INORGANIC POWDER ANALYSIS BY TIME-WAVELENGTH RESOLVED LUMINESCENCE SPECTROSCOPY

By

EDGAR FRANCIS PASKI

B.Sc., University of Waterloo, 1981

A THESIS SUBMITTED IN PARTIAL FULFILLMENT OF

THE REQUIREMENTS FOR THE DEGREE OF

DOCTOR OF PHILOSOPHY

in

THE FACULTY OF GRADUATE STUDIES

Department of Chemistry

We accept this thesis as conforming

to the required standard

THE UNIVERSITY OF BRITISH COLUMBIA

September 1988

© Edgar Francis Paski, 1988

In presenting this thesis in partial fulfilment of the requirements for an advanced degree at the University of British Columbia, I agree that the Library shall make it freely available for reference and study. I further agree that permission for extensive copying of this thesis for scholarly purposes may be granted by the head of my department or by his or her representatives. It is understood that copying or publication of this thesis for financial gain shall not be allowed without my written permission.

Department of _Chemistry_ .

The University of British Columbia
Vancouver, Canada

Date _17 October '88_

ABSTRACT

An investigation into the potential of time-wavelength resolved luminescence spectroscopy for the analysis of inorganic powders was performed. A time-wavelength resolved luminescence spectrometer consisting of an excimer laser, scanning monochromator, and gated integrator was constructed. The spectrometer had wavelength coverage from 265 nm to 800 nm, it was capable of measuring lifetimes between 100 ns and 500 ms. Sample excitation was done at 193 nm and 248 nm.

A luminescence system model of first order decay in the time domain and a Gaussian function for the emission band was assumed. The time-wavelength resolved luminescence spectrum was described by the parameters: lifetime, peak maxima, peak halfwidth, and intensity factor. Parameter estimation was done with an algorithm employing a linear algebra construct and simplex optimization. The algorithm's performance on highly overlapped spectra was evaluated. For two component mixtures having a 1% RSD noise level, overlaps greater than 0.3 halfwidths in the spectral domain and lifetime ratios greater than 1:1.3 were resolved with all parameter estimates having an error of less than ±2%.

The luminescence spectra of $CaMoO_4$, $SrMoO_4$, $BaMoO_4$, $ZnMoO_4$, $CdMoO_4$, $PbMoO_4$, $CaWO_4$, $SrWO_4$, $BaWO_4$, $ZnWO_4$, $CdWO_4$, and $PbWO_4$ consisted of broad featureless bands showing simple exponential decay. Mixed crystals of $Ca(Mo_xW_{1-x})O_4$ and $Sr(Mo_xW_{1-x})O_4$ were examined. Tungstate emission was

quenched by molybdate, the molybdate emission dominated when x was greater than 0.15. The tungstate lifetime was found to be proportional to molybdate concentration.

The luminescence spectra of $CaZrO_3$, $SrZrO_3$, $BaZrO_3$, $CaHfO_3$, $SrHfO_3$, $BaHfO_3$, CaO, SrO, and BaO as pure compounds and doped with Tl, Pb, Sb, and Bi were studied. The pure zirconates and hafnates showed short lived (<100 ns) luminescence with 248 nm excitation; no readily discernible luminescence was observed with 193 nm excitation. Doped compounds tended to show luminescence characteristic of the dopant ion.

TABLE OF CONTENTS   Page

TABLE OF CONTENTS   Page

LIST OF TABLES

LIST OF FIGURES

ACKNOWLEDGEMENTS

This work is dedicated to my daughters Shirley and Alison to make up for all those missed picnics, mountain hikes, Scrabble games, and other fun times.

A very special thanks to my wife Frances for her perseverance, support, and encouragement throughout this exercise.

A sincere thank you to Mike Blades, my research supervisor, for his guidance, stimulating discussions, and support for this project.

I also want to thank members of the mechanical and electronics shops for their invaluable technical support, Elmer Ogryzlo for use of his laboratory, and other members of the Chemistry Department for their encouragement and advice.

Chapter 1

INTRODUCTION

1.1 OVERVIEW

Since the research described in this thesis is mainly concerned with luminescnece, the basic principles of this phenomenon are first discussed, with an emphasis on processes occurring in solid inorganic insulators. A brief sketch of pre-twentieth century human experiences with luminescence phenomena is also given, to put this work in perspective.

1.2 HISTORICAL

Luminescence is the emission of electromagnetic radiation from a substance that is in excess of thermally induced blackbody radiation. Prehistoric humans probably associated objects emitting light with heat since in their everyday experiences all common light sources were incandescent black body radiators such as fire, glowing embers and the sun [1]. Luminescence, or "cold" light, was a distinctly unusual phenomenon that generally induced awe and fear in our ancestors [2]. The recognition of luminescence as a distinct physical phenomenon was likely first associated with the aurora borealis and bioluminescence.

The aurora borealis is a striking phenomenon of transient gas phase luminescence [3] appearing in the night sky against the background of fixed stars. In many ancient cultures the appearance of the aurora borealis was often taken to be an omen since it is an unusual phenomenon in temperate latitudes and a distinct rarity in the tropics

1

[3]. In temperate and tropical regions the aurora is normally a deep red color. To the ancients, this deep red color was often associated with blood and a display of the aurora borealis was invariably linked with impending doom or some other significant change for the worse in human events [4]. In polar latitudes where the aurora is an everyday occurrence benign associations with the aurora are the rule. For example, among the Inuit, a legend common to many tribes around the Arctic [4] ascribes the colored bands of the aurora to their ancestors' spirits playing ball with a walrus skull.

Bioluminescence was evident to early humans in several distinct and sometimes unusual forms. Glowworms and fireflies generally heralded the arrival of summer in damp, temperate regions. Luminescence produced by luminescent bacteria in rotting wood and putrefying flesh were noteworthy events that often carried religious overtones [2]. To ancient Chinese seafarers, the appearance of "burning seas" caused by luminescent plankton was attributed to either dragons or the gods.

Reports of precious stones that shine in the dark are scattered throughout early literature [5,6]. These reports tended to be highly embellished accounts of gemstones' refractive power and cut, although fluorspar and certain types of thermoluminescent diamond may have been observed also. The luminous cobra stone of India and Sri Lanka [2] was likely a type of thermoluminescent fluorite. Western

scholars such as Aristotle, Herodotus, and Thales of Miletus [7] gave accounts of luminescent phenomena but did not make direct reference to luminescent stones.

1.2.1 THE BOLOGNA STONE

Sometime between 1602 and 1604 Vincenzo Casciorolo [5], a Bolognian cobbler and amateur alchemist, made one of the most significant discoveries [2] in the field of luminescence. Casciorolo found a heavy, translucent mineral on the slopes of Monte Paterno near Bologna that would, on calcination, shine in the dark after exposure to either sunlight or candlelight. The stone's reddish colored luminescence, like that of a glowing ember, would gradually fade away and cease to glow after a period of time. The substance Casciorolo found was a sulfur rich form of heavy spar that became contaminated with a small amount of barium sulfide on calcination. Over a period of time, the stone would eventually lose its ability to luminesce due to absorption of moisture from the atmosphere [2].

The discovery of the Bologna stone was a significant event in history, for it was the first artificial light storage device. It is the direct precursor of devices such as the fluorescent lamp, cathode ray tube, and the solid state laser. However, of even more importance is the philosophical impact this material had on human thought for it gave direct evidence that light was a material substance. This concept of light being a material substance is comparable to the concept of the wave-particle duality of

matter in modern physics. The physical evidence exhibited by the Bologna stone discredited the Platonic concept of ocular beams [8] emanating from the eye and the Neoplatonist argument of light as the "illumination of the human intellect by divine truth".

The Bologna stone phosphor was studied by leading 17th century scientists and philosophers including Galileo, Liceti and La Galla. Luminescence from the Bologna stone gave Galileo [9] physical evidence that the contemporary philosophical beliefs that light was a quality of a transparent, illuminated medium were false. In 1652, Nicolai Zucchi of Collegio Romano reported in Optica Philosophia that the luminescence intensity from the Bologna stone was proportional to the intensity of the exciting light and that the stone's luminescence color was independent of the exciting light color. On the basis of his experiments, Zucchi [2] made the conclusion: "Light is not merely absorbed as such, but rather it excites and unites with a spiritous substance contained in the stone, and when the illumination has ceased, this substance gradually dissipates and becomes unsuitable for exhibiting a visible glow". Thus the foundations of luminescence spectroscopy were laid.

The first recorded observation of a luminescence spectrum from an inorganic substance was made by Francesco Maria Zanotti in collaboration with Count Francesco Algarotti in 1713 [2]. They repeated Zucchi's experiment using a prism to disperse the luminescence from the Bologna stone

4

phosphor. The dim, apparently monochromatic emission was noted. However, a true idea of the luminescence spectrum was not gained due to low light intensity and the lack of an entrance slit in their apparatus.

1.2.2 CONTRIBUTIONS OF BECQUEREL AND STOKES

The next major advance in luminescence studies was made in the mid nineteenth century when the scientific treatment of the subject was pursued in earnest. Antoine Cesar Becquerel, in collaboration with his son Edmond, published the first drawings of luminescence spectra in volume II of his "Traitè de Physique" (Paris, 1844) in which he showed emission from calcium and barium sulfides along with a solar spectrum containing the Fraunhofer lines for comparison.

Edmond Becquerel's extensive experimental work laid the foundation for the scientific investigation of luminescence [10]. He was the dominant figure of his time with his studies on excitation and emission spectra as well as his invention of the phosphoroscope for the study of luminescence lifetimes. With his phosphoroscope, which was capable of lifetime measurements as short as 0.1 ms, Becquerel established the decay law with his findings that luminescence intensity decreased exponentially as a function of time. Becquerel recorded the first observations of time-wavelength resolved luminescence [10] with his descriptions of substances studied with his phosphoroscope whose luminescence changed color with time.

In a landmark paper, G. G. Stokes [11] coined the term

"fluorescence" after the light emitted from the mineral fluorspar and provided the correct interpretation of fluorescence in solutions being the optical emission of light rather than scattering. In this paper, he stated the principle that has become known as "Stokes' Law": fluorescent light is always of longer wavelength than the light used to excite a luminescent substance or solution. In formulating this principle, Stokes used a multidimensional approach: the method of spectral illumination or "crossed spectra" where the excitation light passed through a prism to illuminate a sample in such a manner that fluorescence from the sample by any excitation wavelength may be observed. In a sequel [12], Stokes described a simple yet elegant fluorescence spectrometer for chemical analysis and reported preliminary work done using this instrument.

Through the efforts of E. Becquerel and G. Stokes luminescence spectroscopy became firmly established as a major area of study that has had profound influence in diverse fields such as archaeology, nuclear physics, quantum physics, biochemistry and art conservation.

1.3 LUMINESCENCE OF AN ISOLATED ATOM

The simplest electronic system capable of emitting light, aside from an accelerating electron, is a single isolated atom. This atom may be excited to a higher energy level above its ground state by two principal processes. The first process, known as kinetic or thermal excitation, involves an inelastic collision with another particle where

some of the particle's kinetic energy is transferred to the atom, raising the atom to a higher energy level. The second excitation process involves absorption of a photon whose energy closely matches that of a transition from the ground state to an excited state of the atom. When the excited atom relaxes to a lower energy state by photon emission, the emission is said to be thermally stimulated if excitation was by the first process and luminescence if excitation was by the second process. In an atom, if the emitted photon has the same energy as the exciting photon, the emitted light is termed resonance radiation [13]. Kinetic and radiative processes may occur either singly or in combination, as illustrated in Figure 1.1.

1.3.1 EINSTEIN THEORY OF RADIATION

If an isolated atom capable of being raised from an energy state 1 to a higher energy state 2 is in a container containing isotropic radiation of frequency between ν and $\nu + d\nu$ and intensity I_ν, the following probability coefficients may be defined [13]:

$B_{12}I_\nu$ is the probability that the atom in energy state 1 will absorb a quantum $h\nu$ and pass to energy state 2 when it is exposed to the isotropic radiation.

A_{21} is the probability that the atom in energy state 2 will spontaneously emit without spatial coherence a quantum $h\nu$ and pass to energy state 1.

$B_{21}I_\nu$ is the probability that the atom will emit a quantum $h\nu$ spatially coherent with the stimulating quantum

7
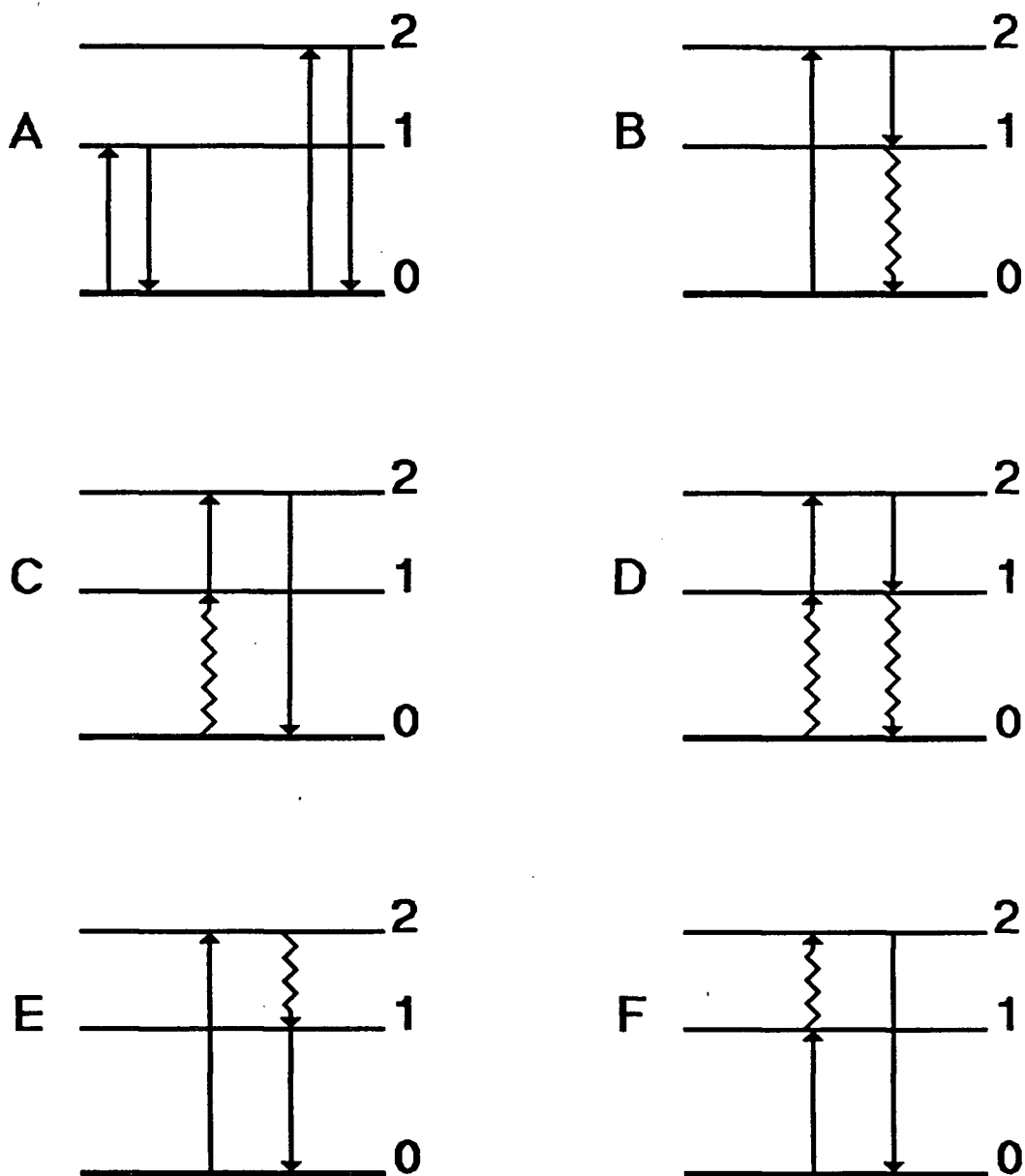
Figure 1.1   Luminescence processes in atoms: (A) resonance
fluorescence, (B) direct line fluorescence,
(C) thermally assisted direct line fluores-
cence, (D) thermally assisted resonance fluo-
rescence, (E) stepwise line fluorescence, (F)
thermally assisted stepwise line fluorescence.

$h\nu'$ when it is exposed to the isotropic radiation.

In the case where local thermodynamic equilibrium (LTE) exists in the container:

$$(A_{21})/(B_{12}) = (2h\nu^3/c^2)(g_1/g_2) \tag{1.1}$$

$$(B_{21})/(B_{12}) = (g_1/g_2) \tag{1.2}$$

where g_1 and g_2 are the statistical weights of the energy states 1 and 2 respectively, h is Planck's constant, and c is the speed of light.

From the definition of the term A_{21}, the lifetime of the atom in energy state 2, τ, is:

$$\tau = 1/(A_{21}) \tag{1.3}$$

and for the transition from an energy state n to all lower energy states m, the lifetime of the atom (τ_n) in energy state n is:

$$\tau_n = 1/(\sum_m A_{nm}) \tag{1.4}$$

Thus, for an isolated atom that is not subject to perturbing influences such as collisions or external force fields, the excited state will have a lifetime that is characteristic of the atom and the particular excited state that the atom is in.

1.3.2 NATURAL LINE BROADENING

If one observes many emission events occurring between the same energy levels from this isolated atom, one will see that the emitted photons are not identical in energy. The

slight energy variation in the photon energy is a consequence of the Heisenberg uncertainty principle. Since the atom spends on the average a time t in the excited state it is impossible to know exactly the energy of the excited state. The excited state may have an energy anywhere in the interval $E \pm (h/2\pi t)$, where E is the average energy of the excited state, h is Planck's constant and t is the average time the atom stays in the excited state.

For an atom undergoing a radiative transition between energy levels 2 and 1, the natural damping factor γ_N is:

$$\gamma_N = (1/\tau_1) + (1/\tau_2) \tag{1.5}$$

where τ_1 and τ_2 are the mean lifetimes for energy states 1 and 2 respectively. The energy distribution of photons for this transition [14] is:

$$\phi_\nu = \gamma_N/[4\pi^2(\nu - \nu_0)^2 + (\gamma_N/2)^2] \tag{1.6}$$

where ϕ_ν represents the probability of photon emission at a frequency ν and ν_0 is the mean frequency of photons emitted.

1.4 LUMINESCENCE OF ATOMS IN A GAS

Consider a transparent container of gas consisting of atoms of one type, say mercury, along with other kinds of atoms and molecules. This system is considerably more complex than that of a single isolated atom, since the mercury atoms will be in motion and be involved in collisions with other mercury atoms as well as other species present in the container. Luminescence from the mercury atoms will be

influenced by interactions with its neighbors in many ways, some of which are discussed in the following sections.

1.4.1 SPECTRAL LINE BROADENING EFFECTS

In a gas, the luminescence from a given transition between energy states 2 and 1 is subject to broadening effects due to the Doppler effect and collisions with other constituents of the gas mixture. Assuming that strong magnetic fields are absent and the number of ions present is negligible, Zeeman and Stark broadening effects may be ignored.

Doppler broadening is produced by the emitting atoms moving about in space at different velocities, without consideration of effects induced by collisions. Assuming a Gaussian velocity distribution for emitting atoms in the gas, a Doppler broadened spectral line is symmetric about the center of the line with a profile, $\phi_{\nu d}$, described by the relationship [14,15]:

$$\phi_{\nu}d = \{\exp-[(\nu-\nu_0)/\Delta\nu_D]^2\}/(\pi^{\frac{1}{2}}\Delta\nu_D) \qquad (1.7)$$

where the Doppler width, $\Delta\nu_D$, the frequency shift of the most probable velocity, is:

$$\Delta\nu_D = (\nu_0/c)[(2kT/M) + V_t^2]^{\frac{1}{2}} \qquad (1.8)$$

where k is Boltzmann's constant, T is temperature, M is mass of the emitting atom, and V_t is the turbulent velocity of the gas.

Collision induced line broadening effects are due to

the perturbation of energy levels in the atom caused by the electric fields of nearby atoms and molecules. Collision broadening of an atomic line is a complex process. The observable effects being overall broadening of the spectral line, a shift in the line maxima and an asymmetric intensity distribution about the line maxima. This complex topic has been studied in detail by the astrophysical community [1,16,17] and has led to an understanding of physical and chemical processes in astronomical objects.

To a first approximation, if the gas in the container is at standard temperature and pressure (STP), the luminescence line profile I_ν, at frequency ν, from an atom may be described by the Voigt equation [15]:

$$I_\nu = I_0(a'/\pi) \int_{-\infty}^{\infty}[\exp(-y^2)]/[a'^2 + (\omega - y)^2] \, dy \quad (1.9)$$

where:

$$\omega = 2(\nu-\nu_0)(\ln 2)^{\frac{1}{2}}/\Delta\nu_D \quad\quad\quad (1.10)$$

$$a' = (\Delta\nu_N + \Delta\nu_L)(\ln 2)^{\frac{1}{2}}/\Delta\nu_D \quad\quad (1.11)$$

$$y = 2\delta(\ln 2)^{\frac{1}{2}}/\Delta\nu_D \quad\quad\quad\quad (1.12)$$

$$\Delta\nu_L = Z_L/\pi \quad\quad\quad\quad\quad\quad (1.13)$$

and I_0 is the intensity at the peak maximum, δ is the frequency displacement from $\nu-\nu_0$, Z_L is the number of broadening collisions per second per luminescent atom.

The approximations for the Lorentz halfwidth, $\Delta\nu_L$, and the form of the Voigt equation yield a line profile that is symmetric with no offset in peak emission wavelength. Despite these limitations, this model for the line profile

is useful in studies of potential spectral overlap problems in analytical applications.

1.4.2 QUANTUM YIELDS AND EXCITED STATE LIFETIMES

Assuming that intrinsic nonlinear optical phenomena are negligible [18], the quantum yield, Φ, for luminescence may be defined as the number of quanta emitted per number of quanta absorbed by a system over a given period of time. In an atom, the quantum yield for a given transition may be reduced by the presence of intermediate excited states, nonradiative internal conversion processes, and nonradiative energy transfer to another species present in the gas.

In the case of resonance fluorescence in a collection of atoms in which nonradiative processes and intermediate excited states are absent, if the atoms are in an excited state p, they will undergo decay to the ground state q at a rate given by the relationship:

$$-dn_p/dt = A_{21} n_p \qquad (1.14)$$

where n_p is the number of atoms in the excited state, A_{21} is the Einstein transition probability (see section 1.3.1) for spontaneous transition from the excited state, p, to the ground state q.

If the exciting radiation is stopped at time t=0, then at some future time, t, the number of excited atoms remaining in the gas, n_p^t, may be found by substituting lifetime for transition probability (1.3) and integrating (1.14):

$$n_p^t = n_p^0 \exp(-t/\tau) \qquad\qquad (1.15)$$

In the case where the excited atoms do not undergo interactions with each other but do undergo relaxation by nonradiative internal conversion processes, the intrinsic lifetime for the atom τ^0 is obtained by combining the transition probabilities for both radiative and nonradiative transitions:

$$\tau^0 = 1/\sum_r A_{pr} \qquad\qquad (1.16)$$

where A_{pr} is the transition probability for the transition between the excited energy state p and a lower state r.

The case where collisional deexcitation occurs along with internal conversion [19] is treated in an analogous manner. If there are s varieties of atoms and molecules in the gas, each having some concentration Q_s, and if the temporal probability for collisional quenching by a species is represented by k_s, then the lifetime for atoms in the excited state τ', is given by the relationship:

$$\tau' = 1/[\sum_r A_{pr} + \sum_s k_s Q_s] \qquad\qquad (1.17)$$

Equation 1.17 is of fundamental importance, for it shows that the lifetime of an excited state in a substance is characteristic of that substance and the environment of the substance. In addition, it provides an avenue for examining environmental effects quantitatively.

1.5 GAS PHASE MOLECULAR LUMINESCENCE

Molecules have a more complex electronic structure than single atoms; this increased complexity is reflected in their luminescence spectra and relaxation behavior. Most gas phase molecular luminescence studies [20] have been limited to aromatic organic molecules. In the gas phase, at low pressures, a molecule may be considered to be an isolated system with negligible interactions with other components of the gas.

In organic molecules, the luminescence processes are involved primarily with excited states of π-electron systems in the molecule [21] and are a function of the molecule's degree of conjugation, shape, rigidity and functional substituents. Organic compounds such as aromatic hydrocarbons, amino acids, and polyenes which contain extensive double bonds are particularly well disposed to luminescence. The Jablonskii diagram in Figure 1.2 outlines the basic luminescence processes in organic molecules.

In π-electron systems, the ground state normally contains an even number of electrons whose spins are paired, this energy state is termed a singlet state and is symbolized as "S_0". There may be several excited states, in which case they are denoted as S_1, S_2, etc.. If spin reversal occurs on excitation the excited states are termed triplet states symbolized as T_1, T_2, etc., with the triplet state energy level always lying below its corresponding singlet state level [22]. Direct electronic transitions
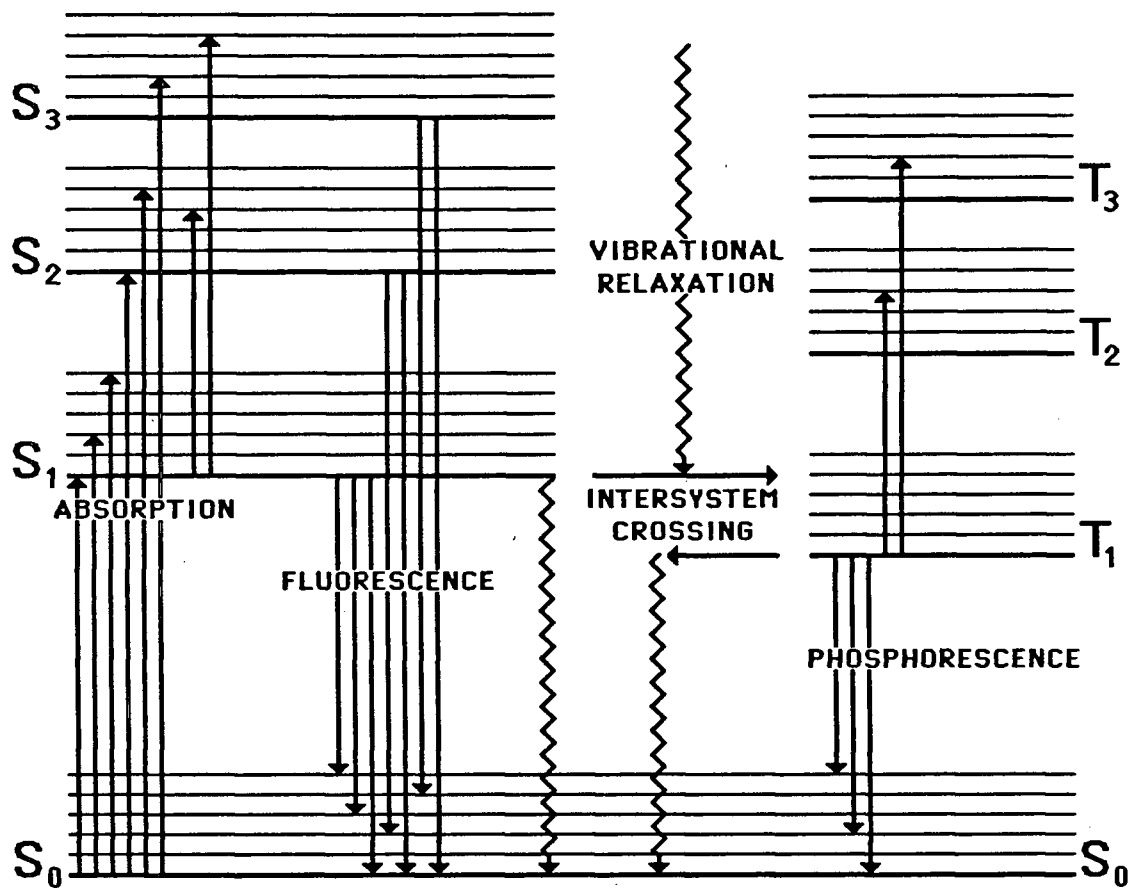
Figure 1.2   Luminescence processes in π-electron systems.

between singlet and triplet states have very low transition probabilities. Within each electronic energy level lies a series of vibrational sublevels.

In organic molecules, the luminescence processes of fluorescence, which involves no change in spin multiplicity, and phosphorescence, where radiative emission is accompanied by a change of spin multiplicity, are readily distinguished. The emission observed for an organic molecule is primarily governed by the following rate processes: $S_1 \rightarrow S_0$, fluorescence; $S_1 \rightarrow S_0$, internal conversion; $S_1 \rightarrow T_1$, intersystem crossing; $T_1 \rightarrow S_0$, phosphorescence; $T_1 \rightarrow S_0$, intersystem crossing. The relative magnitudes of the rate constants are dependent on the overall electronic structure of a particular molecule.

The emission process is highly dependent on the environment of the molecule. Collisional deactivation effects are dependent on the chemical and physical nature of the concomitant as well as the collision frequency. Phosphorescence is normally observed only at low temperatures and pressures since collisional de-excitation of the triplet state is likely to occur before the two slow intersystem crossings are made. However, if a halogen is present in the gas or attached to the molecule, the rate constant for intersystem crossing will be increased significantly and phosphorescence may effectively compete with the fluorescence process. Oxygen effectively quenches all types of luminescence in organic molecules; the oxygen molecule

apparently catalyses [22] nonradiative deactivation processes in the molecule.

Luminescence processes in organic molecules are intimately associated with the bonding within the molecule itself, regardless of the physical state of the molecule. The fine structure observed for an isolated molecule may be altered by the presence of neighbors at increased pressures and in condensed media, but the basic spectral pattern remains with relatively small shifts due to minor alterations in the molecule's π-bonds induced by the neighbors.

1.6 LUMINESCENCE IN THE SOLID STATE

Solid state luminescence is found in a vast array of substances of inorganic and organic composition and in both crystalline and amorphous forms. Although there are numerous luminescence mechanisms in solids, a common thread among them is that luminescence emission is a product of the electronic energy levels of a solid; thus, the luminescence from a solid carries information on these energy levels.

Luminescent solid state materials may be grouped into three broad classifications: organic molecules, semiconductors and inorganic insulators. The luminescence mechanisms dominant within each group differ so much between the groups that separate discussions are warranted for the events that follow the initial excitation.

1.6.1 EXCITATION METHODS

There are numerous methods for inducing luminescence emission in a solid. They may be broadly classified as:

radiation, thermal stimulation, phase change, mechanical deformation, chemical reaction, and superimposed electric field.

Excitation of a solid by irradiation may be done with either nonionizing or ionizing radiation. Nonionizing excitation of solids with UV and visible light is discussed in more detail in succeeding sections.

When a high energy (X-ray or gamma ray) photon or high energy subatomic particle such as an electron or proton passes through a solid; numerous complex processes [23] may be initiated such as: nuclear reactions, bond rupture, ionization, and defect formation as energy is absorbed by the solid. An end result of these interactions is the formation of electron-hole pairs in the solid. Subsequent to the formation of electron-hole pairs, energy release may proceed by: electron-hole recombination, transfer by excitons, or temporary storage in hole trapping metastable energy levels termed traps. In each of these modes relaxation to the ground state may be by a combination of phonons and photons, with luminescence being the route of photon emission.

Thermoluminescence is the thermally stimulated luminescence emission in a solid from metastable energy states known as traps. Traps in a solid are normally populated by irradiation with high energy photons or subatomic particles. The principal applications have been in age dating cultural artifacts and dosimetry.

Crystalloluminescence and lyoluminescence involve phase

changes in a material. Crystalloluminescence [24] is the flash of light emitted from a substance as it crystallizes from a melt. This phenomenon is responsible for the "blick" occurring as the gold bead crystallizes in cupellation [25] and the "shotting" from solidifying slag in the fire assay for gold. The flash colors have been used by fire assayers qualitatively in judging bead purity and assay charges. Lyoluminescence is the light emission from traps as a solid undergoes dissolution. It's principal application is in radiation dosimetry.

Triboluminescence [24,26] is the light emitted from a solid when it undergoes mechanical deformation. Despite its intimate connection with the mechanical, electrical, and spectroscopic properties of materials, it currently remains a laboratory curiosity.

Chemiluminescence occurs when a product of a chemical reaction is left in an electronically excited state and relaxes by photon emission. In solids, this effect is normally associated with reactions occurring on the surface such as the oxidation of phosphorus and unsaturated silicon oxide.

In semiconductors, light emission may follow excitation by an externally applied electric field [27]. The material is normally excited by applying an electric field to an electronic state a few electron volts above the ground state. Subsequent to excitation, there may be energy transport to a radiating site where relaxation by electrolumine-

scent emission occurs.

1.6.2 MOLECULAR SOLIDS

Organic molecules in the solid state may be called molecular solids since the solid is held together by van der Waals forces between the individual molecules. The weak interactions between individual molecules in the solid state do not significantly alter the electronic structure of individual constituent molecules. Therefore, the luminescence is still characteristic of the emitting molecule.

The use of low temperature, rare gas matrix isolation of aromatic hydrocarbons [18] closely approaches the ideal environment of a low pressure gas with minimal interactions of a molecule with its environment. Rigid glass Shpol'skii matrices [29] take advantage of dimensional and geometric correlations between a guest organic molecule and its host solvent in the production of near linelike luminescence spectra.

Emission spectral perturbations due to the presence of neighbors are generally minor in magnitude; they may be produced by: Davydov splitting of energy states, changes in the optical and dielectric properties of the media, and exciton interactions. Excited state lifetimes are markedly dependent on the type of neighbor and its orientation and distance with respect to the luminescent molecule. Radiationless processes in organic solids [30], to a first approximation, tend to be localized to effects between the luminescent molecule and its close neighbors.

1.6.3 SEMICONDUCTORS

Semiconductors are solid materials whose constituent atoms are bonded with each other by covalent bonds, the outer electron orbitals of the constituent atoms overlap each other with the net result that it is impossible to assign a particular electron with a particular atom. Since luminescence is a function of changes in electron energy states, luminescence from a semiconductor [31] is highly dependent on the properties of the entire solid material as well as the properties of its individual constituents. This is in marked contrast to the behavior of molecular crystals.

To illustrate luminescence in semiconductors, consider a typical wide band gap III-V compound such as GaAs. At low temperatures, say around 4 K, and in the dark, pure GaAs is an insulator. If the compound remains at the same temperature and is exposed to light it becomes conductive and is luminescent with line-like and band emission in the near infrared. Now, consider the case where a specimen of GaAs doped with a small amount of silicon ("p-type") is placed in intimate contact with a specimen of tellurium doped GaAs ("n-type"). If a sufficiently high electric potential is applied across the material, it will luminesce and the luminescence will occur only at the p-n junction. In these examples, the luminescence observed is due to electron-hole radiative recombination processes across the gap between conduction and valence bands in GaAs.

The radiative recombination processes in semiconductors

where an electron-hole pair was created by photon absorption are outlined in Figure 1.3 [32]. The conduction band (CB) to valence band (VB) transitions are the highest energy transitions normally possible and are seen at higher temperatures; at low temperatures, this transition is linelike. The exciton (E) to VB transitions are seen only at low temperatures in extremely pure materials. The E to VB transitions may be due to either the decay of free excitons or excitons bound to impurities.

When impurities and defects are present in the semiconductor, energy levels within the band gap may be created. A donor atom is an impurity atom that can readily give up an electron. When present in a semiconductor and when ionized, it gives up an electron to the conduction band. Thus, a donor bound energy level below the conduction band is created. The depth below the conduction band is termed the donor ionization energy and is a function of the composition of both the semiconductor host and dopant atom guest. In an analogous manner, acceptor states (holes) are formed when a dopant capable of accepting electrons is present. The hole is freed when the acceptor is ionized. This input of energy is represented as the acceptor bound energy level above the valence band.

Radiative recombination processes may also take place between CB and acceptor (A) or deep acceptor (DA) levels. The depth of acceptor levels are a function of the composition of the semiconductor material. Similarly,
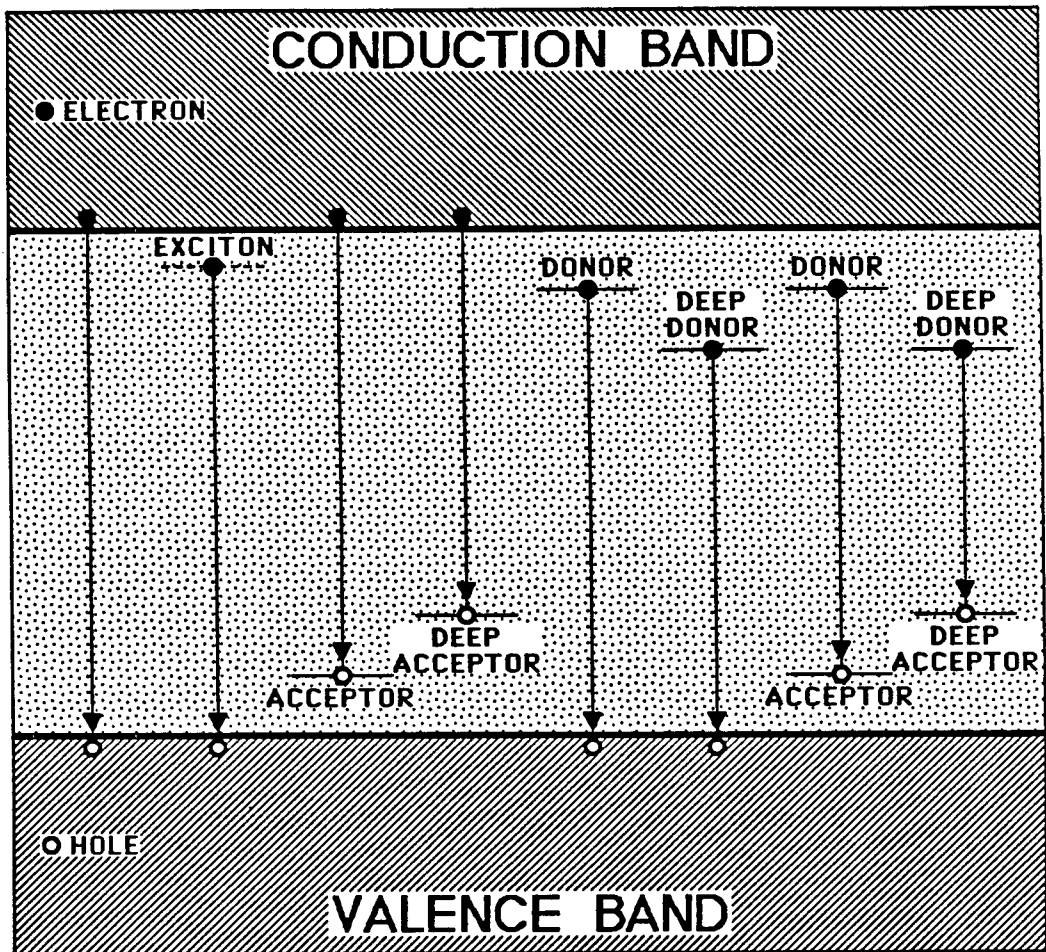
Figure 1.3   Luminescence associated electron-hole pair
             recombination processes in semiconductors.

transitions may take place between donor (D) or deep donor (DD) levels and the VB. In addition, recombination can occur between the D or DD levels and the A or DA levels.

In p-n junctions, the radiative recombination processes are similar. The chief difference in this situation is that, instead of optically pumping the material, the conduction band electrons may be pumped into the p-region by forward biasing the p-n junction with an applied electric potential. Since the luminescence originates in the junction region, the applied bias voltage is approximately that of the band gap itself.

The luminescence spectrum from a semiconductor normally has an amorphous, nondescript appearance that is the result of a complex mixture of broad and narrow bands superimposed on each other. Thus, the apparently featureless luminescence spectrum conveys a tremendous amount of information on the host semiconductor and its dopant guests. For example, studies on the effect of applied bias potential on the luminescence spectrum may provide insights on the composition of a material in the vicinity of the p-n junction.

1.6.4 INORGANIC INSULATORS

The third class of luminescent solid materials is that of the inorganic insulators. This group includes all nonconducting solids that are neither semiconductors nor organic molecules, for example: naturally occurring rocks and minerals, gemstones, ceramics, glass, and inorganic

construction materials. The common feature of these substances is that luminescence from them is almost inevitably associated with impurity atoms and defects in their crystal structure, although there are a few notable exceptions to this generalization.

Inorganic insulator host lattices are transparent to visible light, have large band gaps and have bonding ranging from covalent (diamond) to ionic (CsF). Common host lattice types include: 1) the alkali metal and alkaline earth halides, 2) oxygen dominated lattices such as Al_2O_3, $CaCO_3$ and $CaWO_4$, 3) some II-IV compounds such as ZnS, 4) glass, and 5) diamond. Luminescence from this diverse group of materials involves several quite different processes, some of which are considered in the following sections.

1.6.4.1 THE COLOR CENTER IN ALKALI HALIDES

Consider a perfect crystal of pure sodium chloride, a substance which is normally transparent from about 175 nm to 14500 nm. If this crystal is exposed to high energy photons such as X-rays [33] it will become yellow in color and will retain that color after cessation of the X-ray irradiation provided that the crystal is kept at cryogenic conditions. On exposure to visible light the cooled crystal will exhibit strong broad band luminescence in the near infrared.

Some of defects in the crystal lattice produced by the X-ray bombardment may be color centers [34] such as the F center which consists of an anion vacancy in which a single electron is trapped. In an F center, the trapped electron

may be considered to be a particle in a box with walls made up of the neighboring ions that interact with the particle. The ion neighbor orbitals will overlap with those of the trapped electron resulting in electronic states that are intimately coupled to the crystal lattice. Thus the absorption and luminescence spectra of an F center convey information on the crystal lattice in the neighborhood of the F center.

The spectra associated with an F center consist of single broad absorption and emission bands. Even though both absorption and emission transitions occur between the same two energy states there is a large Stokes' shift between them. The band width for the absorption and emission bands is a function of the neighboring ions vibrational motion. The Stokes' shift is a result of the different electrostatic environments between the ground and excited states in the F center. On excitation, the neighboring ions are suddenly in a different electrostatic environment and they rapidly reposition themselves to a new minimum potential energy arrangement. Subsequent to this rearrangement, relaxation to the ground state may occur by either photon emission or radiationless deactivation.

1.6.4.2 TRIVALENT RARE EARTH IONS IN LANTHANUM CHLORIDE

A perfect, pure crystal of $LaCl_3$ will not luminesce when excited by a broadband source such as a Xenon flash lamp. However, if the same source is used to excite a $LaCl_3$ crystal doped with a trivalent rare earth ion such as Pr^{+3},

very weak luminescence will be observed. The emission and absorption spectra of the doped crystal consist of a series of sharp lines similar in appearance to that of an isolated atom.

In trivalent rare earth doped luminescent substances, the spectral lines originate from transitions wholly within the 4f manifold of the rare earth ion and are characteristic of energy levels within that particular electron shell. Since the 4f electrons are shielded from the external environment, the energy levels of the rare earth ion are only slightly perturbed by the crystal field of the host lattice. The perturbations in the spectral lines do reflect the different crystal fields of various host lattices by minor shifts in wavelength and splittings within energy levels [35].

The transitions involved are essentially purely electronic with minimal direct interaction with host lattice vibrations. There is no Stokes' shift and consequently, thermal quenching [36] due to crossing of excited state and ground state parabolae does not occur. The principal effect of temperature on emission and absorption spectra is band broadening, with quenching primarily due to electromagnetic coupling and tunneling effects. Luminescence from a trivalent rare earth ion may be perturbed by impurities present in the host lattice. These perturbation effects were used by Miller [37] to analyze for impurities in a host lattice.

1.6.5 THE CONFIGURATION COORDINATE MODEL

The absorption and emission spectra of a localized excitation in an inorganic insulator may be approximated by a one dimensional configuration coordinate model [38-41]. Although this model is valid only if the electron-phonon interaction involves one vibrational mode in the lattice, predictions for more complex systems based on this model agree favorably with experimental data.

A configuration coordinate model diagram for a localized excitation, say a dopant ion in a host lattice, is shown in Figure 1.4. The vertical axis represents system energy, E, and the horizontal axis is the configuration coordinate, Q, which represents the distance from the dopant ion to the nearest neighbor ions in the lattice. The equilibrium value of Q for the ion in its ground state is zero. The potential energy, E_g, as a function of the configuration coordinate is then given by:

$$E_g = \tfrac{1}{2}k_g Q^2 \tag{1.18}$$

where k_g is the force constant for the ground state ion. For the ion in the excited state, the potential energy function is

$$E_e = \tfrac{1}{2}k_e(Q-Q_0)^2 + E_0 \tag{1.19}$$

where k_e is the force constant for the excited state ion, Q_0 is the equilibrium value for the ion in its excited state, and E_0 is the electronic energy difference between the
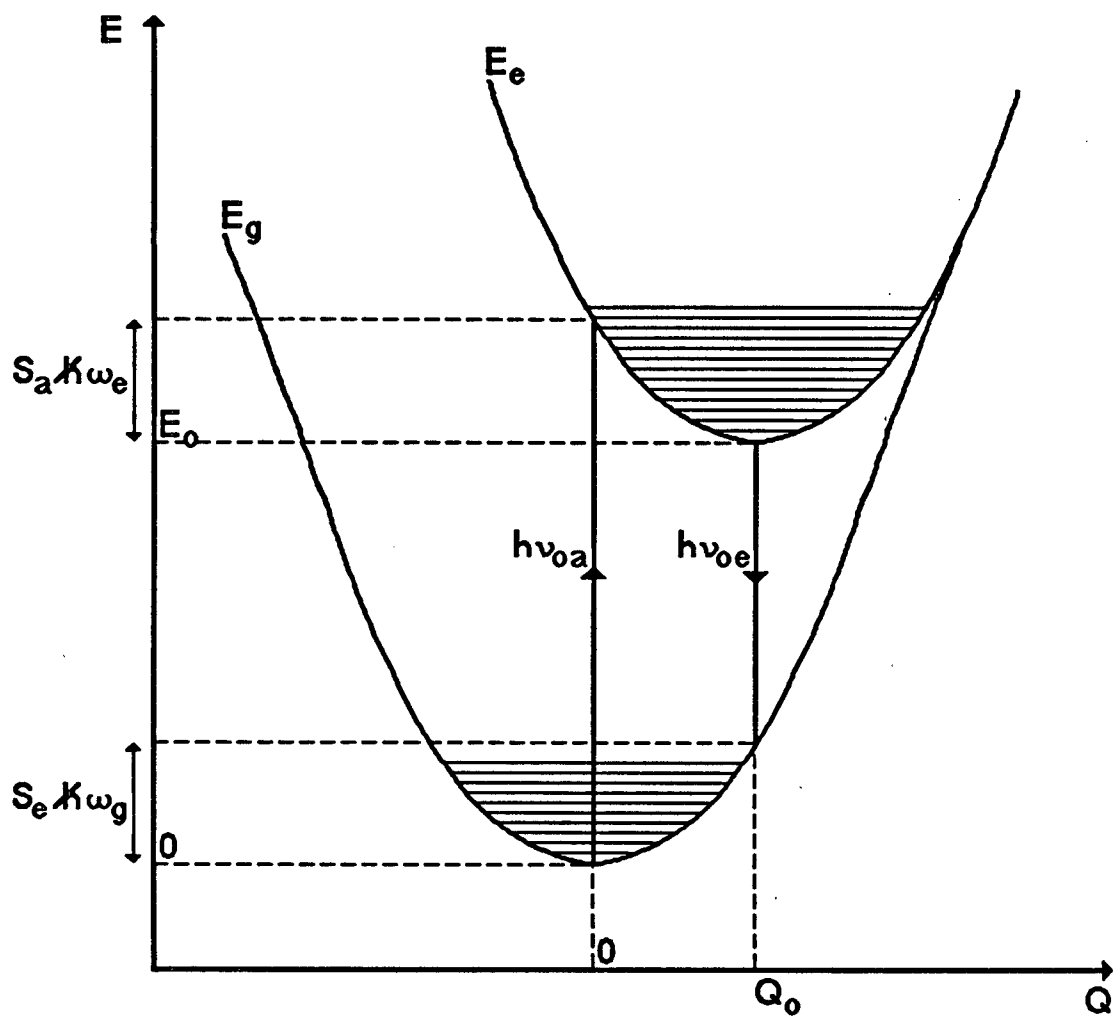
Figure 1.4   Configuration coordinate diagram for transitions between an excited state and the ground state.

excited and ground state equilibrium values.

Neglecting the zero point energies in the ground and excited states, the band maxima for absorption, $h\nu_{0a}$, and emission, $h\nu_{0e}$ are

$$h\nu_{0a} = E_0 + S_a \hbar\omega_e \qquad (1.20)$$

$$h\nu_{0e} = E_0 - S_e \hbar\omega_g \qquad (1.21)$$

where S_a and S_e are the average number of phonons emitted after photon absorption and emission respectively; $\hbar\omega_e$, $\hbar\omega_g$, are the average phonon energies for the excited and ground states, respectively.

For a dipole transition, assuming that both the semiclassical approximation and the Franck-Condon principle are followed, the emission band profile is described by the relationship:

$$I(h\nu) = [64\pi^4\nu^4/3c^3] \; G(h\nu) \qquad (1.22)$$

where the term $G(h\nu)$ is the spectrum shape function. The spectrum shape function is:

$$G(h\nu) = \sum \text{weighted } |M_{if}|^2 \qquad (1.23)$$

where the initial states in the matrix element M_{ij} are weighted by the appropriate Boltzmann factor. The spectrum shape factor is Gaussian in profile and the resulting emission profile is slightly skewed due to the ν^4 term in equation (1.22).

Since the emission spectral profile is a Gaussian

shape, it may be described in terms of moments [42]. The second moment (variance) at zero Kelvin is:

$$\sigma_e^2 = S_e(\hbar\omega_g)^3/(\hbar\omega_e) \qquad (1.24)$$

and has a temperature dependence:

$$\sigma_e(T) = \sigma_e(0K) \; [\tanh(\hbar\omega_g/2kT)]^{-\frac{1}{2}} \qquad (1.25)$$

The absorption spectral profile relationships follow an analogous argument. Skewness and peakedness [42] relationships have been derived. However, in many simple luminescent systems, these higher terms are not required to describe the observed emission band shapes.

1.6.6 ENERGY TRANSFER

When a region in a solid absorbs energy and becomes electronically excited, some or all of that energy may be transferred to another region in the solid before the excitation energy is radiated by the emission of photons or heat as illustrated in Figure 1.5. Energy transfer from one region to another is dependent on the local environments of the sensitizer and activator sites as well as the propagation path between them. Luminescence from a substance is highly dependent on energy transfer phenomena and conveys information on the various energy transfer processes occurring in the solid. In solids, there are three fundamental mechanisms of energy transfer: charge transport, radiative, and nonradiative transfer.

Charge transport, or photoconductivity, occurs when a
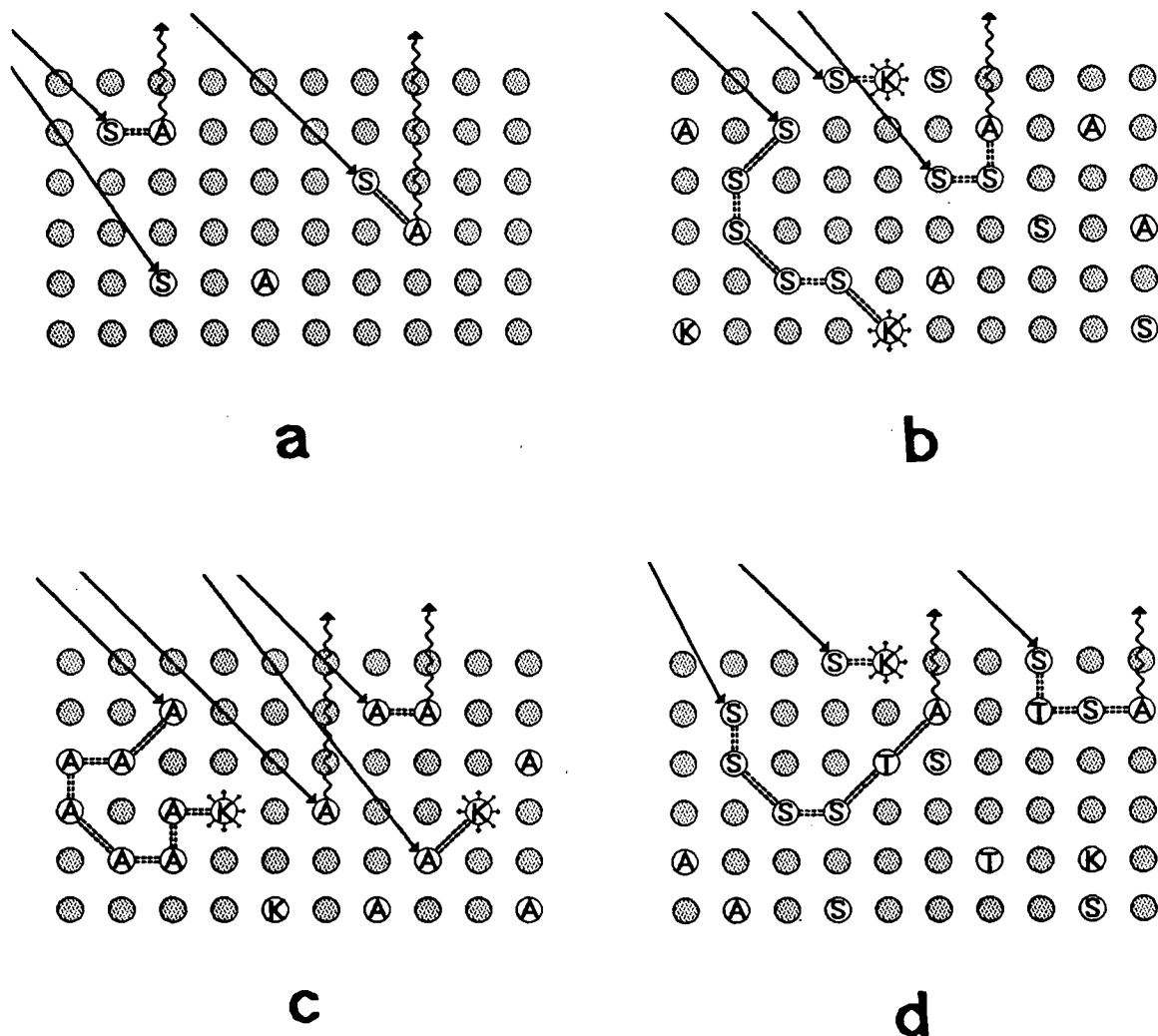
Symbol key:

ⓢ sensitizer		→ excitation	
Ⓐ activator		⤳ luminescence	
Ⓚ killer site		⋯⋯ nonradiative transfer	
Ⓣ trap site		☼ phonon emission	

Figure 1.5   Nonradiative energy movement in solids: (a) energy transfer, (b) energy migration, (c) concentration quenching with transfer to killer sites, (d) traps and delayed luminescence.

photon of sufficient energy is absorbed in the solid and promotes an electron into the conduction band. This process is important in metals and semiconductors. However, in most inorganic insulators, this process is not a significant means of energy transport.

The resonance radiative transfer process occurs when a sensitizer emits a photon which travels through the solid and is subsequently absorbed by an activator which in turn luminesces. The distinguishing features associated with this transfer process are 1) the transfer is a function of sample geometry, and 2) the sensitizer lifetime is independent of activator concentration. However, the emission spectrum is a function of activator concentration. The probability for energy transfer between sensitizer and activator as a function of the distance between them, $P_{SA}(R)$, is given by the relationship [43]:

$$P_{SA} = \sigma_A/(4\pi R^2 \tau_S) \int G_S(\nu)G_A(\nu)d\nu \qquad (1.26)$$

where R is the distance between sensitizer and activator, σ_A is the integrated activator absorption cross section, τ_S is the sensitizer lifetime, and the integral term represents the spectral overlap between sensitizer emission and activator absorption.

The third fundamental mechanism of energy transfer in solids is that of radiationless energy transfer where the basic interaction is electromagnetic coupling between an energy donor and an energy acceptor. This mechanism is best

34

subdivided into two cases: resonance radiationless transfer and nonresonance radiationless transfer.

In resonance radiationless energy transfer, the energy levels between energy donor and energy acceptor are overlapped and the transfer is solely by direct electromagnetic coupling between donor and acceptor. A "virtual photon" may be considered to be the transfer agent. The basic quantum mechanical theoretical treatment was done by Forster [44] for the case of dipole-dipole interactions between solid organic molecules. This transfer mode is an additional path for sensitizer deexcitation. Consequently, a decrease in sensitizer lifetime that is proportional to activator concentration is characteristic of this mode of energy transfer.

A quantitative treatment for resonance radiationless energy transfer has been summarized by Powell and Blasse [45]. For a dipole-dipole interaction between sensitizer and activator, the overlap integral may be simplified to the form:

$$\Omega = \int g_s(\tilde{\nu}) G_a(\tilde{\nu}) d\tilde{\nu} \qquad (1.27)$$

where the g_s and G_a terms are the normalized spectral band-shape functions for the square of the orientation angle between the sensitizer and activator dipoles. The critical interaction distance (R_0), the distance at which the transfer rate is equal to the intrinsic sensitizer decay rate, is defined as:

$$R_0 = \{[3f_a e^2 \Omega \phi_s]/[4(2\pi n \tilde{\nu}_{sa})^4 mc^2]\}^{1/6} \qquad (1.28)$$

where f_a is the activator oscillator strength, e is electron charge, ϕ_s is the sensitizer quantum efficiency, n is the host lattice refractive index, $\tilde{\nu}_{sa}$ is the average value for the wave number in the spectral overlap region, m is electron mass, and c is the speed of light. Thus, for any given sensitizer-activator pair the dipole-dipole interaction energy transfer rate between them is given by

$$\omega_{sa}^{DD} = (\tau_s^0)^{-1} (R_0/R_{sa})^6 \qquad (1.29)$$

where τ_s^0 is the intrinsic sensitizer lifetime and R_{sa} is the distance between sensitizer and activator. The transfer rates for dipole-quadrupole and quadrupole-quadrupole interactions are analogous, with the exponential factors of 8 and 10 respectively.

In nonresonance radiationless energy transfer, the donor and acceptor energy levels do not overlap. The energy level match and subsequent transfer is made possible by creation or destruction of phonons in the host lattice. The transfer rate is dependent on the overlap integral which in turn is dependent on the distribution of phonons present.

The quantitative treatment of nonresonance radiationless energy transfer, as summarized by Powell and Blasse [45], provides the background for the equations that follow. In a solid the temperature dependent occupation number for phonons of polarization j and wave vector k, n_{jk}, is given by the relationship:

$$n_{jk} = 1/[\exp(\Delta E_{sa}/kT)-1] \qquad (1.30)$$

where ΔE_{sa} is the energy difference between sensitizer and activator energy levels, k is Boltzmann's constant, and T is temperature in Kelvin. For phonon absorption, the phonon population number is given as $n_a = n_{jk}$; for phonon emission, the phonon population number is given as $n_e = n_{jk} + 1$.

There are two limiting cases for phonon assisted energy transfer: the first where the phonon wavelength is very large with respect to sensitizer-activator separation and the second where the phonon wavelength is much shorter than the distance between sensitizer and activator.

In the case where the phonon wavelength is greater than the distance between sensitizer and activator, the energy transfer rate is given by

$$\omega'_{sa} = [(D|\Delta E_{sa}|^3 R_{sa})/6\hbar^2] \sum_j n_p(\alpha_j/v_j^7) \qquad (1.31)$$

where ΔE_{sa} is the energy level difference between sensitizer and activator, R_{sa} is the distance between sensitizer and activator, $\hbar$ is Planck's constant, n_p is the phonon population number (n_e for emission or n_a for absorption), α_j is the angular average of the lattice strain parameter, v_j is the phonon velocity, and D is a constant term defined as

$$D = [J^2(f-g)^2]/\pi\hbar^4\rho \qquad (1.32)$$

where J is a quantum mechanical matrix element for the system independent of phonon state. The parameters f and g are coupling constants for the ground and excited states respectively (their difference is assumed to be equal for

37

sensitizer and activator), and ρ is the host lattice density.

In the case where the phonon wavelength is shorter than the distance between sensitizer and activator the energy transfer rate is given as

$$\omega_{sa}'' = D|\Delta E_{sa}| \sum n_p(\alpha_j/v_j^5) \quad . \tag{1.33}$$

In comparing the behavior described by equations (1.31) and (1.33), the important points are that for both cases the temperature dependencies are similar. However, the energy transfer rate is markedly dependent on the differences in energy levels between sensitizer and activator.

Only the most salient points of energy transfer in solids have been considered in this discussion. In depth treatments of this complex topic are given in references [46-49].

1.6.7 ENERGY MIGRATION

Energy migration is a multistep process consisting of a series of energy transfer steps from one sensitizer to another, with each step in this cascade occurring by any of the three basic energy transfer mechanisms. The resulting complex behavior effectively precludes attempts to formulate a general theoretical expression applicable to all physical cases. Models based on exciton motion [50] have been successful in explaining energy migration influenced luminescence decay kinetics found in selected cases.

In real solids, the sensitizer-sensitizer energy

migration chain may terminate by energy transfer to a trap or killer site before an activator site is encountered, as illustrated in Figure 1.5. When energy is transferred from a sensitizer to a killer site, internal processes occur that convert all transferred energy to phonons, the net result of which is a quenching of luminescence. Traps are metastable states in a lattice. They may be either a level with a very low transition probability for spontaneous emission or a defect site where an electron can be captured and remain for a significant time before recombination. The end result of energy transfer to a trap is the long lifetime luminescence that is characteristic of the trap site.

If a solid material is excited by a pulsed source such as a nitrogen laser pumped dye laser, the luminescence decay kinetics may be modeled for the two extreme cases of sensitizer-sensitizer energy migration [36,51]. The first case is that of fast diffusion among sensitizers i.e., where the probability for energy transfer between sensitizers is much greater than that for energy transfer between a sensitizer and Z, which is a trap or killer site. In this case, the emission intensity, I, may be described by the relationship [36]:

$$I = I_0 \exp(-t/\tau)\exp(-C_Z P_{SZ} t) \tag{1.34}$$

where τ is the intrinsic lifetime of the emitting species, C_Z is the concentration of species Z, P_{SZ} is the probability for the energy transfer from the sensitizer to species Z,

and t is time. The overall result is that the decay rate is an exponential function and is determined by the concentration of trapping or killer species Z.

The second limiting case is that of diffusion limited energy migration where the probability of energy transfer between sensitizers is much less that that between a sensitizer and species Z. In this case, the relatively slow sensitizer-sensitizer energy migration may proceed through the lattice along one, two, or three dimensional pathways until the migration is terminated by energy transfer to species Z. Intensity relationships for these pathways for the limiting situation where t→∞ are as follows. In a one dimensional system, the intensity relationship is [51,52] given as

$$I = I_0 exp(-t/\tau)exp[-3(\pi^2 C_z P_{ss} t/4)^{1/3}] \qquad (1.35)$$

where P_{ss} is the probability of the sensitizer-sensitizer energy transfer process. The result of energy migration by this pathway is that the decay curve is nonexponential. For energy migration by a two dimensional pathway [36]:

$$I = I_0 exp(-t/\tau)/(4\pi C_z Z^{-2} Dt) \qquad (1.36)$$

where Z is the trapping radius for species Z, and D is the diffusion constant for the excitation energy migration among the sensitizers. Here, as in the one dimension case, the decay curve is nonexponential. In most situations, the energy migration takes a random three dimensional path

through the lattice. In this case, the intensity relationship is [36,51,53] given as

$$I = I_0 \exp(-t/\tau)\exp(-11.404 C_z C^{1/4} D^{3/4} t) \qquad (1.37)$$

where C is an interaction parameter for the energy transfer from sensitizer to species Z.

Energy migration is responsible for concentration quenching effects [51,54,55] in solids. It is an important process in lanthanide doped materials due to the narrow spectral bands of the intra f orbital transitions and the relatively small perturbations induced by the host lattice. An important consequence of slow diffusion energy migration is that quenching and decay kinetics are a function of both crystal size and transfer geometry within the host lattice.

1.7 LUMINESCENCE IN ANALYTICAL CHEMISTRY

Luminescence spectroscopy is a very useful and powerful technique for chemical analysis as it is inherently a nondestructive process well suited for remote analysis. Luminescence detection is sensitive, has wide dynamic range, and is readily applied at any stage in the analytical protocol. The ultimate detection limit, the detection and identification of a single ion [56] has been achieved using luminescence spectroscopy. Nguyen et al. [57] have reported a detection limit of a single species containing the equivalent of eight Rhodamine 6G fluorophores using laser-induced fluorescence detection.

Despite these attributes, luminescence spectroscopy has

been considered [6] to be a less desirable analytical technique due to an apparent lack of specificity and a high susceptibility to quenching and enhancement interference effects. Stokes [12] noted the effects of chemical environment on luminescence from aqueous quinine solutions.

Early analytical uses of luminescence were primarily qualitative and empirical [58,59] with the principal applications being in forensic science, mineralogy, pharmaceuticals, and food analysis. One of the first published uses in quantitative analysis was by King [60] in enhancing the sensitivity of the Gutzeit test for trace arsenic. Most early analytical work was done using mercury discharge lamps as an excitation source; generally, total emission was recorded with minimal efforts to do measurements on narrow spectral regions.

In current analytical practice, luminescence based methods are applied primarily to liquid solutions of organic molecules [61-63]. Inorganic analysis by luminescence is normally done on liquid samples using luminescent organic complexes [61] and flame (plasma) atomic fluorescence [64]. The analysis of inorganic solids by luminescence spectroscopy has been limited mainly to microscopy [65] and situations where the analyte has been incorporated into a host lattice such as in the determination of trace quantities of uranium [66,67] or heavy metals [68].

Luminescence from an inorganic solid is inherently a rich source of information on electronic processes occurring

in the material. A consequence of this high information content is that single parameter luminescence measurements may have little, if any, direct relationship to a given attribute of a luminescent solid. An increase in the luminescence measurement dimensionality affords an increased utilization of information carried by the luminescence signal. The multidimensional approach has been successful in the analysis of individual components [69] present in solid mixtures of polynuclear aromatic hydrocarbons using a phosphorescence excitation-emission matrix method.

Few reports on the analysis of inorganic solids in situ by luminescence spectroscopy have appeared in the recent literature. This is likely due to a combination of the complex processes occurring in inorganic solids and the use of single parameter measurements. A multidimensional approach to measuring luminescence may yield a direct correspondence between a measured parameter and a particular attribute of the solid. The emission and absorption spectra should be characteristic of the activator and sensitizer species in the solid. The decay time behavior carries information on the environment of the sensitizers and activators, particularly energy transfer and energy migration processes occurring in the solid.

In this thesis, the multidimensional approach of time-wavelength resolved luminescence spectroscopy is examined to see if it may be applied to chemical analysis of some simple luminescent inorganic solids.

Chapter 2

EXPERIMENTAL

2.1 OVERVIEW

This chapter describes the construction and operating characteristics of the time-wavelength resolved luminescence spectrometer as well as the preparation of compounds used in this study.

2.2 SPECTROMETER

A computer controlled time-wavelength resolved luminescence spectrometer was constructed. A block diagram of the instrument is shown in Figure 2.1. The spectrometer has wavelength coverage of 250 nm to 700 nm and is capable of measuring decay lifetimes from 100 ns to 0.1 s

2.2.1 COMPUTER SYSTEM

A Corona Model PC400-HD2 computer with 10 megabyte hard disc (Corona Data Systems Inc., Thousand Oaks, CA), Roland Model CC-121 color monitor (Roland Corp US, Los Angeles, CA) and STB GRAPHIX PLUS II video board (STB Systems Inc., Richardson, TX) was used to control and acquire data from the spectrometer. Communications with and control of the spectrometer components were done through the system serial and parallel ports.

2.2.2 SOFTWARE

The instrument control and data acquisition software was written in BASIC. The program is listed in Appendix 1. The graphics software EnerGraphics Version 1.3 (Enertronics Research Inc., St. Louis MO) was used for the display of
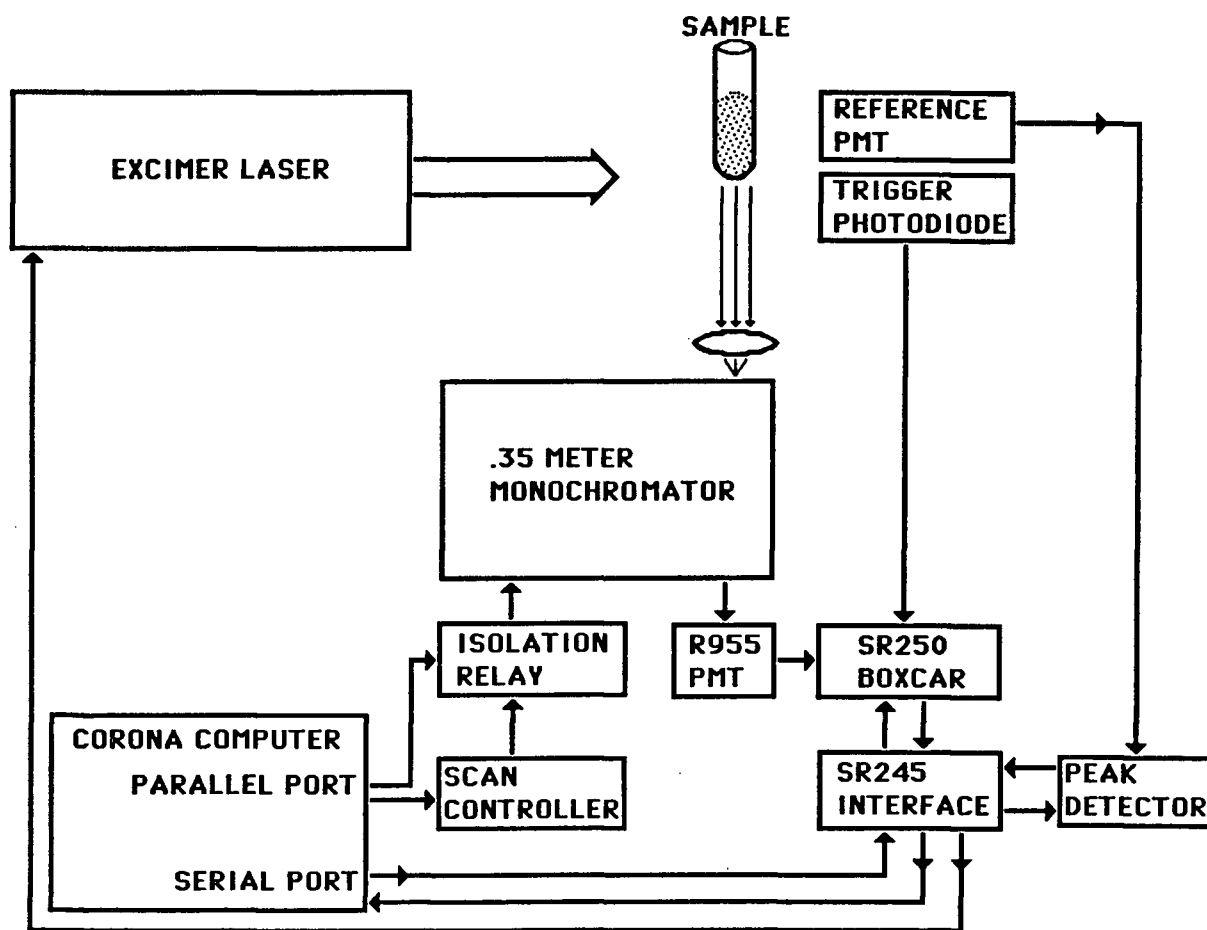
Figure 2.1   Block diagram of the time-wavelength resolved
              luminescence spectrometer.

spectra. A major limitation of EnerGraphics is that the program requires equal spacing of data on the x and y axes.

2.2.3 EXCITATION SOURCE

A Lumonics Model TE-861T-3 excimer laser (Lumonics Inc., Kanata, Ont.) with magnesium fluoride optics was used to excite sample materials. Excitation at 193 nm and 248 nm was done using ArF and KrF gas mixtures respectively. Standard operating conditions recommended by the manufacturer were used as they were found to provide the maximum fill gas lifetimes with minimal pulse to pulse variations in output beam intensity.

Laser performance was markedly dependent on the gas mixture used and recent use history [70,71]. For optimal fill gas lifetimes and uniform pulse energies, the laser had to be run several hours every day, seven days a week. Performance was reduced significantly by even a two day hiatus in operation. If the unit was idle for more than one week it would take several days and numerous gas fills to regain acceptable performance. All gases used for KrF operation were research grade. For ArF operation, prepurified grade helium was substituted for economy.

For ArF operation the pulse-to-pulse reproducibility was better than ± 3% relative standard deviation (RSD), with an initial pulse energy of approximately 100 mJ and a useful gas fill lifetime of about four hours. For KrF operation the pulse-to-pulse reproducibility was better than ± 1% RSD with an initial pulse energy of about 200 mJ and a useful

gas fill lifetime of about 15 hours. The gas fill was considered spent when pulse energy dropped to less than about 2 mJ with pulse-to-pulse reproducibility greater than ± 10% RSD.

Short and long term changes in laser output encountered during the measurement of a typical spectrum using ArF excitation are illustrated in Figure 2.2. Intensities have been normalized to the maximum pulse energy observed in a given run. Every tenth pulse is plotted. Run A was done on a fresh gas fill; run B was done toward the end of the gas fill's useful life. The data shown in Figure 2.2 were taken in this project's earlier stages before the operating parameters were optimized.

Serious problems were encountered in initial attempts to use ArF. Laser operation was unstable with high voltage arcing and spurious radio frequency emissions strong enough to lock up both the computer system and interface module, as well as raising havoc with other experiments being carried out in the laboratory. Stable laser operation with ArF was achieved only after modifying the thyratron circuit by adding component RV4, a V420PA40A varistor as shown in Figure 2.3.

2.2.4 LASER PULSE ENERGY MONITOR

Laser pulse energy was monitored with a photomultiplier tube (PMT) and a peak detector circuit. The reference PMT housing is shown in Figure 2.4. The detector used was a 1P28 PMT with base wired for fast response [72,73] and

47
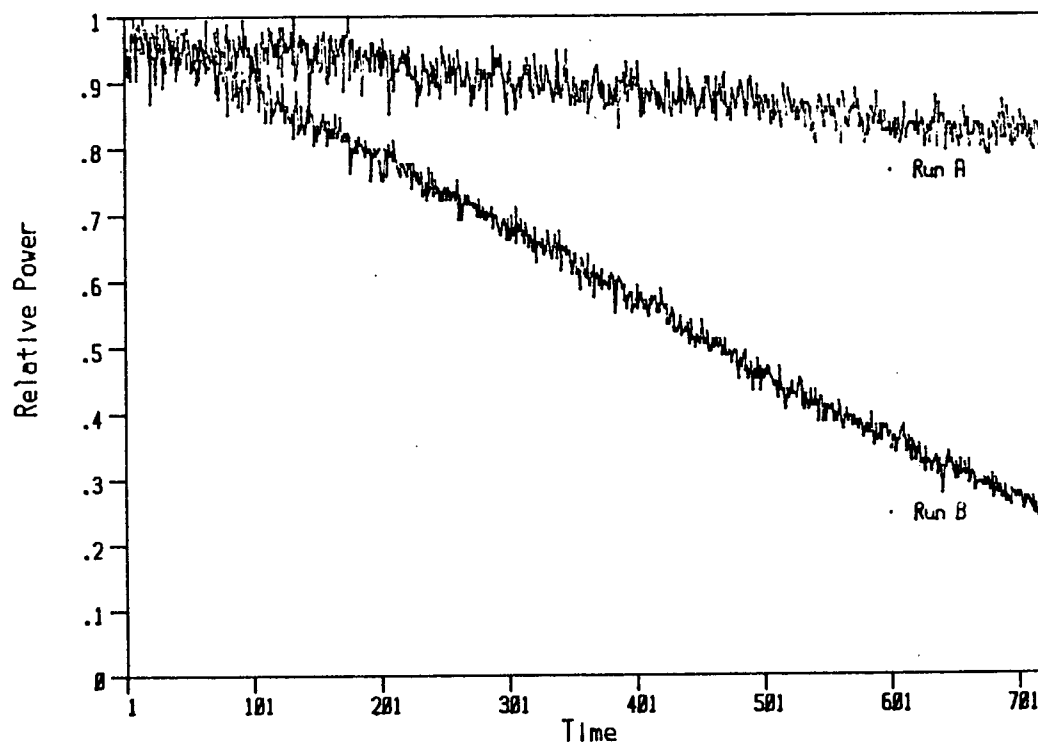
Figure 2.2   Excimer laser power output fluctuations, time
              scale is shot number ÷ 10; at 3 Hz: (A) fresh
              fill gas, (B) same fill gas three hours later.

Figure 2.3   Modification to laser thyratron circuit.

49
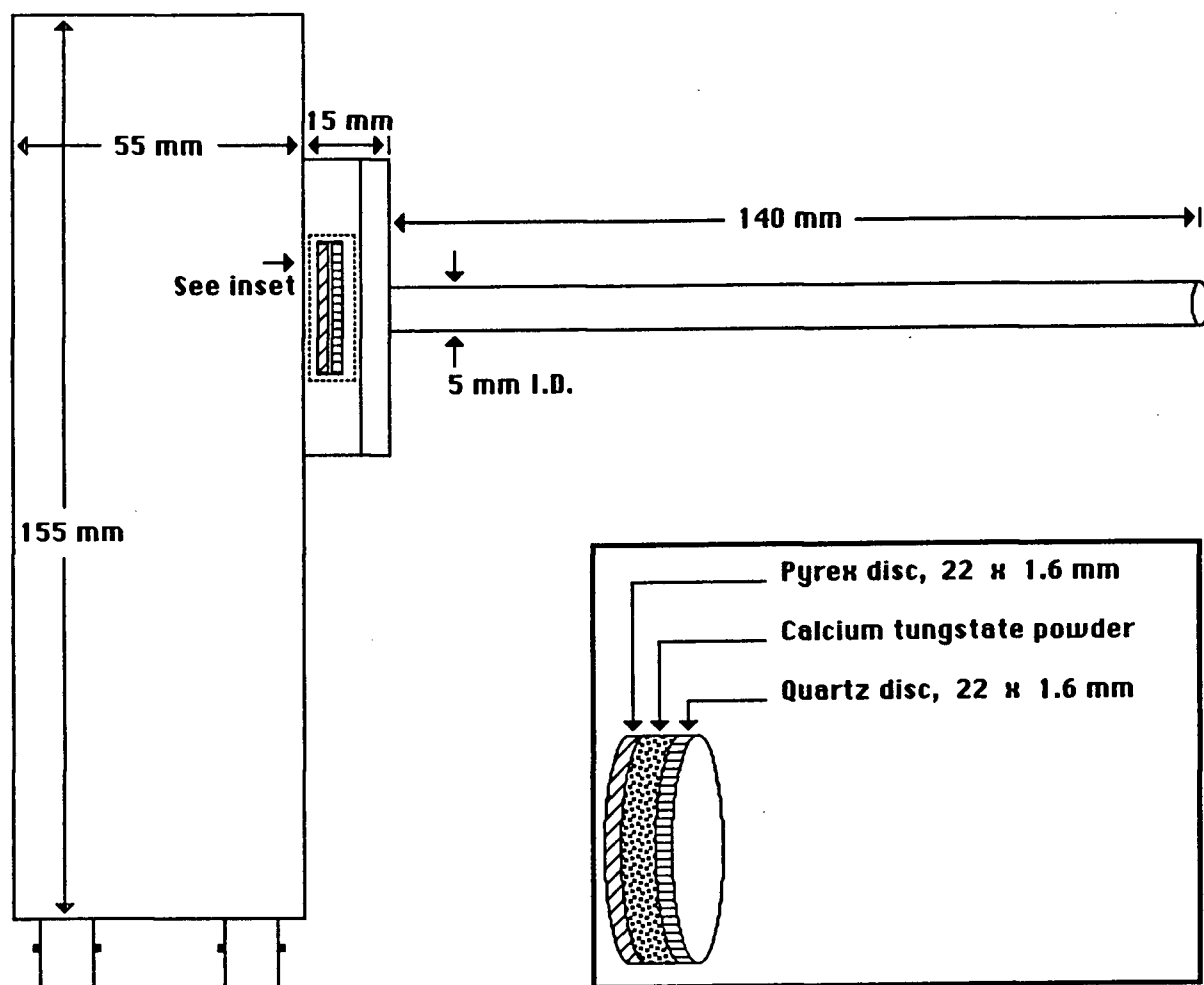
Figure 2.4   Reference PMT housing.

terminated with a 50 Ω load. A Kepco Model ABC 1500M high voltage power supply (Kepco Inc., Flushing, NY) was used for the PMT. The screen consists of a thin layer of calcium tungstate powder sandwiched between quartz and pyrex discs. The screen serves three functions: 1) it effectively blocks out ambient room light, 2) it converts laser UV radiation to visible, and 3) it protects the PMT from direct exposure to laser radiation.

The peak detector circuit used is shown in Figure 2.5. The circuit is built around a Burr-Brown 4085KG peak detector module (Burr-Brown Corp., Tucson, AZ) with external buffer amplifiers and logic gates to protect the module and provide additional signal control.

2.2.5 SAMPLE HOLDERS

Two types of sample holders were used for powder specimens. In initial work, sample powders were held in 50 mm long test tubes made from 7 mm outer diameter by 1 mm wall quartz tubing. The test tubes gave off significant luminescence in the UV and visible regions. Despite the fact that all test tubes were fabricated from the same lot of tubing, the time-wavelength resolved luminescence spectra of the test tubes was not uniform and their use was abandoned. In later work, sample powders were sandwiched between two 22 mm diameter by 1.6 mm thick suprasil discs (Amersil Inc., Hillside, NJ). The suprasil discs exhibited faint luminescence, with uniform time-wavelength resolved spectra for the different discs used.

Figure 2.5   Peak detector circuit diagram.

52
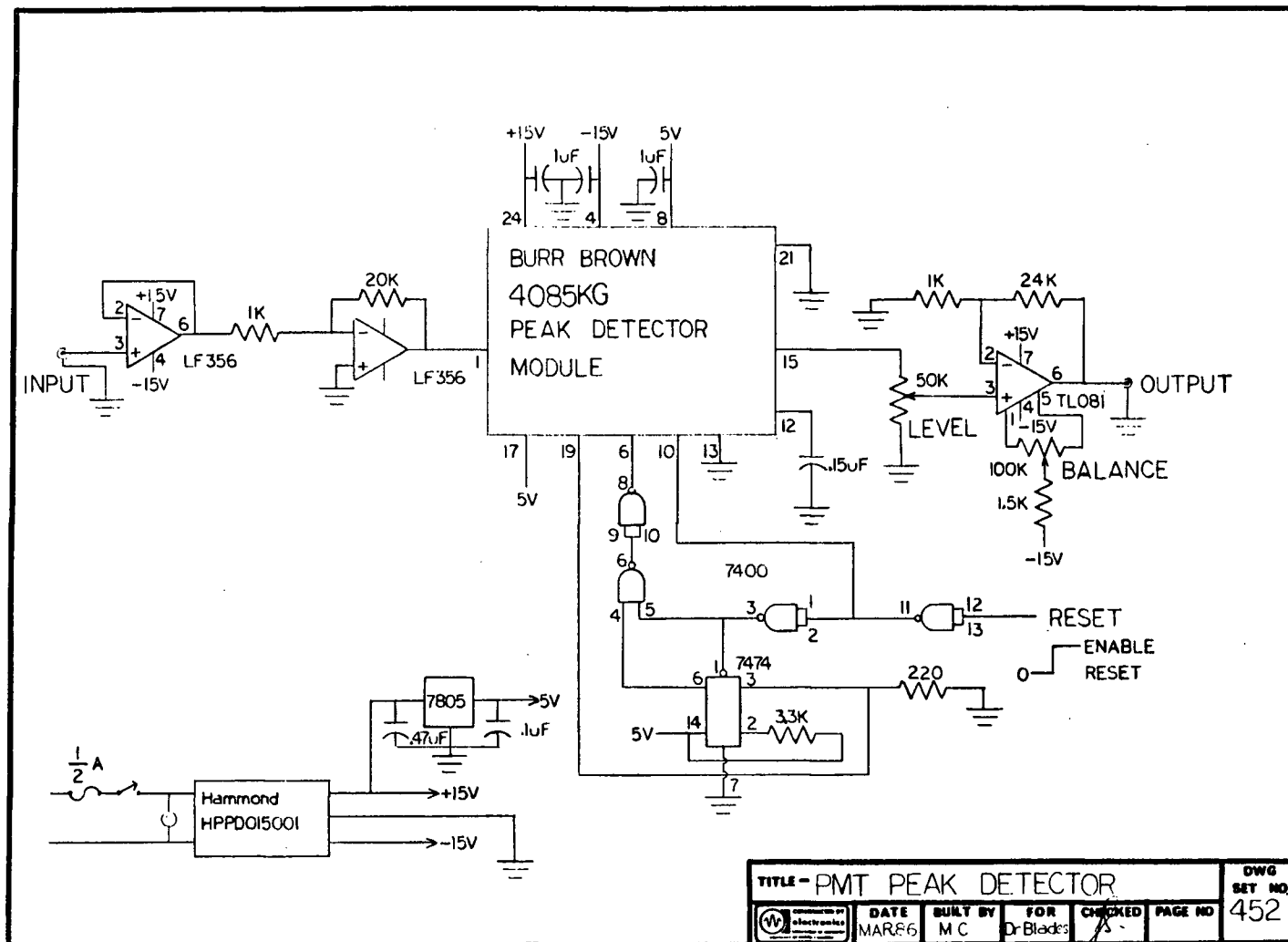
2.2.6 SPECTROMETER OPTICS

The spectrometer optical arrangement is shown in Figure 2.6. The sample holder and quartz collection lenses were mounted on an optical rail. The optical rail and monochromator were mounted on an aluminum plate for alignment stability. A UV cutoff filter consisting of a 1 cm quartz cell filled with either methanol or carbon tetrachloride was placed in front of the monochromator entrance slits to prevent scattered laser radiation entering the monochromator. In early work a pyrex disc was used for a cutoff filter. However, this disc was found to luminesce intensely from scattered laser radiation and its use was discontinued.

A GCA/McPherson Model 270 monochromator with a Model 700-51 scan controller (McPherson Division, S.I. Corp., Acton, MA) along with a 1200 line/mm holographic diffraction grating having peak efficiency at 500 nm were used.

2.2.7 WAVELENGTH SCANNING

The Model 700-51 scan controller was highly susceptible to electromagnetic interference (EMI) from the excimer laser as well as other laboratory noise sources. To eliminate spurious changes in wavelength and scan direction caused by EMI, all electrical lines between the scan controller and monochromator were connected by an isolation relay only when scanning wavelength. The isolation relay was controlled by toggling a line on the Corona parallel printer port.

Wavelength scanning was accomplished by connecting a second line on the Corona parallel port to the external
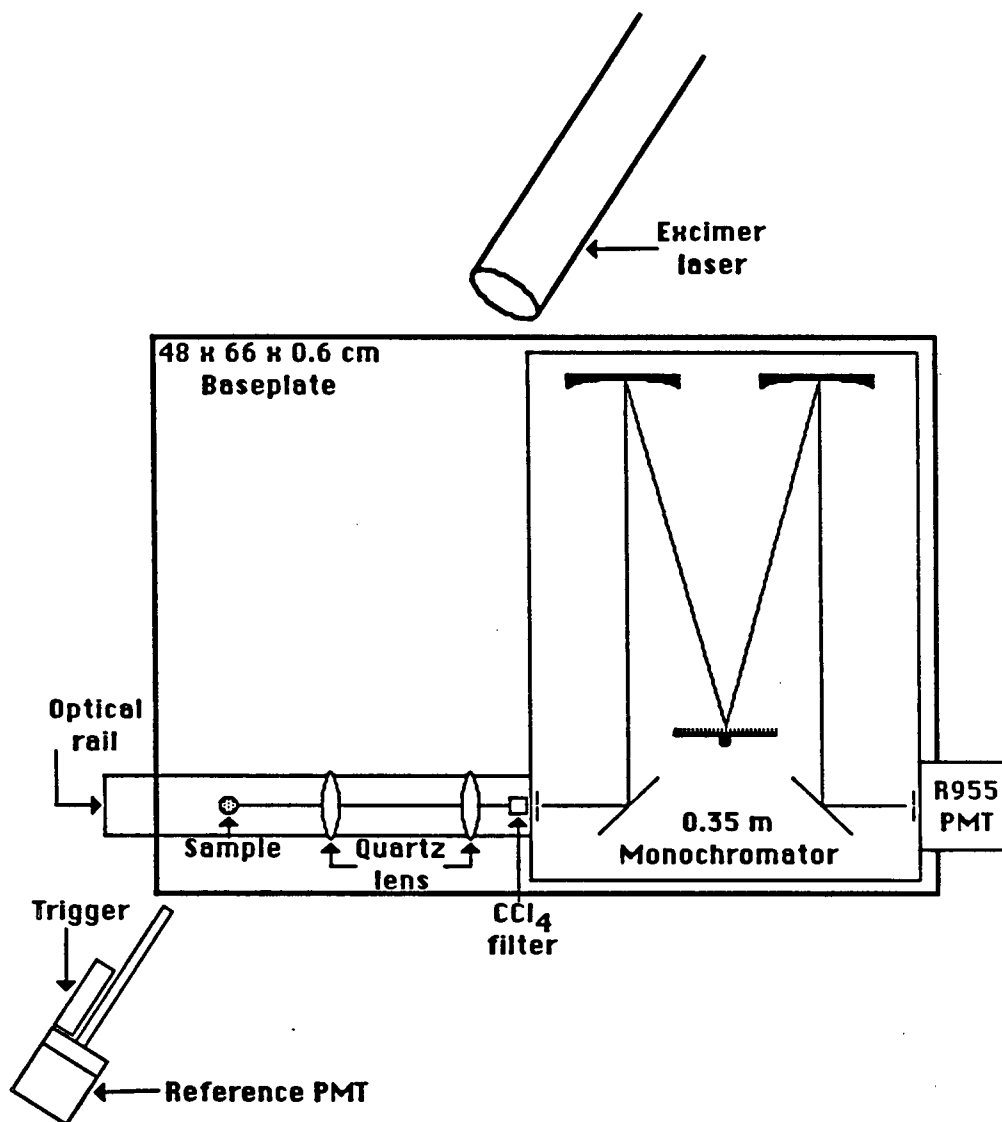
Figure 2.6   Spectrometer optical diagram.

oscillator input of the Model 700-51 scan controller. The machine language routine listed in Appendix 2 was used to toggle the parallel port line at about 600 Hz for an appropriate number of pulses to scan from one wavelength to another.

2.2.8 DETECTOR

Sample luminescence was detected with a Hamamatsu R955 PMT (Hamamatsu Corp., Bridgewater, NJ) mounted in a McPherson Model EU-701-93 PMT housing. The PMT socket was wired for fast response using the base circuit described by Harris [72], and a 50 Ω load resistor was used for termination. High voltage power supplies used were a Fluke Model 413C (John Fluke Mfg. Co. Inc., Seattle, WA) and a Cintel Type 1892 (Cinema-Television Ltd., London, England).

2.2.9 SIGNAL ACQUISITION

A Stanford Research Systems Model SR245 computer interface and a Model SR250 gated integrator and boxcar averager (Stanford Research Systems Inc., Palo Alto, CA) were used to acquire intensity data from the reference and signal sources. The Model SR245 interface was also used to fire the excimer laser. Communications between the Corona and Model SR245 interface were by the system serial port.

The Model SR250 gated integrator was triggered with an EG&G SGD-040D photodiode mounted near the sample holder and reference PMT. The photodiode was illuminated indirectly by the excimer laser. A screen consisting of a pyrex disc coated with a smear of Apiezon Type L vacuum grease (Apiezon

Products Ltd., London, England) was placed in front of the photodiode to convert the UV laser radiation to visible. The photodiode trigger housing and circuit is shown in Figure 2.7. An all metal housing was used to shield against the intense EMI exiting from the laser snout.

2.2.10 SPECTRAL RESPONSE CORRECTION

All reported spectra have been corrected for system spectral response. The system spectral response was determined with an Electro Optics Associates Model L-10 quartz lamp and Model P-101 power supply (Electro Optics Associates, Palo Alto, CA) using the method of Stair [74]. Spectral response correction factors were applied to raw data files created by the instrument control and data acquisition program listed in Appendix 1 with the BASIC program listed in Appendix 3. Correction factors used for the other UV cutoff filters are also listed in Appendix 3. Spectra were not corrected for higher order diffraction.

2.2.11 CABLING

The serial port cable between the Corona and the Model SR245 interface had two external metal braid shields connected to all metal shielded connector sockets and plugs. The cable between the Corona parallel printer port and isolation relay and Model 700-51 scan controller also had two external metal braid shields connected to all metal sockets and plugs. 50 Ω triax cable (Belden 9222) with BNC connectors was used for the signal line between the R955 PMT and the Model SR250 gated integrator as well as for the connection

Battery container

Brass tubing, black interior

40 Mesh copper screen

Apiezon "L" gease coated
pyrex disc, 22 x 1.6 mm

EG & G SGD-040D photodiode

Trigger output BNC connector

EG & G
SGD-040D

TRIGGER
OUT

A

C

G

1 MEG

9 V

+
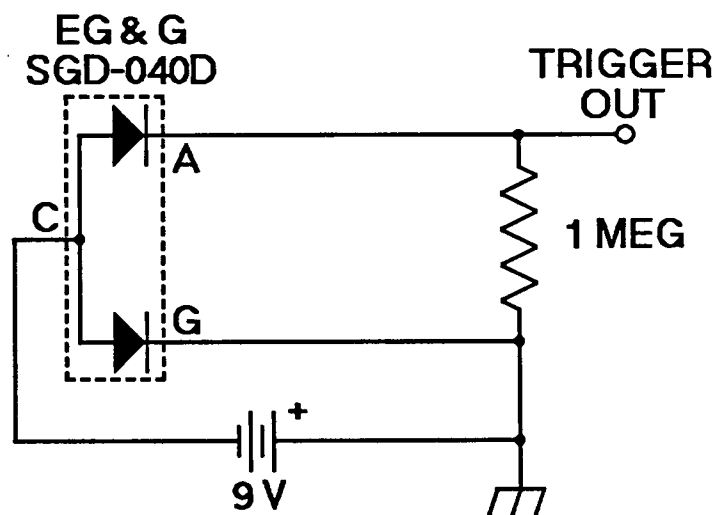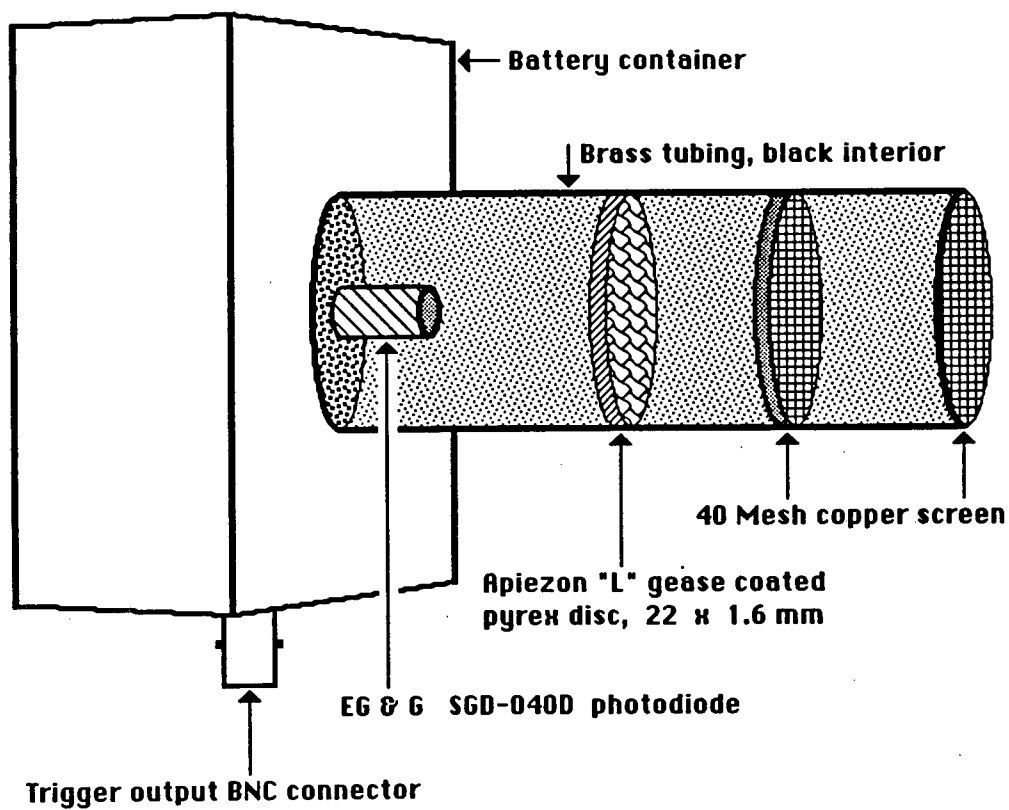
Figure 2.7   Photodiode trigger housing and circuit diagram.

between the excimer laser and the Model SR245 interface. All other control and signal lines were 50 Ω coaxial cable (Amphenol 03554) with BNC connectors. All instrument components were connected to a common single-point ground.

2.2.12 ELECTRICAL POWER

Serious problems were encountered with electrical power distribution lines in the building. The problem first became apparent by a rapidly shrinking and expanding display on the computer monitor. Significant short and long term fluctuations in power line voltage were a daily occurrence and adversely affected measurements. A simple monitor consisting of a stepdown transformer and bridge rectifier connected to a laboratory chart recorder was used to follow line voltage fluctuations. Typical line voltage swings encountered are illustrated in Figure 2.8.

This problem was alleviated by having a new supply circuit installed for laser use only and using constant voltage supply devices for other instrument components. A Sola Model 20-25-220E829 constant voltage transformer (Sola Electric Company, Chicago, IL) was used to supply the computer, and Model 700-51 scan controller. An RTE DELTEC Model MPC 1560 120/120 (RTE DELTEC, San Diego, CA) line conditioner was used to power the PMT power supplies, peak detector, Model SR245 interface and Model SR250 gated integrator.

2.2.13 ELECTROMAGNETIC INTERFERENCE

Electromagnetic interference (EMI) was a source of
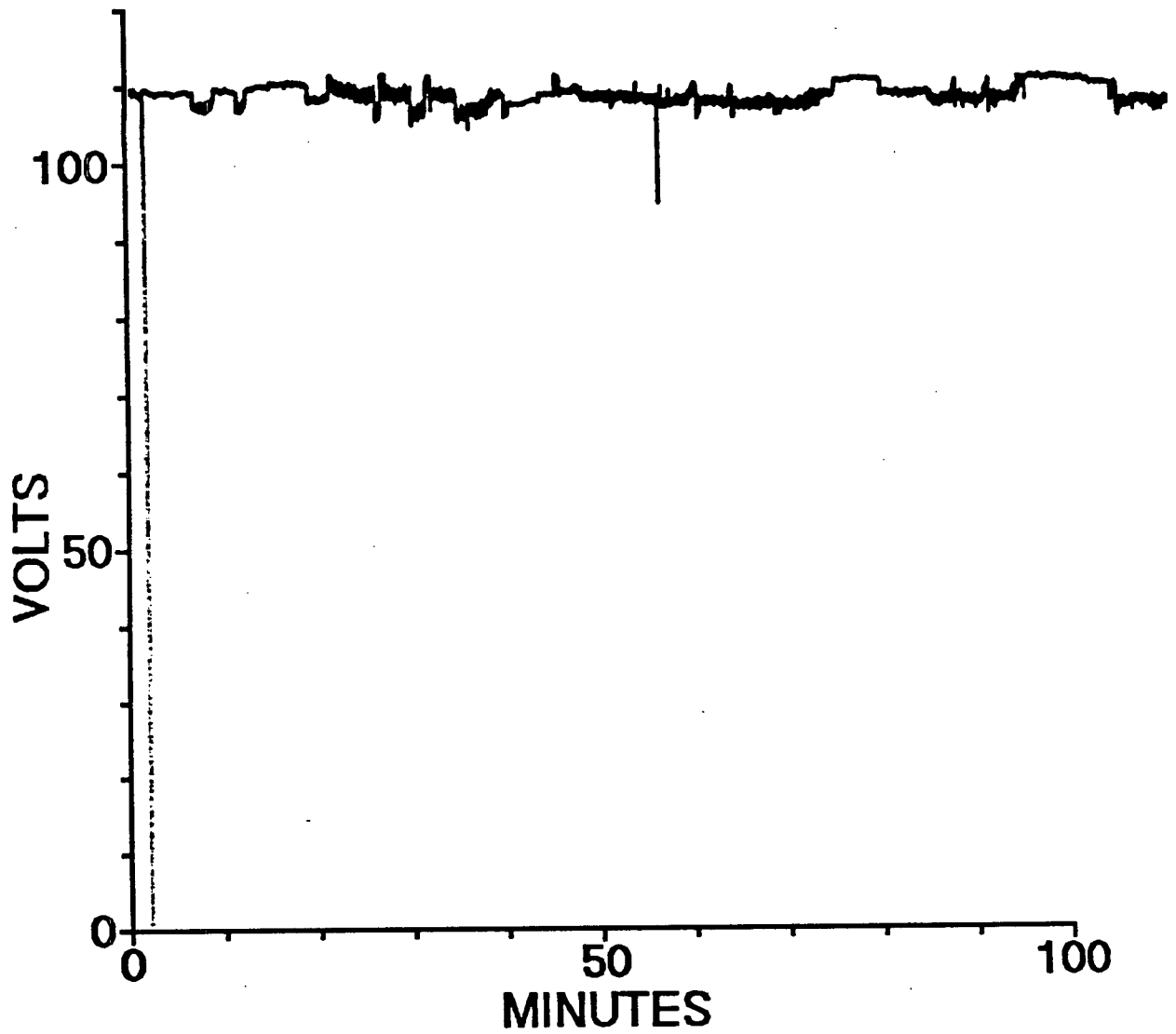
Figure 2.8   Power line voltage fluctuations.

considerable difficulty and frustration in attempts to take reliable measurements. Despite using many standard [75-77] techniques to alleviate this problem, EMI was the limiting factor in obtaining credible lifetime measurements. Some of the practical consequences of EMI encountered were digital equipment lockup, anomalous triggering, corrupted data files, signal noise, and insidious equipment malfunctions.

Some of the EMI sources encountered were microwave discharges, Tesla coils, warning sign flasher, the excimer laser, and several sources of unknown origin that were external to the laboratory. The combination of transient EMI phenomena with several independently acting EMI sources consumed an inordinate amount of time and effort in attempts to obtain reliable data.

The EMI from all laboratory sources other than the excimer laser and Tesla coil was successfully controlled by a combination of robust shielding and single-point grounding [75] of all instrument components. The Corona computer would lock up whenever a Tesla coil was used in an adjoining laboratory, the EMI apparently entering the computer through its keyboard. An effective EMI shield was impractical and Tesla coil use was brief and infrequent, so the instrument was not run whenever an energized Tesla coil was nearby.

The excimer laser was an intractable, vexing source of EMI. The beam snout and power cord were the points of EMI emission from the excimer laser, all other leaking areas having been sealed with RF gasket or low pass filters.

Effective emission reduction from the snout and power cord was impractical since it would have involved major modifications to the excimer laser without guaranteed success. Power line introduction of EMI to the instrument components was eliminated by use of a power line conditioner. Radiated EMI was particularly troublesome since its severity at any given point in space was altered by the presence of nearby objects.

The waveforms in Figure 2.9 were taken with a Tektronix Model 2430A digital storage oscilloscope (Tektronix, Beaverton, OR) and illustrate the magnitude of the EMI problem. The signals shown are an average of 256 waveforms captured from the 1P28 reference PMT for two different lengths of cable between the reference PMT output terminal and oscilloscope input terminal. Oscilloscope triggering was done by the signal from the 1P28 reference PMT. The sharp rise at point T and the gradual decay in region F is due to light emitted by the the calcium tungstate screen on excitation at 193 nm from the excimer laser. The fluctuations in regions P are spurious signals caused by EMI from the excimer laser that are emitted immediately prior to the actual laser pulse. The fluctuations in regions F are also due to EMI from the excimer laser. The principal period of the fluctuations is about 9 ns, regardless of signal cable length; this is also the nominal laser pulse width when using an ArF fill gas. Earlier attempts to characterize excimer laser EMI failed because the oscilloscopes available

61

SINGLE LENGTH CABLE

DOUBLE CABLE LENGTH
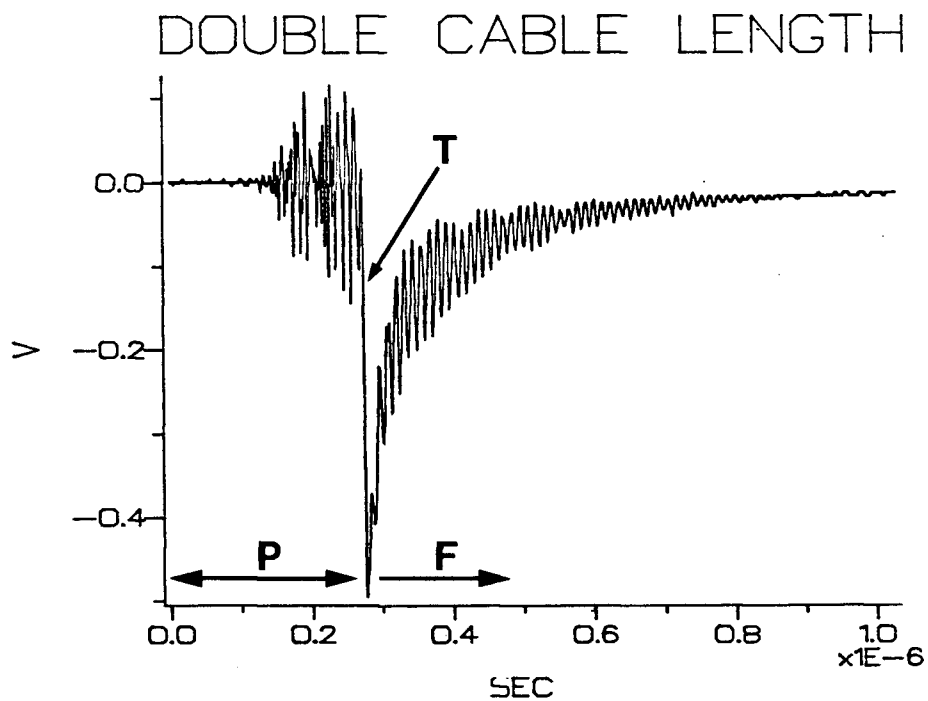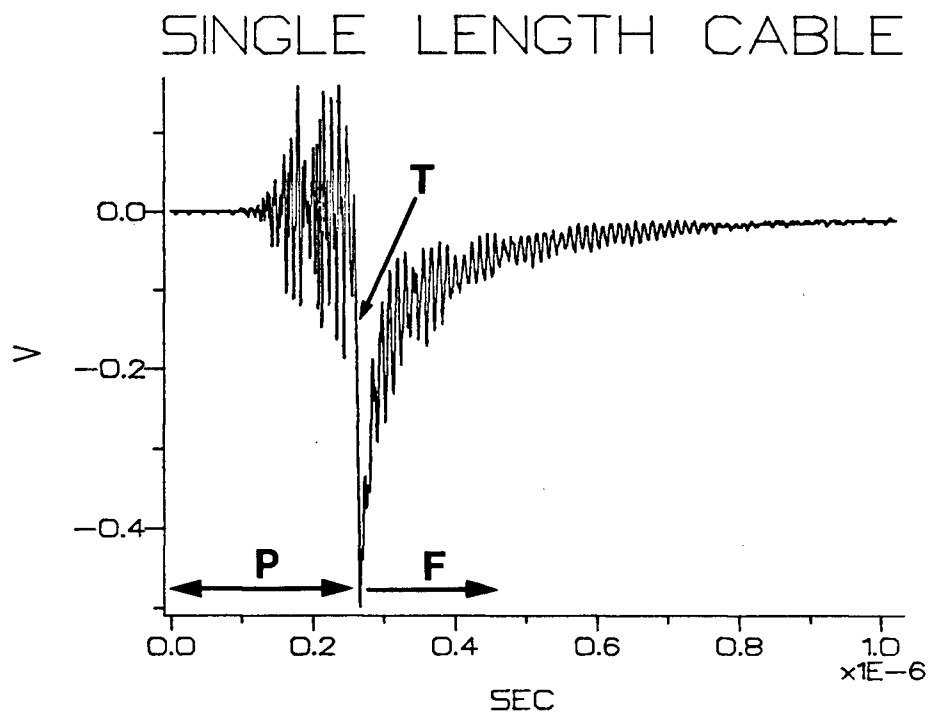
Figure 2.9   EMI from excimer laser; region P - before laser pulse, region T - during pulse, region F - after laser pulse: (A) 1.0 m signal cable length, (B) 2.0 m signal cable length.

were subject to spurious triggering caused by EMI emitted prior to the actual laser pulse.

Consequently, credible data may only be collected when there is at least a 100 ns delay from the time the laser pulse arrives to the sample gate opening on the Model 250 gated integrator. Thus, the spectrometer is effectively limited to studies on species having luminescence lifetimes greater than about 100 ns.

2.3 COMPOUND PREPARATION

The compounds examined in this study were mixed oxide inorganic insulators in powder form. All compounds were prepared by precipitation from aqueous solution. The compounds prepared were pulverized in an agate mortar and pestle prior to storage in glass vials. Deionized water of ionic purity better than 10 MΩ-cm was used in all procedures. Reagents used are listed in Table I.

Care was taken in all stages to minimize contamination. All glassware used was cleaned by soaking in 4 M HNO_3, washing with a 1% Extran® (BDH Chemicals, Toronto, Ont.) solution, a final rinse with deionized water followed by oven drying. Platinum crucibles were cleaned by soaking in 4 M HNO_3 overnight [78], followed by ultrasonic agitation in a 50% Extran solution, deionized water final rinse and oven drying. Operations were carried out in covered vessels wherever possible.

2.3.1 MOLYBDATES AND TUNGSTATES

Alkaline earth and heavy metal tungstates were prepared

Table I

REAGENTS

Compound	Grade	Source[1]	Catalog No.
$Ba(NO_3)_2$	ACS	MCB	BX 100
Bi	TMI 2	Spex	BI 03-20
$CaCO_3$	ACS	BDH	ACS 174
$CdCl_2 \cdot 2\frac{1}{2}H_2O$	ACS	Fisher	72065
HCl, Conc.	ACS	BDH	ACS 393-41
$HfOCl_2 \cdot 8H_2O$	Gold Label	Aldrich	22,965-2
HNO_3, Conc.	ACS	BDH	ACS 579-43
Methanol	Pesticide	BDH	B90234
MgO	ACS	MCB	MX 65
$Na_2MoO_4 \cdot 2H_2O$	ACS	BDH	ACS 822
$Na_2WO_4 \cdot 2H_2O$	ACS	BDH	ACS 873
Oxalic acid	ACS	BDH	ACS 594
PbO	TMI 10	Spex	PB 75-10
Sb	TMI 2	Spex	SB 03-5
$SrCl_2 \cdot 6H_2O$	ACS	BDH	ACS 882
$TlNO_3$	Analar	BDH	B042310
Zn	Reagent	Fisher	Z-11
$ZrOCl_2 \cdot 8H_2O$	Gold Label	Aldrich	20,502-8

1) Source:

    Matheson, Coleman & Bell, Norwood, OH

    Spex Industries, Inc., Edison, NJ

    BDH Chemicals Ltd., Toronto, Ont.

    Fisher Scientific Co., Pittsburgh. PA

    Aldrich Chemical Co., Inc., Milwaukee, WI

as follows [79,80]:

Ten ml of 1.00M alkaline earth or heavy metal chloride solution was added to a 125 ml Erlenmeyer flask containing 0.010 moles of $Na_2WO_4 \cdot 2H_2O$ dissolved in approximately 25 ml water. The slurry was warmed to approximately 90 °C for about two hours with periodic agitation, and then allowed to sit overnight at room temperature [81]. The supernatant liquid was decanted off and precipitates were washed three times by adding about 25 ml water, warming for about one hour at about 90 °C with periodic agitation, allowing to settle out overnight at room temperature and then decanting off the supernatant liquid. The washed precipitates were then dried by filtering off excess water by vacuum filtration using Whatman No. 52 filter paper, then drying at 110 °C. The dried compounds were then annealed [82] in covered platinum crucibles at 800 °C for 4 h in a muffle furnace.

The corresponding molybdates [83] as well as the mixed crystal series $Ca(Mo_x W_y)O_4$, $Sr(Mo_x W_y)O_4$, $(Ca_x Sr_y)MoO_4$ and $(Ca_x Sr_y)WO_4$, where $x+y = 1$, were prepared in an analogous manner. The zinc, cadmium and lead precipitates were gelatinous and took several days to settle out. Yields were better than 98% for the alkaline earth compounds and exceeded 80% for the heavy metal salts.

2.3.2 ZIRCONATES AND HAFNATES

Alkaline earth zirconates and hafnates were prepared via oxalate intermediates [84-87] in the following manner:

65

One ml of 1.00 M alkaline earth chloride (5.00 ml of 0.2 M $BaNO_3$) was added to a 125 ml Erlenmeyer flask containing 0.0010 moles of zirconyl (or hafnyl) chloride dissolved in about 5 ml water, The solution was warmed to about 80 °C and 2.5 ml of hot 1.0 M oxalic acid was added. The solution was warmed to near boiling for 30 minutes and periodically agitated [88]. The solution was allowed to settle overnight at room temperature. The solution was then cooled in an ice bath and supernatant liquid decanted off. The precipitate was then washed three times with cold water [89] in an ice bath and transferred as a slurry to a covered platinum crucible. On settling, the supernatant liquid was decanted off, the precipitate was dried at 110 °C, and then ignited in a muffle furnace for 4 h at 900 °C.

Doped zirconates and hafnates were prepared in an analogous manner with 1.00 ml of 0.001 M dopant solution (Bi, Pb, Tl in 0.1 M HNO_3, Sb in 0.1 M HCl) added prior to addition of the alkaline earth solution. Yields for all alkaline earth zirconates and hafnates prepared exceeded 90%.

2.4 COMPOUND ANALYSIS

Representative samples of the compounds prepared were analyzed by x-ray powder diffraction [90]. The instrument used was a Philips Model PW1008/85 X-ray powder diffracto-meter with Model PW1024/10 powder camera, Model PW1033 motor driver and Model PW1012/20 camera mount and filter holder (Philips Electronic Instruments, Mahwah, NJ). The X-ray

source used was a copper target X-ray tube run at 38 kV, 25 mA with a nickel filter. Powder samples were held in 0.3 mm capillary tubes; exposure was 4 h using Kodak type DEF-392 direct exposure film.

For each sample, the calculated d values and their associated visually estimated peak intensities were compared against values listed in the ASTM X-ray powder data file. Results are tabulated in Table II. The X-ray powder data is in good agreement with literature data for the compounds examined and also shows that contamination from simple metal oxides is not present in appreciable quantities.

Selected samples were analyzed by neutron activation to confirm their elemental composition and check for the presence of impurities. The analyses were done by Novatrack at the TRIUMF facility on the University of British Columbia campus. Results are listed in Table III. Approximately 100 mg samples were used for the molybdate and tungstate salts.

Table II

X-ray Power Diffraction Data for Alkaline Earth Zirconates and Hafnates

$CaZrO_3$		$SrZrO_3$		$BaZrO_3$	
d, Å	100 I/I_{max}	d, Å	100 I/I_{max}	d, Å	100 I/I_{max}
2.408	1	2.600	<1	1.792	1
2.002	20	2.368	<1	1.704	60
1.816	40	2.049	30	1.610	<1
1.792	2	1.983	<1	1.526	2
1.650	5	1.674	50	1.479	20
1.621	10	1.450	10	1.322	20
1.547	10	1.296	10	1.274	1
1.480	<1	1.183	2	1.247	2
1.441	<1			1.209	10
1.416	5				
1.283	1				
1.266	1				
1.199	<1				
1.176	2				
1.148	2				

Table II (contd.)

X-ray Power Diffraction Data for Alkaline Earth Zirconates and Hafnates

CaHfO$_3$		SrHfO$_3$		BaHfO$_3$	
d, Å	100 I/I$_{max}$	d, Å	100 I/I$_{max}$	d, Å	100 I/I$_{max}$
3.969	100	4.599	<1	2.931	100
2.936	50	4.623	10	2.078	30
2.849	10	4.745	2	1.799	<1
2.814	100	2.880	100	1.698	80
2.780	10	2.560	1	1.471	10
2.550	5	2.173	1	1.316	20
2.405	1	2.040	40	1.203	5
2.330	<1	1.822	10		
2.279	<1	1.667	60		
1.994	80	1.541	2		
1.807	20	1.444	20		
1.784	20	1.361	5		
1.642	30	1.292	30		
1.616	30	1.179	5		
1.540	10	3.507	2		
1.477	<1				
1.413	5				
1.338	<1				
1.262	10				

TABLE III

Expected and Measured Composition of Molybdate and Tungstate Salts Prepared

Compound	Ca, %	Sr, %	Mo, %	W, %
$Sr(Mo_{.02}W_{.98})O_4$		26.26* (24.5)	0.575 (<0.5)	53.99 (50.5)
$Sr(Mo_{.05}W_{.95})O_4$		26.45 (27.8)	1.449 (2.3)	52.76 (50.2)
$Sr(Mo_{.10}W_{.90})O_4$		26.82 (19.5)	2.937 (3.8)	50.65 (45.2)
$Sr(Mo_{.15}W_{.85})O_4$		27.19 (21.7)	4.465 (5.8)	48.49 (45.6)
$Sr(Mo_{.20}W_{.80})O_4$		27.56 (24.7)	6.036 (7.0)	46.27 (41.5)
$Sr(Mo_{.25}W_{.75})O_4$		27.95 (24.7)	7.651 (7.4)	43.99 (43.0)
$Sr(Mo_{.30}W_{.70})O_4$		28.35 (28.9)	9.312 (9.5)	41.64 (40.0)
$Ca(Mo_{.01}W_{.99})O_4$	13.96 (14.9)		0.334 (<.05)	63.41 (60.1)
$Ca(Mo_{.02}W_{.98})O_4$	14.01 (15.2)		0.671 (<0.9)	62.96 (60.6)
$Ca(Mo_{.05}W_{.95})O_4$	14.14 (10.7)		1.692 (2.9)	61.60 (52.3)
$Ca(Mo_{.10}W_{.90})O_4$	14.36 (14.8)		3.437 (3.8)	59.23 (55.2)
$Ca(Mo_{.15}W_{.85})O_4$	14.59 (16.0)		5.238 (6.0)	56.88 (53.9)
$Ca(Mo_{.20}W_{.80})O_4$	14.83 (16.8)		7.098 (8.7)	54.40 (53.5)
$Ca(Mo_{.25}W_{.75})O_4$	15.07 (15.9)		9.019 (9.5)	51.85 (51.8)
$Ca(Mo_{.30}W_{.70})O_4$	15.23 (15.6)		11.004 (12.8)	49.20 (48.7)

* Values measured by neutron activation in parentheses, all values are expressed in percent by weight.

Chapter 3

DATA REDUCTION

3.1 OVERVIEW

In this chapter the data reduction technique used for extracting useful information from a time-wavelength resolved luminescence spectrum is described and the algorithm's performance is evaluated.

3.2 SYSTEM MODEL

In an inorganic solid, the configuration coordinate model discussed in section 1.6.5 generally gives a good description of the emission and absorption spectra associated with a localized excitation. To a first approximation, the emission band shape is Gaussian and can be described by a function which inclues the parameters of peak maxima, peak width, and an intensity factor:

$$S_\nu = K_a \exp((m-\nu)^2/(cw^2)) \tag{3.1}$$

where ν is frequency (cm^{-1}), K_a is a constant proportional to the quantity of emitter, m is the peak maxima (cm^{-1}), w is the peak halfwidth (cm^{-1}), S_ν is the observed luminescence intensity at frequency ν, and c is a constant relating halfwidth to standard deviation. In many simple systems the skewness and kurtosis terms [40,91] are insignificant.

In simple systems where energy migration processes are negligible, luminescence decay proceeds by first-order kinetics as discussed in section 1.3.1. The instantaneous luminescence intensity observed at a time t following pulsed

excitation is given by the relationship:

$$T_t = K_b \exp(-t/\tau) \tag{3.2}$$

where T_t is the observed luminescence intensity at time, t, after the excitation pulse, K_b is a constant proportional to the quantity of emitter, τ is the intrinsic lifetime of the emitting species. When luminescence intensity is measured with a gated integrator having a time window width of Δt:

$$T_t = K_b \int_t^{t+\Delta t} \exp(-t/\tau)\, dt \tag{3.3}$$

after integrating (3.3) and collecting terms, the measured intensity is given by the relationship:

$$T_t = K_b \tau [\exp(-t/\tau) - \exp(-(t+\Delta t)/\tau)] \tag{3.4}$$

By combining (3.1) and (3.4), the time-wavelength resolved luminescence spectrum may be expressed in matrix form as:

$$[D] = [S][T] \tag{3.5}$$

where [D] is a i x j data matrix of luminescence intensities for i wavelengths and j times, [S] is a i x 1 concentration term and spectrum vector, [T] is a 1 x j normalized time behavior vector. The ith and jth values for the [S] and [T] vectors are given by the relationships:

$$S_i = C \exp((m-\nu_i)^2/(cw^2)) \tag{3.6}$$

$$T_j = \tau \left[\exp(-t_j/\tau) - \exp(-(t_j+\Delta t)/\tau) \right] \qquad (3.7)$$

where S_i is the spectral response value at frequency ν_i, C is a constant term proportional to the quantity of emitter, and T_j is the normalized intensity value at gate opening time t_j for a gate width Δt.

In the situation where several emitting species are present, the observed luminescence is a function of all species present and any interactions that may take place between them and concomitants in the lattice. If each species acts independently and the observed luminescence is a linear combination of the emission from each species present, then for the case where n species are present, the i x 1 [S] (3.6) and the 1 x j [T] (3.7) vectors may be replaced by i x n and n x j matrices respectively in (3.5).

The system model (3.5) describes the time-wavelength resolved spectrum from any given component in terms of four parameters: peak maxima, peak width, intensity factor, and lifetime. Thus, in principle, the spectrum from a material containing n emitting components may be described with 4n parameters.

3.3 OPTIMIZATION AND PARAMETER ESTIMATION

The system model is a non linear function of the parameters on both the time and wavelength domains, it cannot be linearized for a system containing two or more components. Solving the matrix equation (3.5) and computing the parameter values from experimental data was attempted by using

optimization techniques to arrive at a minimum error value between experimental data and a spectrum computed from estimated parameter values. Two optimization methods were attempted to find parameter values: simplex optimization and the extended Kalman filter.

3.3.1 SIMPLEX OPTIMIZATION

A simplex [92] is a geometric figure that has one more vertex than the dimensions of the space in which it is defined; it includes all interconnecting line segments and polygonal faces. For example, it is a triangle in two dimensions and is a tetrahedral figure in three dimensional space. In simplex optimization, each vertex of the simplex is assigned to an attribute of the system under study that is to be minimized. The optimization procedure is a collection of rules for tumbling the simplex through parameter space in order to achieve the minimization of the attribute in question.

The simplex algorithm originally formulated by Spendley et al. [93] has been modified by numerous investigators [94-98] to accelerate convergence or avoid trapping in local minima. The simplex algorithm used in this study is the modification of Nelder and Mead [99]. The implementation follows that described by Daniels [100]. This version is one of the simplest implementations, yet it is robust [92,100,101] with slow convergence being its only serious drawback. The procedure for a two parameter system is as follows:

(1) Create a three point simplex by guessing three different values for each parameter, evaluate the function (or carry out the process) and plot the responses as in Figure 3.1. The three response values are: low point (LP), high point (HP) and next highest point (NHP).

(2) Calculate the centroid, CN, (in a two parameter system it lies midway between the LP and NHP); then carry out a reflection operation by extending a line from HP through CN. The distance between HP and CN is x, the reflected point, R, lies along the line at a distance ax from CN as illustrated in Figure 3.1. The constant, a, is called the reflection coefficient and is slightly less than 1 to avoid oscillation problems. A new response value for the system at point R is obtained by evaluating the function (or carrying out the process) for the parameters at that point.

(3) If the reflection operation is moderately successful, where the response values are: LP≤R<HP, then a new simplex is formed by replacing HP with R, and carrying out the reflection operation again in step (2).

(4) If the reflection operation is very successful, where the response values are: R<LP, an expansion operation is carried out by forming a new point, E, at a distance cx from CN along the reflection line as illustrated in Figure 3.1. The expansion coefficient, c, is slightly less than 2 to avoid oscillation problems. A new response value is obtained at E. If the expansion is succes-

75
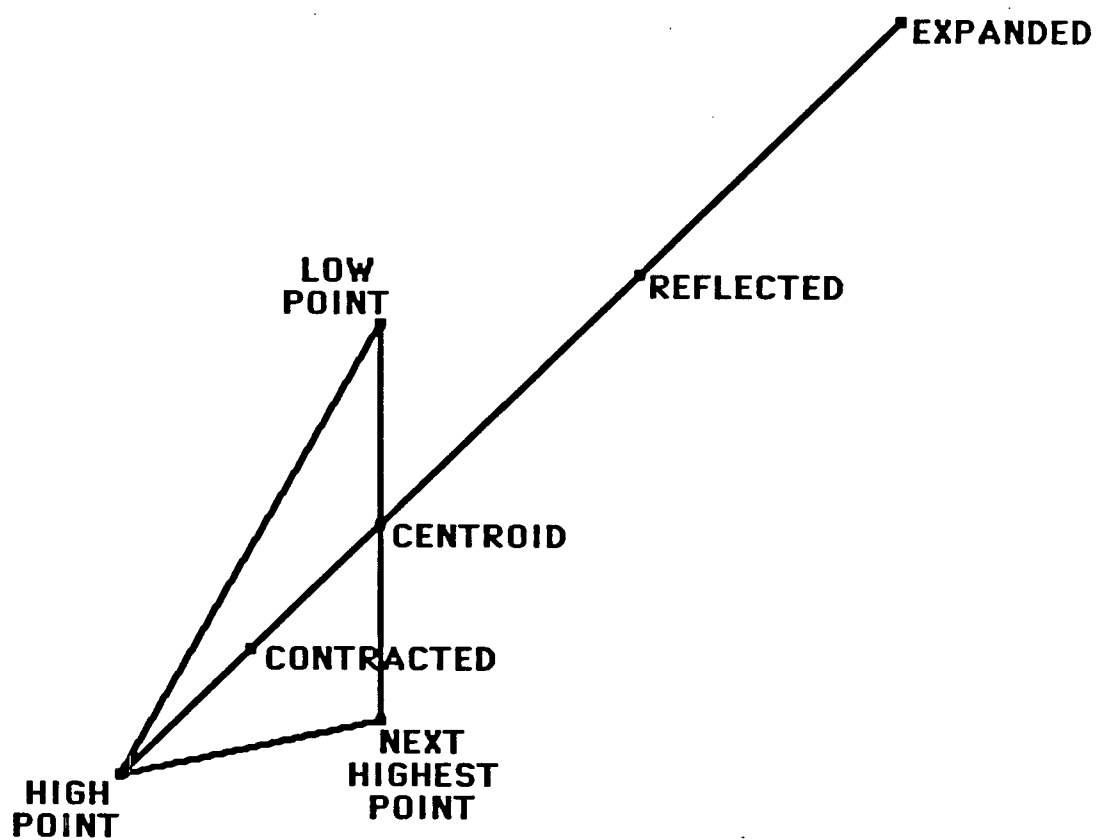
Figure 3.1 Two dimensional simplex illustrating reflection, expansion, and contraction operations.

sful, that is, E<R, then E replaces HP. Otherwise, R
replaces HP and the reflection operation is carried out
again in step (2).

(5) If the initial reflection operation fails, where R≥HP,
then a contraction operation is carried out by forming a
new point, C, at a distance bx from CN along the refle-
ction line as illustrated in Figure 3.1. The contra-
ction coefficient, b, is slightly less than 0.5 to avoid
oscillation problems. If the contraction is successful,
that is, C<HP, the point HP is replaced by C and the
reflection operation is carried out again in step (2).

(6) In rare cases the contraction operation may fail. If
this occurs, then the entire simplex, except for point
LP, is scaled [100] and the optimization procedure is
started again.

(7) The reflection operations are carried out unless some
termination criterion is met. The termination criterion
may be set to be something like when a sequence of
reflections fails to reduce the response value below a
set point or produces a reduction less than some pre-
determined value.

3.3.2 THE KALMAN FILTER

Digital filters [102-104] have proven useful in para-
meter estimation and optimization problems, the digital
filter serving to separate one component of a signal from
another. The Kalman filter is a series of equations that is
the optimal solution [102] to the general linear filter

problem. If the system to be examined is a linear system and has only Gaussian noise, the minimum variance estimates for the system parameters given by the Kalman filter will be the best possible estimates obtainable. No other linear or nonlinear estimator [105] can produce parameter estimates having lower variance.

The extended Kalman filter has been applied to non-linear systems [102,105,106] successfully to derive system parameters and deconvolute overlapped spectral peaks [105]. The Kalman filter has been applied to two dimensional systems to process images [107] and to two and three dimensional systems [108] to fit enzyme kinetic data in multicomponent systems.

In principle, the extended Kalman filter [105,108] should be readily applied to finding parameters describing time-wavelength resolved luminescence spectra. Considerable effort was expended in implementing the extended Kalman filter to resolve highly overlapped spectral envelopes and obtain their parameters. The lack of noise data for the measured luminescence spectra was a suspected trouble spot. However, when this data was collected and applied the system still failed to converge. The extended Kalman filter program was very sensitive to the initial guess values for the parameters. This sensitivity may be due to the system being nonlinear in both the time and wavelength domains. Another possibility is that the computer program written to implement the filter may have contained errors. A satis-

factory solution to the sensitivity problem was not obtained and work on the Kalman filter approach was abandoned.

3.4 THE DATA REDUCTION ALGORITHM

Data reduction of multicomponent fluorescence spectra [109] and chromatographic peaks [110] was done for a single parameter for multiple components present by using a linear algebra construct and simplex optimization. This approach was incorporated in the first stage of a two stage data reduction scheme to extract the concentration factor, peak maxima, peak width, and lifetime for each emitting species present in a time-wavelength resolved luminescence spectrum. Stage I: Estimate the lifetime behavior for each emitter by the method of Knorr and Harris [109].

(a) Guess the number of emitting species present, n, and a lifetime value, τ_n for each species.

(b) Use equation 3.7 to construct an estimated n x j normalized time behavior matrix [TE].

(c) Use equation 3.8 to compute an estimated spectral behavior matrix [SE] by multiplying the data matrix by the pseudoinverse of the estimated time behavior matrix; then an estimated data matrix [DE] using equation 3.9, and finally use equation 3.10 to compute the squared error, SQE, between [D] and [DE].

$$[SE] = [D] [TE]^T ([TE] [TE]^T)^{-1} \qquad (3.8)$$

$$[DE] = [SE] [TE] \qquad (3.9)$$

$$SQE = \sum_{a=1}^{i} \sum_{b=1}^{j} (D_{ab} - DE_{ab})^2 \qquad (3.10)$$

79

(d) Guess new values for lifetimes, then repeat steps (b) and (c) using simplex optimization to minimize SQE.

Stage II:

(e) Compute estimated from [SE] for the parameters C, m, and w for each of the n components present.

(f) Using equation 3.6 and estimates of C, m, and w for each component, construct a new i x n estimated spectral behavior matrix [SE].

(g) Using equation 3.7 and estimated values for τ, construct a new n x j estimated time behavior matrix [TE] .

(h) Compute an estimated data matrix [DE] using equation 3.9, and the squared error, SQE from 3.10.

(i) Guess new values for C, m, w, and τ; repeat steps (f) to (g) using simplex optimization minimize SQE.

In step (i) one may set fixed values for any parameters for any components. This approach may be useful when attempting to characterize an unknown in the presence of known emitters or to examine small changes in selected parameters.

3.5 COMPUTERS AND FORTRAN COMPILERS USED

The data reduction program was run on the following systems: (a) Perkin-Elmer 7500 series professional computer system (Perkin-Elmer Corp., Norwalk, CT), (b) Compupro IEEE 696/S-100 system with CPU 68K processor board (Compupro, Hayward, CA), (c) Corona Model PC400-HD2 computer with 8087 coprocessor. A Silicon Valley Systems FORTRAN 77 compiler (Silicon Valley Systems, Inc., Cupertino, CA) compiler was

used on the Perkin-Elmer and Compupro systems. A WATFOR-77 (WATCOM Systems Inc., Waterloo, Ont.) compiler was used on the Corona system.

Processing times on the Perkin-Elmer and Compupro systems were similar and about twice as fast as the Corona. Aside from some technical problems with the Perkin-Elmer system, all three systems required the same number of iterations to arrive at similar estimated parameter values.

3.6 ALGORITHM EVALUATION

The program listed in Appendix 4 was used in evaluating the algorithm's performance on sets of synthetic spectra. The synthetic spectra were computed using parameters similar to those of common luminescent salts such as calcium tungstate and calcium molybdate. All synthetic spectra were corrupted with Gaussian noise [92] at levels commonly found in experimental data taken with the time-wavelength resolved luminescence spectrometer. In order to simulate real data as closely as possible, the synthetic spectra were stored in data files having exactly the same format as files produced by the program listed in Appendix 1. The synthetic spectra time coverage was from 1 µs to 20 µs in 1 µs steps and a window width of 1 µs; wavelength coverage was from 300 nm to 700 nm in steps of 10 nm.

3.6.1 PERFORMANCE ON TWO COMPONENT MIXTURES

The algorithm was tested for the effects of noise, initial guess values, and relative concentrations of the two components on their parameter estimates at various degrees

of overlap in both the time and wavelength domains. In this series of experiments, the parameters assigned to component A were held constant while those assigned to component B were varied as shown in Table IV.

The principal question regarding a two component mixture is how close can the luminescence emission envelopes be before the algorithm fails to produce parameter estimates that are within acceptable error limits. The algorithm's performance for the case where both components have similar initial intensities is illustrated in Figure 3.2. The peak separation in the spectral domain is plotted on the abscissa in units of peak halfwidths, and the ratio of lifetimes of component B to component A is plotted on the ordinate. The shaded areas represent regions where the relative error between actual and estimated parameter values lie within the bounds stated. This figure is the result of applying the data reduction algorithm to 161 synthetic spectra and plotting the maximum error found for the parameters for both components A and B.

A feature common to most situations examined is that as the peak separation increases in the wavelength domain, the error in the parameter estimates decreases to a minimum value and then increases again as the peak separation becomes greater. The increasing error in parameter estimates as peak separation becomes greater is due to the decreasing amount of the component B spectral envelope included in the data collection window. For example, less than one half of

Table IV

Parameter Assignments for Two Component Mixtures

Component	A	B
Lifetime, μs	10	vary, 0.25 to 250
Peak maxima, cm^{-1}	23000	vary, 14000 to 23000
Peak halfwidth, cm^{-1}	6000	6000
Intensity	10	vary, 1 to 50
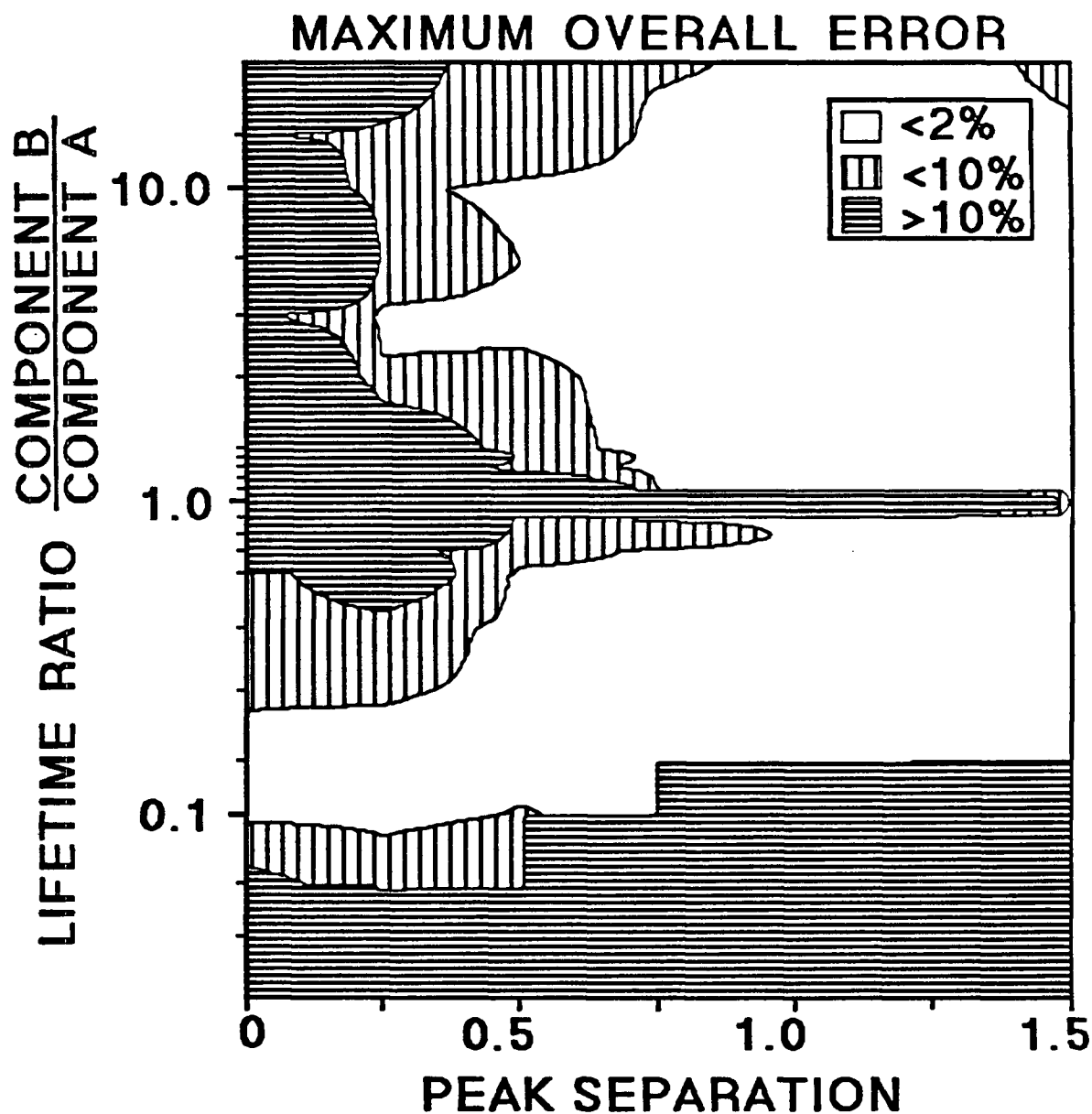
Figure 3.2 Maximum error in estimated parameters for both
components A and B as a function of peak separa-
tion in both time and wavelength domains. Syn-
thetic data with: 1% RSD noise, component B inte-
nsity = 10, other parameters as in Table I.
Guess values used: A = 12.3 μs, B = 123 μs.

the component B spectral envelope is present in the data collection window at a peak separation of 1.5 halfwidths.

Similar behavior is seen in the time domain, particularly so at short lifetimes for component B. This is due to the very small contribution component B makes to the overall observed signal. So little of component B is present that it tends to get lost in the noise, as well as being highly sensitive to truncation errors introduced with the data storage format used. When component B has a relatively long lifetime, there is little change in its intensity within the data collection window. This results in an increasing uncertainty in its lifetime estimate.

These effects are illustrated in Figure 3.3. In Figure 3.3a, all parameters for both components were estimated with a maximum error of less than 2%. In Figure 3.3b, all parameters for component A were estimated within 1% of the actual values whereas the parameter estimates for component B were all greater than 10%. This poor performance is due to the small signal envelope from component B; its peak maxima lies outside the data collection window and its short lifetime yields scant information on time behavior.

The algorithm's performance for estimating individual parameters for each component are illustrated in Figures 3.4, 3.5, and 3.6. Of the four parameters, peak maxima and peak width consistently showed the least error regardless of peak separation, added noise, lifetimes, or relative intensities. The errors for component A parameter estimates are
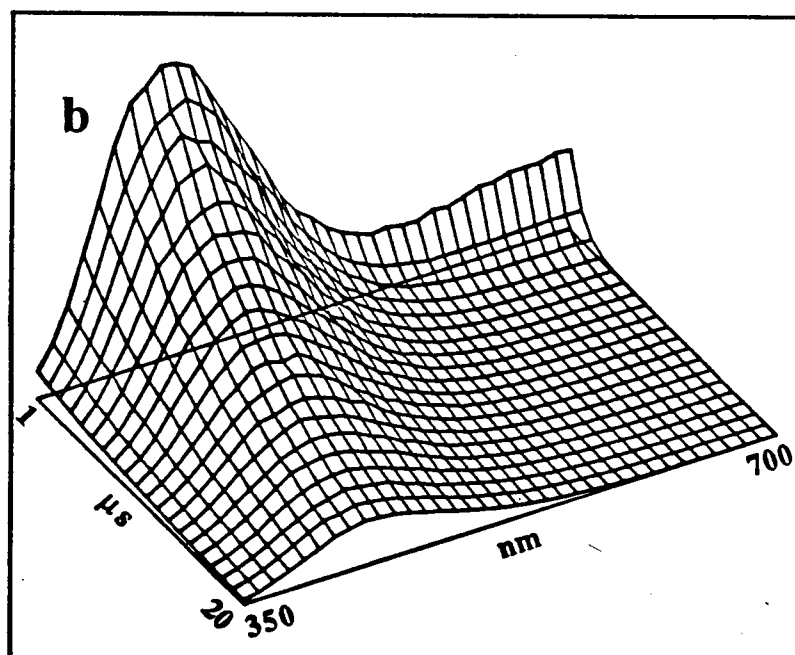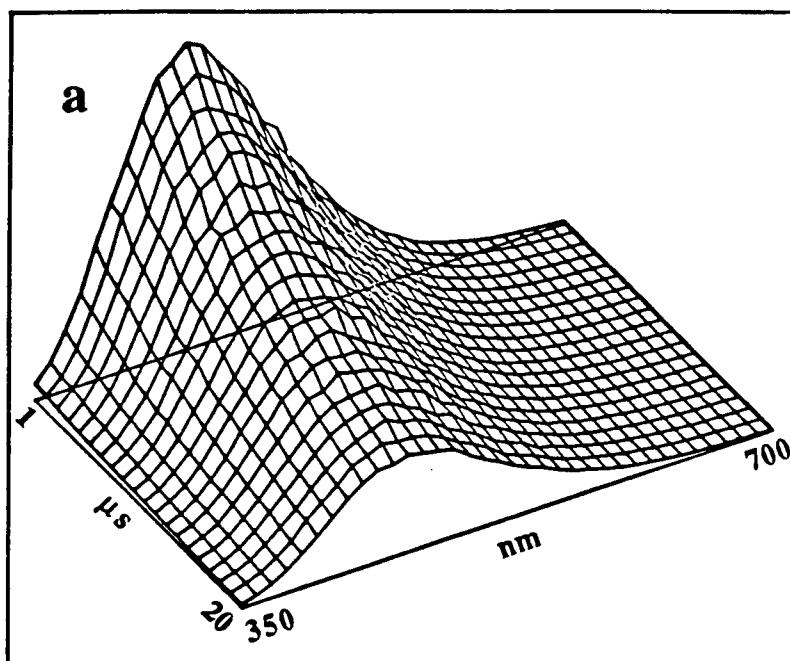
Figure 3.3 Synthetic spectra with 1% RSD noise added, verti-
cal axis: intensity. (a) Lifetimes: A = 10 μs,
B = 25μs; peak maxima: A = 435 nm, B = 465 nm.
(b) Lifetimes: A = 10 μs, B = 1 μs; peak maxima:
A = 435 nm, B = 714 nm.
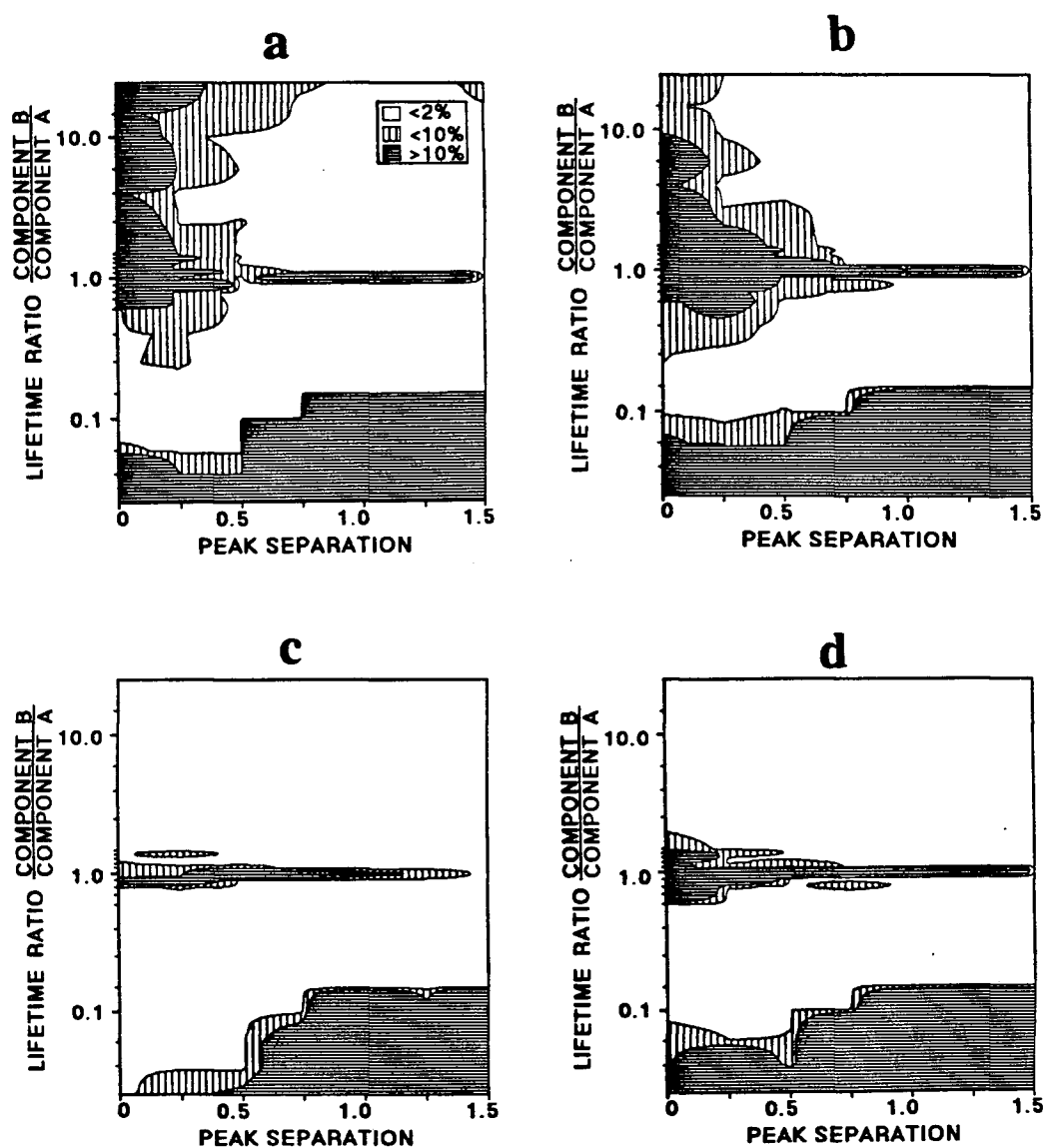
Figure 3.4 Maximum error in estimated parameters for both
components A and B. (a) Lifetimes, (b) peak
intensities, (c) peak maxima, (d) peak halfwidth.
Synthetic data with: 1% RSD noise, component B
intensity = 10, other parameters as in Table I.
Guess values used: A = 12.3 µs, B = 123 µs.
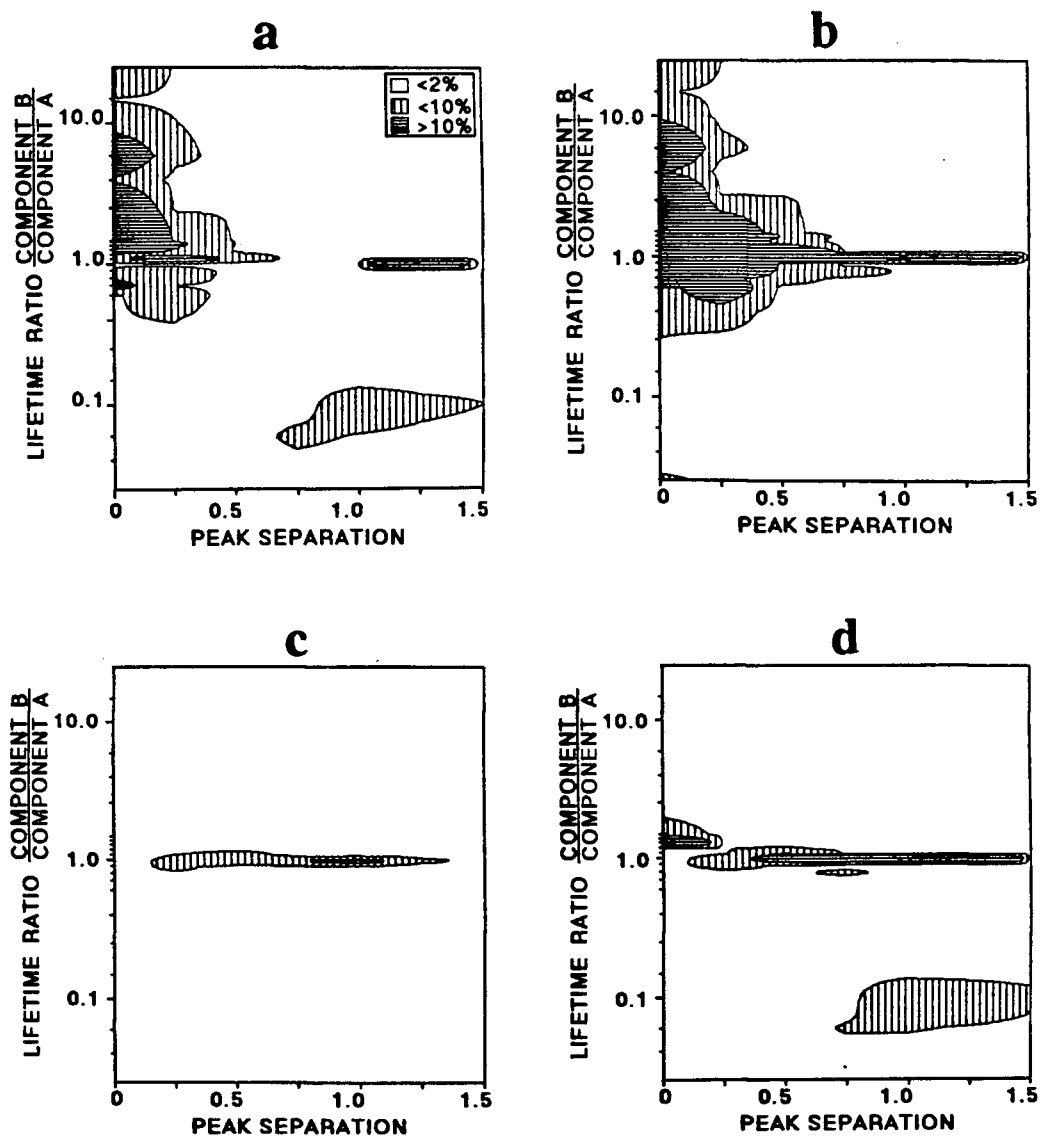
Figure 3.5 Maximum error in estimated parameters for component A only. (a) Lifetimes, (b) peak intensity, (c) peak maxima, (d) peak halfwidths. Synthetic data with: 1% RSD noise, component B intensity = 10, other parameters as in Table I. Guess values used: A = 12.3 μs, B = 123 μs.
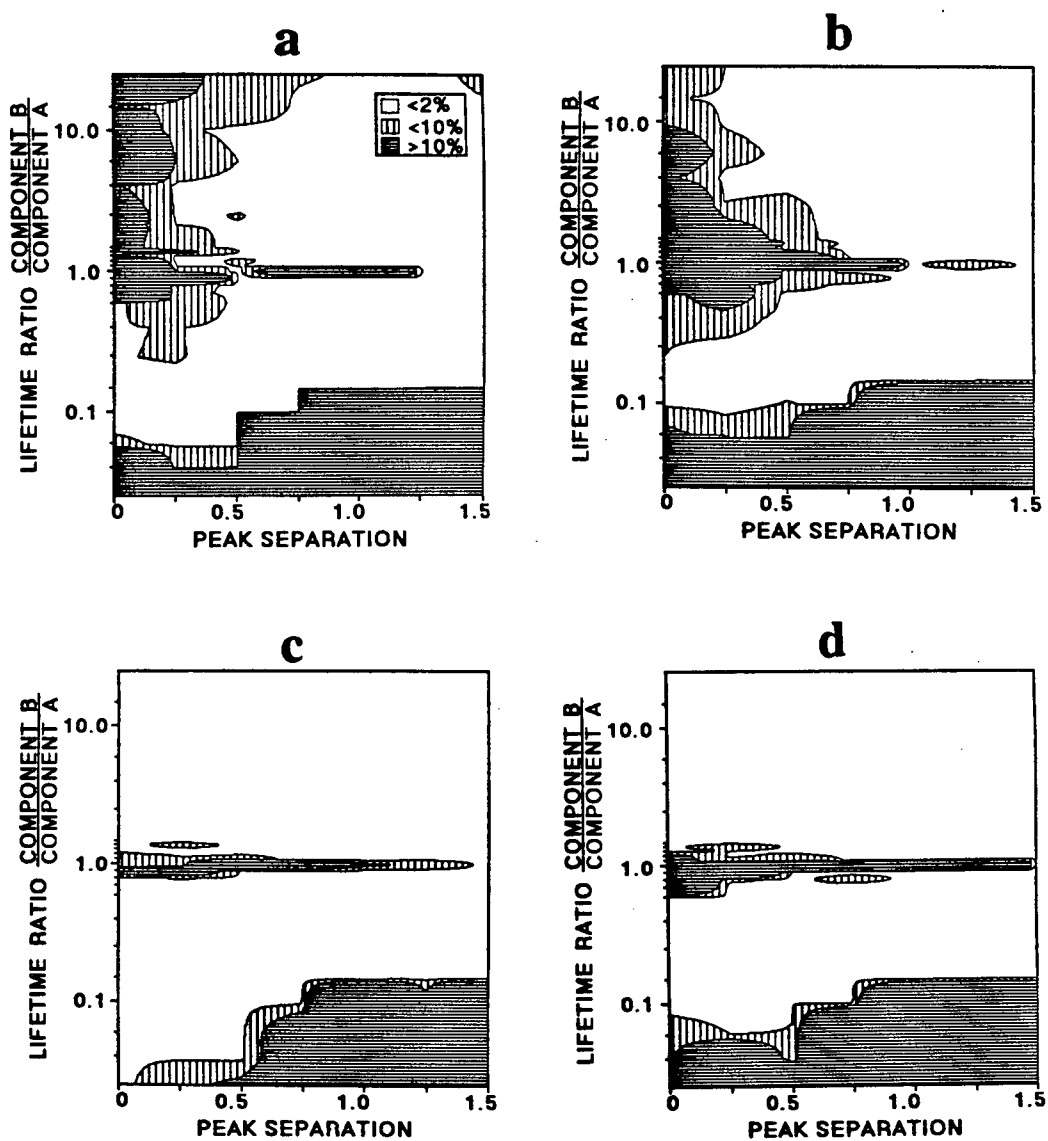
Figure 3.6 Maximum error in estimated parameters for compo-
nent B only. (a) Lifetimes, (b) peak intensity,
(c) peak maxima, (d) peak halfwidths. Synthetic
data with: 1% RSD noise, component B intensity =
10, other parameters as in Table I. Guess values
used: A = 12.3 μs, B = 123 μs.

shown in Figure 3.5, they are generally acceptable with the intensity factor being most prone to error. The results for component B parameter estimates are given in Figure 3.6. This figure illustrates well the difficulties encountered with low signal levels from component B due to short lifetimes and large portions of the spectral envelope lying outside the data collection window.

The effect of noise on the algorithm's performance is demonstrated in Figure 3.7. The error shown is the maximum found for any parameter for any component. To the synthetic spectra, Gaussian noise was added at levels ranging from zero to five percent relative standard deviation. In this particular experiment the lifetime values from stage I of the data reduction algorithm were held constant during stage II of the data reduction process. The previously noted trends in estimated parameter reliability were reinforced in this series of experiments as can be seen in Figure 3.7. To a first approximation, the error level found the parameter estimates is proportional to the noise level in the data examined. A signal noise level of 1% RSD was normally achieved with the spectrometer used in this study and this noise level was applied to the synthetic spectra in subsequent experiments.

The algorithm's sensitivity to initial guess values for lifetimes is shown in Figure 3.8. The algorithm seems to perform better when lifetime guesses are higher than the
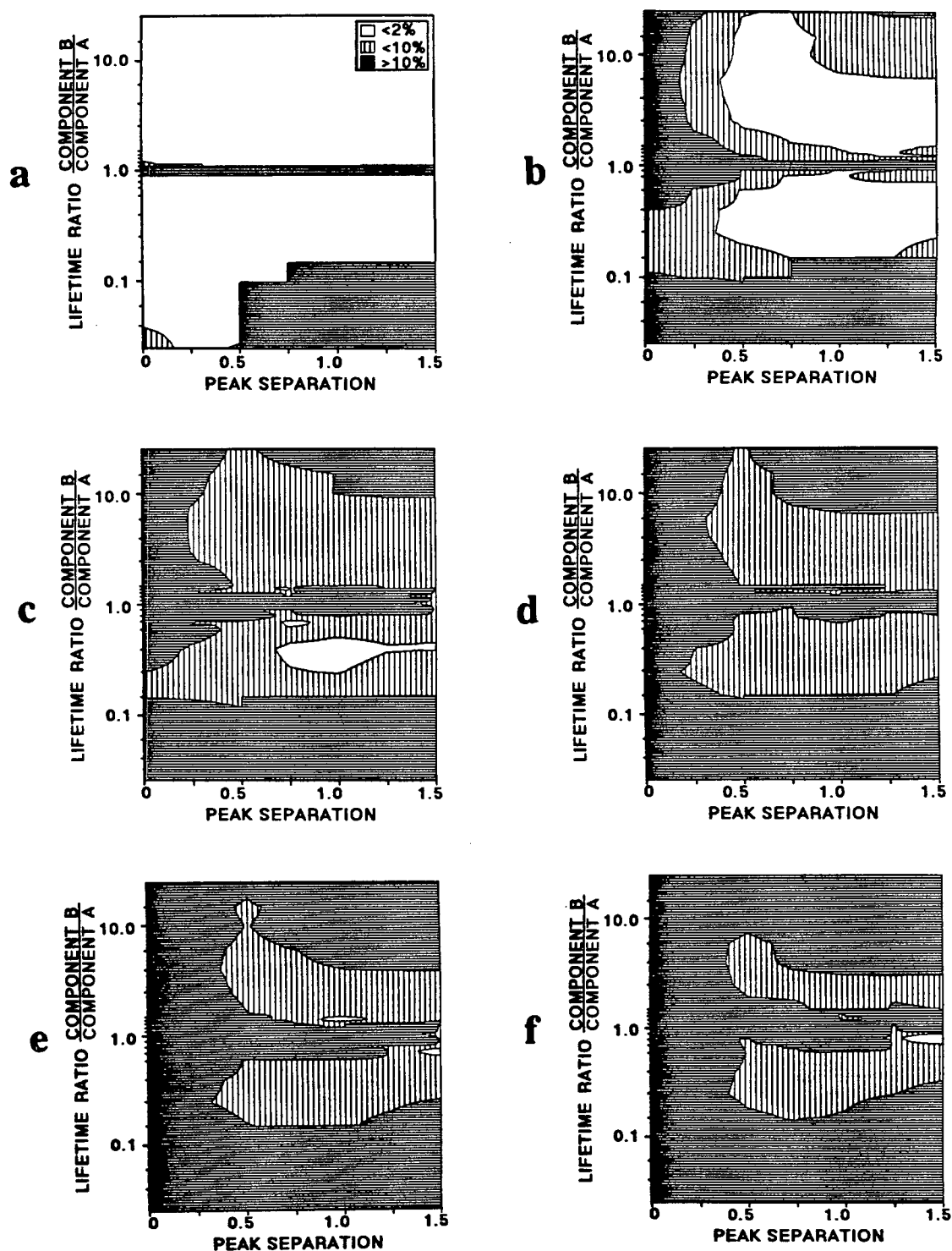
Figure 3.7 Maximum error in estimated parameters for both components A and B as a function of added noise. (a) no noise added, (b) 1% RSD, (c) 2% RSD, (d) 3% RSD, (e) 4% RSD, (f) 5% RSD. Synthetic data with: component B intensity = 10, other parameters as in Table I. Guess values used: A = 12.3 μs, B = 123 μs.
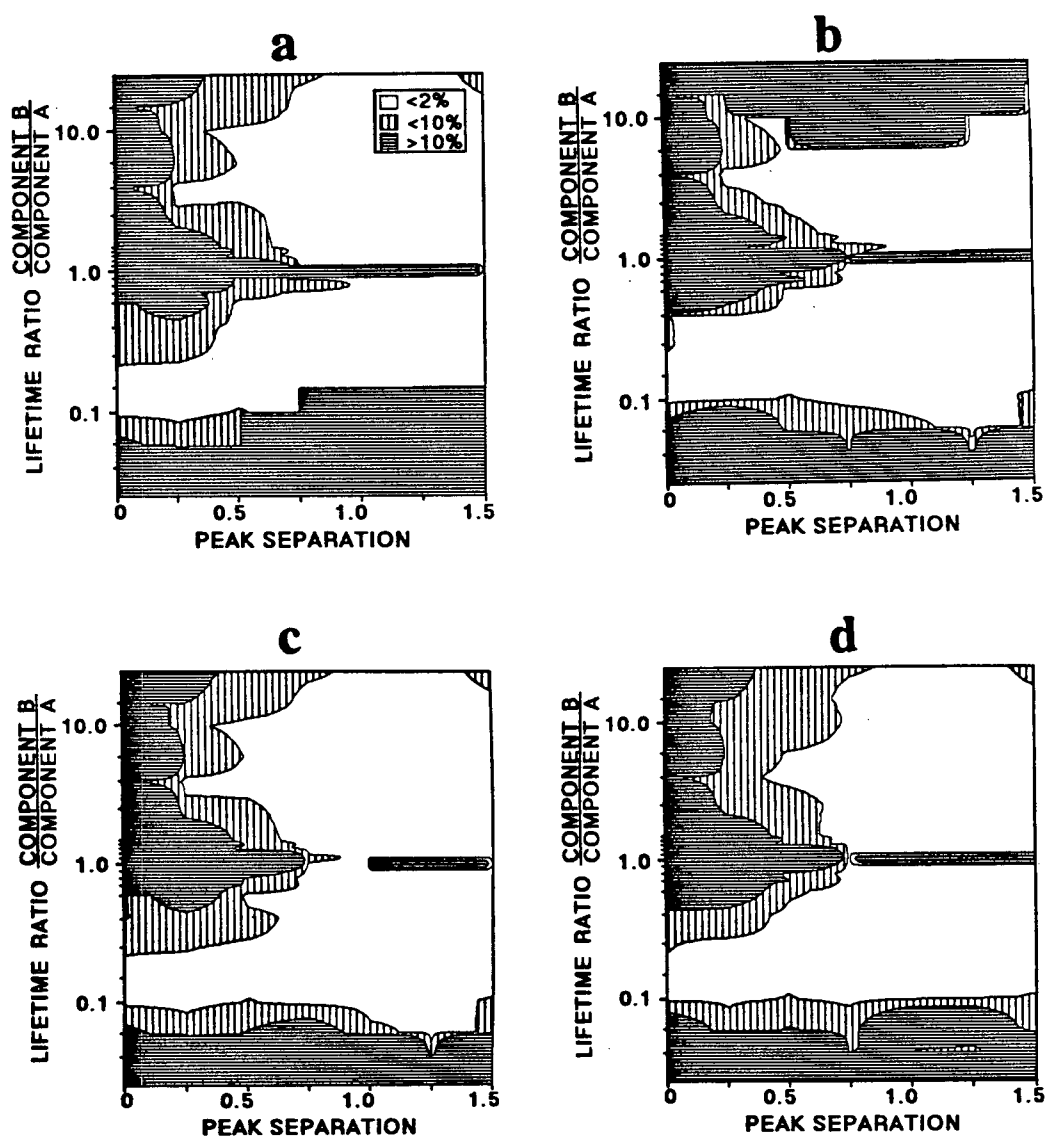
Figure 3.8 Maximum error in estimated parameters for both components A and B as a function of lifetime guess values. Guess values (μs) used: (a) 12.3, 123; (b) 12.3, 1.23; (c) 12.3, 7.89; (d) 123, 1.23. Synthetic data with: 1% RSD noise, component B intensity = 10, other parameters as in Table I.

actual lifetimes. Generally, the algorithm appears to have relatively low sensitivity to guess values provided that they are within a factor of 10 of the real lifetime values.

In Figure 3.9, the effect of varying the amount of component B in the system is presented. The overall trend here is that the error in estimated parameter values is related to the size of the spectral envelope captured within the data collection window. This trend reinforces the notion that the errors in parameter estimates are more dependent on the volume contained within the observed spectral envelope than on the overlap of components A and B in either the time or wavelength domains.

3.6.2 PERFORMANCE ON THREE COMPONENT MIXTURES

Synthetic spectra consisting of three components were successfully resolved into the individual components. The algorithm's performance for systems containing three highly overlapped components is shown in the examples listed in Table V. Generally, if the lifetime ratio between any two components is greater than 2:1, and if the peak separation is breater than 0.5 halfwidths then the data reduction operation would normally be successful as demonstrated when comparing results for the #1 and #3 mixtures in Table V.

The algorithm was used to find the number of components present in an unknown mixture. The algorithm was run using an increasing number of guessed components in the initial guess. The values for SQE at termination were plotted against the number of constituents guessed as shown in
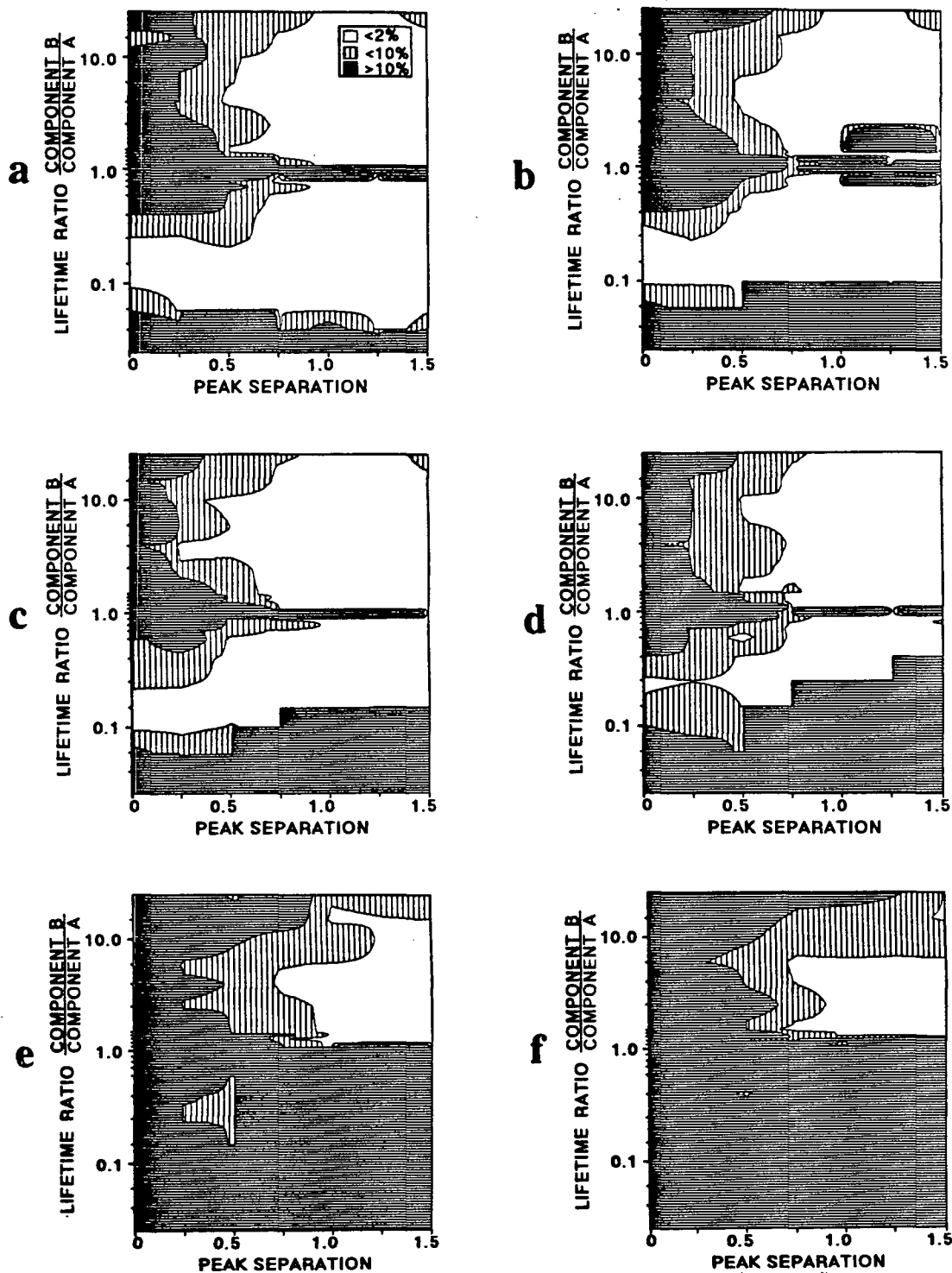
Figure 3.9 Maximum error in estimated parameters for both components A and B as a function of peak intensity. Peak intensities used: (a) A = 10, B = 50; (b) A = 10, B = 20; (c) A = 10, B = 10; (d) A = 10, B = 5; (e) A = 10, B = 2; (f) A = 10, B = 1. Synthetic data with 1% RSD noise, other parameters as in Table I. Guess values used: A = 12.3 μs, B = 123 μs.

Table V

Comparison of Actual and Estimated Parameters for Three Component Mixtures[a]

Component	Lifetime μs	Maxima cm^{-1}	Halfwidth cm^{-1}	Intensity
A	10.00 (10.05)	23000 (22964)	6000 (6023)	10.00 (10.10)
B	25.00 (25.23)	19400 (19382)	6000 (5999)	10.00 (9.87)
C	2.50 (2.48)	18200 (18204)	6000 (6008)	10.00 (10.07)
A	10.00 (10.02)	23000 (22989)	6000 (6019)	10.00 (9.97)
B	25.00 (25.09)	19400 (19403)	6000 (6017)	10.00 (9.95)
C	2.50 (2.50)	15800 (15838)	6000 (6013)	10.00 (10.01)
A	10.00 (10.22)	23000 (22734)	6000 (6208)	10.00 (10.90)
B	25.00 (1.85)	19400 (20398)	6000 (1E-8)	10.00 (0.72)
C	40.00 (33.62)	18200 (18673)	6000 (6101)	10.00 (9.95)

[a]Estimated values are in parentheses. 1% RSD noise added; guess times, μs: 36.9, 12.3, 7.89.

Figure 3.10. In most situations, the value of SQE decreases rapidly until the correct number of components present is reached and then the curve decreases at a much slower rate or increases. The rise in SQE when passing the correct number of components present is likely due to numerical instabilities associated with the calculation of the pseudo-inverse.

This approach was applied successfully to find the number of components present in a real material. A powder sample of $Sr(Mo_{0.05} W_{0.95})O_4$ was excited at 193 nm and 248 nm, the measured spectra are shown in Figure 3.11. Three components are present: WO_4^-, MoO_4^-, and a long lived component from the quartz cell used to hold the sample powder.

In Figure 3.12 the difference between the measured spectrum in Figure 3.11a and a spectrum created by the computed parameters are shown. The cause for the rise in SQE when guessing four components is likely due to numerical instabilities in the pseudoinverse calculation, a consequence of this is shown in Figure 3.12. Additional refinements to the simplex algorithm may reduce these abnormalities in real systems.

THREE COMPONENT SYSTEM
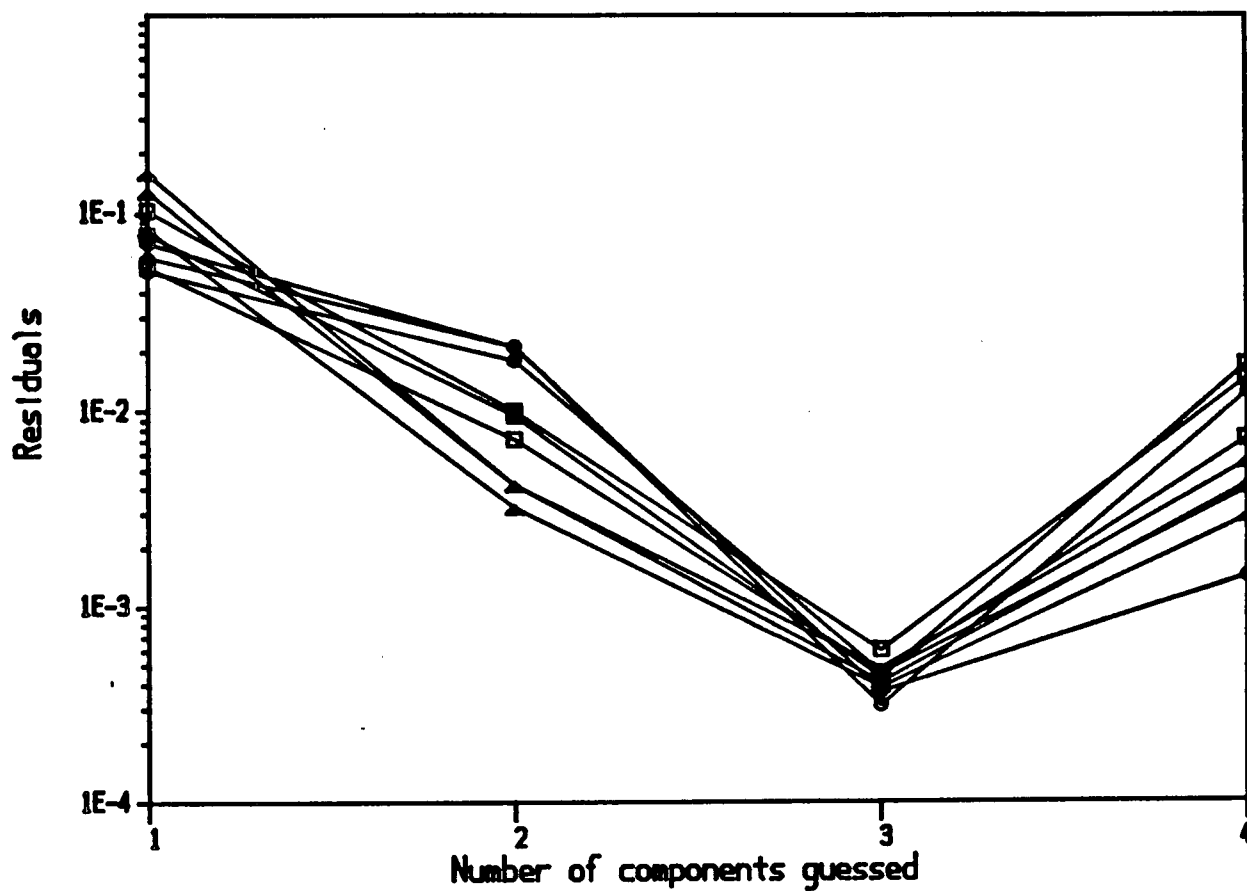
Figure 3.10 Plot of residual error vs number of components
guessed. Lifetimes, μs: A = 10, B = 25, C = 2.5;
peak separations range: A - B: 0.2 to 0.6 half-
widths, A - C: 0.8 to 1.2 halfwidths; 1% RSD
noise; equal peak intensities.
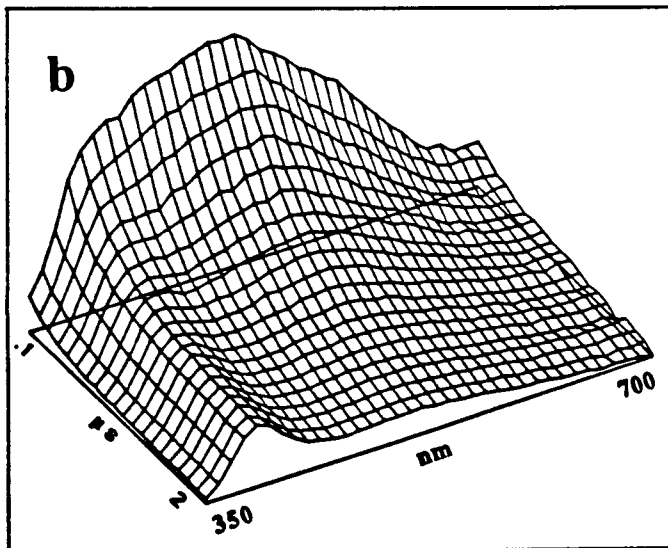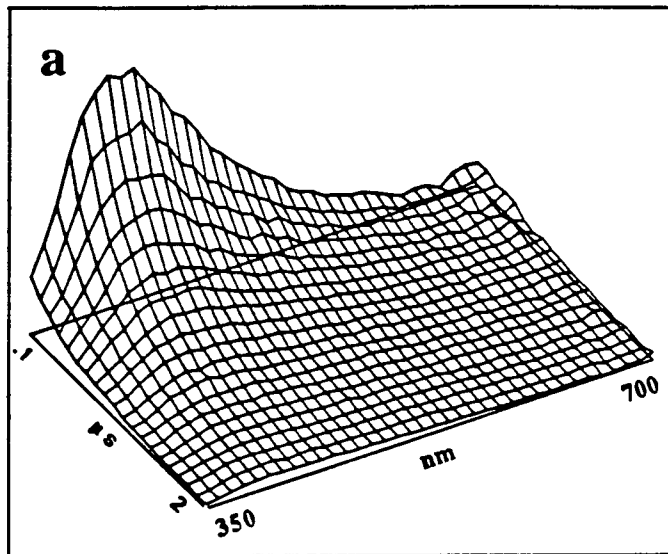
Figure 3.11 Measured spectra for Sr(Mo$_{.05}$ W$_{.95}$)O$_4$: (a) 193 nm excitation; (b) 248 nm excitation.
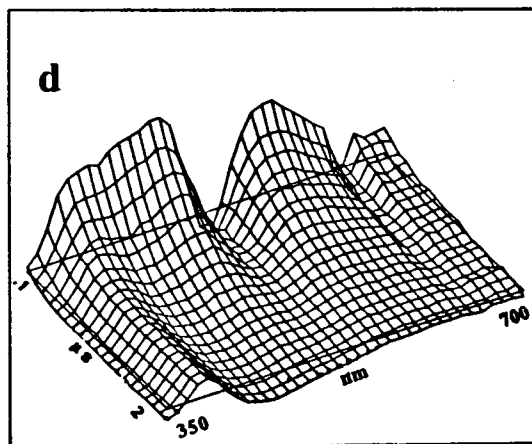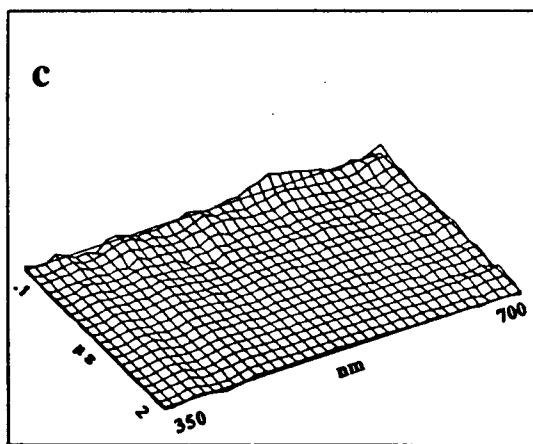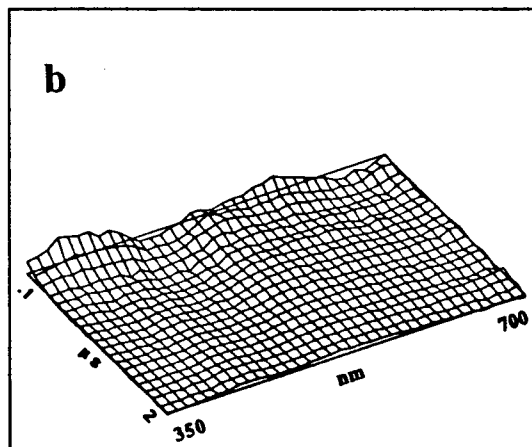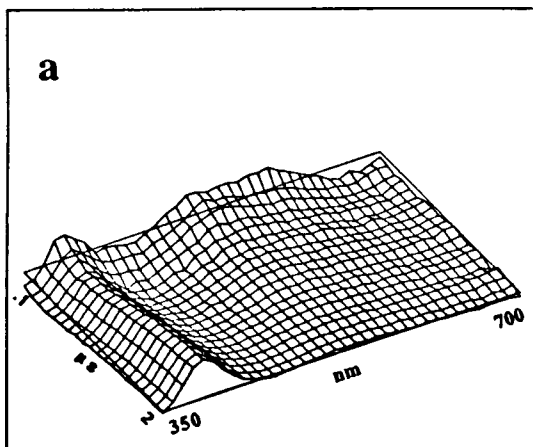
Figure 3.12 Difference spectra as a function of the number of components guessed for $Sr(Mo_{.05} W_{.95})O_4$ excited at 248 nm. (a) one; (b) two; (c) three; (d) four components.

Chapter 4

INORGANIC POWDERS

4.1 OVERVIEW

In this chapter the results of studies on the time-wavelength luminescence spectra of two groups of inorganic powders are presented.

4.2 TUNGSTATES AND MOLYBDATES

Scheelite (calcium tungstate) is a technologically important compound; it is the principal commercial source of tungsten as well as being used as a phosphor, scintillator, and host lattice for solid state lasers. Among inorganic compounds, the luminescence properties of scheelites have been studied extensively. The absorption and emission spectra of the individual alkaline earth molybdate and tungstate salts as well as their mixed crystals was reported by Kroger [111] as part of an extensive study on luminescent inorganic solids.

The currently accepted model [112,113] for absorption and emission in calcium tungstate is that the intense emission band at 420 nm is due to a charge transfer transition within the tungstate anion. This model may be applied to other compounds containing the tungstate or molybdate anions [114-118].

In this study, sample powders of molybdate and tungstate salts held in quartz test tube cells were excited at 193 and 248 nm, the time-wavelength resolved luminescence spectra were collected with the apparatus described in
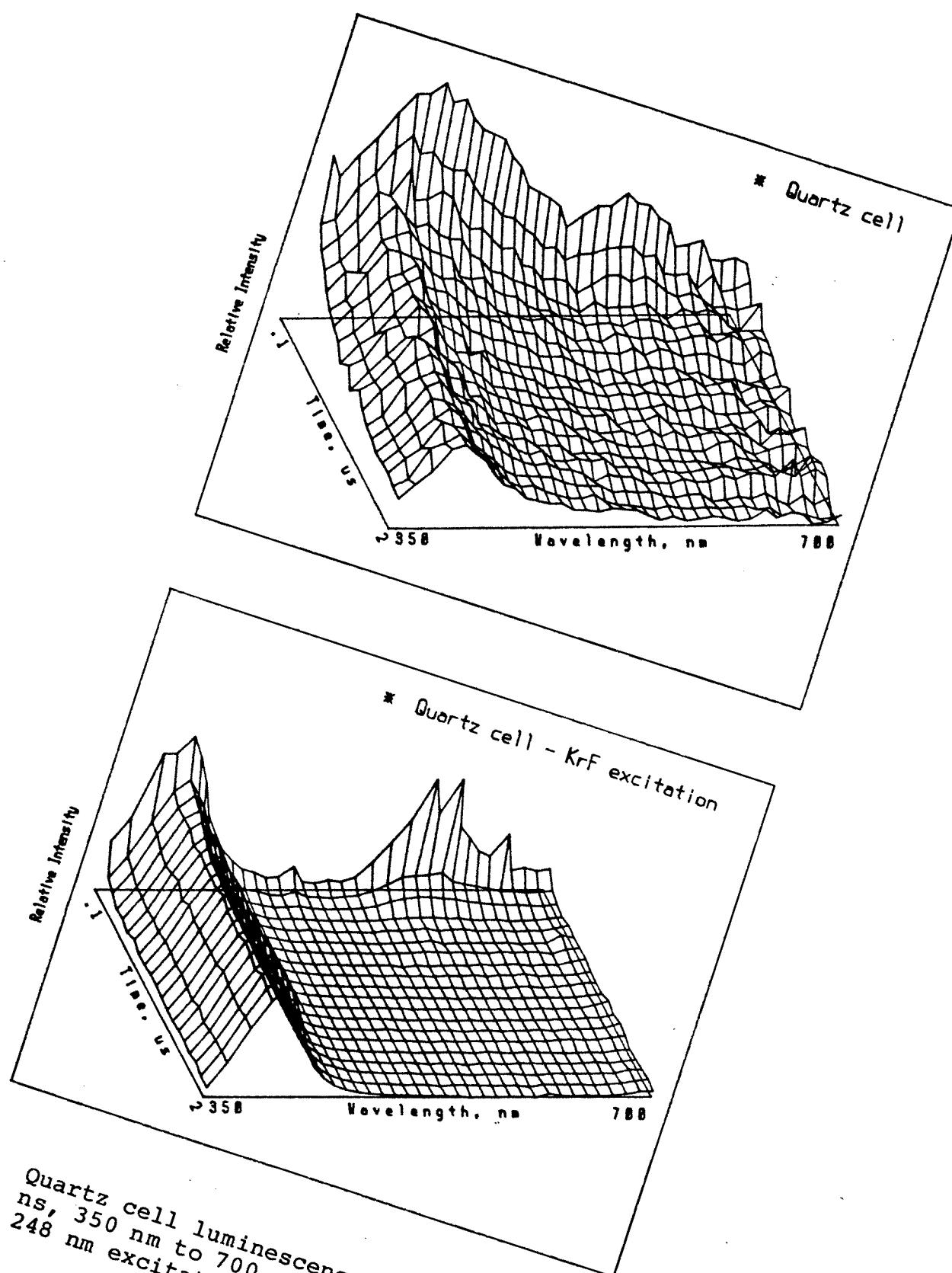
Figure 4.1 Quartz cell luminescence spectra, 100 ns to 2000 ns, 350 nm to 700 nm. (a) 193 nm excitation. (b) 248 nm excitation.
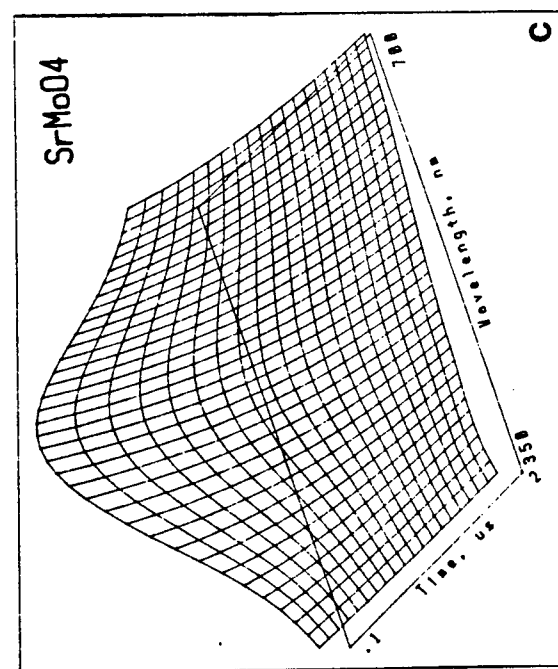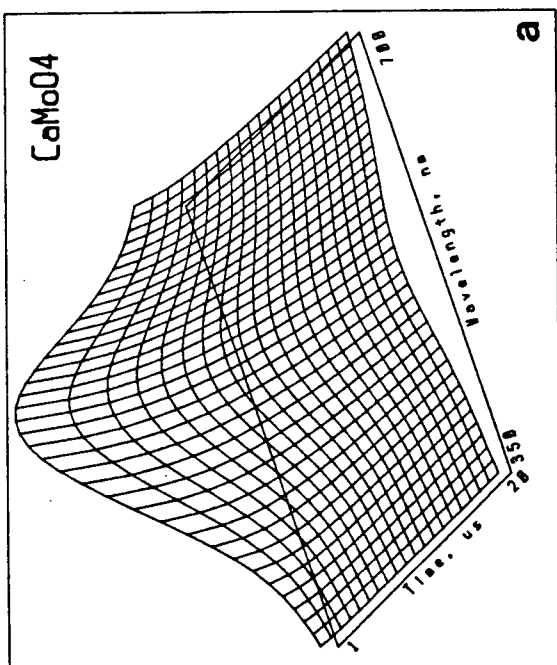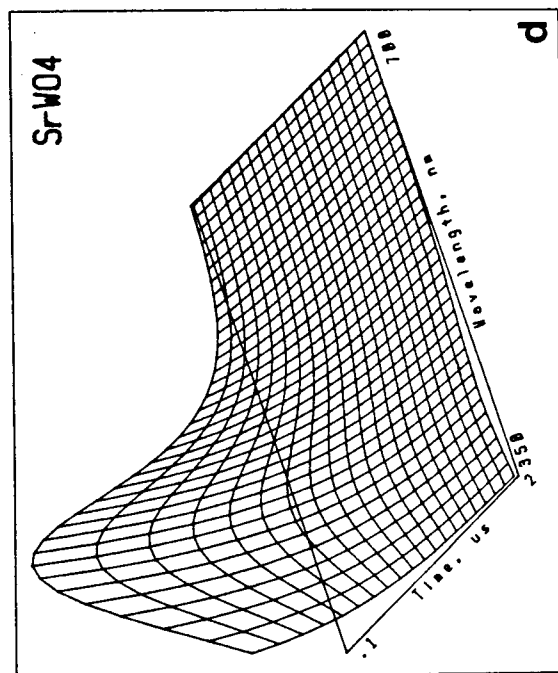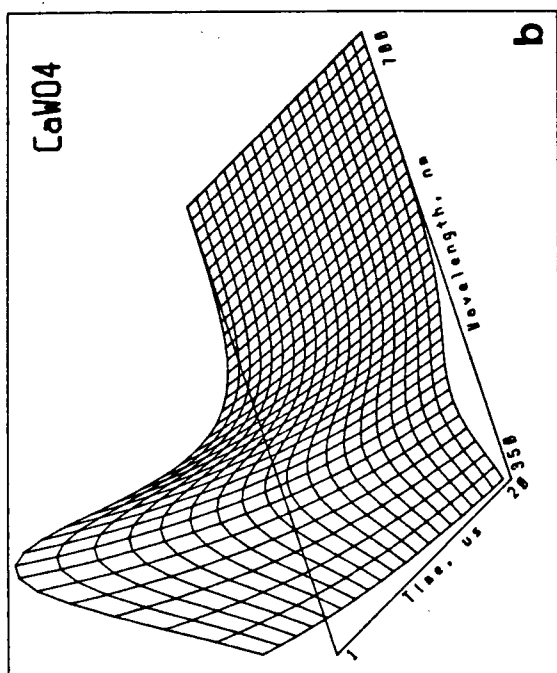
Figure 4.2   Luminescence spectra, 193 nm excitation, 350 to 700 nm. (a) Calcium molybdate, 1000 ns to 20000 ns. (b) Calcium tungstate, 1000 ns to 20000 ns. (c) Strontium molybdate, 100 ns to 2000 ns. (d) Strontium tungstate, 100 ns to 2000 ns.
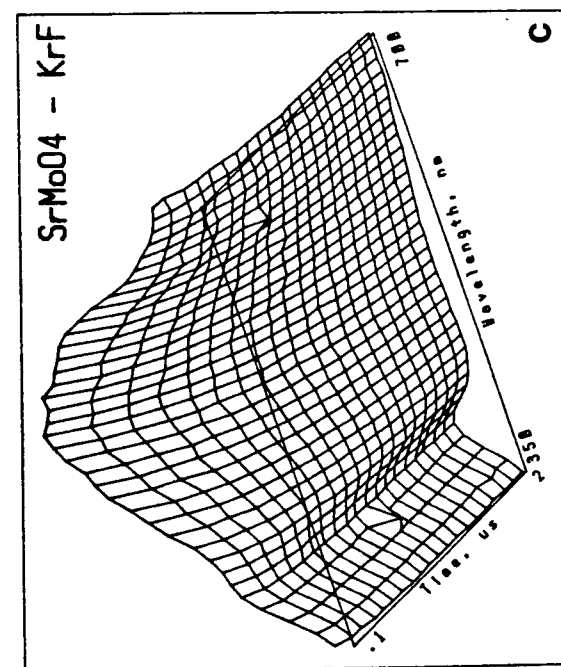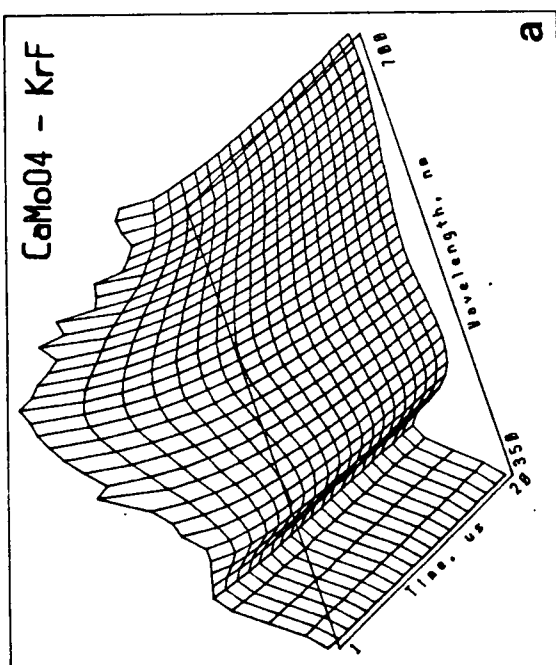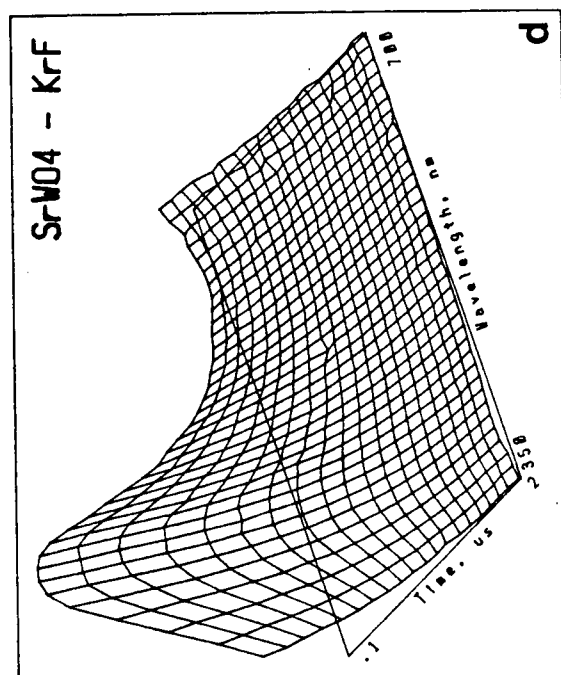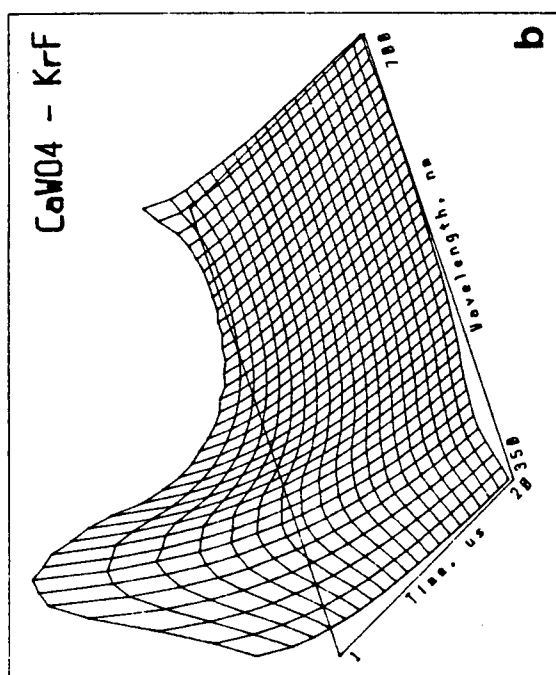
Figure 4.3   Luminescence spectra, 248 nm excitation, 350 to 700 nm.   (a) Calcium molybdate, 1000 ns to 20000 ns. (b) Calcium tungstate, 1000 ns to 20000 ns. (c) Strontium molybdate, 100 ns to 2000 ns. (d) Strontium tungstate, 100 ns to 2000 ns.

chapter 2. The background luminescence from the quartz cell is shown in Figure 4.1. Under 193 nm excitation the quartz cell luminesces strongly with a very broad short lifetime emission and a long lived band at 390 nm. Excitation at 248 nm produces intense, long lifetime emission at 390 nm and a minor short lifetime band in the 600 nm region. The long lifetime emission band at 390 nm is likely due to trap sites [119] present in the quartz.

The alkaline earth molybdates and tungstates having the scheelite structure were examined. The barium salts prepared had lifetimes less than 50 ns and credible measurements could not be made due to the technical problems described in chapter 2. Spectra for the calcium and strontium salts are shown in Figures 4.2 and 4.3 for 193 nm and 248 nm excitation respectively. The spectra shown in Figure 4.2 were smoothed for visual display.

The emission band positions, halfwidths, and lifetimes were independent of the excitation wavelengths used. However, the luminescence intensities appeared to be dependent on excitation wavelength. Absolute luminescence intensity measurements were not made due to limitations imposed by the spectrometer and excitation source. The emission bands from both tungstate and molybdate were affected by the cation. The peak maxima positions were similar for both calcium and strontium compounds. The bandwidths for the strontium salts were about 20% wider than those of the calcium salts. The calcium salts had lifetimes about 20

times greater than the corresponding strontium salt. Assuming that this trend continues on for the barium salts, their expected lifetimes would be on the order of 10 ns. This appears to agree with observations made in previous attempts to measure luminescence on barium salts [82].

Zinc and cadmium salts were also examined. Their spectra are shown in Figures 4.4 and 4.5 for 193 nm excitation and 248 nm excitation respectively. The spectra in Figure 4.4 were smoothed for visual display. The measurements on zinc molybdate appear to be due entirely to the quartz cell (Figure 4.1). Cadmium molybdate exhibited weak luminescence under both excitation wavelengths. The most notable feature is that the characteristic molybdate peak maxima is shifted to about 580 nm. The tungstate emission bands showed a similar shift with their peak maxima going to about 480 nm. The zinc and cadmium compounds peak maxima, halfwidths, and lifetimes appeared to be independent of excitation wavelength. Both compounds showed greater luminescence intensity under 193 nm excitation. The zinc tungstate band halfwidth was about 15% wider than the cadmium compound. Zinc and cadmium tungstate [120,121] have the wolframite structure. The difference in tungstate and molybdate peak maxima positions of the zinc and cadmium salts when compared to the alkaline earth compounds is principally due to the different crystal structures for these compounds.

Results for the parameters describing the luminescence
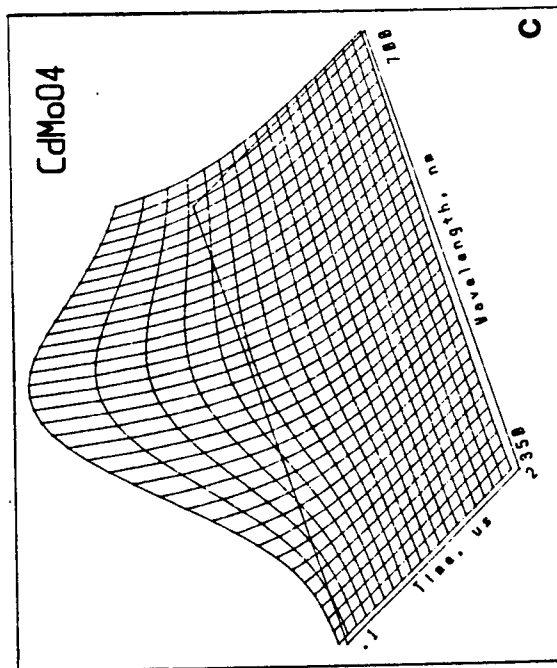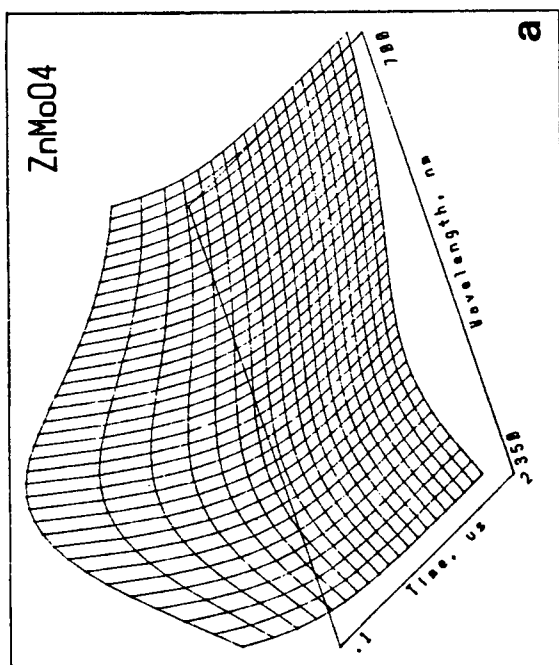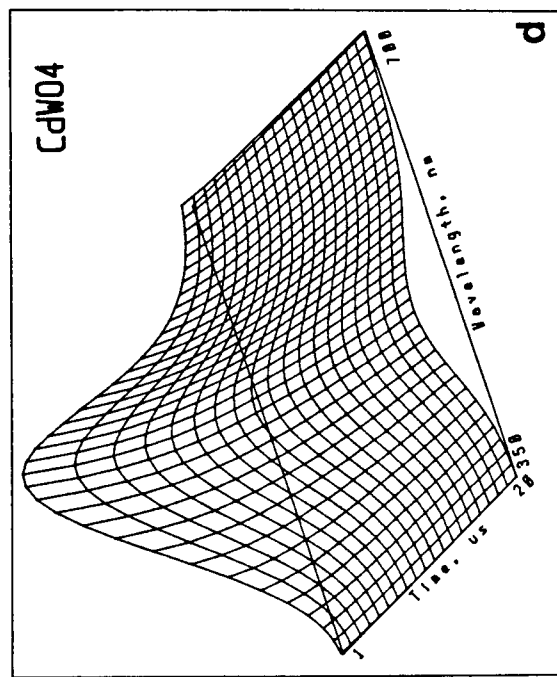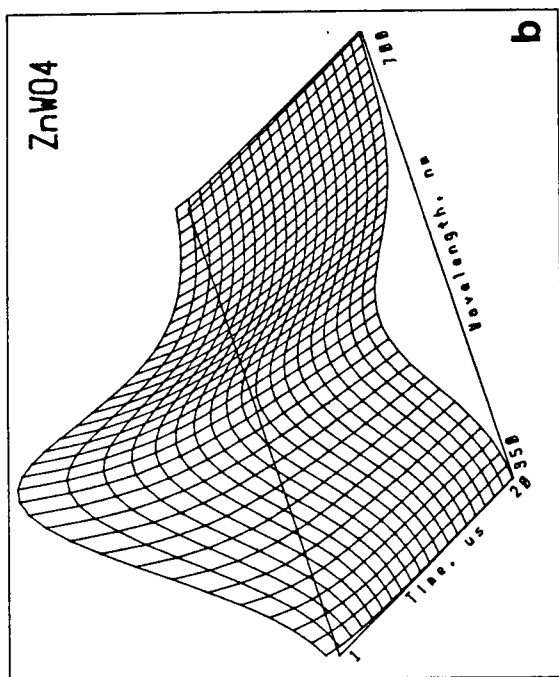
Figure 4.4   Luminescence spectra, 193 nm excitation, 350 to 700 nm. (a) Zinc molybdate, 100 ns to 2000 ns, (b) Zinc tungstate, 1000 ns to 20000 ns, (c) Cadmium molybdate, 100 ns to 2000 ns, (d) Cadmium tungstate, 1000 ns to 20000 ns.
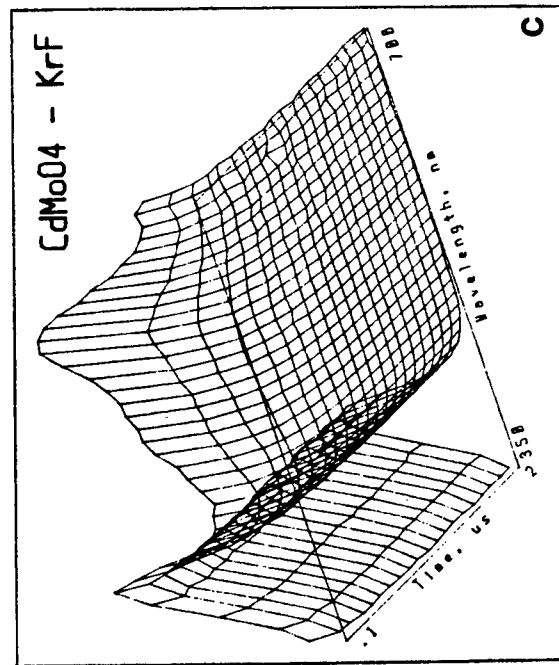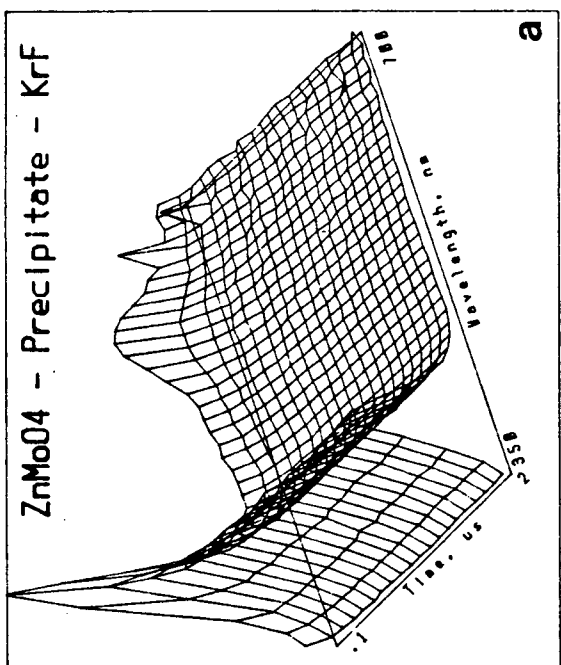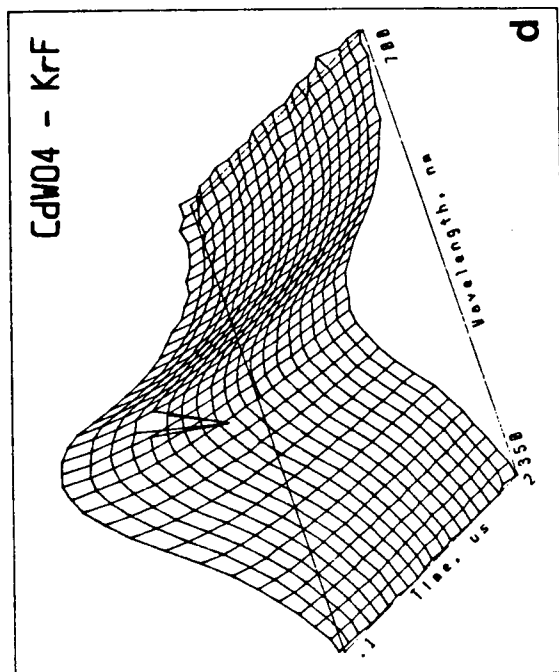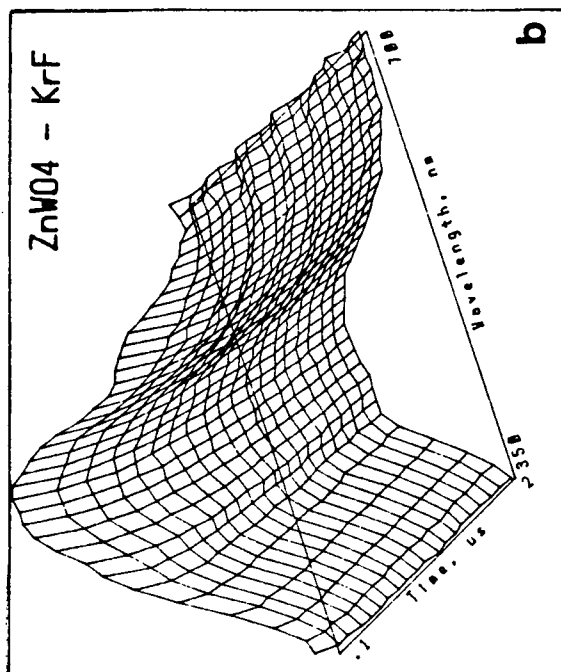
Figure 4.5   Luminescence spectra, 248 nm excitation, 350 to
700 nm.   (a) Zinc molybdate, 100 ns to 2000 ns,
(b) Zinc tungstate, 100 ns to 2000 ns, (c)
Cadmium molybdate, 100 ns to 2000 ns, (d)
Cadmium tungstate, 1000 ns to 20000 ns.

from the single molybdate and tungstate salts excited at 193 nm are summarized in Table VI.

Naturally occurring substances such as minerals are rarely found as pure compounds; invariably they contain contaminants of various composition and concentration. If two different compounds have the same or similar crystalline form they are said to be isomorphous. The tungstate and molybdate ions are of similar size and they tend to form direct replacements for each other in crystal lattices to form an isomorphic series of compounds. The substitution of molybdate for tungstate is common in naturally occurring scheelite. This isomorphous substitution of molybdate for tungstate is reflected in luminescence observed [122,123] from the scheelite-powellite series, $Ca(Mo,W)O_4$, associated with various ore deposit types. A similar effect has been reported [124,125] for the wulfenite-stolzite series $Pb(Mo,W)O_4$. In these reports, the common observation is that when molybdate substitution for tungstate approaches the 10% level, tungstate emission vanishes and the system exhibits luminescence characteristic of molybdate.

Two isomorphous series were prepared: $Ca(Mo,W)O_4$ and $Sr(Mo,W)O_4$. The spectra observed for these compounds are shown in Figures 4.6, 4.7, and 4.8.

The calcium molybdate-tungstate series in Figure 4.6 was excited at 193 nm. The most striking feature shown in this series is that the tungstate lifetime is appreciably shortened by relatively small quantities of molybdate. The

Table VI

Spectral Parameters for Molybdate and Tungstate Salts

Compound	Lifetime μs	Peak maxima cm^{-1}	Peak halfwidth cm^{-1}
$CaMoO_4$	9.7	19210	6950
$SrMoO_4$	0.75	19430	7770
$CdMoO_4$	0.33	18350	6430
$CaWO_4$	8.6	24110	6330
$SrWO_4$	0.48	23920	7420
$ZnWO_4$	15.8	21104	6150
$CdWO_4$	13.9	20670	5780
$PbWO_4$	1.9	23800	12100
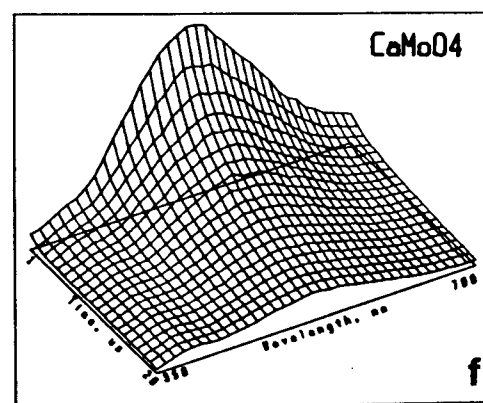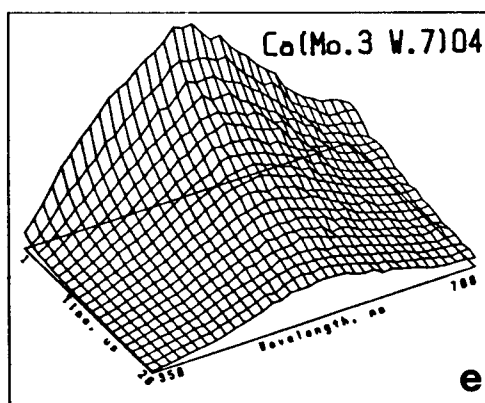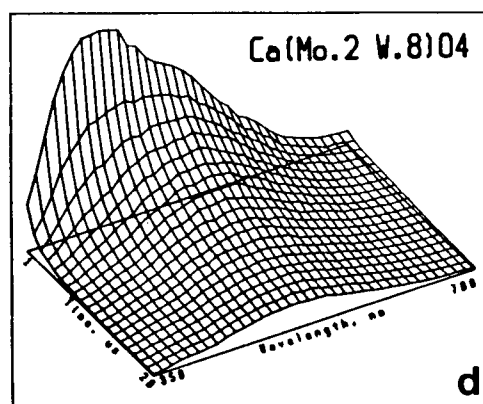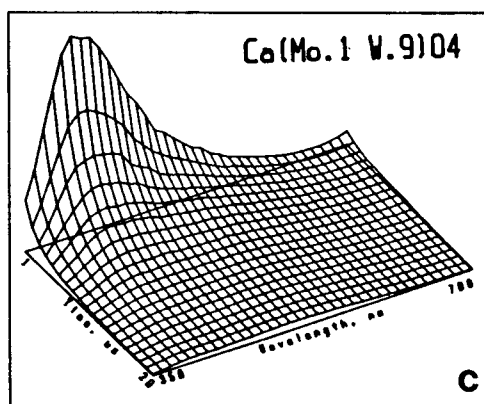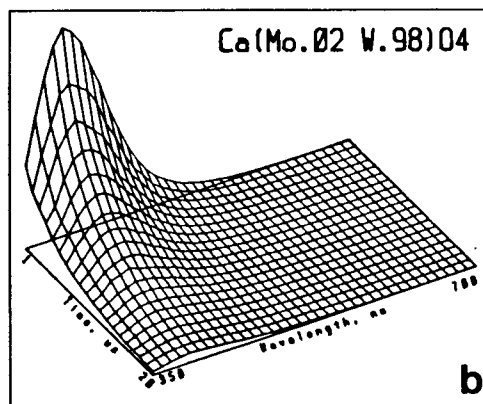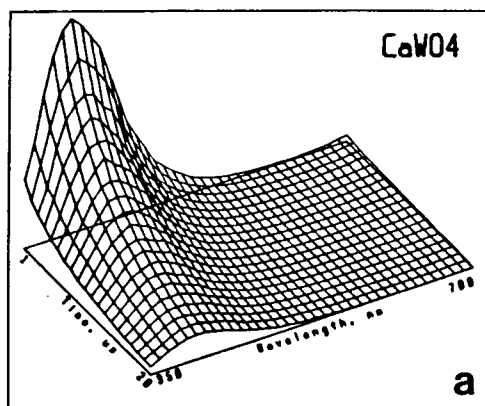
Figure 4.6   Luminescence spectra, 193 nm excitation, 1000 ns
to 20000 ns, 350 nm to 700 nm. (a) $CaWO_4$, (b)
$Ca(Mo_{.02} W_{.98})O_4$,(c) $Ca(Mo_{.1} W_{.9})O_4$, (d)
$Ca(Mo_{.2} W_{.8})O_4$, (e) $Ca(Mo_{.3} W_{.8})O_4$, (f) $CaMoO_4$.
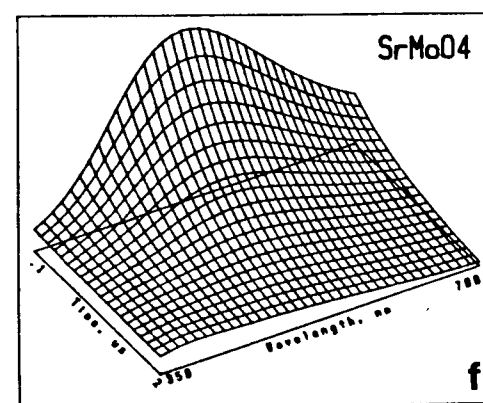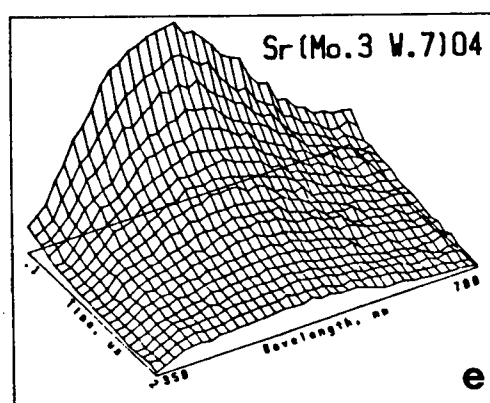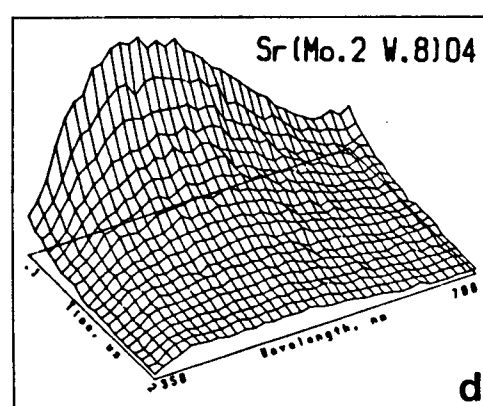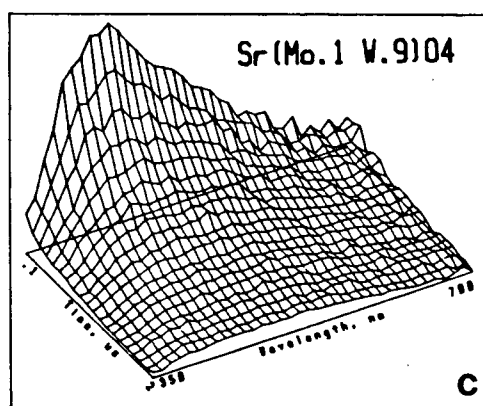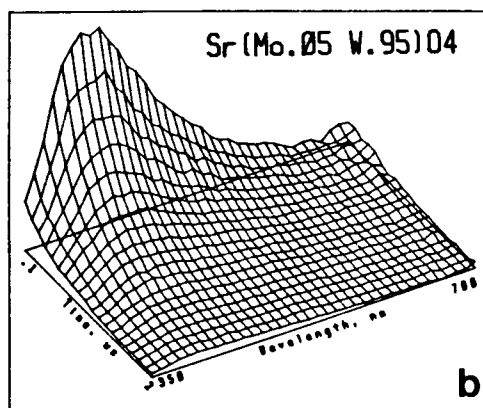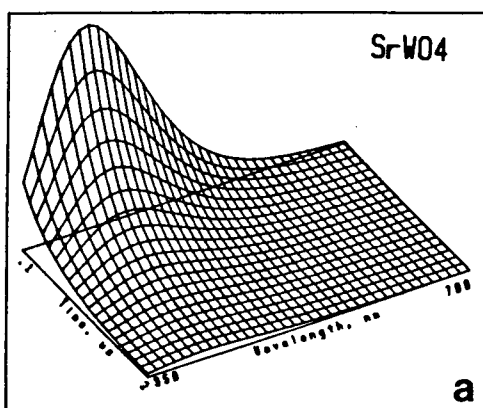
Figure 4.7   Luminescence spectra, 193 nm excitation, 100 ns
to 2000 ns, 350 nm to 700 nm. (a) $SrWO_4$, (b)
$Sr(Mo_{.02}W_{.98})O_4$,(c) $Sr(Mo_{.1}W_{.9})O_4$, (d)
$Sr(Mo_{.2}W_{.8})O_4$, (e) $Sr(Mo_{.3}W_{.8})O_4$, (f) $SrMoO_4$.
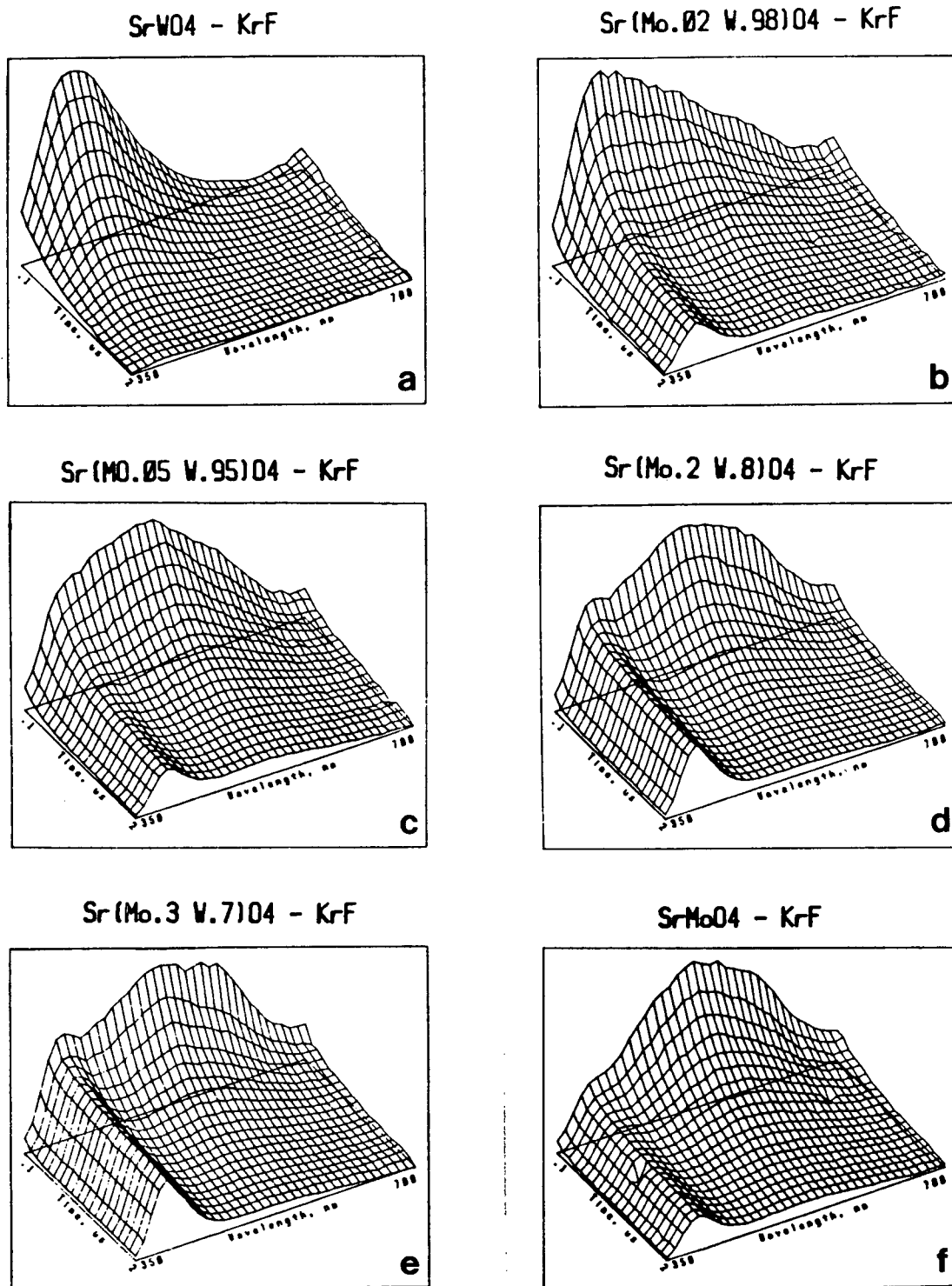
Figure 4.8 Luminescence spectra, 248 nm excitation, 100 ns to 2000 ns, 350 nm to 700 nm. (a) $SrWO_4$, (b) $Sr(Mo_{.02} W_{.98})O_4$, (c) $Sr(Mo_{.1} W_{.9})O_4$, (d) $Sr(Mo_{.2} W_{.8})O_4$, (e) $Sr(Mo_{.3} W_{.8})O_4$, (f) $SrMoO_4$.

quenching effect is somewhat understated in the display format used; the intensity of pure calcium molybdate is approximately one eighth that of pure calcium tungstate. Similar behavior is observed for the strontium molybdate-tungstate series excited at 193 nm as illustrated in Figure 4.7. The trend in the strontium series is similar to that of the calcium series, with the quenching effect of molybdate being even more pronounced.

The strontium series excited at 248 nm was examined; the series spectra are presented in Figure 4.8. Again, the quenching pattern is similar with the effect of molybdate being even more pronounced. In this series, molybdate luminescence dominates when present at levels less than 5%.

Tungstate luminescence lifetime is related to molybdate concentration as illustrated in the plots in Figure 4.9. The two isomorphous series were excited at 193 nm, and the lifetime information was extracted from the time-wavelength resolved spectra using the data reduction program listed in Appendix 4. The relationship shown between lifetime and molybdate concentration is empirical without appeal to any specific energy transfer model.

The quenching effects seen in these isomorphous series demonstrate the advantage of taking the multidimensional approach of time-wavelength resolved luminescence to extract additional information from the luminescence signal. This approach affords a more comprehensive understanding of the processes occurring in the system under study, which in turn

113
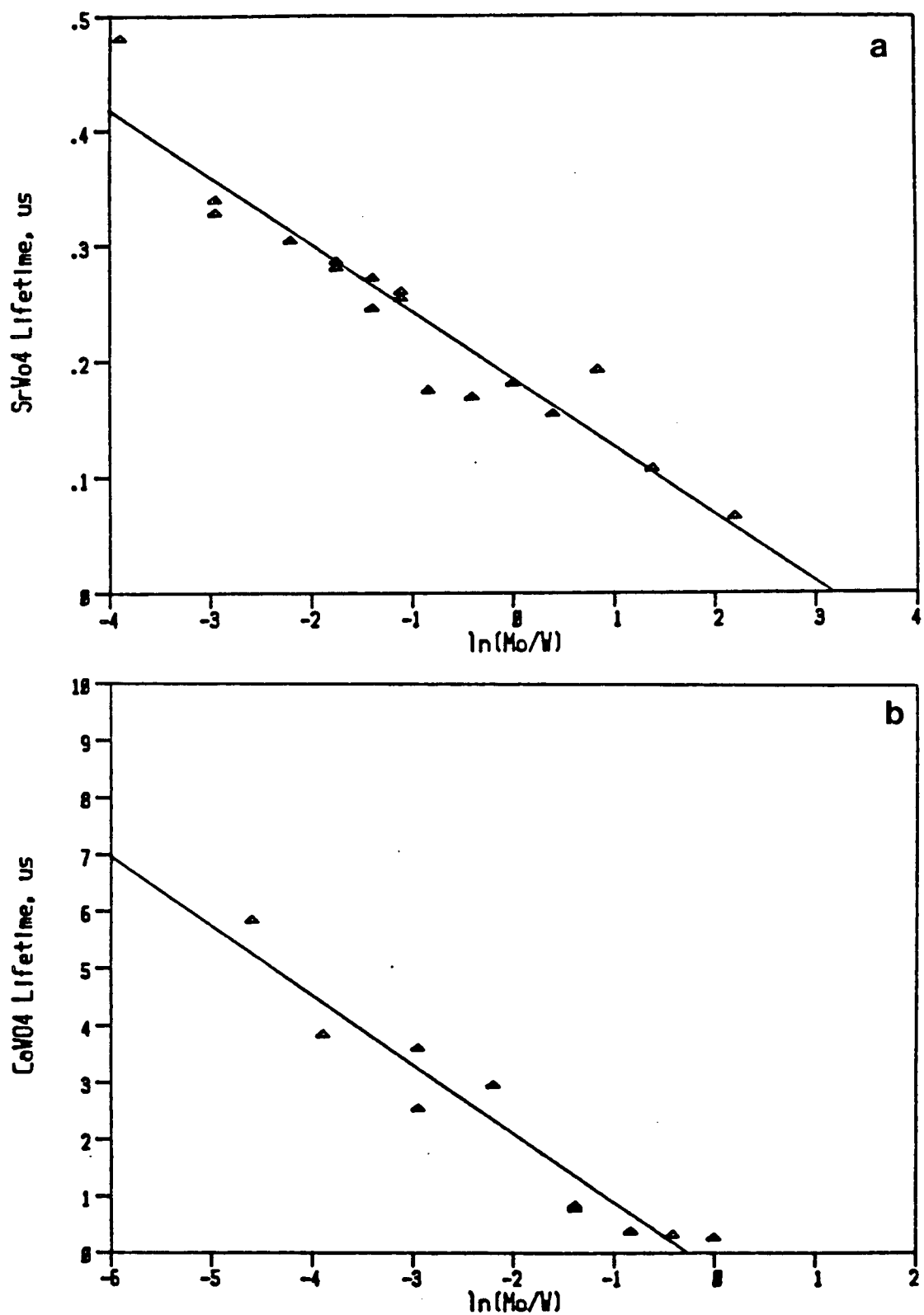
Figure 4.9   Relationship between tungstate lifetime and molybdate to tungstate ratio in mixed crystals, 193 nm excitaton. (a) Sr(Mo,W)O$_4$ system. (b) Ca(Mo,W)O$_4$ system.

leads to a more robust analytical scheme.

4.3 ZIRCONATES AND HAFNATES

Zirconium and hafnium have the most similar chemistries of all elements in the periodic chart. This similarity is exhibited both in their natural occurrence [89] and the extreme difficulties in their separation and analysis by chemical techniques. Both elements form extensive isomorphous series of compounds with each other. Atomic and mass spectroscopy are the most robust analytical techniques for the identification and quantitation of these elements.

Very little work has been reported in the literature on the luminescence properties of the alkaline earth zirconates and there are no reports on alkaline earth hafnate luminescence. The most reliable reports of zirconate luminescence are for mixed zirconium-silicon oxides [126-128], although trace titanium may have been the activator in the Gaft [126] and Lysakov [127] reports. Blasse [129] states that, for the weakly luminescent $BaZrSi_3O_9$, excitation is possible only for wavelengths less than 220 nm.

The properties of calcium zirconate as a host lattice for activators such as lead [130], manganese [131], and trivalent lanthanides [132] have been reported. However, no mention was made in these reports on the levels of hafnium present in the calcium zirconate host lattice.

The alkaline earth zirconates and hafnates used in this study were prepared from ultrapure zirconate and hafnate starting materials as outlined in chapter 2. Initial

115

attempts to measure luminescence spectra on the undoped compounds held in the quartz test tube cells were unsuccessful due to a combination of strong luminescence from the quartz cells and very weak luminescence from the compounds examined. A sample consisting of two Suprasil discs, clamped together to hold sample powders, was satisfactory. The Suprasil discs were weakly luminescent under either 193 nm or 248 nm excitation. Their time-wavelength resolved luminescence spectra are shown in Figure 4.10. The time-wavelength resolved spectra for pure and doped alkaline earth zirconates, hafnates, and oxides appear at the end of this chapter.

Contamination of the zirconate and hafnate powders with alkaline earth oxide was a distinct possibility, even though their presence was not indicated in the X-ray powder data. Spectra measured for the pure and doped alkaline earth oxides are included for comparison.

Attempts to extract spectral parameters from data collected on the pure alkaline earth zirconates and hafnates with the algorithm and model described earlier were unsuccessful. Luminescence decay does not appear to follow simple first order kinetics. This may be due to the presence of several emitting components or to energy migration effects. The observed luminescence decay is rapid and instrumental limitations may be responsible for apparent non-first order decay behavior.

The pure alkaline earth zirconates and hafnates do not

appear to luminesce at wavelengths greater than 270 nm when excited at 193 nm. However, under 248 nm excitation a prominent band centered in the 500 nm region appears along with a long lived band at 650 nm. The 650 nm band may be due to lattice defects or trace quantities of alkaline earth oxide present. The band in the 500 nm region shows changes in position, width, and lifetime among the different compounds investigated. Further exploitation of the data contained in these spectra is dependent on having a suitable data reduction process.

The effects of dopants added to the alkaline earth zirconates and hafnates was investigated. Generally, the added activator dominates the observed luminescence spectrum. Few differences were observed in the wavelength domain between excitation at 193 nm and 248 nm among the compounds studied. However, in the time domain some striking effects were observed.

In the lead activated compounds, the lifetime of the band associated with lead was markedly dependent on excitation wavelength. This phenomenon was observed for all the alkaline earth zirconates and hafnates studied without exception.

In the bismuth activated compounds, excitation wavelength dependent effects on the emission characteristic to bismuth were also observed. In this case, the effects appear to be more closely correlated with the alkaline earth ion rather than zirconate or hafnate.

In the thallium and antimony activated compounds, excitation wavelength dependent effects were noted but readily discernible patterns were not seen.

The differentiation between zirconate and hafnate in inorganic powders by time-wavelength resolved luminescence appears possible in simple systems such as the calcium and strontium compounds as can be seen in comparing Figures 4.12 (a) with 4.24 (a) and Figures 4.16 (a) with 4.28 (a).
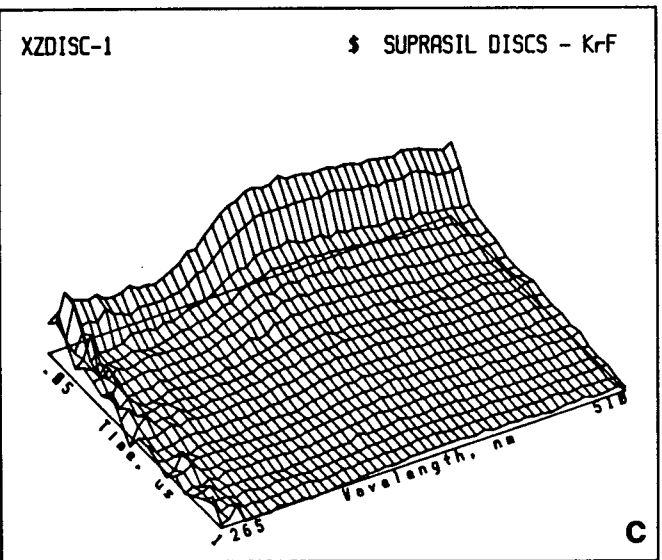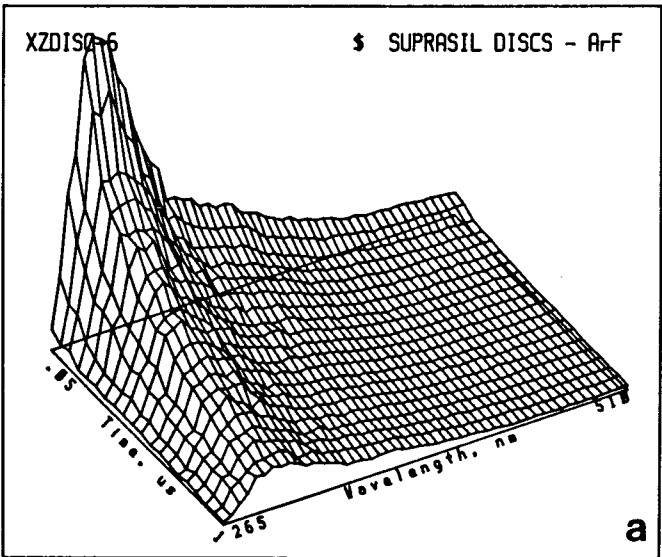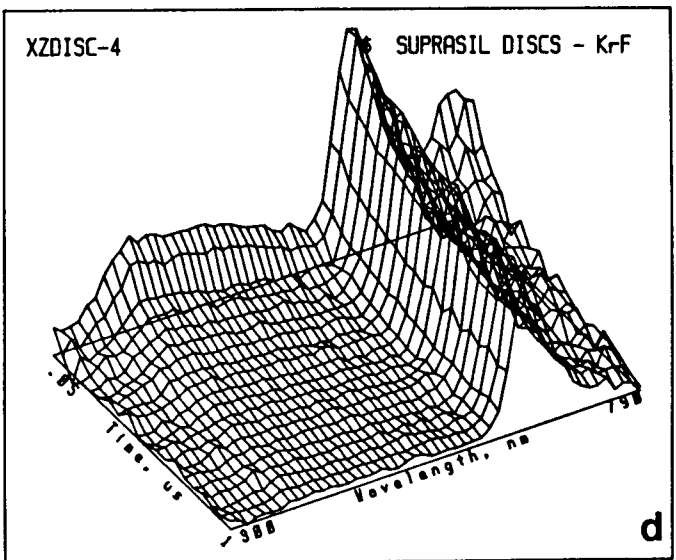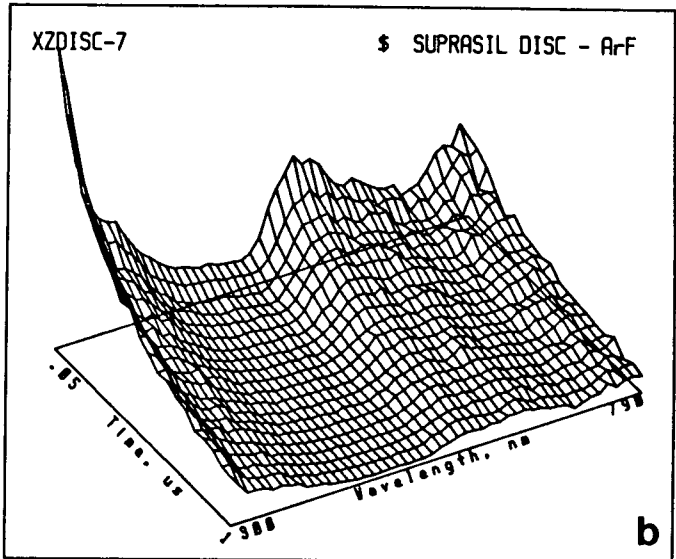
Figure 4.10 Suprasil disc luminescence spectra, 50 ns to 1000 ns. (a) 193 nm excitation, 265 nm to 510 nm. (b) 193 nm excitation, 300 to 790 nm. (c) 248 nm excitation, 265 nm to 510 nm. (d) 248 nm excitation, 300 nm to 790 nm.
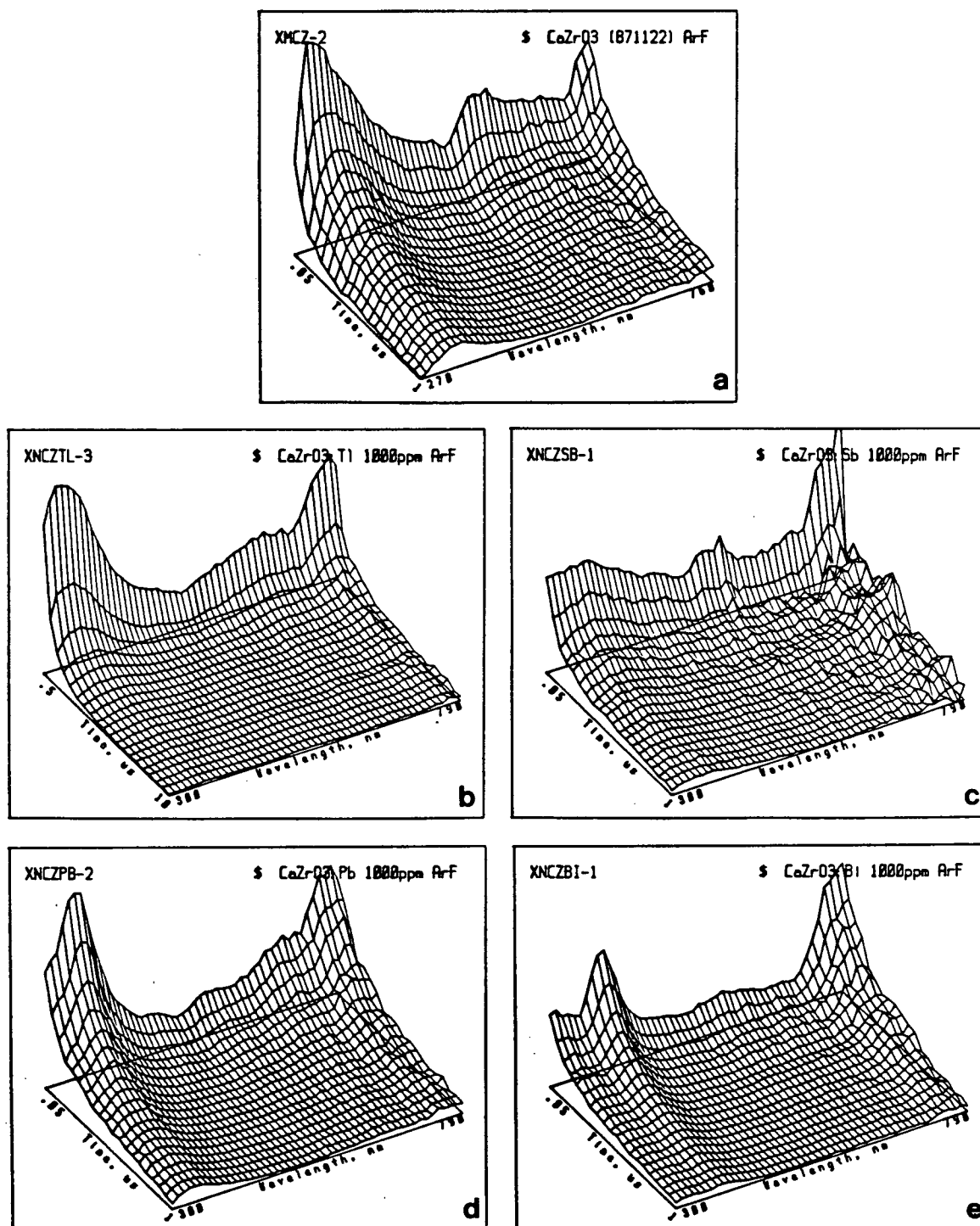
Figure 4.11 Calcium zirconate; excitation: 193 nm.
             (a) no dopant, 50 ns to 1000 ns, 270 nm to 760 nm
             (b) Tl doped, 500 ns to 10000 ns, 300 nm to 790 nm
             (c) Sb doped, 50 ns to 1000 ns, 300 nm to 790 nm
             (d) Pb doped, 50 ns to 1000 ns, 300 nm to 790 nm
             (e) Bi doped, 50 ns to 1000 ns, 300 nm to 790 nm

Figure 4.12 Calcium zirconate; excitation: 193 nm.
          (a) no dopant, 50 ns to 1000 ns, 265 nm to 570 nm
          (b) Tl doped, 500 ns to 10000 ns, 265 nm to 510 nm
          (c) Sb doped, 50 ns to 1000 ns, 265 nm to 510 nm
          (d) Pb doped, 50 ns to 1000 ns, 265 nm to 510 nm
          (e) Bi doped, 50 ns to 1000 ns, 265 nm to 510 nm

Figure 4.13 Calcium zirconate; excitation: 248 nm.
        (a) no dopant, 50 ns to 1000 ns, 300 nm to 790 nm
        (b) Tl doped, 50 ns to 1000 ns, 300 nm to 790 nm
        (c) Sb doped, 50 ns to 1000 ns, 300 nm to 790 nm
        (d) Pb doped, 50 ns to 1000 ns, 300 nm to 790 nm
        (e) Bi doped, 50 ns to 1000 ns, 300 nm to 790 nm

122

Figure 4.14 Calcium zirconate; excitation: 248 nm.
               (a) no dopant, 50 ns to 1000 ns, 265 nm to 510 nm
               (b) Tl doped, 50 ns to 1000 ns, 265 nm to 510 nm
               (c) Sb doped, 50 ns to 1000 ns, 265 nm to 510 nm
               (d) Pb doped, 50 ns to 1000 ns, 265 nm to 510 nm
               (e) Bi doped, 50 ns to 1000 ns, 265 nm to 510 nm
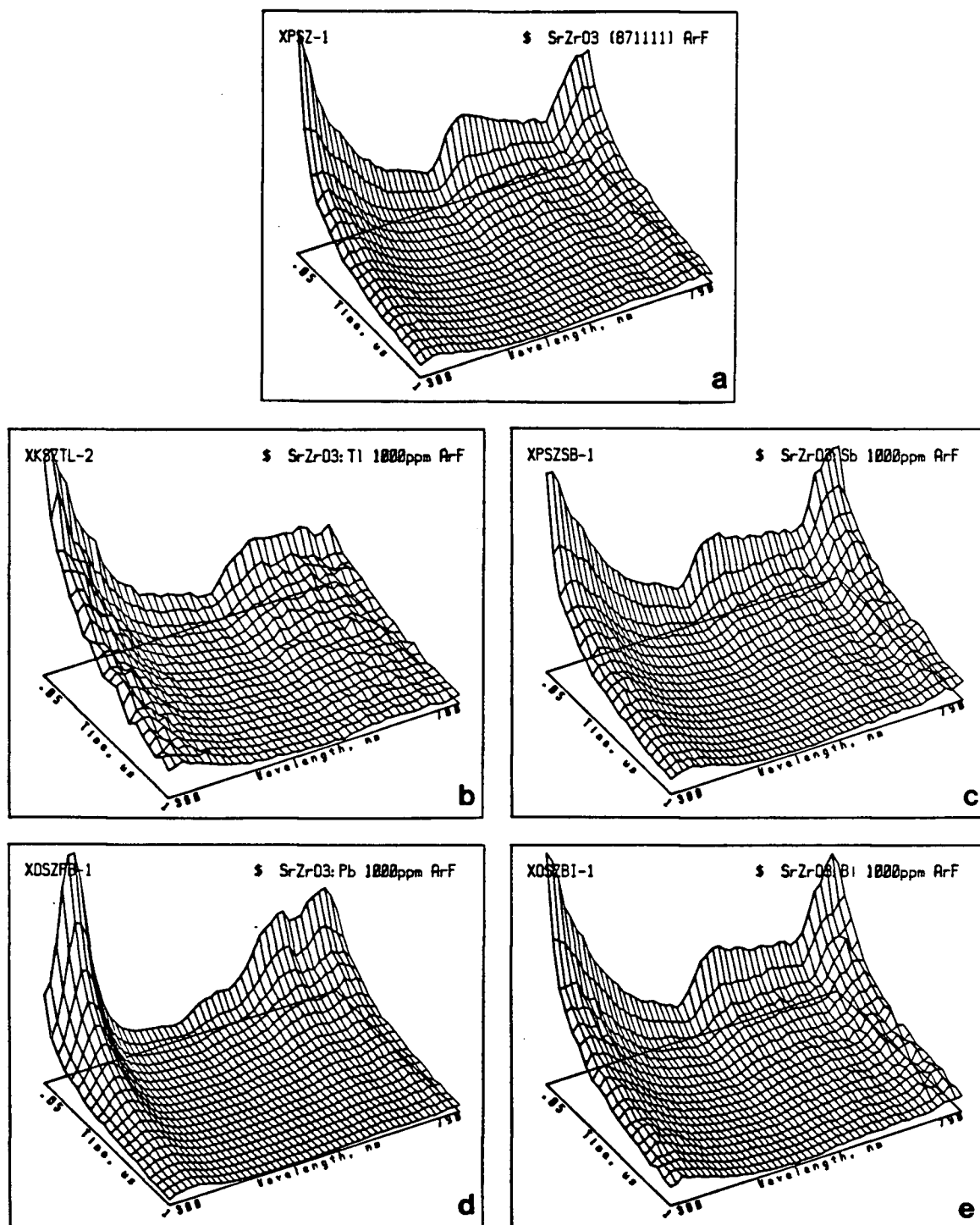
Figure 4.15 Strontium zirconate; excitation: 193 nm.
                (a) no dopant, 50 ns to 1000 ns, 300 nm to 790 nm
                (b) Tl doped, 50 ns to 1000 ns, 300 nm to 700 nm
                (c) Sb doped, 50 ns to 1000 ns, 300 nm to 790 nm
                (d) Pb doped, 50 ns to 1000 ns, 300 nm to 790 nm
                (e) Bi doped, 50 ns to 1000 ns, 300 nm to 790 nm
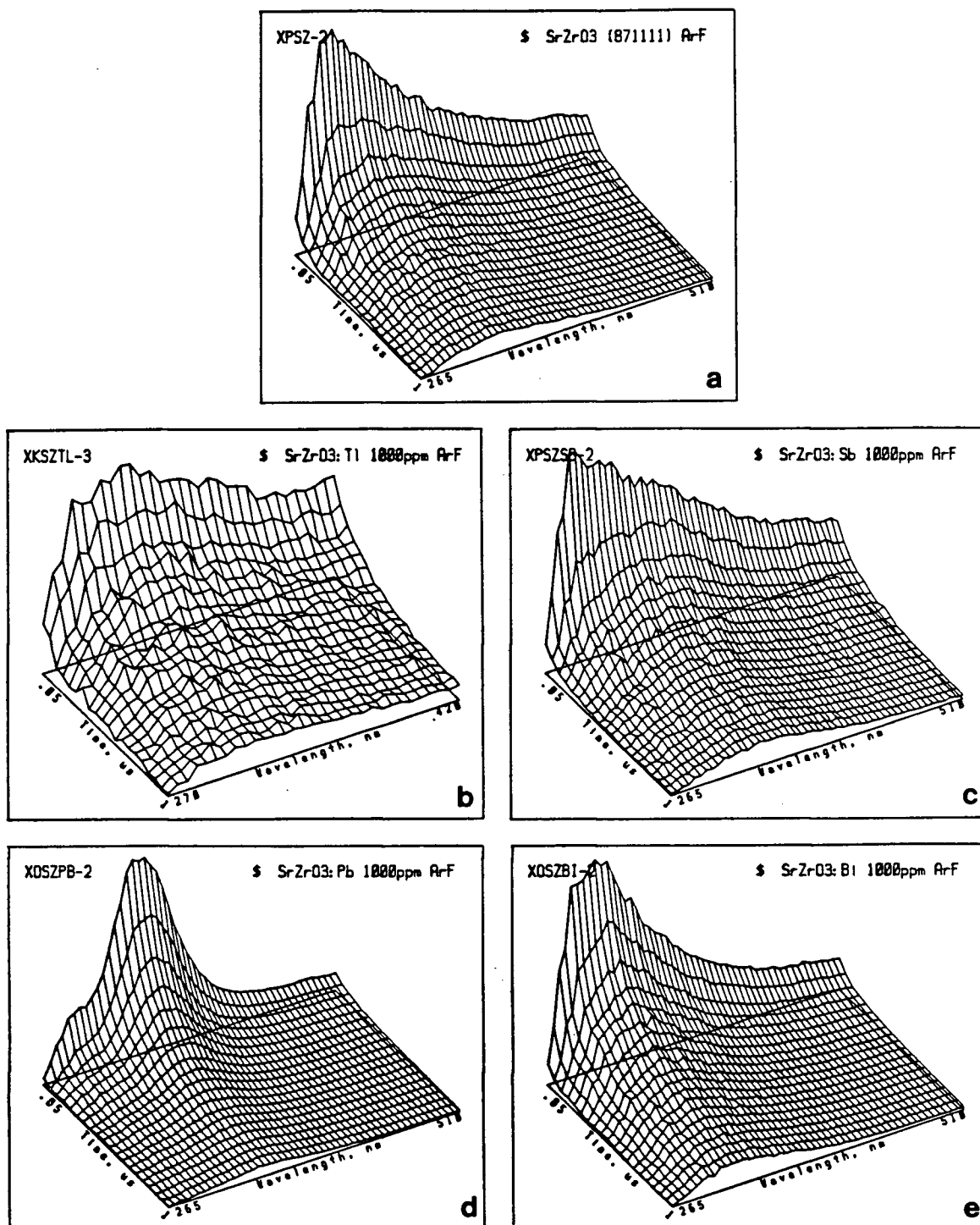
Figure 4.16 Strontium zirconate; excitation: 193 nm.
    (a) no dopant, 50 ns to 1000 ns, 265 nm to 510 nm
    (b) Tl doped, 50 ns to 1000 ns, 270 nm to 420 nm
    (c) Sb doped, 50 ns to 1000 ns, 265 nm to 510 nm
    (d) Pb doped, 50 ns to 1000 ns, 265 nm to 510 nm
    (e) Bi doped, 50 ns to 1000 ns, 265 nm to 510 nm

125
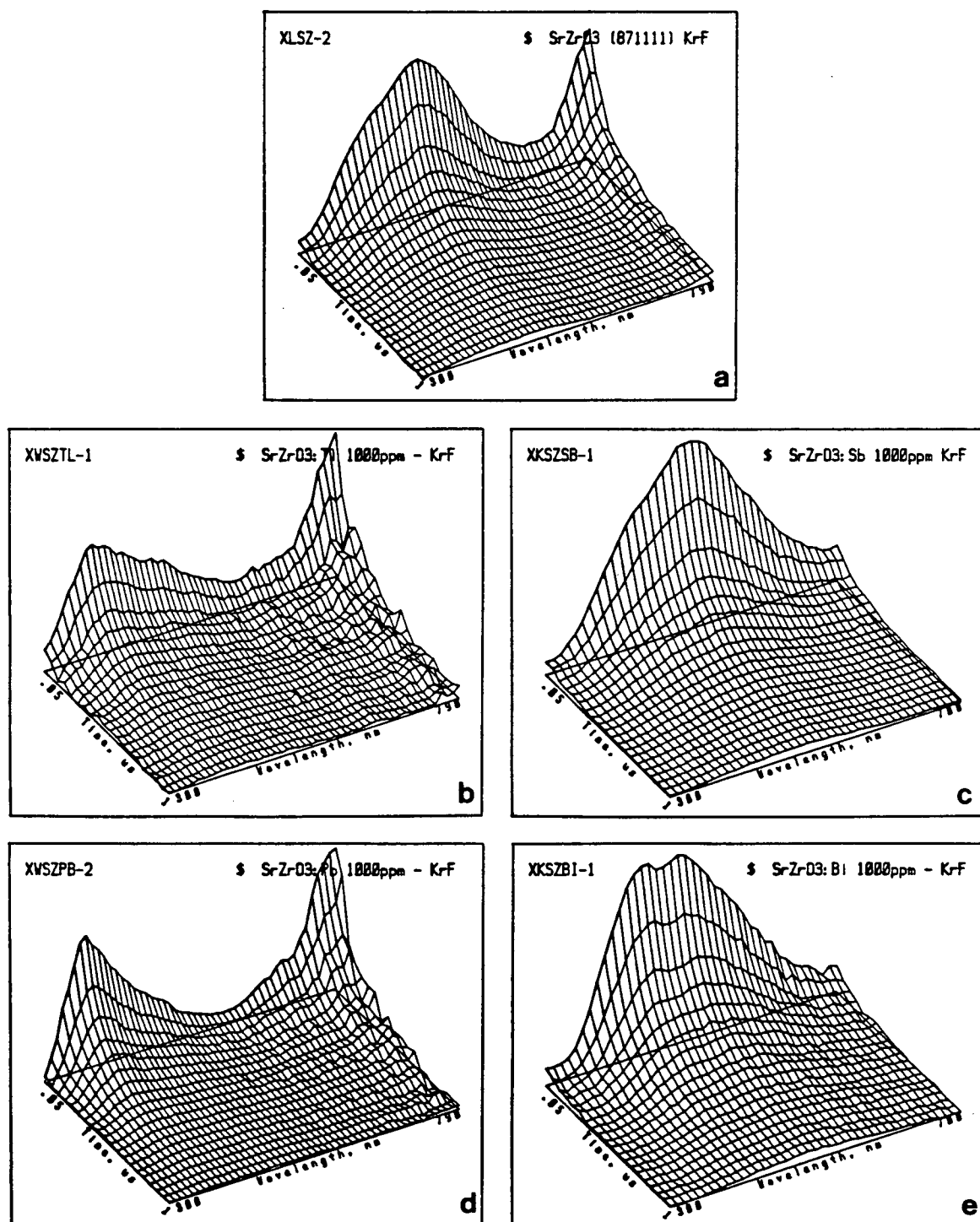
Figure 4.17 Strontium zirconate; excitation: 248 nm.
    (a) no dopant, 50 ns to 1000 ns, 300 nm to 790 nm
    (b) Tl doped, 50 ns to 1000 ns, 300 nm to 790 nm
    (c) Sb doped, 50 ns to 1000 ns, 300 nm to 700 nm
    (d) Pb doped, 50 ns to 1000 ns, 300 nm to 790 nm
    (e) Bi doped, 50 ns to 1000 ns, 300 nm to 700 nm
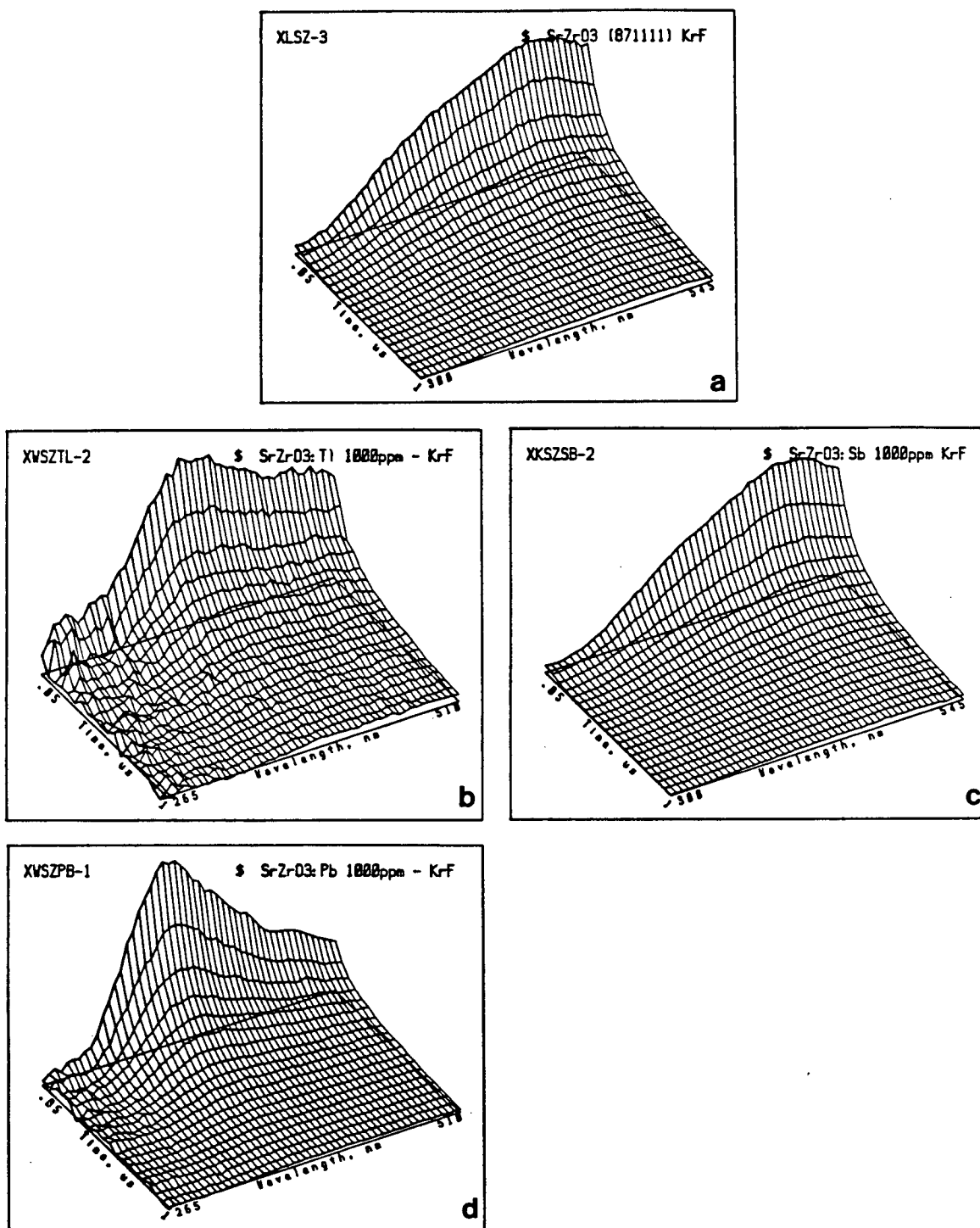
Figure 4.18 Strontium zirconate; excitation: 248 nm.
(a) no dopant, 50 ns to 1000 ns, 300 nm to 545 nm
(b) Tl doped, 50 ns to 1000 ns, 265 nm to 510 nm
(c) Sb doped, 50 ns to 1000 ns, 300 nm to 545 nm
(d) Pb doped, 50 ns to 1000 ns, 265 nm to 510 nm
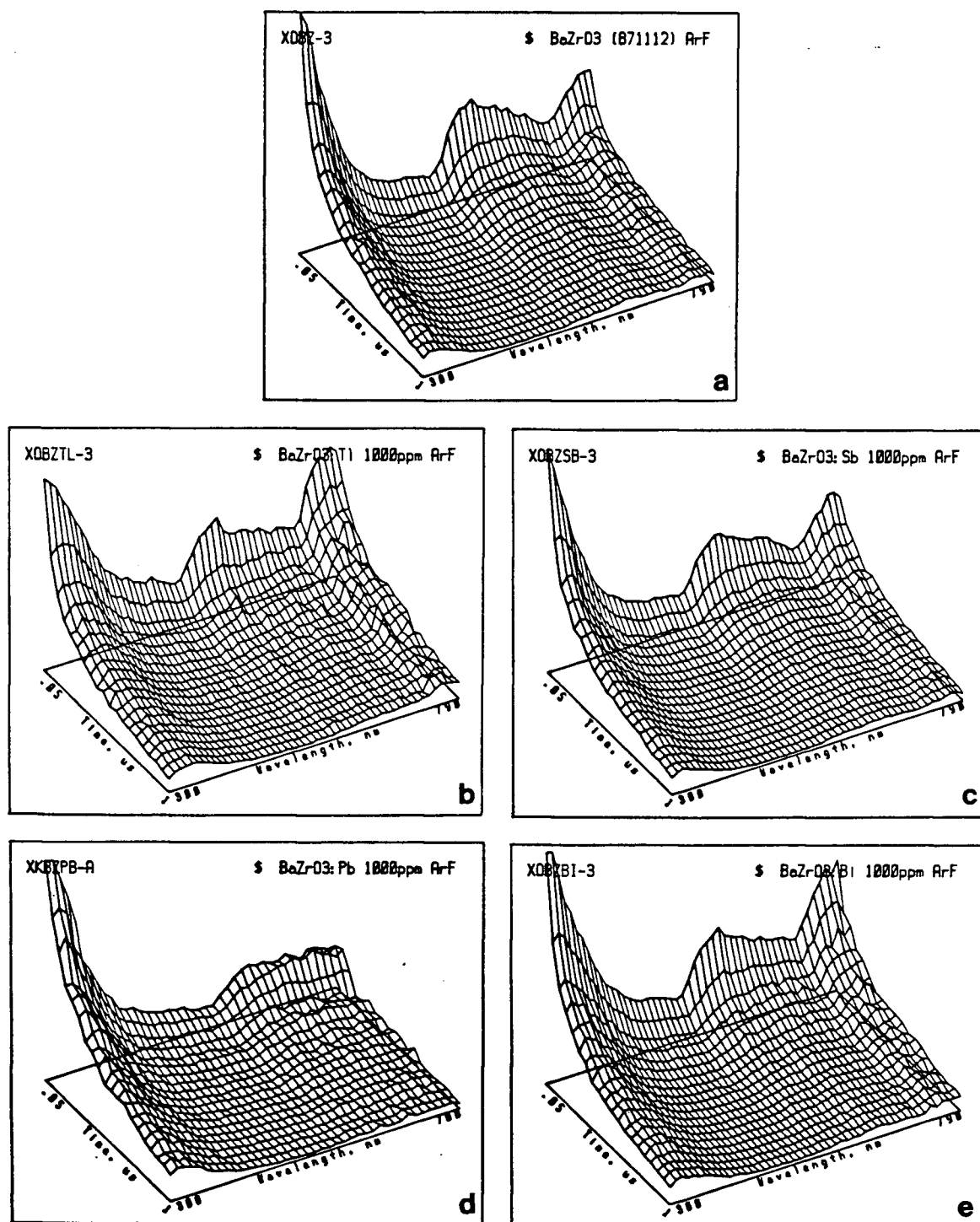
Figure 4.19 Barium zirconate; excitation: 193 nm.
          (a) no dopant, 50 ns to 1000 ns, 300 nm to 790 nm
          (b) Tl doped, 50 ns to 1000 ns, 300 nm to 790 nm
          (c) Sb doped, 50 ns to 1000 ns, 300 nm to 790 nm
          (d) Pb doped, 50 ns to 1000 ns, 300 nm to 700 nm
          (e) Bi doped, 50 ns to 1000 ns, 300 nm to 790 nm
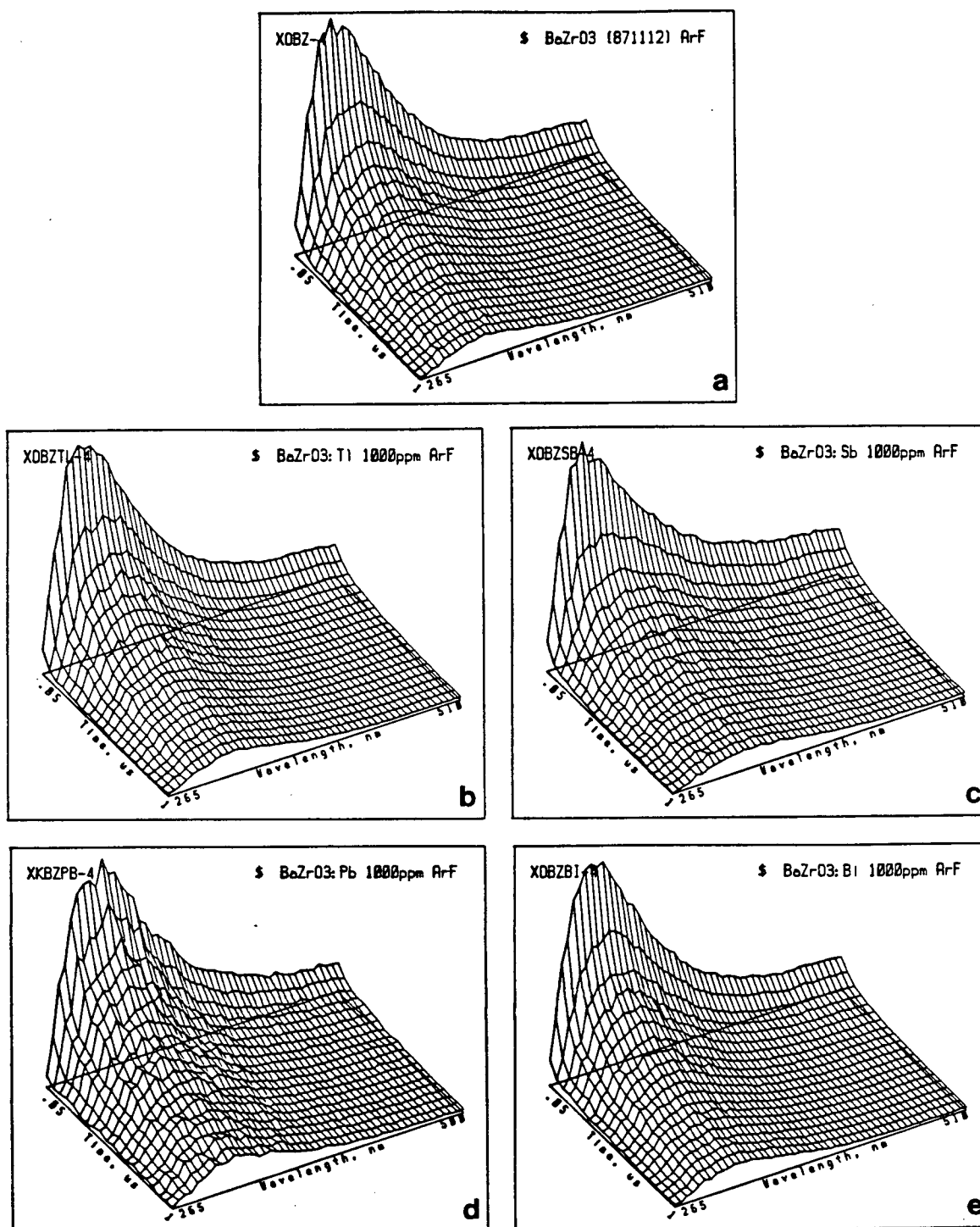
Figure 4.20 Barium zirconate; excitation: 193 nm.
(a) no dopant, 50 ns to 1000 ns, 265 nm to 510 nm
(b) Tl doped, 50 ns to 1000 ns, 265 nm to 510 nm
(c) Sb doped, 50 ns to 1000 ns, 265 nm to 510 nm
(d) Pb doped, 50 ns to 1000 ns, 265 nm to 500 nm
(e) Bi doped, 50 ns to 1000 ns, 265 nm to 510 nm
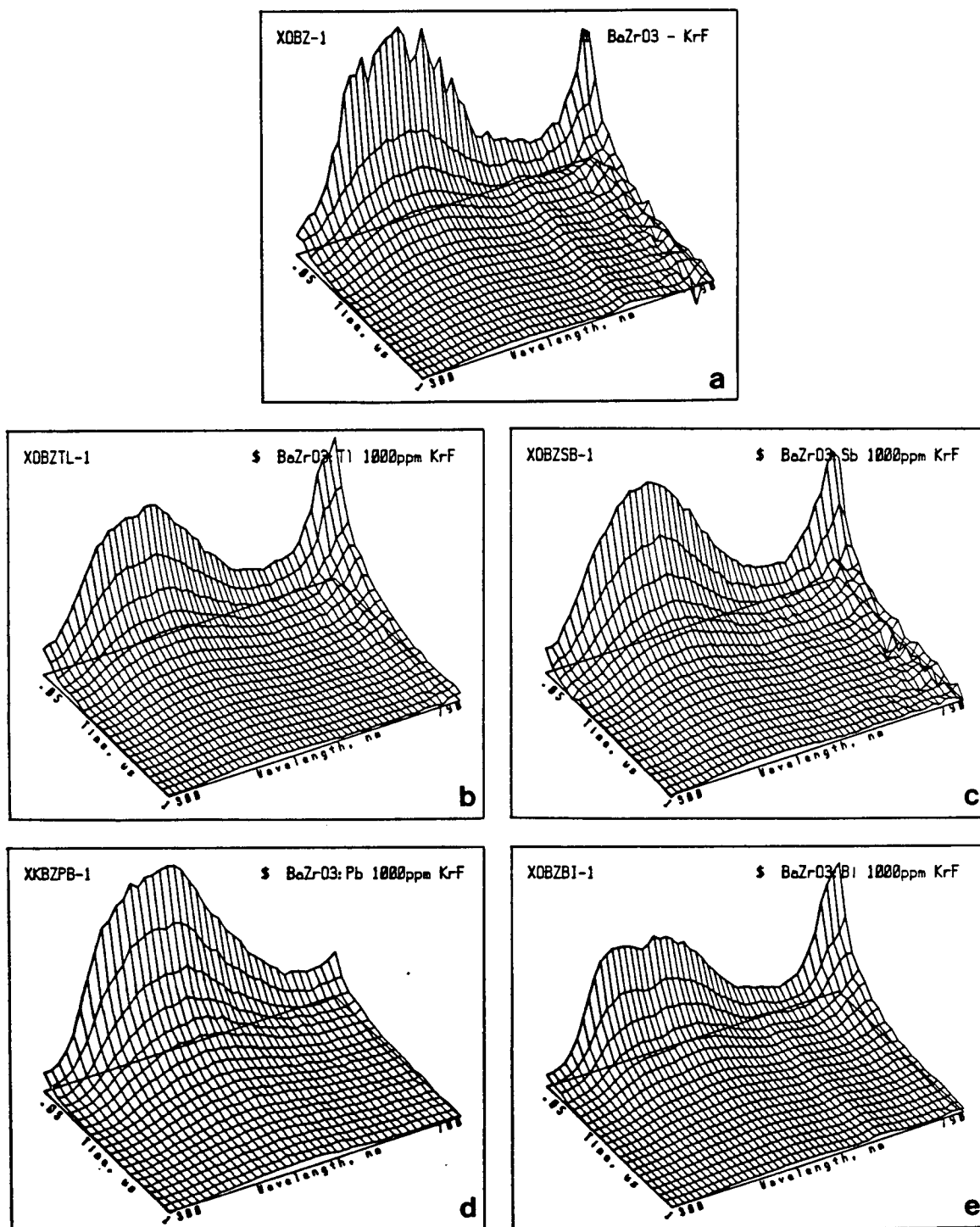
Figure 4.21 Barium zirconate; excitation: 248 nm.
(a) no dopant, 50 ns to 1000 ns, 300 nm to 790 nm
(b) Tl doped, 50 ns to 1000 ns, 300 nm to 790 nm
(c) Sb doped, 50 ns to 1000 ns, 300 nm to 700 nm
(d) Pb doped, 50 ns to 1000 ns, 300 nm to 790 nm
(e) Bi doped, 50 ns to 1000 ns, 300 nm to 700 nm
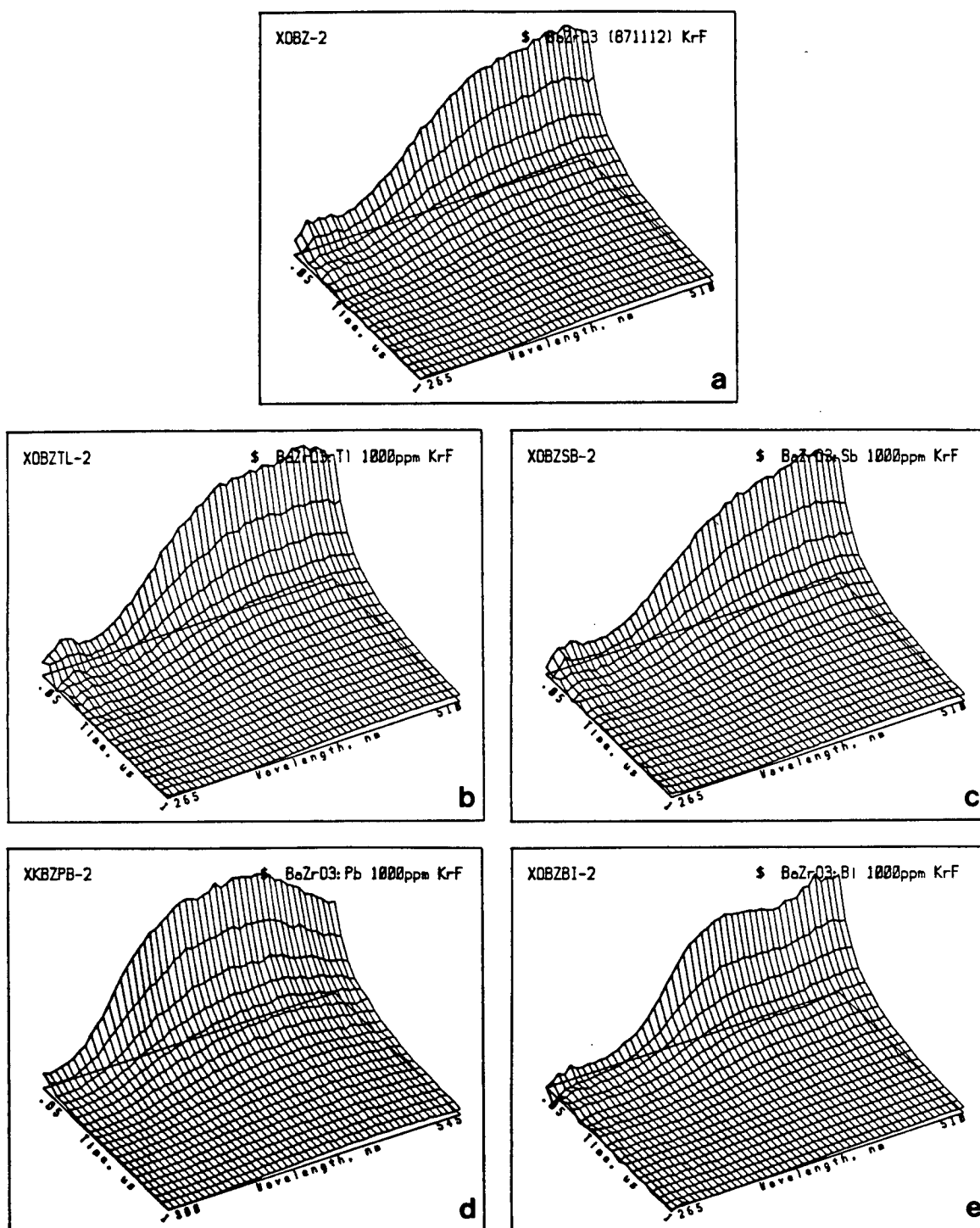
Figure 4.22 Barium zirconate; excitation: 248 nm.
(a) no dopant, 50 ns to 1000 ns, 265 nm to 510 nm
(b) Tl doped, 50 ns to 1000 ns, 265 nm to 510 nm
(c) Sb doped, 50 ns to 1000 ns, 265 nm to 510nm
(d) Pb doped, 50 ns to 1000 ns, 300 nm to 545 nm
(e) Bi doped, 50 ns to 1000 ns, 265 nm to 510 nm
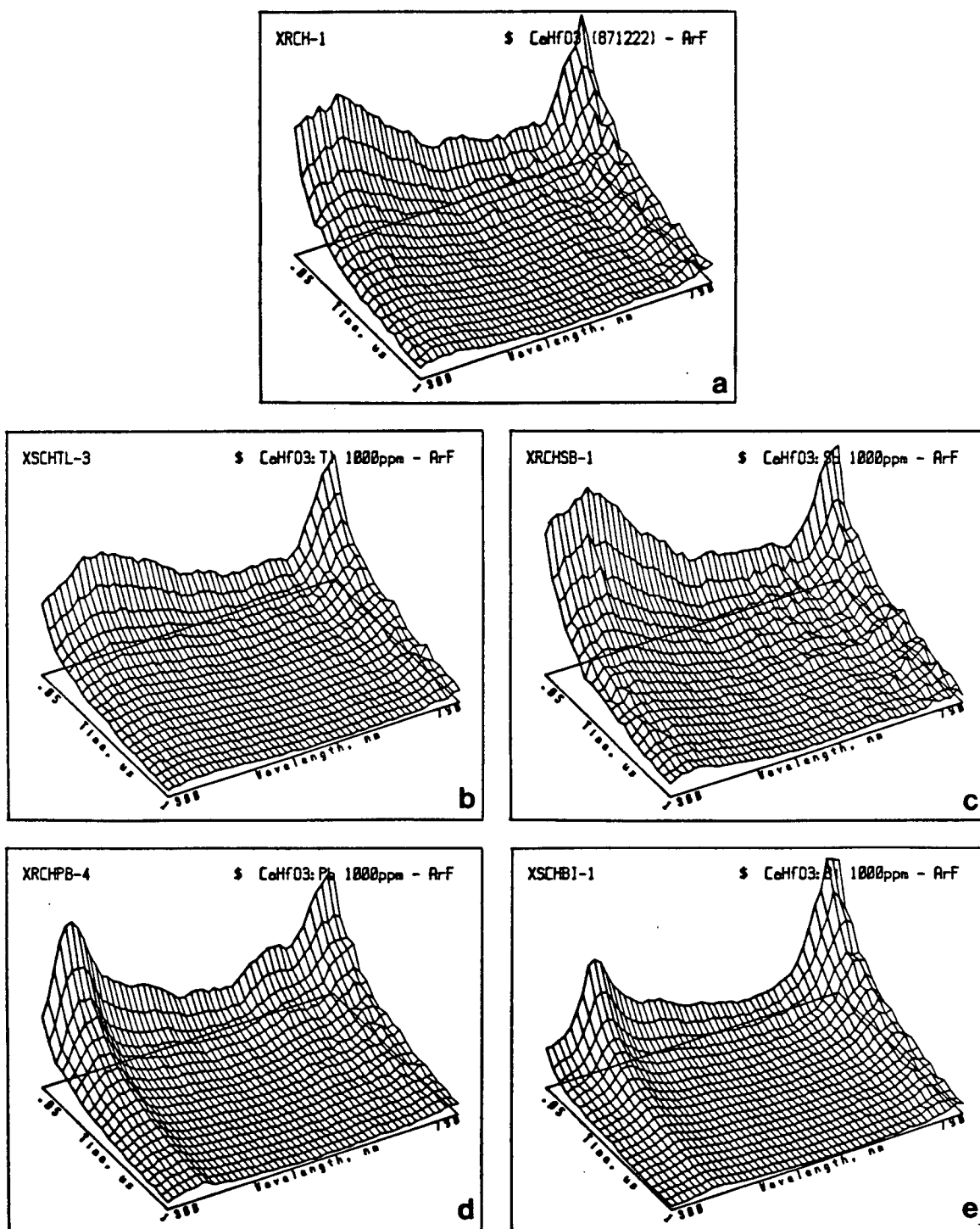
Figure 4.23 Calcium hafnate; excitation: 193 nm.
(a) no dopant, 50 ns to 1000 ns, 300 nm to 790 nm
(b) Tl doped, 50 ns to 1000 ns, 300 nm to 790 nm
(c) Sb doped, 50 ns to 1000 ns, 300 nm to 790 nm
(d) Pb doped, 50 ns to 1000 ns, 300 nm to 790 nm
(e) Bi doped, 50 ns to 1000 ns, 300 nm to 790 nm
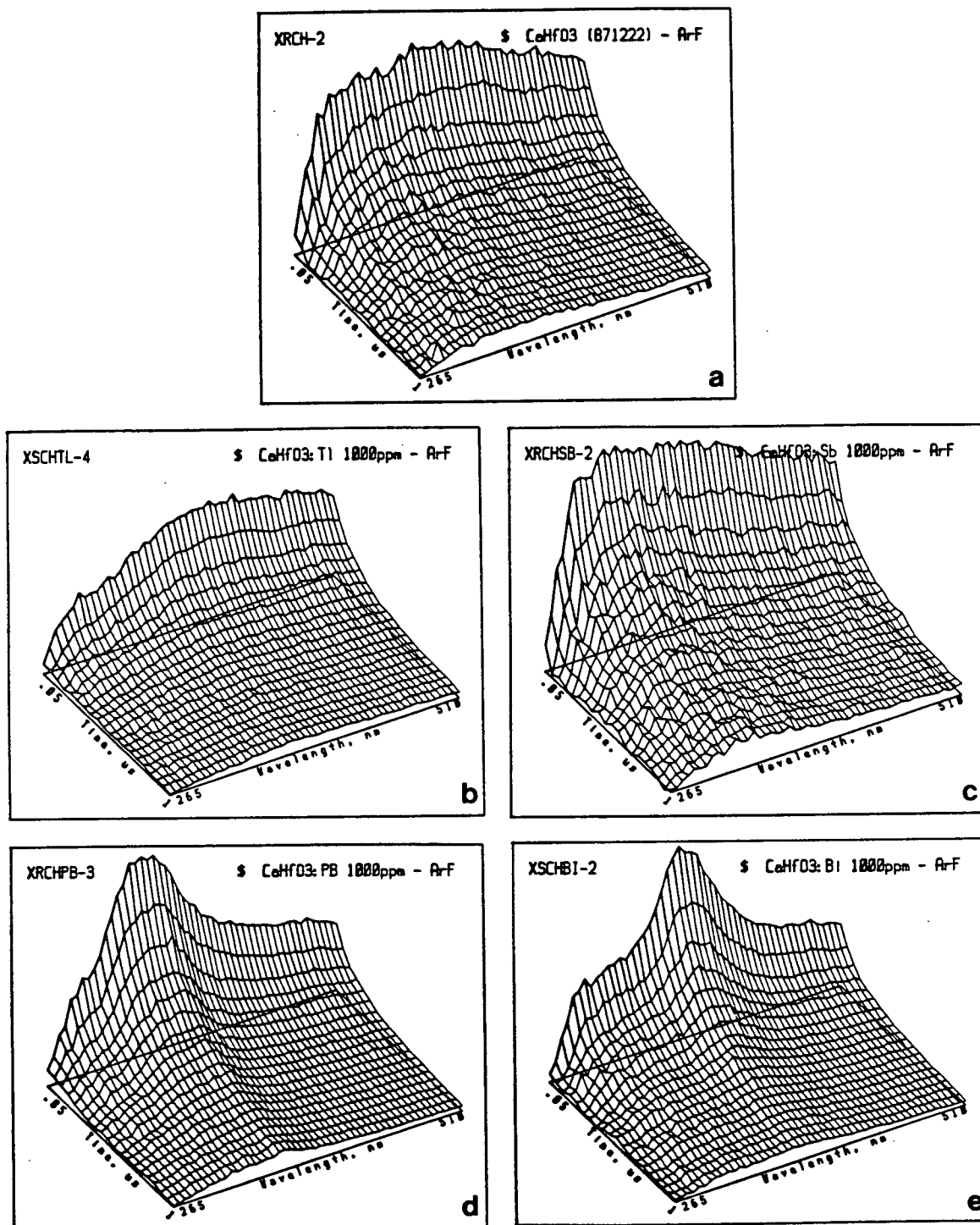
Figure 4.24 Calcium hafnate; excitation: 193 nm.
(a) no dopant, 50 ns to 1000 ns, 265 nm to 510 nm
(b) Tl doped, 50 ns to 1000 ns, 265 nm to 510 nm
(c) Sb doped, 50 ns to 1000 ns, 265 nm to 510 nm
(d) Pb doped, 50 ns to 1000 ns, 265 nm to 510 nm
(e) Bi doped, 50 ns to 1000 ns, 265 nm to 510 nm
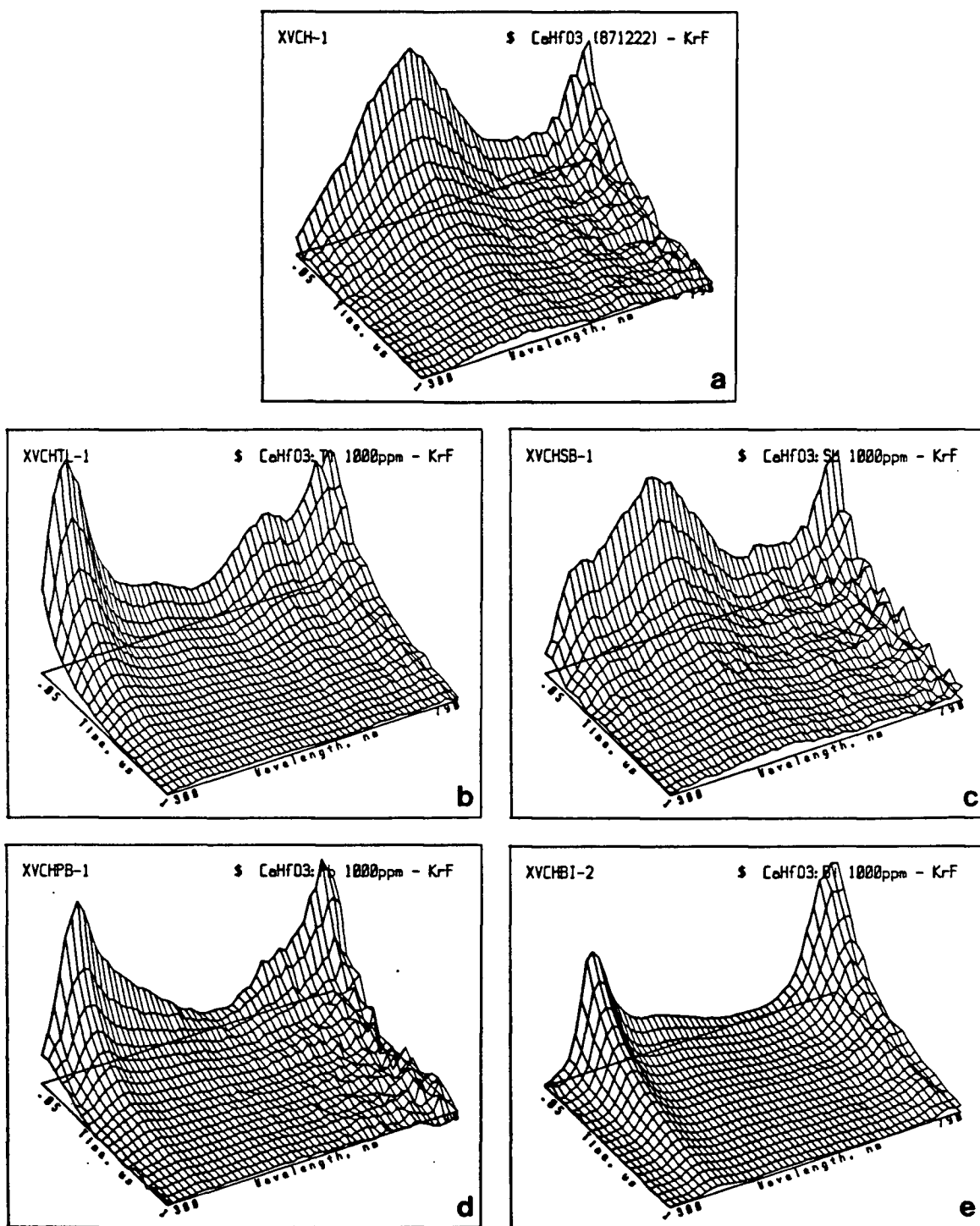
Figure 4.25 Calcium hafnate; excitation: 248 nm.
        (a) no dopant, 50 ns to 1000 ns, 300 nm to 790 nm
        (b) Tl doped, 50 ns to 1000 ns, 300 nm to 790 nm
        (c) Sb doped, 50 ns to 1000 ns, 300 nm to 790 nm
        (d) Pb doped, 50 ns to 1000 ns, 300 nm to 790 nm
        (e) Bi doped, 50 ns to 1000 ns, 300 nm to 790 nm
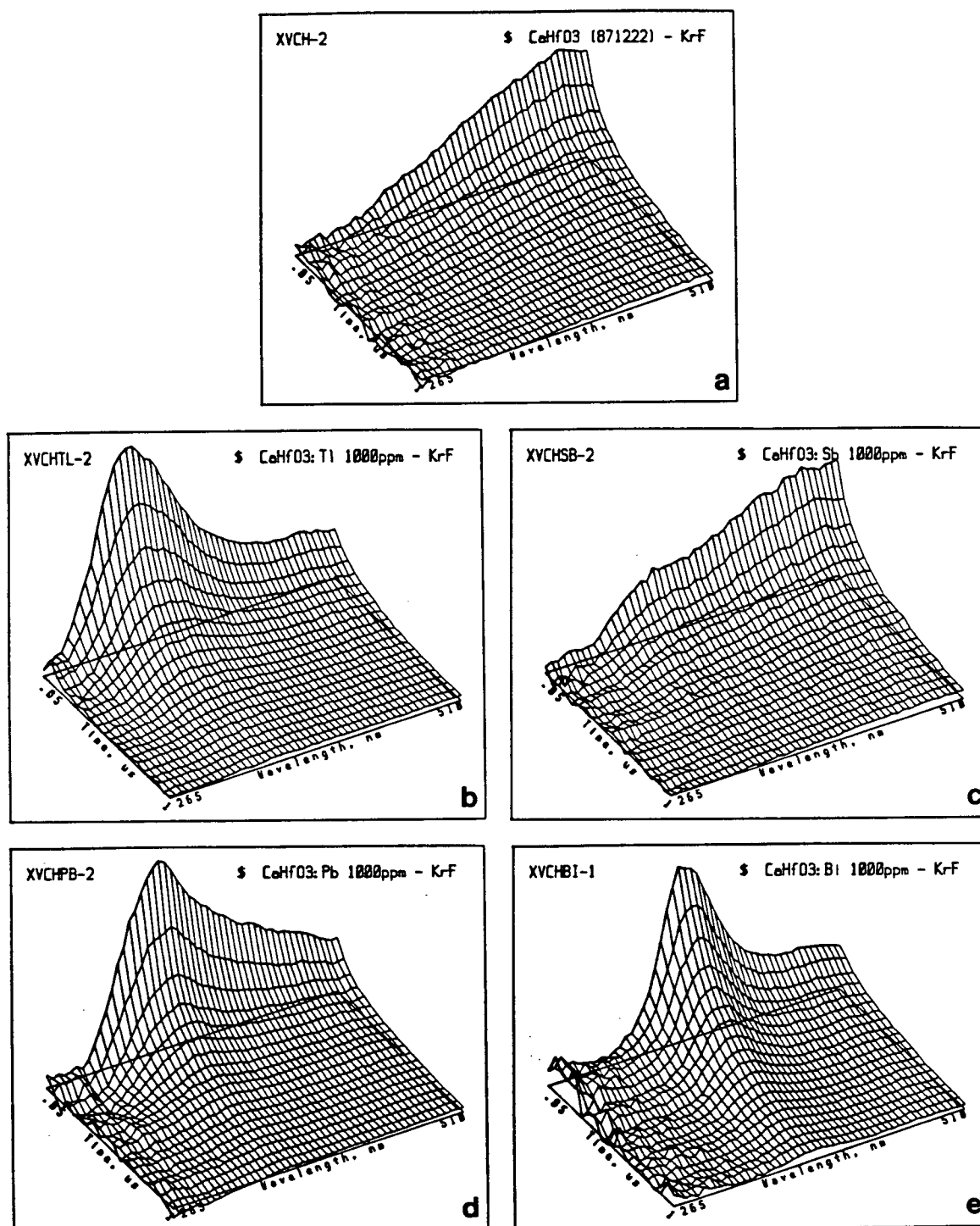
Figure 4.26 Calcium hafnate; excitation: 248 nm.
    (a) no dopant, 50 ns to 1000 ns, 265 nm to 510 nm
    (b) Tl doped, 50 ns to 1000 ns, 265 nm to 510 nm
    (c) Sb doped, 50 ns to 1000 ns, 265 nm to 510 nm
    (d) Pb doped, 50 ns to 1000 ns, 265 nm to 510 nm
    (e) Bi doped, 50 ns to 1000 ns, 265 nm to 510 nm

135
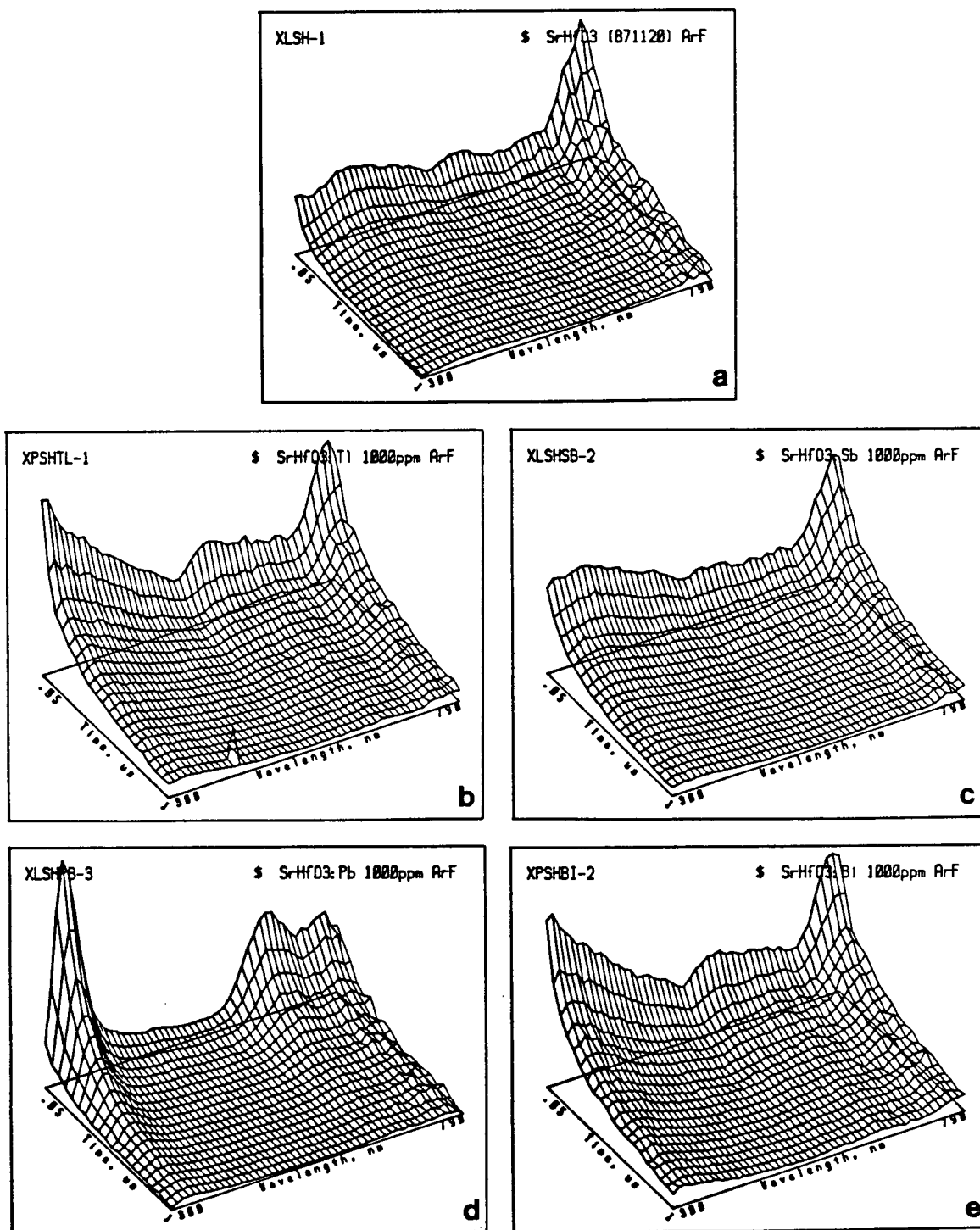
Figure 4.27 Strontium hafnate; excitation: 193 nm.
        (a) no dopant, 50 ns to 1000 ns, 300 nm to 790 nm
        (b) Tl doped, 50 ns to 1000 ns, 300 nm to 790 nm
        (c) Sb doped, 50 ns to 1000 ns, 300 nm to 790 nm
        (d) Pb doped, 50 ns to 1000 ns, 300 nm to 790 nm
        (e) Bi doped, 50 ns to 1000 ns, 300 nm to 790 nm

136
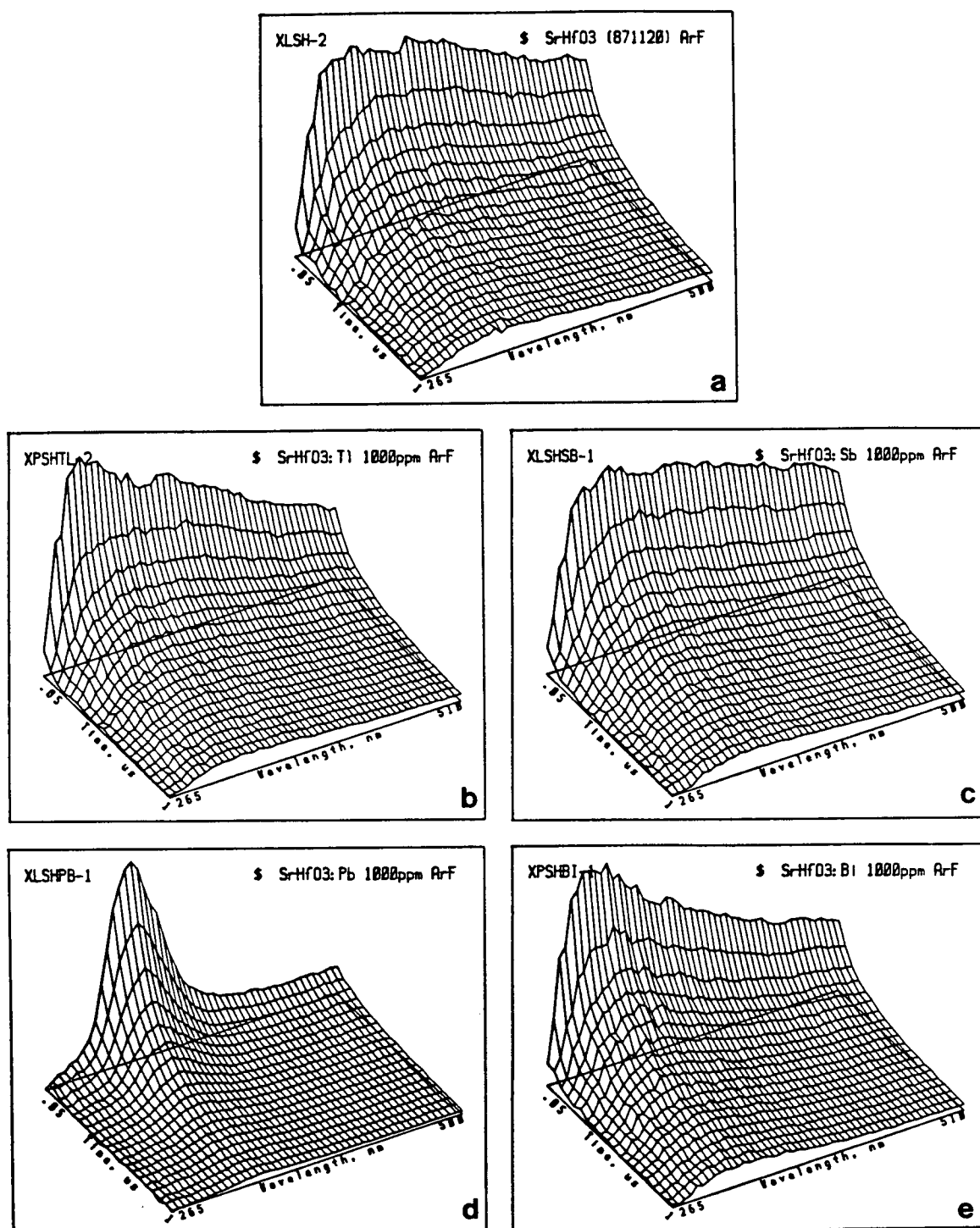
Figure 4.28 Strontium hafnate; excitation: 193 nm.
        (a) no dopant, 50 ns to 1000 ns, 265 nm to 500 nm
        (b) Tl doped, 50 ns to 1000 ns, 265 nm to 500 nm
        (c) Sb doped, 50 ns to 1000 ns, 265 nm to 500 nm
        (d) Pb doped, 50 ns to 1000 ns, 265 nm to 500 nm
        (e) Bi doped, 50 ns to 1000 ns, 265 nm to 500 nm

137
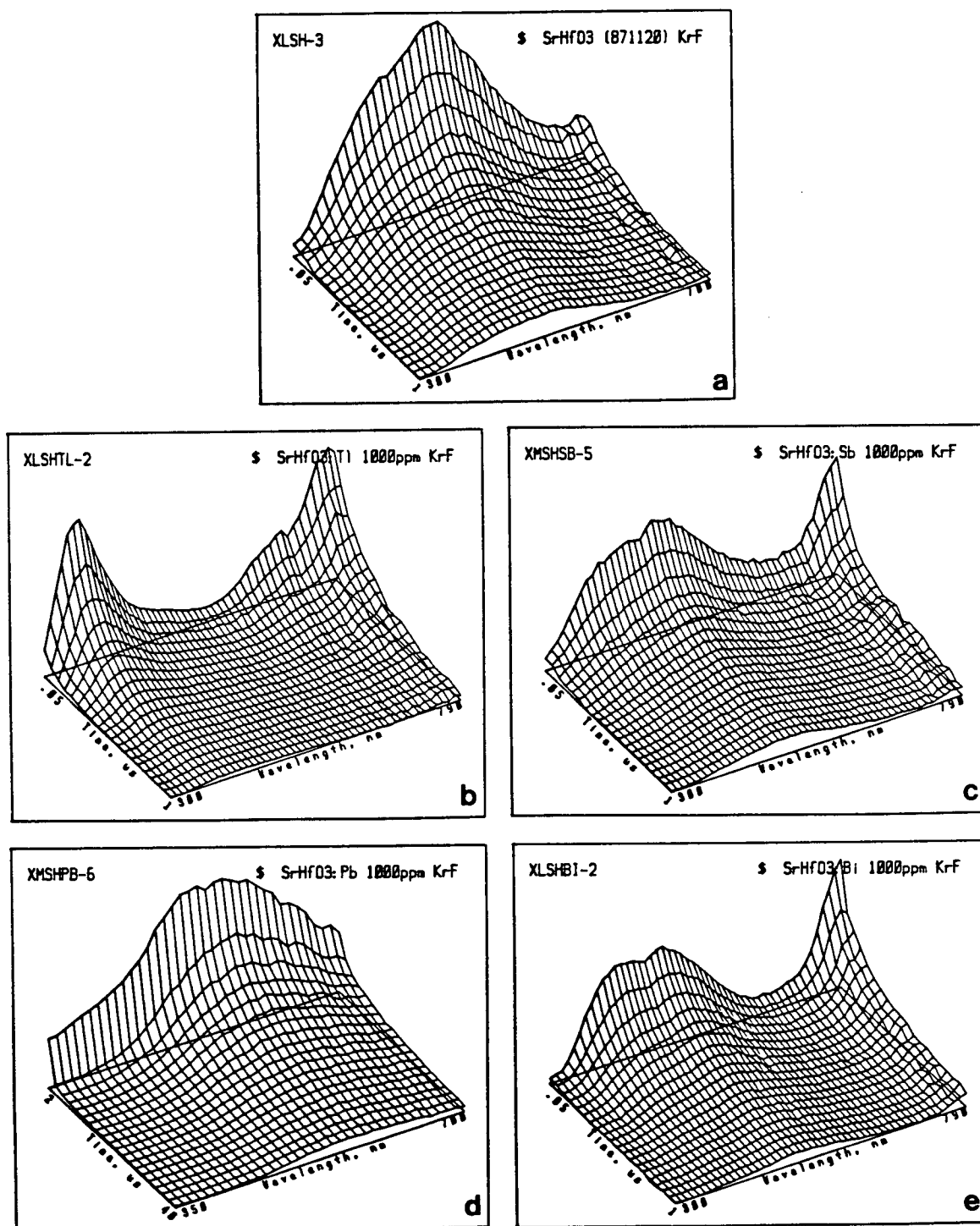
Figure 4.29 Strontium hafnate; excitation: 248 nm.
(a) no dopant, 50 ns to 1000 ns, 300 nm to 700 nm
(b) Tl doped, 50 ns to 1000 ns, 300 nm to 790 nm
(c) Sb doped, 50 ns to 1000 ns, 300 nm to 790 nm
(d) Pb doped, 2000 ns to 40000 ns, 350 nm to 700 nm
(e) Bi doped, 50 ns to 1000 ns, 300 nm to 790 nm
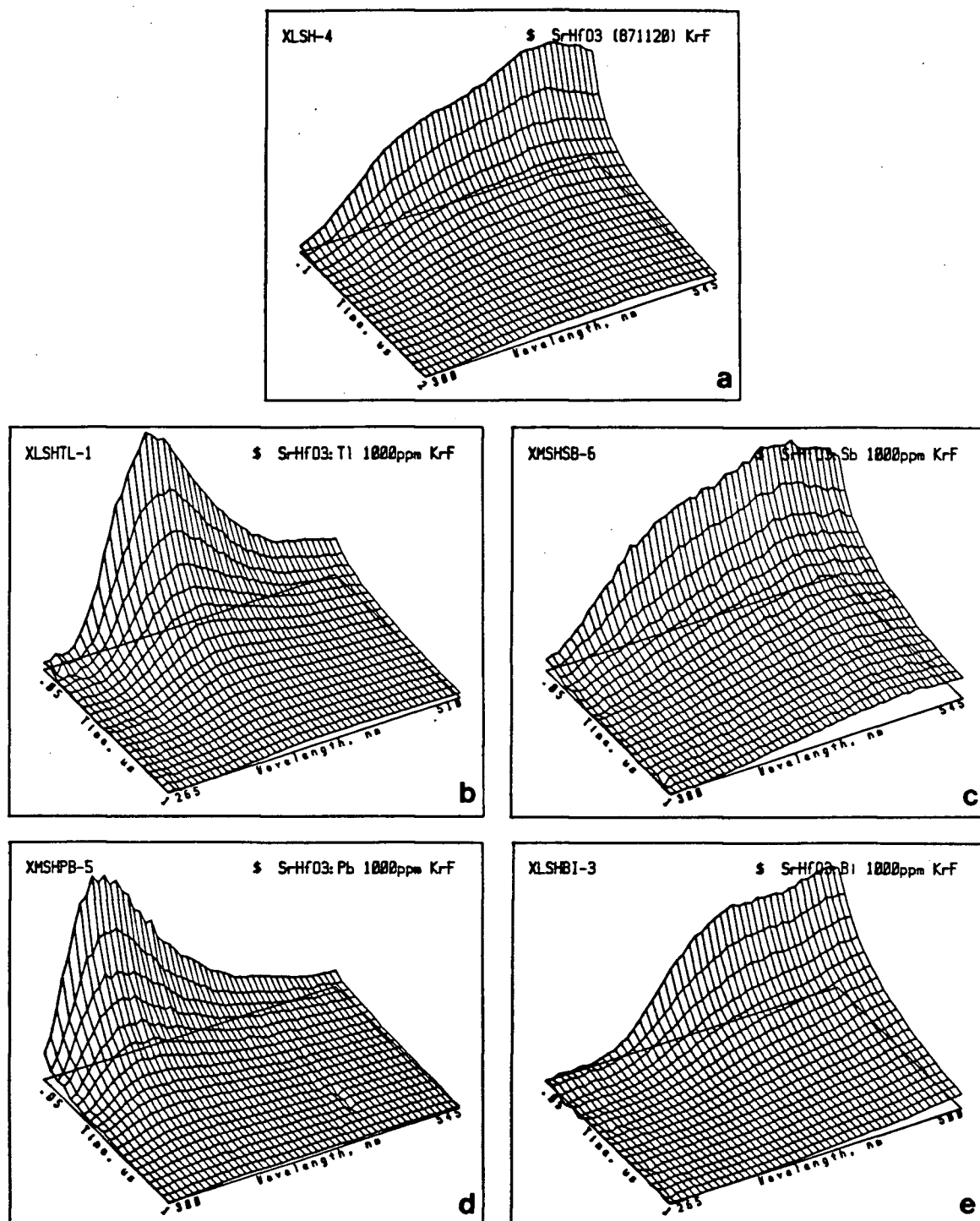
Figure 4.30 Strontium hafnate; excitation: 248 nm.
          (a) no dopant, 100 ns to 2000 ns, 300 nm to 545 nm
          (b) Tl doped, 50 ns to 1000 ns, 265 nm to 510 nm
          (c) Sb doped, 50 ns to 1000 ns, 300 nm to 545 nm
          (d) Pb doped, 50 ns to 1000 ns, 300 nm to 545 nm
          (e) Bi doped, 50 ns to 1000 ns, 265 nm to 500 nm
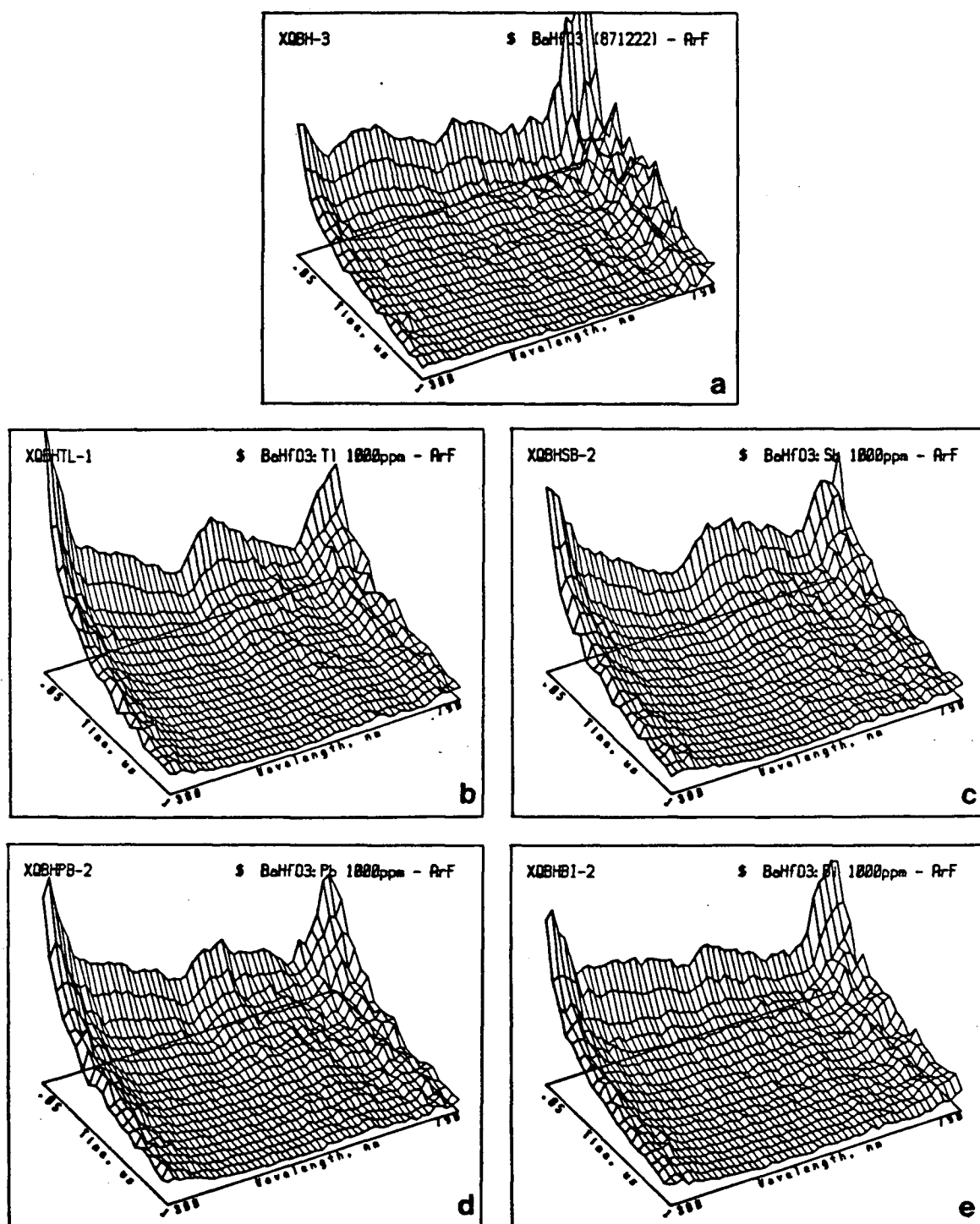
Figure 4.31 Barium hafnate; excitation: 193 nm.
(a) no dopant, 50 ns to 1000 ns, 300 nm to 790 nm
(b) Tl doped, 50 ns to 1000 ns, 300 nm to 790 nm
(c) Sb doped, 50 ns to 1000 ns, 300 nm to 790 nm
(d) Pb doped, 50 ns to 1000 ns, 300 nm to 790 nm
(e) Bi doped, 50 ns to 1000 ns, 300 nm to 790 nm
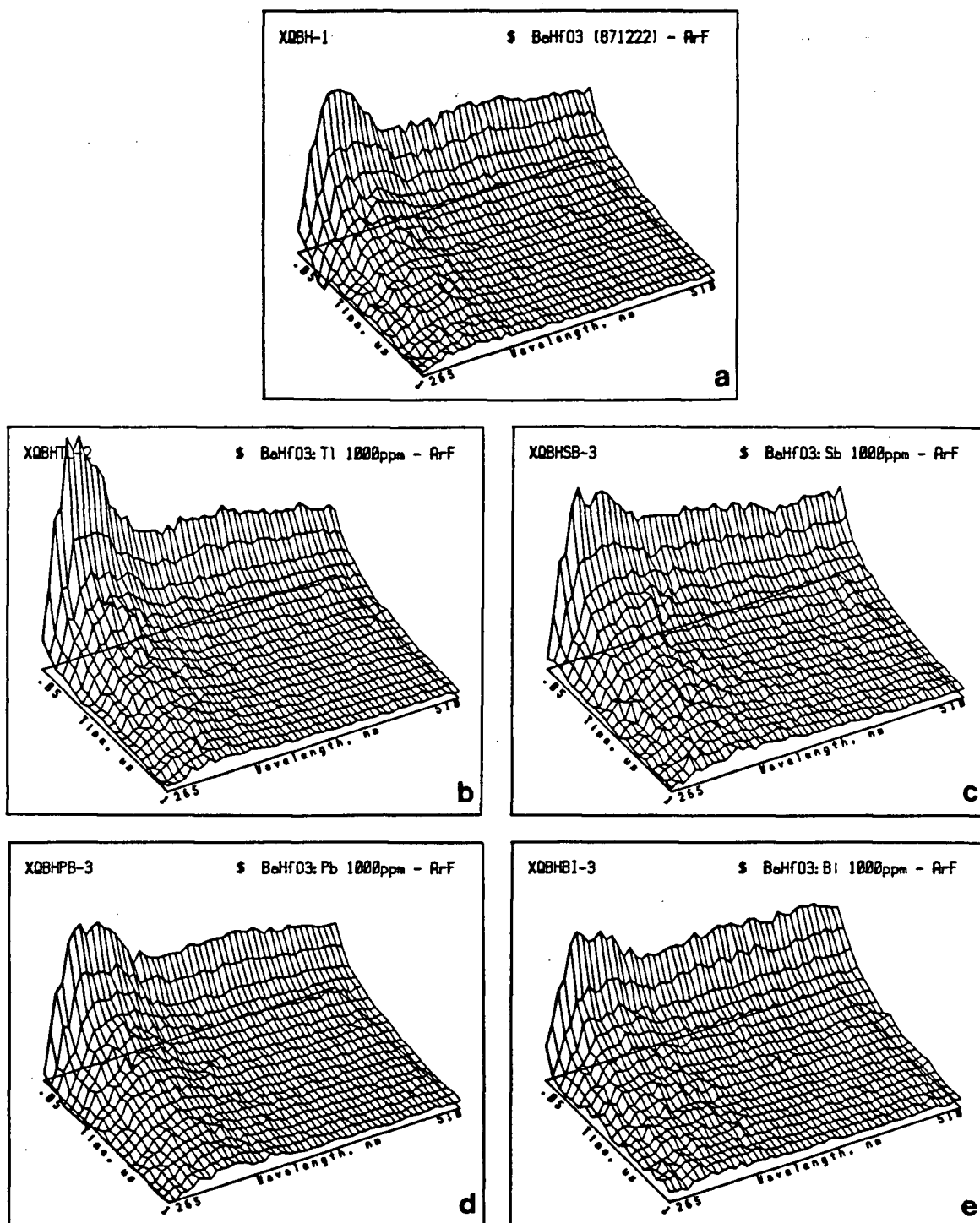
Figure 4.32 Barium hafnate; excitation: 193 nm.
        (a) no dopant, 50 ns to 1000 ns, 265 nm to 510 nm
        (b) Tl doped, 50 ns to 1000 ns, 265 nm to 510 nm
        (c) Sb doped, 50 ns to 1000 ns, 265 nm to 510 nm
        (d) Pb doped, 50 ns to 1000 ns, 265 nm to 510 nm
        (e) Bi doped, 50 ns to 1000 ns, 265 nm to 510 nm
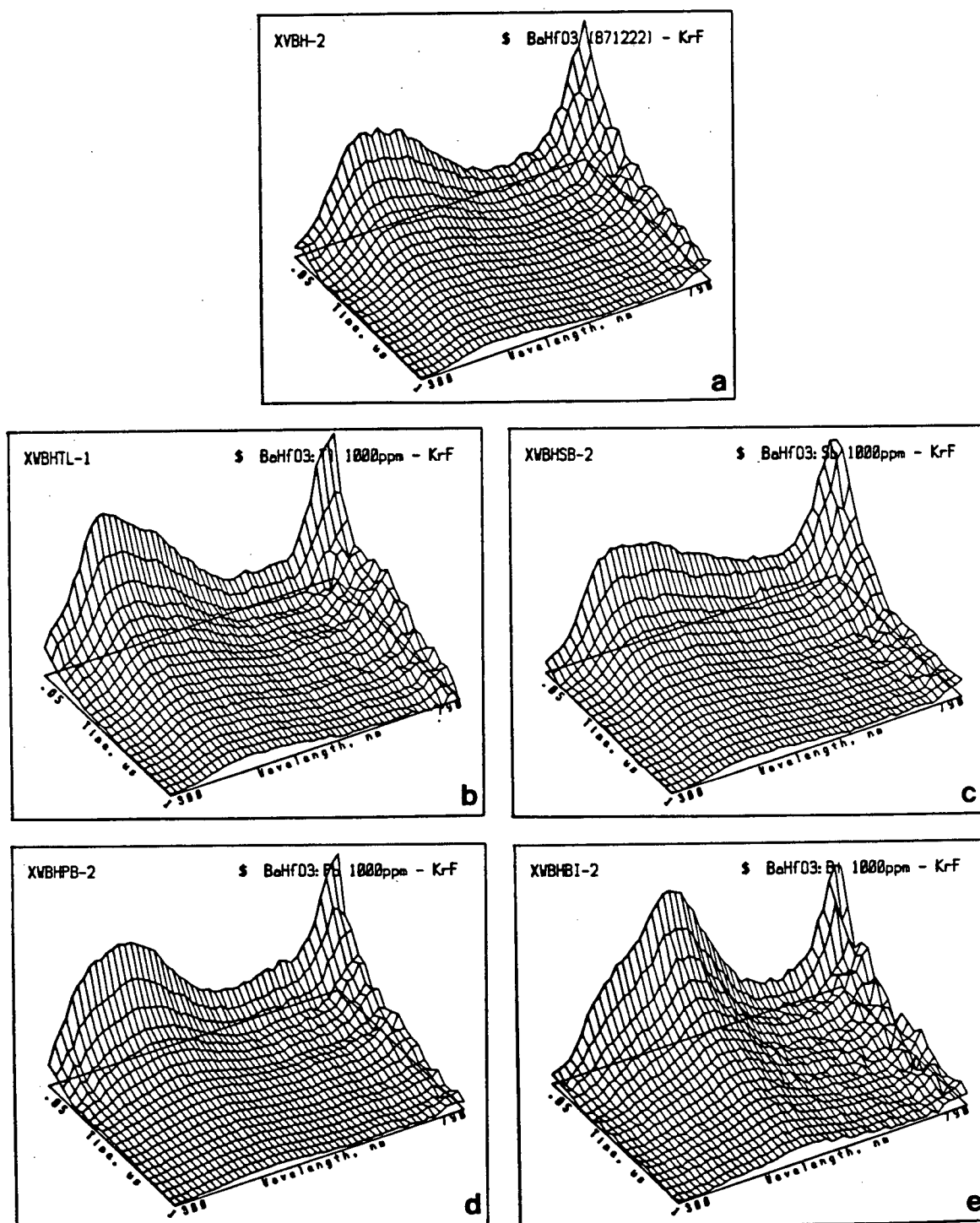
Figure 4.33 Barium hafnate; excitation: 248 nm.
　　　　　(a) no dopant, 50 ns to 1000 ns, 300 nm to 790 nm
　　　　　(b) Tl doped, 50 ns to 1000 ns, 300 nm to 790 nm
　　　　　(c) Sb doped, 50 ns to 1000 ns, 300 nm to 790 nm
　　　　　(d) Pb doped, 50 ns to 1000 ns, 300 nm to 790 nm
　　　　　(e) Bi doped, 50 ns to 1000 ns, 300 nm to 790 nm
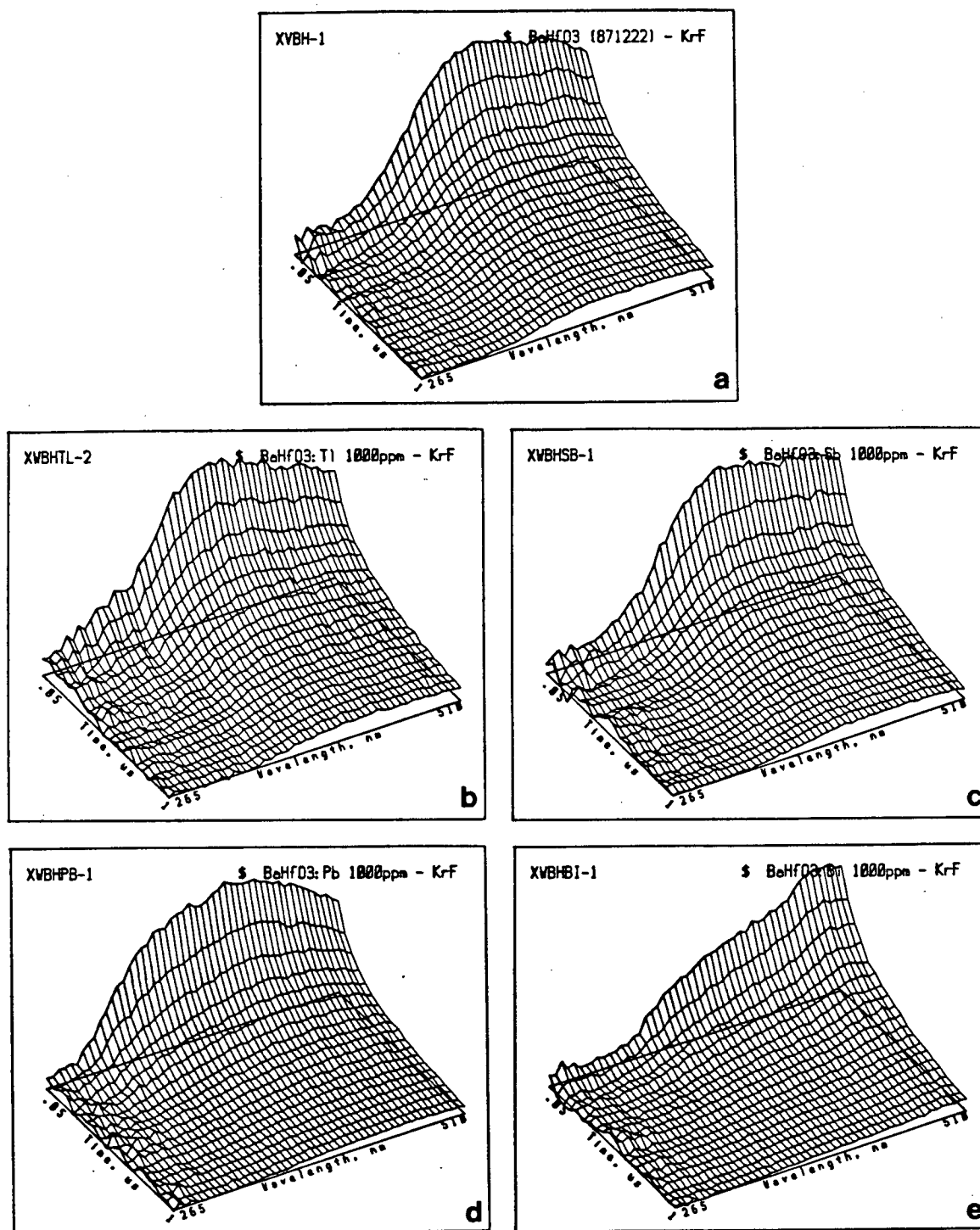
Figure 4.34 Barium hafnate; excitation: 248 nm.
       (a) no dopant, 50 ns to 1000 ns, 265 nm to 510 nm
       (b) Tl doped, 50 ns to 1000 ns, 265 nm to 510 nm
       (c) Sb doped, 50 ns to 1000 ns, 265 nm to 510 nm
       (d) Pb doped, 50 ns to 1000 ns, 265 nm to 510 nm
       (e) Bi doped, 50 ns to 1000 ns, 265 nm to 510 nm
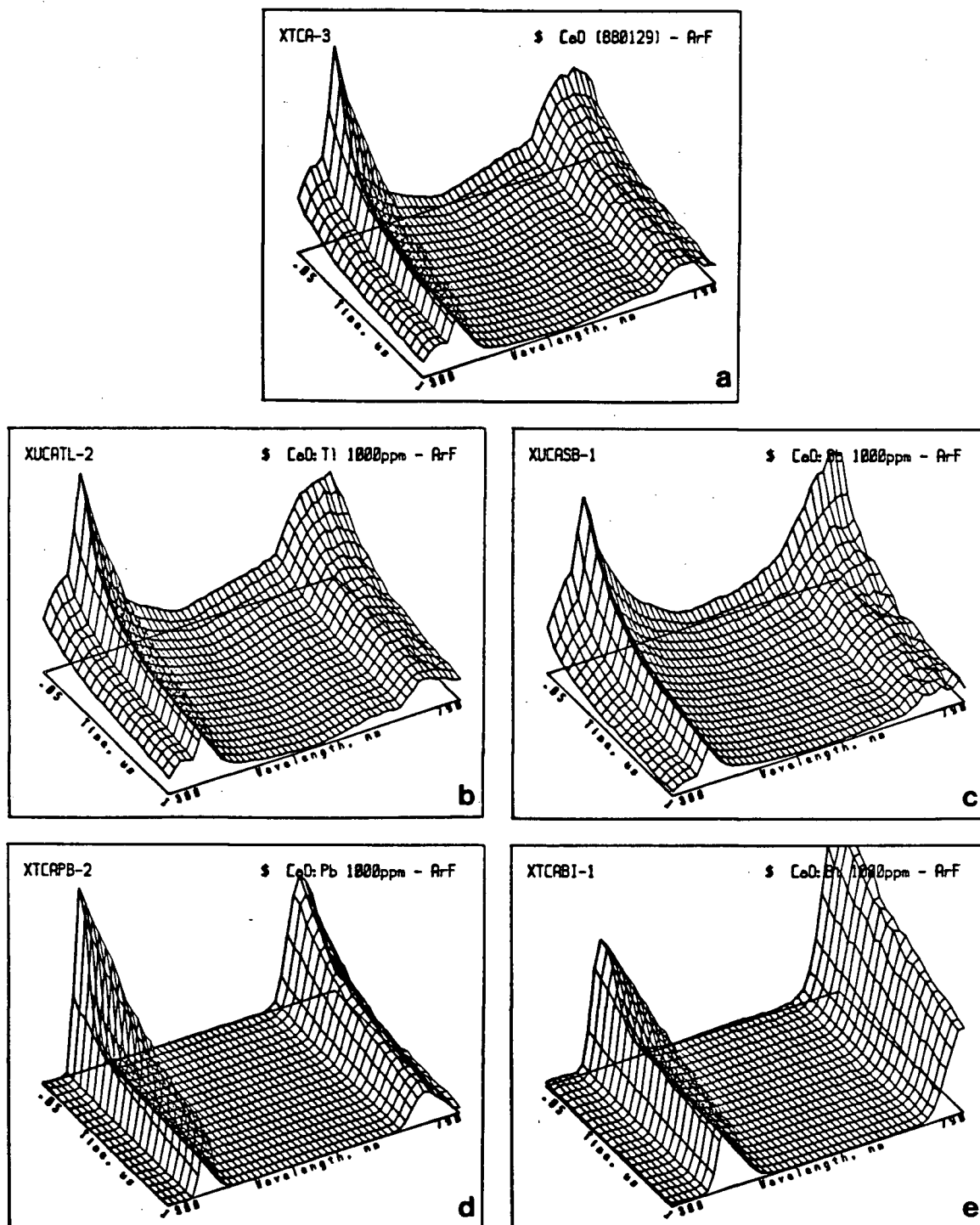
Figure 4.35 Calcium oxide; excitation: 193 nm.
(a) no dopant, 50 ns to 1000 ns, 300 nm to 790 nm
(b) Tl doped, 50 ns to 1000 ns, 300 nm to 790 nm
(c) Sb doped, 50 ns to 1000 ns, 300 nm to 790 nm
(d) Pb doped, 50 ns to 1000 ns, 300 nm to 790 nm
(e) Bi doped, 50 ns to 1000 ns, 300 nm to 790 nm
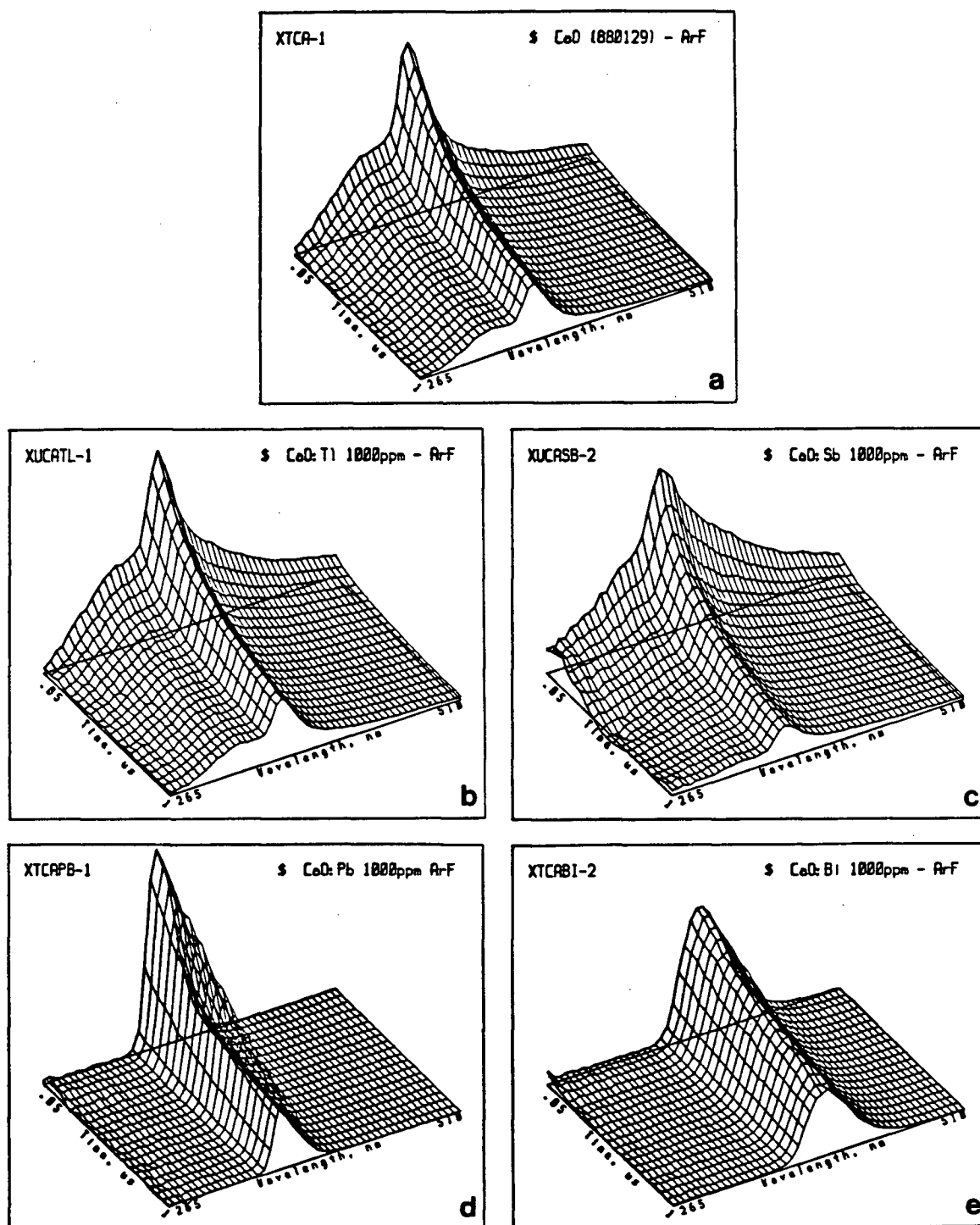
Figure 4.36 Calcium oxide; excitation: 193 nm.
(a) no dopant, 50 ns to 1000 ns, 265 nm to 510 nm
(b) Tl doped, 50 ns to 1000 ns, 265 nm to 510 nm
(c) Sb doped, 50 ns to 1000 ns, 265 nm to 510 nm
(d) Pb doped, 50 ns to 1000 ns, 265 nm to 510 nm
(e) Bi doped, 50 ns to 1000 ns, 265 nm to 510 nm
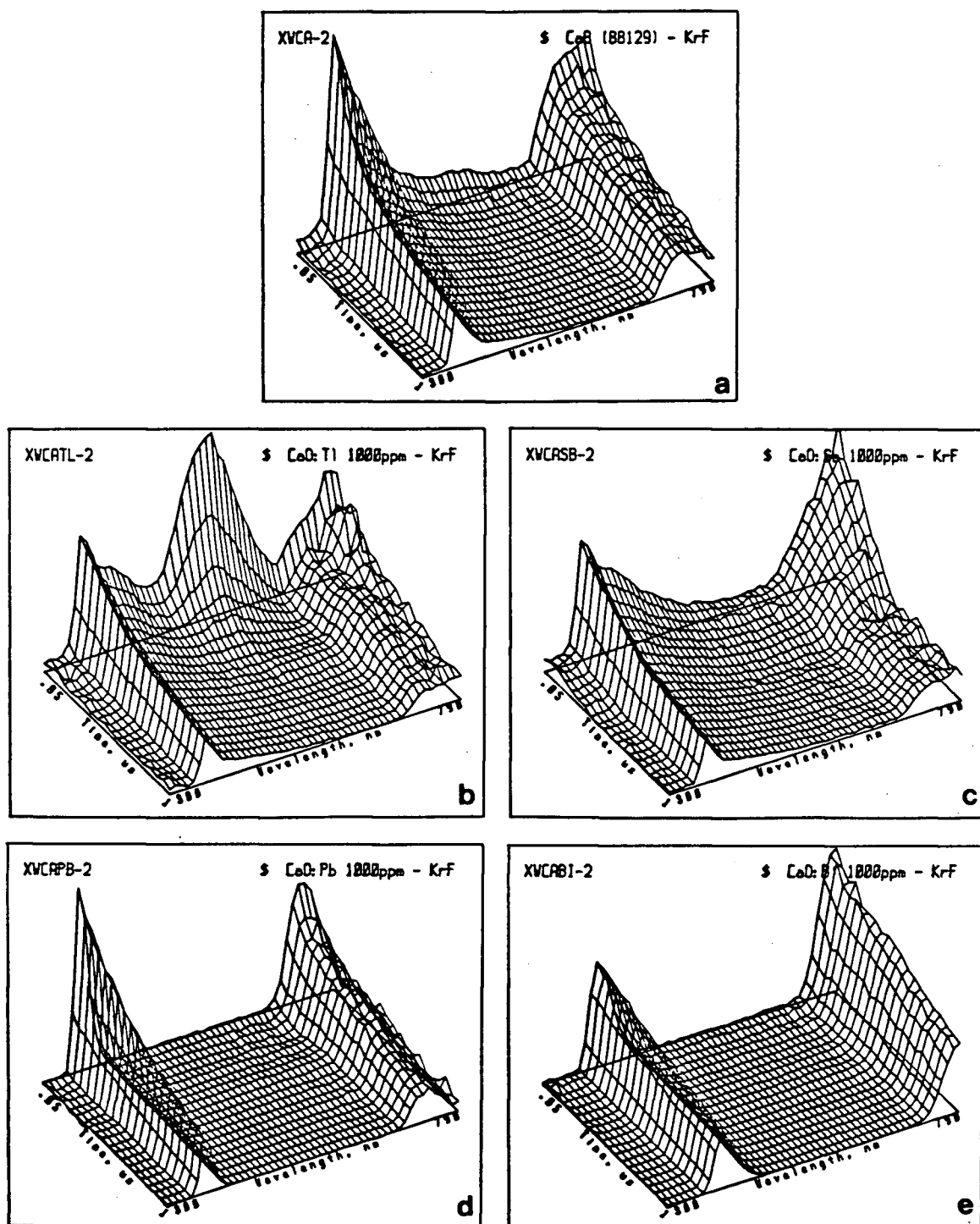
Figure 4.37 Calcium oxide; excitation: 248 nm.
    (a) no dopant, 50 ns to 1000 ns, 300 nm to 790 nm
    (b) Tl doped, 50 ns to 1000 ns, 300 nm to 790 nm
    (c) Sb doped, 50 ns to 1000 ns, 300 nm to 790 nm
    (d) Pb doped, 50 ns to 1000 ns, 300 nm to 795 nm
    (e) Bi doped, 50 ns to 1000 ns, 300 nm to 790 nm
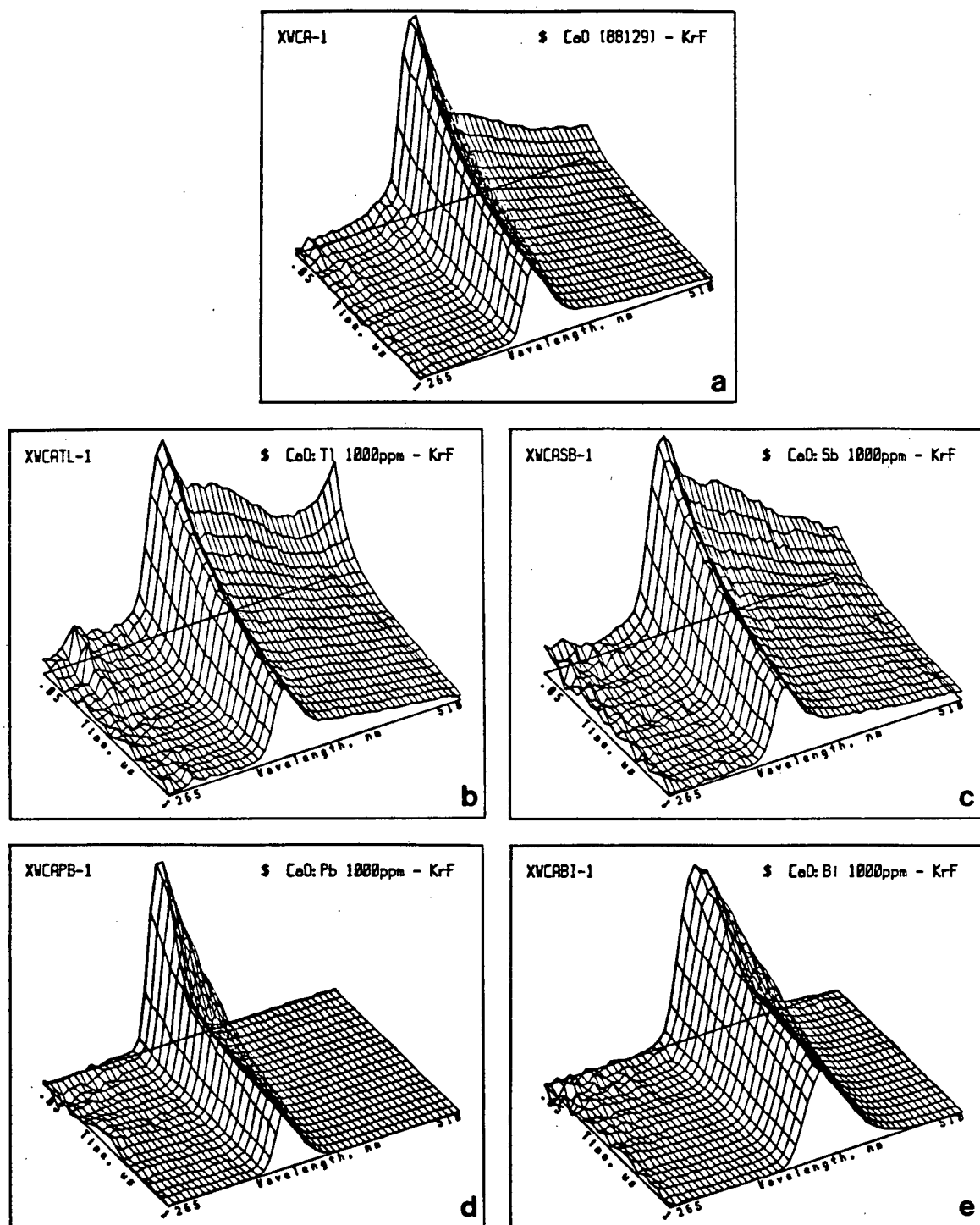
Figure 4.38 Calcium oxide; excitation: 248 nm.
          (a) no dopant, 50 ns to 1000 ns, 265 nm to 510 nm
          (b) Tl doped, 50 ns to 1000 ns, 265 nm to 510 nm
          (c) Sb doped, 50 ns to 1000 ns, 265 nm to 510 nm
          (d) Pb doped, 50 ns to 1000 ns, 265 nm to 510 nm
          (e) Bi doped, 50 ns to 1000 ns, 265 nm to 510 nm
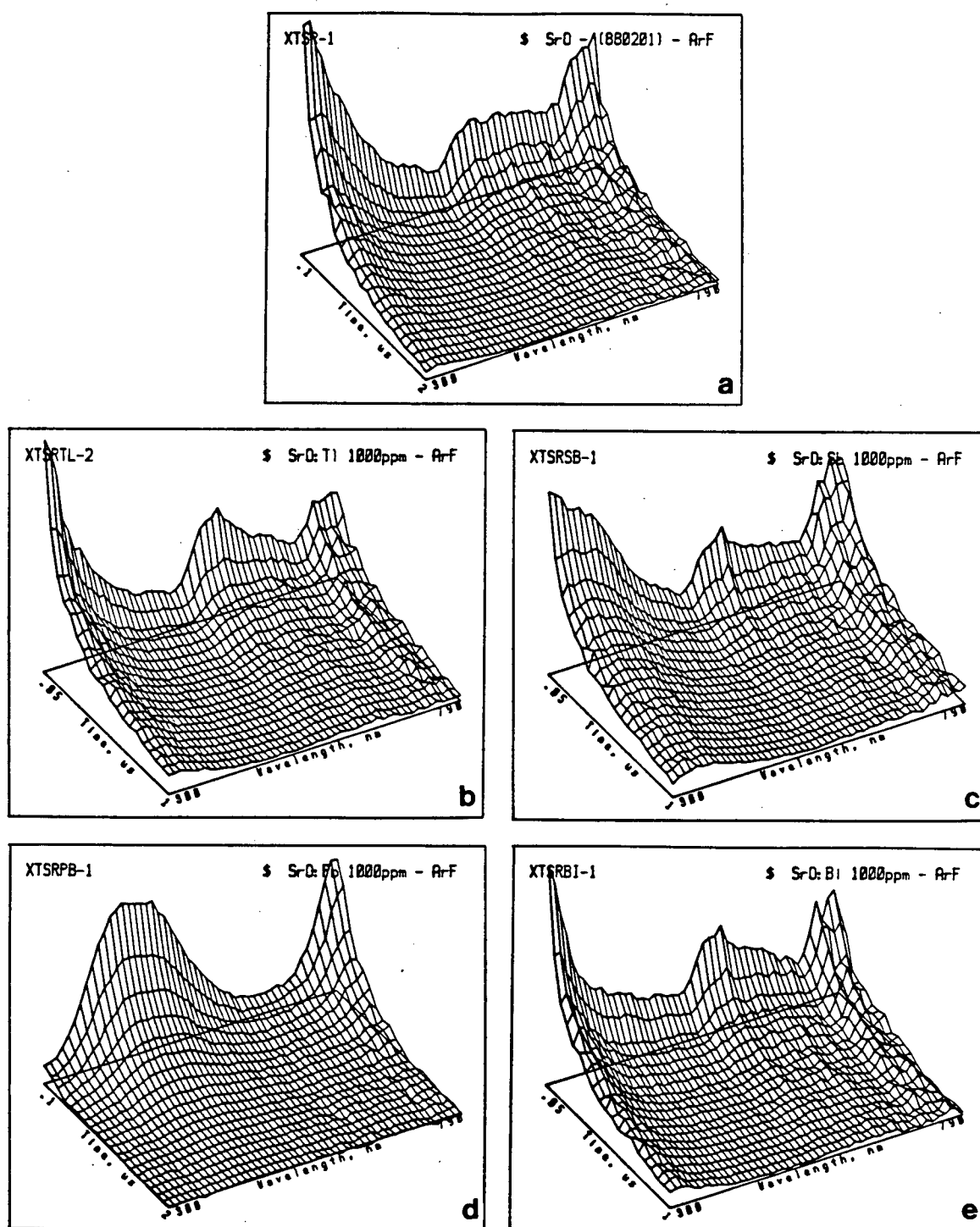
Figure 4.39 Strontium oxide; excitation: 193 nm.
(a) no dopant, 100 ns to 2000 ns, 300 nm to 790 nm
(b) Tl doped, 50 ns to 1000 ns, 300 nm to 790 nm
(c) Sb doped, 50 ns to 1000 ns, 300 nm to 790 nm
(d) Pb doped, 100 ns to 2000 ns, 300 nm to 790 nm
(e) Bi doped, 50 ns to 1000 ns, 300 nm to 790 nm
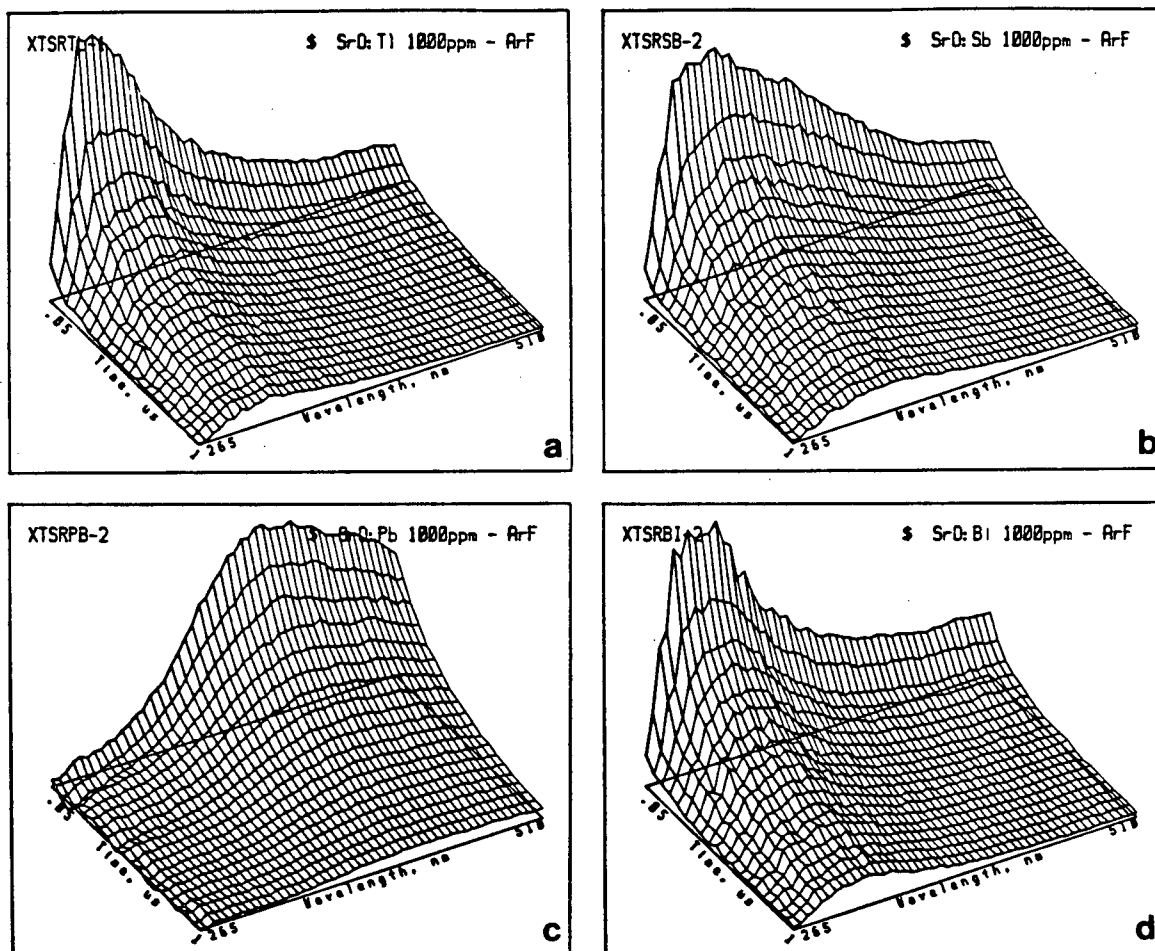
Figure 4.40 Strontium oxide; excitation: 193 nm.
    (a) Tl doped, 50 ns to 1000 ns, 265 nm to 510 nm
    (b) Sb doped, 50 ns to 1000 ns, 265 nm to 510 nm
    (c) Pb doped, 50 ns to 1000 ns, 265 nm to 510 nm
    (d) Bi doped, 50 ns to 1000 ns, 265 nm to 510 nm

149
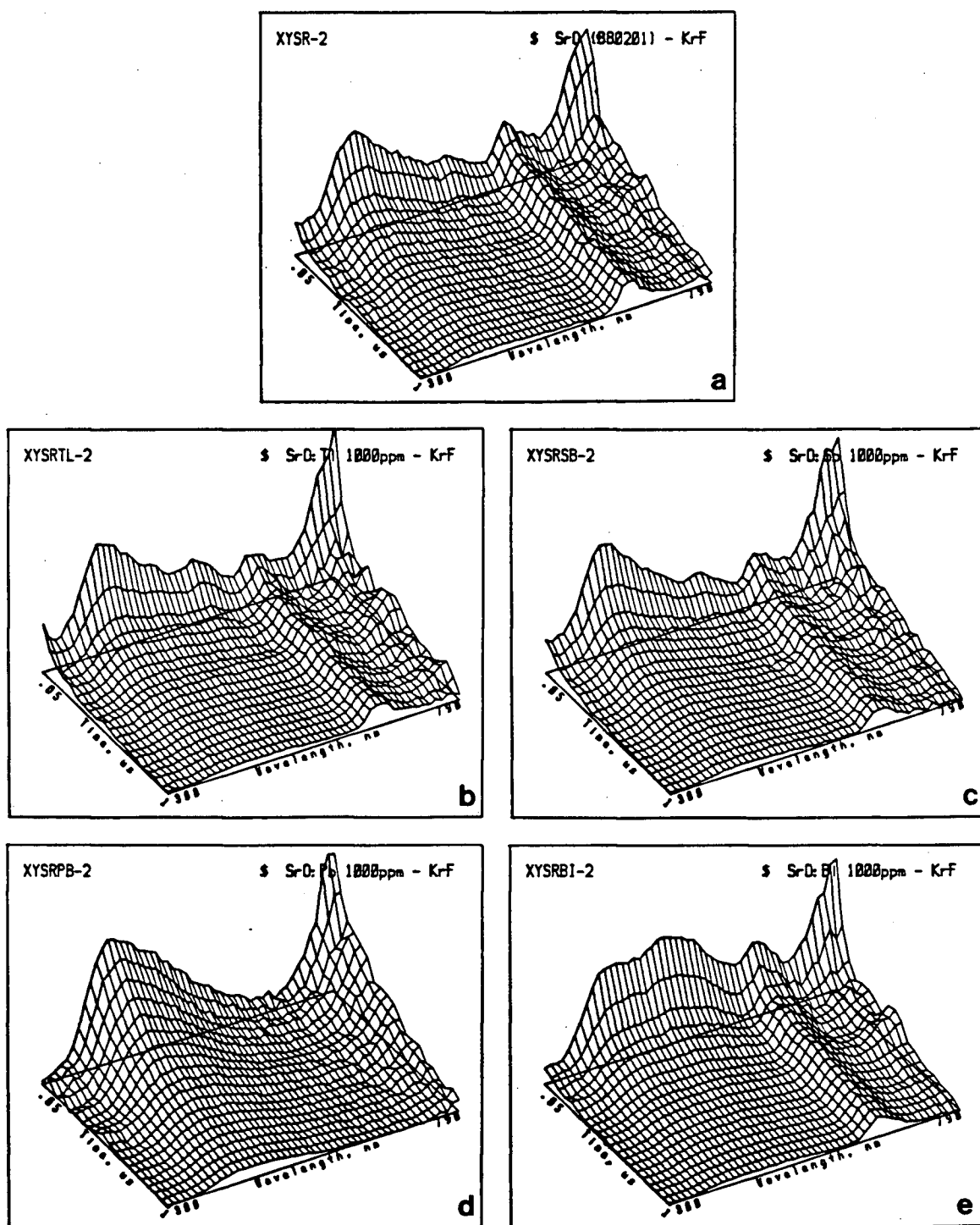
Figure 4.41 Strontium oxide; excitation: 248 nm.
(a) no dopant, 50 ns to 1000 ns, 300 nm to 790 nm
(b) Tl doped, 50 ns to 1000 ns, 300 nm to 790 nm
(c) Sb doped, 50 ns to 1000 ns, 300 nm to 790 nm
(d) Pb doped, 50 ns to 1000 ns, 300 nm to 790 nm
(e) Bi doped, 50 ns to 1000 ns, 300 nm to 790 nm
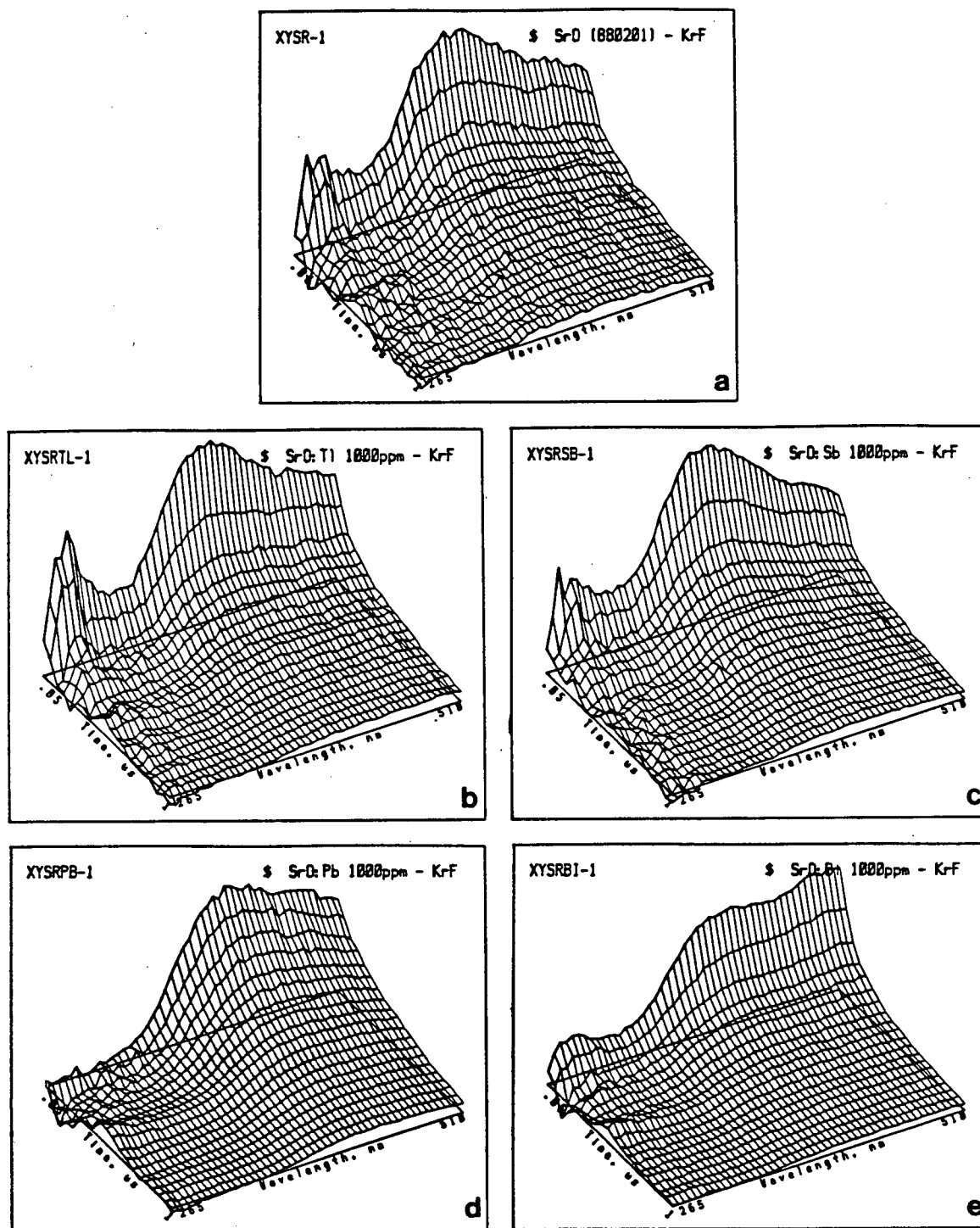
Figure 4.42 Strontium oxide; excitation: 248 nm.
        (a) no dopant, 50 ns to 1000 ns, 265 nm to 510 nm
        (b) Tl doped, 50 ns to 1000 ns, 265 nm to 510 nm
        (c) Sb doped, 50 ns to 1000 ns, 265 nm to 510 nm
        (d) Pb doped, 50 ns to 1000 ns, 265 nm to 510 nm
        (e) Bi doped, 50 ns to 1000 ns, 265 nm to 510 nm

151
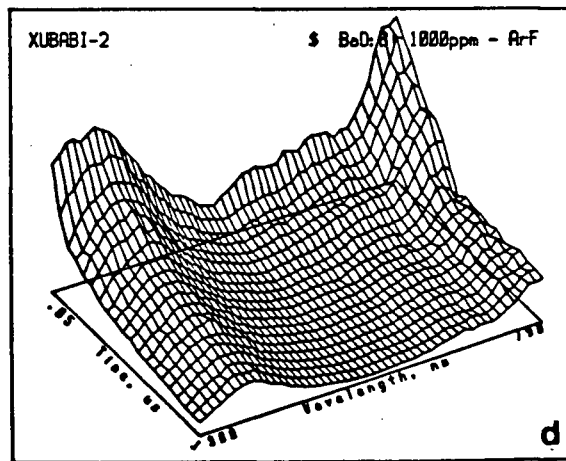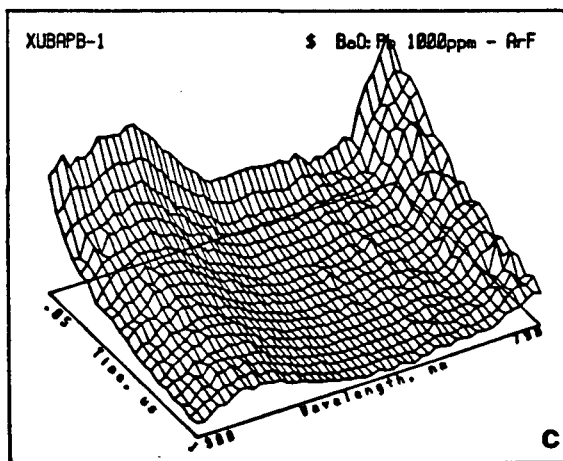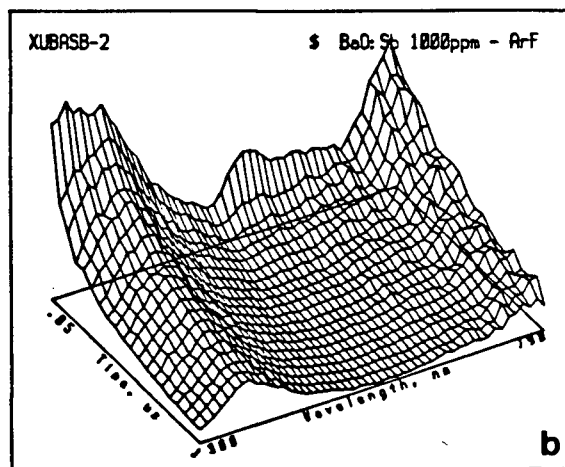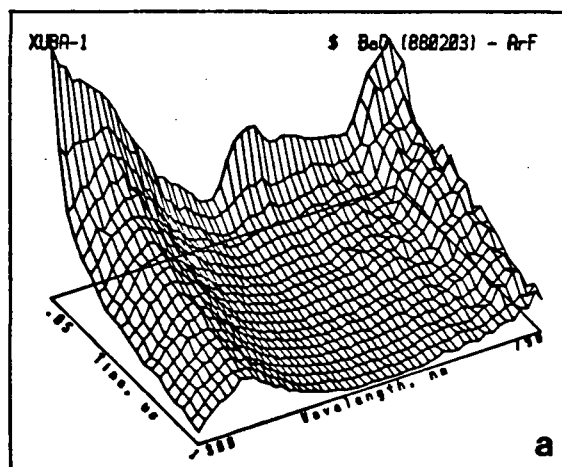
Figure 4.43 Barium oxide; excitation: 193 nm.
             (a) no dopant, 50 ns to 1000 ns, 300 nm to 790 nm
             (b) Sb doped, 50 ns to 1000 ns, 300 nm to 790 nm
             (c) Pb doped, 50 ns to 1000 ns, 300 nm to 790 nm
             (d) Tl doped, 50 ns to 1000 ns, 300 nm to 790 nm
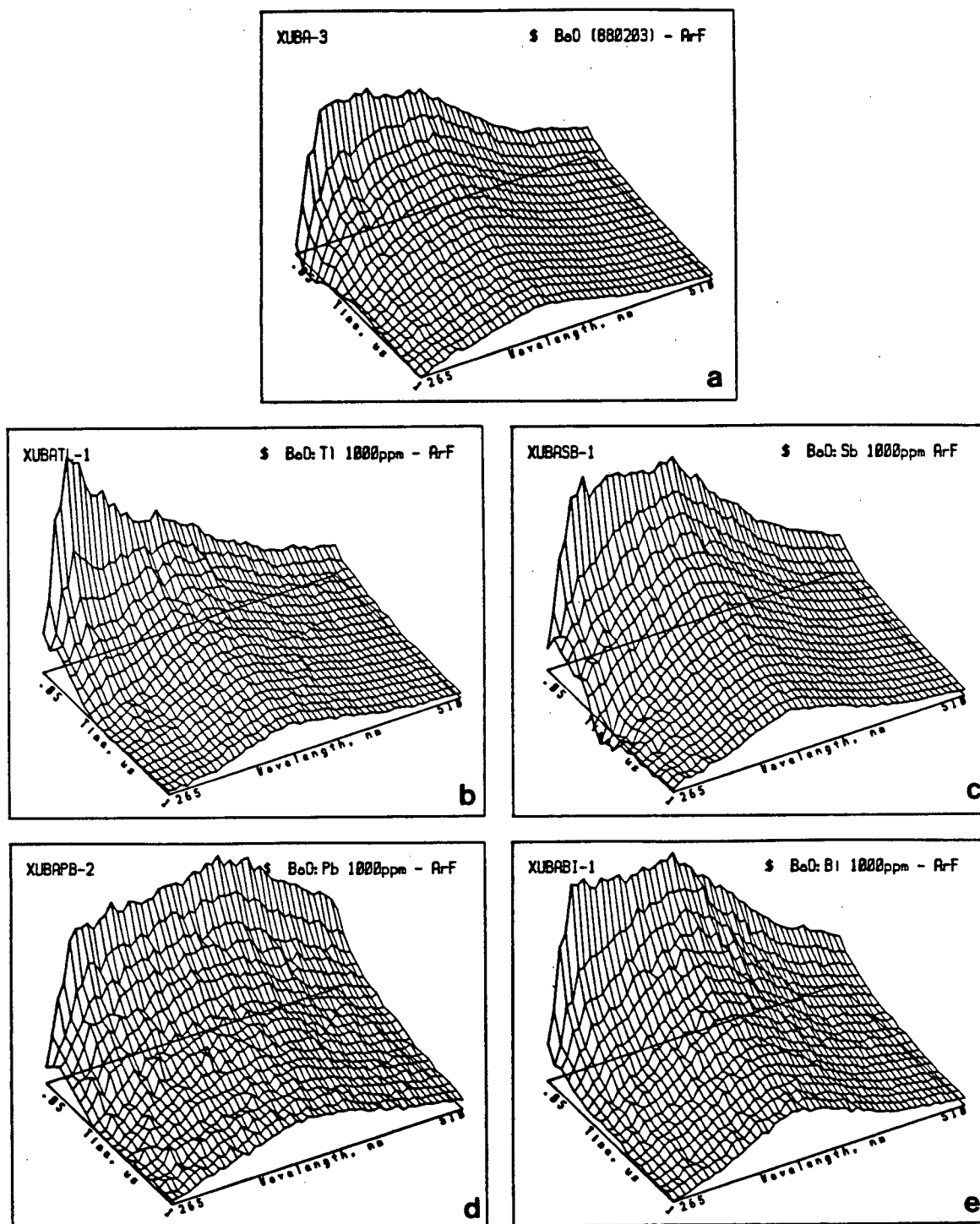
Figure 4.44 Barium oxide; excitation: 193 nm.
        (a) no dopant, 100 ns to 1000 ns, 265 nm to 510 nm
        (b) Tl doped, 50 ns to 1000 ns, 265 nm to 510 nm
        (c) Sb doped, 50 ns to 1000 ns, 265 nm to 510 nm
        (d) Pb doped, 100 ns to 1000 ns, 265 nm to 510 nm
        (e) Bi doped, 50 ns to 1000 ns, 265 nm to 510 nm
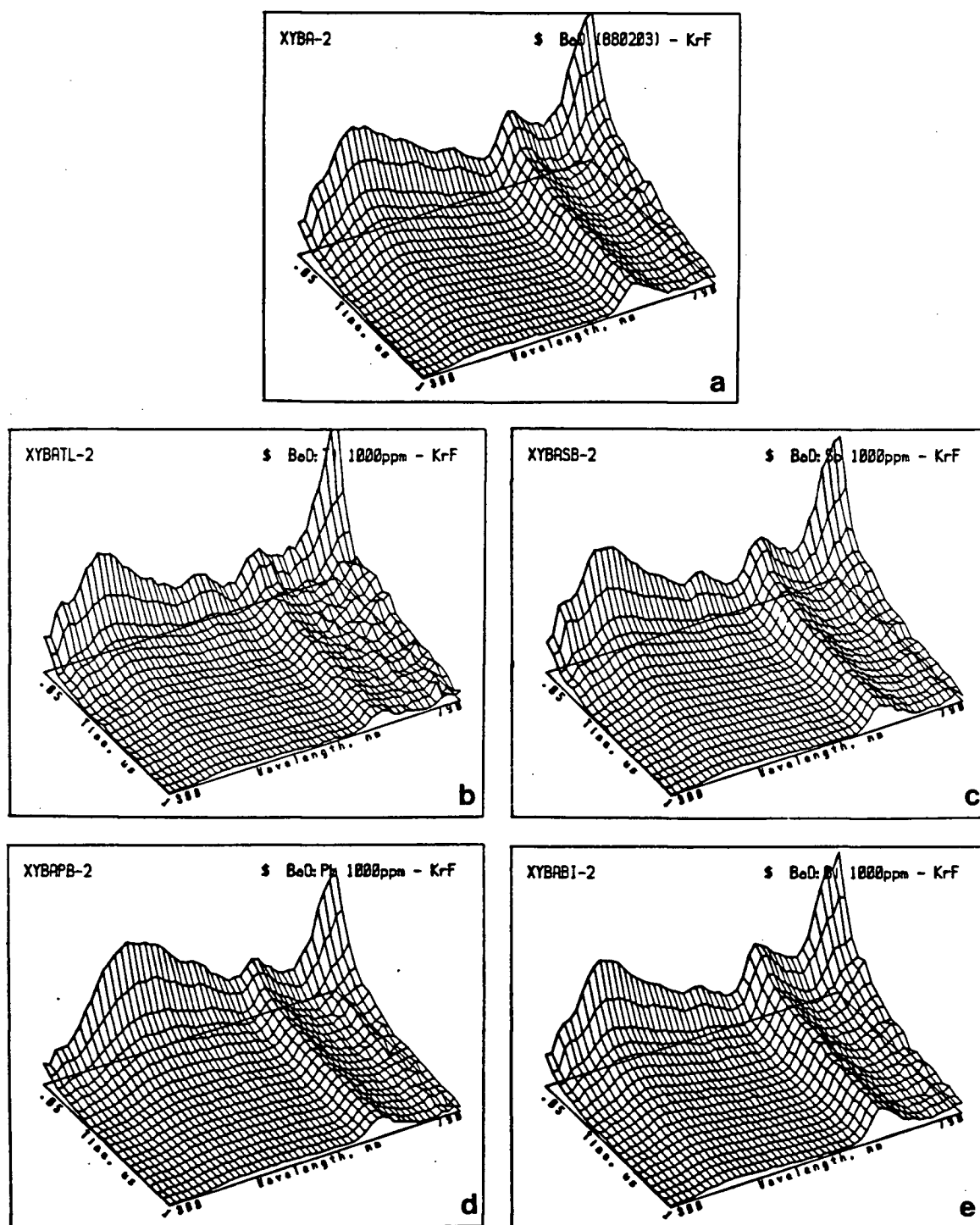
Figure 4.45 Barium oxide; excitation: 248 nm.
            (a) no dopant, 50 ns to 1000 ns, 300 nm to 790 nm
            (b) Tl doped, 50 ns to 1000 ns, 300 nm to 790 nm
            (c) Sb doped, 50 ns to 1000 ns, 300 nm to 790 nm
            (d) Pb doped, 50 ns to 1000 ns, 300 nm to 790 nm
            (e) Bi doped, 50 ns to 1000 ns, 300 nm to 790 nm
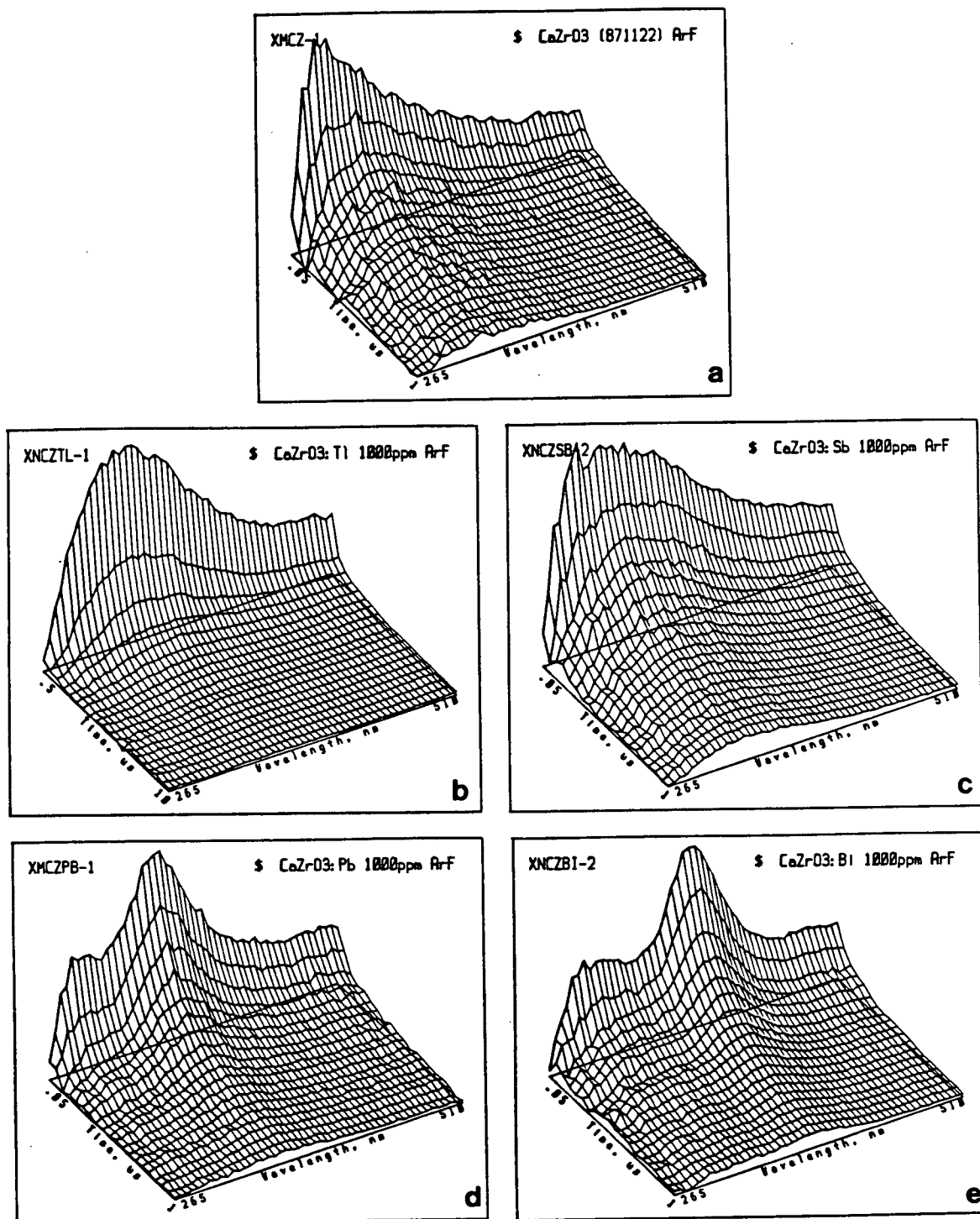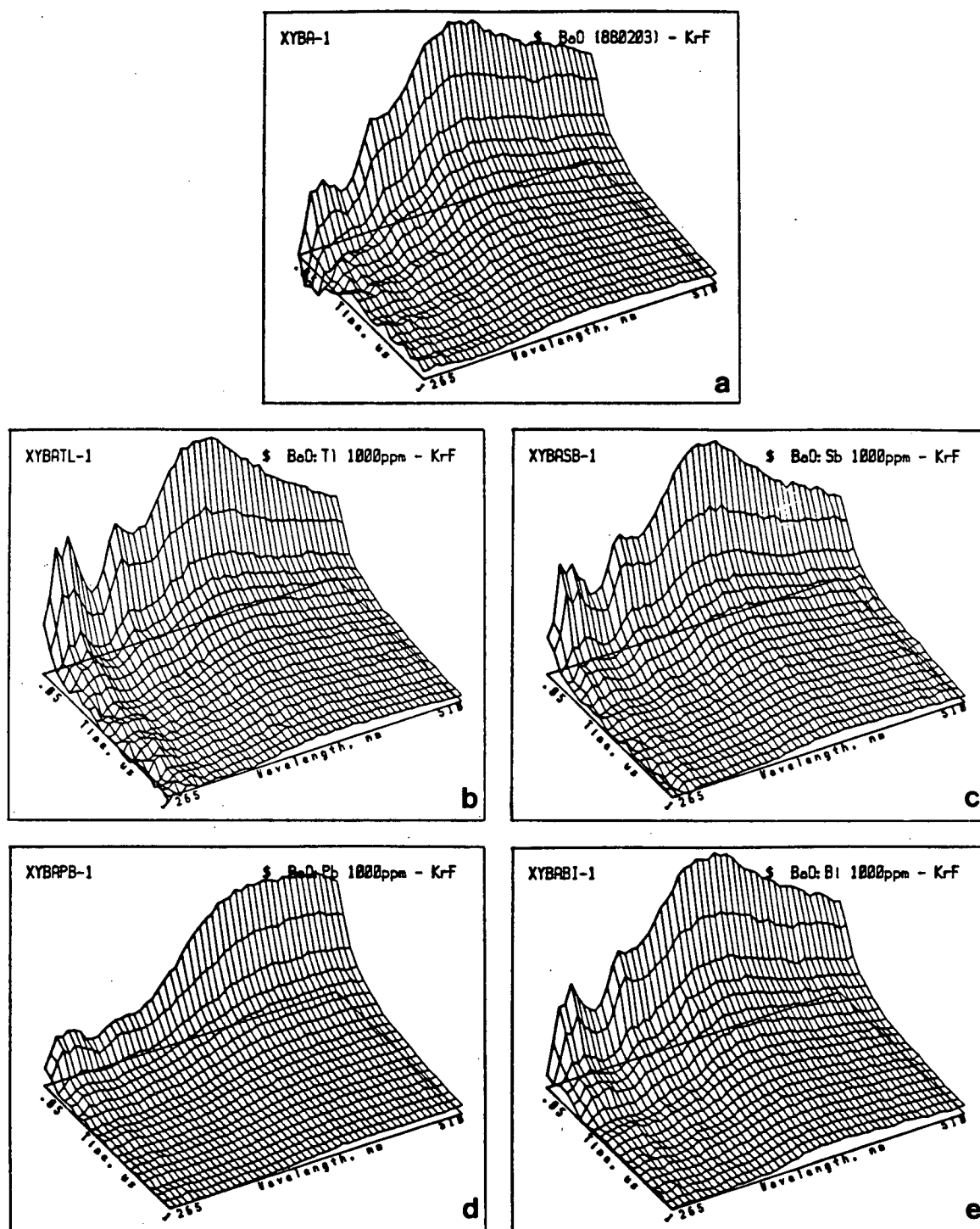
Figure 4.46 Barium oxide; excitation: 248 nm.
(a) no dopant, 50 ns to 1000 ns, 265 nm to 510 nm
(b) Tl doped, 50 ns to 1000 ns, 265 nm to 510 nm
(c) Sb doped, 50 ns to 1000 ns, 265 nm to 510 nm
(d) Pb doped, 50 ns to 1000 ns, 265 nm to 510 nm
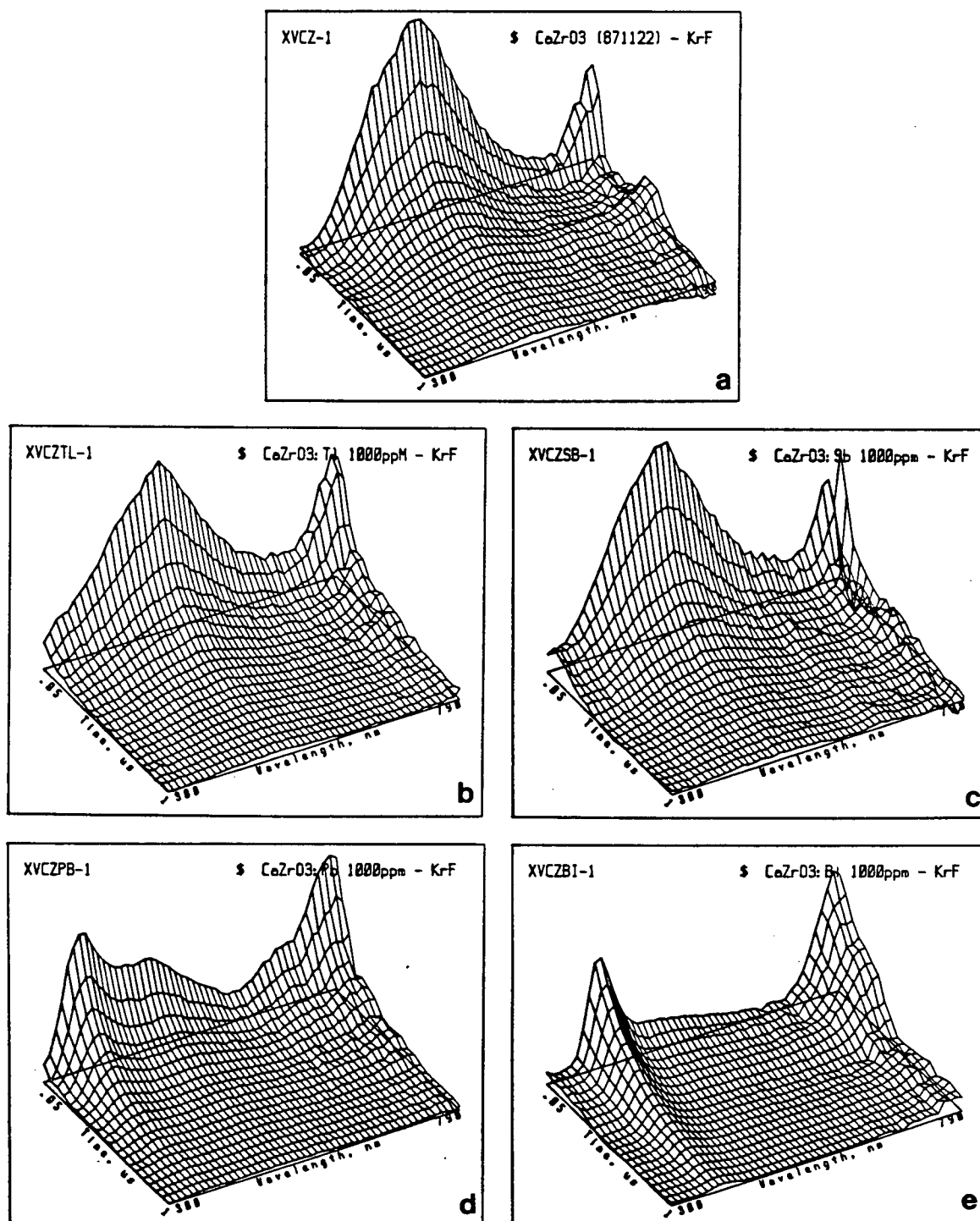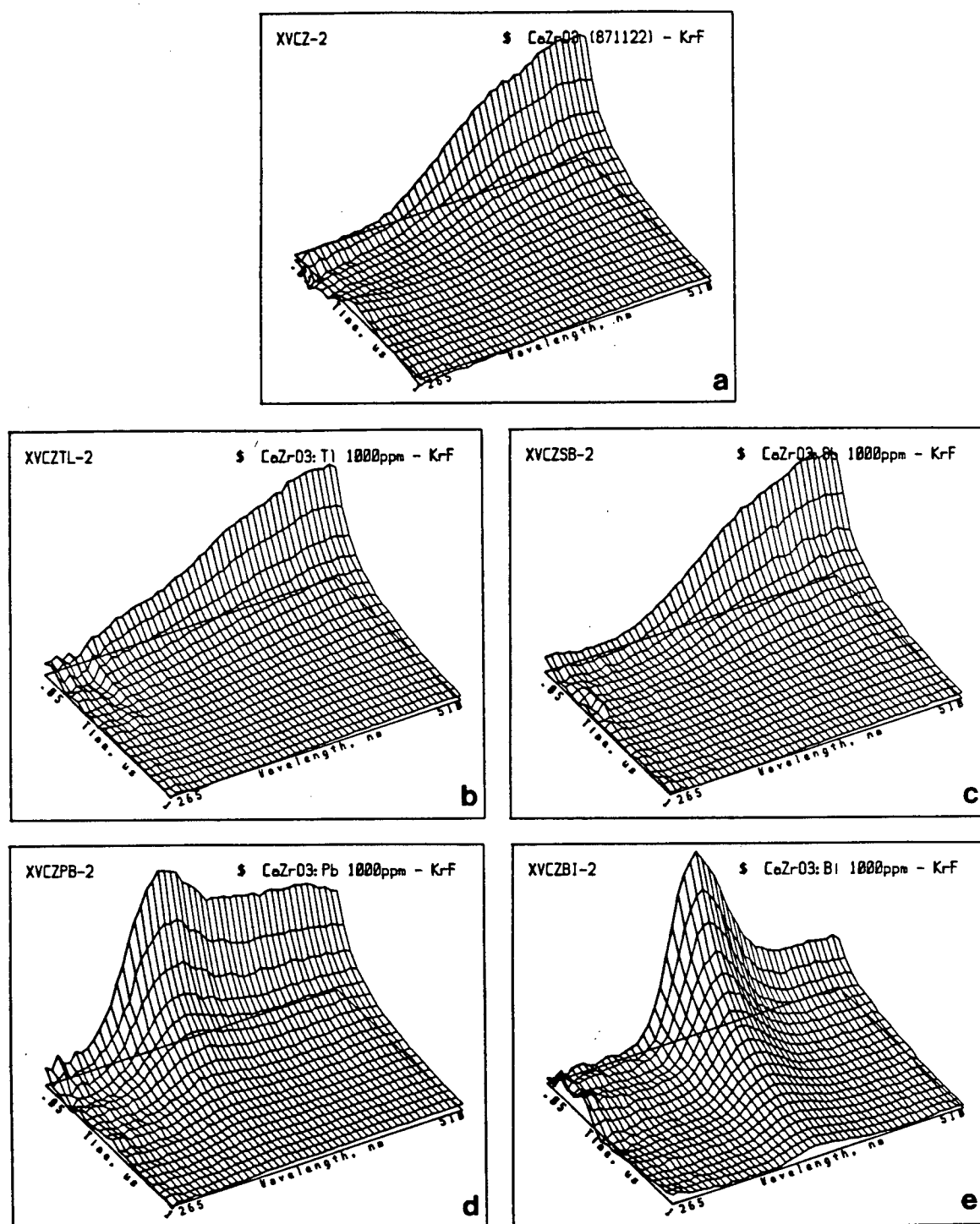(e) Bi doped, 50 ns to 1000 ns, 265 nm to 510 nm

Chapter 5

CONCLUDING REMARKS

In this study, the multidimensional approach of time-wavelength resolved luminescence spectroscopy was examined to see if analytically useful information could be extracted from the complex luminescence signals intrinsic to inorganic solids. The results presented in this thesis clearly show the advantages inherent to this approach. Information present in the time-wavelength resolved spectrum allows the use of energy transfer and energy migration phenomena in inorganic substance characterization. This is potentially a very powerful analytical tool since it may be applied to quantitative trace analysis as well as to describing the gross structure of a substance.

The simple molybdate-tungstate systems studied illustrate the potential of using energy transfer in the quantitative analysis of inorganic powders. The mechanism for energy transfer from tungstate to molybdate is likely by a nonresonance radiationless route, since the decay appears to be first order for both molybdate and tungstate emission. Other modes of energy transport and energy migration in solids may have interesting analytical applications. For example, when energy migration processes occur in a host lattice, the decay lifetime may be a function of individual particle size. This phenomenon may be readily applied to the rapid, remote monitoring of particle size in a milling operation.

The degree of success of a multidimensional approach to luminescence spectroscopy is markedly dependent on the data reduction operations employed. The two stage process employed in this study provided reliable estimates for the number of components present and their parameters. This algorithm works well for up to three components. However, the computational burden becomes excessive for systems containing more than three components. For more complex systems, highly efficient digital filter techniques appear to be the optimal solution.

The adaptive Kalman filter is an optimal approach for real time data reduction. This powerful algorithm is well suited to applying both empirical and theoretical models to a data set. For example, a spectrum from an unknown material could be rapidly compared with empirical wavelength domain spectra while applying various models for the luminescence decay. This type of data treatment is particularly well suited to industrial process control or to rapid screening tests on clinical specimens.

The lanthanides are particularly interesting since their line-like spectra and participation in energy migration carry much information on the local and global environments of a solid. The multidimensional approach provides relatively easy access to this information, particularly when used in conjunction with site selective excitation. A potential application is the nondestructive determination of the distribution of trace lanthanides in

cultural artifacts such as pottery, stone sculpture, and paint pigments.

The studies on zirconates and hafnates gave indications of short lifetime luminescence in the near infrared. Very little attention has been paid to near infrared luminescence from natural substances such as rocks and minerals. These materials should produce rich emission spectra due to the charge transfer absorption bands associated with iron ions in many minerals and energy transfer phenomena. Time-wavelength resolved luminescence in this region offers exciting possibilities for remote sensing since the atmosphere is transparent for both excitation and emission.

The exploratory work reported in this thesis was subject to limitations imposed by the equipment available. Studies on energy transfer and energy migration require time domain measurements spanning the range from sub nanosecond to seconds. Multichannel spectral domain measurements are essential for efficient data collection. For future work, a spectrometer consisting of a polychromator with a gated, intensified diode array detector is required. The excitation source should be able to supply pulsed, high intensity radiation from the red to ultraviolet regions. A convenient source would consist of a pulsed tuneable dye laser coupled with a frequency multiplying crystal.

The work presented in this thesis has shown that time-wavelength resolved luminescence is a potentially valuable analytical tool for the characterization of luminescent

inorganic solids. Thus, the objectives of this study have been met. Hopefully, the background information and experimental data presented in this thesis will stimulate and encourage others to continue investigations in this area.

REFERENCES

1 Harwit, M. Astrophysical Concepts; Wiley: New York, 1973.

2 Harvey, E. N. A History of Luminescence; American Philosophical Society: Philadelphia, PA, 1957.

3 Akasofu, S-I. Scientific American; 1965, 213(6), 54-62.

4 Weiner, J. Planet Earth; Bantam: Toronto, 1986, pp. 238-242.

5 Partington, J. R. A History of Chemistry; Macmillan: New York, 1946, Vol. 2.

6 Pringsheim, P.; Vogel, M. Luminescence of Liquids and Solids and its Practical Applications; Interscience: New York, 1943.

7 Burke, J. The Day the Universe Changed; Little, Brown: Boston, 1985, p16.

8 Lovell, D. J. Optical Anecdotes; SPIE: Bellingham, WA, 1981.

9 Redondi, P. Galileo Heretic; Princeton University: Princeton, NJ, 1987, pp. 9-20.

10 Becquerel, E. La Lumière, ses Causes et ses Effets; L'Institut de France: Paris, 1867, Vol. 1, pp. 247-260.

11 Stokes, G. G. Phil. Trans. 1852, 142, 463-562.

12 Stokes, G. G. Phil. Trans. 1853, 143, 385-396.

13 Mitchell, A. C. G.; Zemansky, M. W. Resonance Radiation and Excited Atoms; Cambridge University: London, 1961.

14 Swihart, T. L. Astrophysics and Stellar Astronomy; Wiley: New York, 1968.

15 L'vov, B. V. Atomic Absorption Spectrochemical Analysis; Elsevier: New York, 1970.

16 Mihalas, D. Stellar Atmospheres, 2nd ed.; Freeman: San Francisco, 1978.

17 Dufay, J. Introduction to Astrophysics: The Stars; Dover, New York, 1964.

18 Baldwin, G. C. An Introduction to Nonlinear Optics; Plenum: New York, 1969.

19 Winefordner, J. D.; Schulman, S. G.; O'Haver, T. C. Luminescence Spectrometry in Analytical Chemistry; Wiley-Interscience: New York, 1972.

20 Stockburger, M. In <u>Organic Molecular Photophysics</u>; Birks, J. B., Ed.; Wiley: London, 1973, Vol. 1, pp. 57-99.

21 Lakowicz, J. R. <u>Principles of Fluorescence Spectroscopy</u>; Plenum: New York, 1983.

22 Lumb, M. D. In <u>Luminescence Spectroscopy</u>; Lumb, M. D., Ed.; Academic Press: London, 1978, Chapter 2.

23 Friedlander, G.; Kennedy, J. W.; Miller, J. M. <u>Nuclear and Radiochemistry</u>, 2nd. ed.; Wiley: New York, 1964, pp. 86-140.

24 Walton, A. J. <u>Adv. Phys.</u> 1977, <u>26</u>, 887-948.

25 Bugbee, E. E. <u>A Textbook of Fire Assaying</u>, 3rd. ed.; Wiley: New York, 1940.

26 Zink, J. I. <u>Naturwissenschaften</u> 1981, <u>68</u>, 507-512.

27 Williams, F. In <u>Luminescence of Inorganic Solids</u>; Goldberg, P., Ed.; Academic Press: New York, 1966, Chapter 1.

28 Imasaka, T.; Fukuoka, K.; Hayashi, T.; Ishibashi, N. <u>Anal. Chim. Acta</u> 1984, <u>156</u>, 111-120.

29 D'Silva, A. P.; Fassel, V. A. <u>Anal. Chem.</u> 1984, <u>56</u>, 985A-1000A.

30 Henry, B. R.; Siebrand, W. In <u>Organic Molecular Photophysics</u>; Birks, J. B. Ed.; Wiley: London, 1973; Vol. 1, pp. 153-233.

31 Kittel, C. <u>Introduction to Solid State Physics</u>; 5th. ed.; Wiley: New York, 1976.

32 Imbusch, G. F. In <u>Luminescence Spectroscopy</u>; Lumb, M. D., Ed.; Academic Press: London, 1978, Chapter 1.

33 Pollock, C. R. <u>J. Lumin.</u> 1986, <u>35</u>, 65-78.

34 Townsend, P. D.; Kelly, J. C. <u>Colour Centres and Imperfections in Insulators and Semiconductors</u>; Chatto & Windus: London, 1973.

35 Doorn, S. K.; Wright, J. C. <u>Anal. Chem.</u> 1985, <u>57</u>, 2869-2873.

36 Blasse, G. <u>Mater. Chem. Phys.</u> 1987, <u>16</u>, 201-236.

37 Miller, M. P.; Tallant, D. R.; Gustafson, F. J.; Wright, J. C. <u>Anal. Chem.</u> 1977, <u>49</u>, 1474-

38 Curie, D. <u>Luminescence in Crystals</u>; Meuthen: London, 1963.

39 Curie, D. In _Optical Properties of Ions in Solids_;
   DiBartolo, B. Ed.; Plenum: New York, 1975, pp. 71-105.

40 Tyner, C. E.; Drotning, W. D.; Drickamer, E. G. _J. Appl._
   Phys. 1976, _47_, 1044-1047.

41 DiBartolo, B. _Optical Interactions in Solids_; Wiley: New
   York, 1968.

42 Kelley, C. S. _Phys. Rev._ 1979, _20_, 5084-5089.

43 Auzel, F. In _Radiationless Processes_; DiBartolo, B. Ed.;
   Plenum: New York, 1980, pp. 238-264.

44 Forster, T. _Discuss. Faraday Soc._ 1959, _27_, 7-17

45 Powell, R. C.; Blasse, G. _Structure and Bonding_ 1980, _42_,
   43-96.

46 Lin, S. H., Ed. _Radiationless Transitions_; Academic Press:
   New York, 1980.

47 Yen, W. M.; Selzer, P. M., Ed. _Laser Spectroscopy of Solids_;
   Springer-Verlag: Berlin, 1981.

48 DiBartolo, B., Ed. _Radiationless Processes_; Plenum: New
   York, 1980.

49 Hufner, S. _Optical Spectra of Transparent Rare Earth_
   Compounds; Academic Press: New York, 1978.

50 Agranovich, V. M.; Galanin, M. D. _Electronic Excitation_
   Energy Transfer in Condensed Matter; North-Holland:
   Amsterdam, 1982, pp. 171-290.

51 Blasse, G. _J. Less-Common Metals_ 1985, _112_, 1-8.

52 Movaghar, B.; Sauer, G. W.; Wurtz, D. _J. Stat. Phys._ 1982,
   _27_, 473-485.

53 Yokota, M.; Tanimoto, O. _J. Phys. Soc. Japan_ 1967, _22_,
   779-784.

54 Bernard, J. E.; Berry, D. E.; Williams, F. In _Energy_
   Transfer Prcesses in Condensed Matter; DiBartlo, B. Ed.;
   Plenum: New York, 1984, pp. 49-73.

55 Blasse, G. In _Energy Transfer Prcesses in Condensed Matter_;
   DiBartlo, B. Ed.; Plenum: New York, 1984, pp. 251-261.

56 Neuhauser, W.; Hohenstatt, M.; Toschek, P. E. _Phys. Rev. A_
   1980, _22_, 1137-1140.

57 Nguyen, D. C.; Keller, R. A.; Trkula, M. J. Opt. Soc. Am. B: Opt. Phys. 1987, 4 138.

58 Radley, J. A.; Grant, J. Fluorescence Analysis in Ultra-Violet Light; Chapman & Hall: London, 1933.

59 Gleason, S. Ultraviolet Guide to Minerals; Van Nostrand: New York, 1960.

60 King, A. A. Chem. and Ind. 1928, 4, 301.

61 Warner, I. M.; McGown, L. B. Anal. Chem. 1988, 60, 162R-175R.

62 Gilbault, G. G. Practical Fluorescence; Marcel Dekker: New York, 1973.

63 Seitz, W. R. In Treatise on Analytical Chemistry; 2nd. ed.; Elving, P. J.; Meehan, E. W.; Kolthoff, I. M. Eds.; Wiley: New York, 1981, pp. 230-241.

64 Holcombe, J. A.; Bass, D. A. Anal. Chem. 1988, 60, 226R-252R.

65 Cooke, P. M. Anal. Chem. 1988, 60, 221R-226R.

66 Johnson, W. M.; Maxwell, J. A. Rock and Mineral Analysis; 2nd. ed.; Wiley: New York, 1981, pp. 201-205.

67 Feigl, F.; Anger, V. Spot Tests in Inorganic Analysis; 6th. ed.; Elsevier: Amsterdam, 1972, pp 500-501.

68 Ryan, D. E.; Prime, R. J.; Holzbecher, J.; Young, R. E. Anal. Lett. 1973, 6, 721-729.

69 Ho, C.-N.; Warner, I. M. Anal. Chem. 1982, 54, 2486-2491.

70 Excimer Laser Fuel Gas Lifetimes: What to Believe?; Technical Note No. 3; Questek Inc., Billerica, MA, May, 1983;

71 Hans, W.; Scott, P. Laser Focus/Electro Optics 1983, 19(10), 86-92.

72 Harris, J. M.; Lytle, F. E.; McCain, T. C. Anal. Chem. 1976, 48, 2095-2098.

73 Engstrom, R. W. Photomultiplier Handbook; RCA: Lancaster, PA; 1980.

74 Stair, R.; Schneider, W. E.; Jackson, J. K. Appl. Opt. 1963, 12, 1151-1154.

75 Ott, H. W. Noise Reduction Techniques in Electronic Systems; Wiley: New York, 1976.

163

76 Violette, J. L.; White, D. R. J.; Violette, M. F. Electro-magnetic Compatibility Handbook; Van Nostrand Reinhold: New York, 1987.

77 The Radio Amateur's Handbook, 61st ed.; American Radio Relay League: Newington, CT, 1983, Chapter 15.

78 Farnsworth, Marie; The Theory and Technique of Quantitative Analysis; Wiley: New York, 1928.

79 Cotton, F. A.; Wilkinson, G. Advanced Inorganic Chemistry, 2nd ed.; Interscience: New York, 1966.

80 Rieck, G. D. Tungsten and its Compounds; Pergamon: Oxford, 1967.

81 Vogel, A. I. A Textbook of Quantitative Inorganic Analysis, 3rd ed.; Longmans: London, 1961.

82 Kroger, A. Some Aspects of the Luminescence of Solids; Elsevier: New York, 1948.

83 Parker, G. A. Analytical Chemistry of Molybdenum; Springer-Verlag: Berlin, 1983.

84 Reddy, V. P.; Mehrotra, P. N. Thermochim. Acta 1979, 31, 31-37.

85 Sharma, A. K.; Kaushik, N. K. Thermochim. Acta 1985, 83, 347-376.

86 Reddy, V. B.; Mehrotra, P. N. Thermochim. Acta 1980, 42, 363-367.

87 Mittal, S.; Sharma, A. K.; Kaushik, N. K. Thermochim. Acta 1985, 89, 195-202.

88 Larsen, E. M. In Advances in Inorganic Chemistry and Radio-chemistry; Academic Press: New York, 1981; Vol.13, pp 1-133.

89 Blumenthal, W. B. The Chemical Behavior of Zirconium; Van Nostrand: Princeton, NJ, 1958.

90 Azaroff, L. V.; Buerger, M. J. The Powder Method in X-ray Crystallography; McGraw-Hill: New York, 1958.

91 Tyner, C. E.; Drickamer, H. G. J. Chem. Phys. 1977, 67, 4103-4115.

92 Press, W. H.; Flannery, B. P.; Teukolsky, S. A.; Vetterlung, W. T. Numerical Recipes; Cambridge Univ. Press: Cambridge, 1986, Chapter 10.

93 Spendley, W.; Hext, G. R.; Himsworth, F. R. <u>Technometrics</u> 1962, <u>4</u>, 441.

94 Parker, L. R.; Cave, M. R.; Barnes, R. M <u>Anal. Chim. Acta</u> 1985, <u>175</u>, 231-237.

95 Ryan, P. B.; Barr, R. L.; Todd, H. D. <u>Anal. Chem.</u> 1980, <u>52</u>, 1460-1467.

96 Cave, M. R. <u>Anal. Chim. Acta</u> 1986, <u>181</u>, 107-116.

97 Burgess, D. D. <u>Anal. Chim. Acta</u> 1986, <u>181</u>, 97-106.

98 Van Der Wiel, P. F. A.; Massen, R.; Kateman, G. <u>Anal. Chim. Acta</u> 1983, <u>153</u>, 83-92.

99 Nelder, J. A.; Mead, R. <u>Comput. J.</u> 1965, <u>7</u>, 308-313.

100 Daniels, R. W. <u>An Introduction to Numerical Methods and Optimization Techniques</u>; North-Holland: New York, 1978, pp. 177-202

101 Caceci, M. S.; Cacheris, W. P. <u>Byte</u>, 1984, May, 340-362.

102 Gelb, A. Ed. <u>Applied Optimal Estimation</u>; MIT Press: Cambridge MA, 1974.

103 Brown, R. G. <u>Introduction to Random Signal Analysis and Kalman Filtering</u>; Wiley: New York, 1984.

104 Dudgeon, D. E.; Mersereau, R. M. <u>Multidimensional Digital Signal Processing</u>; Prentice-Hall: Englewood Cliffs, NJ, 1984.

105 Brown, S. D. <u>Anal. Chim. Acta</u> 1986, <u>181</u>, 1-26.

106 Rutan, S. C. <u>J. Chemometrics</u> 1987, <u>1</u>, 7-18.

107 Woods, J. W. <u>Top. Appl. Phys.</u> 1982, <u>42</u>, 155-205.

108 Rutan, S. C.; Brown, S. D. <u>Anal. Chim. Acta</u> 1985, <u>175</u>, 219-229.

109 Knorr, F. J.; Harris, J. M.; <u>Anal. Chem.</u> 1981, <u>53</u>, 272-276.

110 Knorr, F. J.; Thorsheim, H. R.; Harris, J. M. <u>Anal. Chem.</u> 1981, <u>53</u>, 821-825.

111 Kroger, A. <u>Some Aspects of the Luminescence of Solids</u>; Elsevier: New York, 1948.

112 Treadaway, M. J.; Powell, R. C. <u>J. Chem. Phys.</u> 1974, <u>61</u>, 4003-4011.

113 Gurvitch, A. M.; Gutan, V. B.; Meleshkin, B. N.; Mikhailin, V. V.; Mikhalev, A. A.; Tombak, M. I. J. Lumin. 1977, 15, 187-199.

114 Ivanovskii, A. L.; Zhukov, V. P.; Slepukhin, V. K.; Gubanov, V. A.; Shveikin, G. P. Zh. Strukt. Khim. 1980, 21, 30-36.

115 Tyner, C. E.; Drickamer, H. G. J. Chem. Phys. 1977, 67, 4103-4115.

116 Van Loo, V. J. Lumin. 1975, 10, 221-235.

117 Blasse, G.; Van den Heuvel, G. P. M. J. Lumin., 1974, 9, 74-78.

118 Grasser, R.; Scharmann, A. J. Lumin. 1976, 12/13, 473-478.

119 Wong, J,; Angell, C. A. Glass Structure by Spectroscopy; Marcel Dekker: New York, 1976.

120 Wyckoff, R. W. G. Crystal Structures, 2nd. ed.; Inter-science: New York, 1965, Vol. 3, pp. 41-43.

121 Palache, C.; Berman, H.; Fronel, C. The System of Mineralogy, 7th. ed.; Wiley: New York, 1951, Vol. II, pp. 1064-1071.

122 Gorobets, B. S.; Nauchitel, M. A. Konstitutsiia i Svoistva Mineralov, 1975, 9, 98-105.

123 Nauchitel, M. A. Zakonomren. Raspred. Primesnykh Tsentrov Ionnykh Krist. 1974, 3, 71-79.

124 Efendiev, Sh. M; Darvishov, N. G.; Gabrielyan, V. T. Phys. Stat. Sol. A 1984, 86, K105-K108.

125 Darvishov, N. G.; Godzhaeva, Sh. M.; Efendiev, Sh. M.; Yusifov, F. K.; Deposited Doc. 1984, VINITI 1678-84, 12pp.

126 Gaft, M. L.; Gorobets, B. S.; Khomyakov, A. P. Dokl. Akad. Nauk SSSR 1981, 260, 1234-1237.

127 Lysakov, V. S.; Solntsev, V. P.; Eliseev, A. P. Zh. Prikl. Spektrosk. 1976, 25, 823-826.

128 Blasse, G.; Bril, A. J. Solid State Chem. 1970, 2, 105-108.

129 Blasse, G. Structure and Bonding 1980, 42, 1-41.

130 Braam, A. W.; Blasse, G. Solid State Commun. 1976, 20, 717-719.

131 Blasse, G.; De Korte, P. H. M. J. Inorg. Nucl. Chem. 1981, 43, 1505-1506.

132 Kravets, N. V.; Zakharov, V. M.; Polezhaev, Yu. M.;
    Kruzhalov, A. V.; Shul'gin, B. V. Zh. Fiz. Khim. 1978, 52,
    1810.

133 Wyckoff, R. W. G. Crystal Structures, 2nd. ed.; Inter-
    science: New York, 1965, Vol. 2, pp. 390-402.

SPECTROMETER CONTROL PROGRAM IN BASIC

```
1     'PROGRAM ZAPIT-9C  - REVISION 7.6 - 870826 - USES ISOLATION RELAY
:
2     'BY  E. F. PASKI   *   (C) COPYRIGHT 1987   *    ALL RIGHTS RESERVED
:
3     'ACQUISITION PROGRAM FOR CORONA - BOXCAR - MONOCHROMATOR - PEAK DETECTOR
:
10    'MONOCHROMATOR DRIVER ROUTINE IN MACHINE LANGUAGE
11    CLEAR,&HFF00 : DEF SEG : DEF USR0=&HFF00
12    FOR I%=&HFF00 TO &HFFFF : POKE I%,0 : NEXT I%    'INITIALIZE MEMORY
13    'READ AND STORE MONOCHROMATOR DRIVER PROGRAM
14     FOR I%=&HFF00 TO &HFF45 : READ X% : POKE I%,X% : NEXT I%
15      DATA &HB8,&H0,&H0,&HA3,&HF2,&HFF,&HFF,&H06,&HF2,&HFF,&HBA,&HBC,&H03
16      DATA &HB0,&H7F,&HEE
17      DATA &HB8,&H0,&H0,&HA3,&HF6,&HFF,&HFF,&H06,&HF6,&HFF,&HBE,&HF4,&HFF
18      DATA &HBF,&HF6,&HFF,&HA7,&H75,&HF3
19      DATA &HBA,&HBC,&H03,&HB0,&H7E,&HEE
20      DATA &HB8,&H0,&H0,&HA3,&HF6,&HFF,&HFF,&H06,&HF6,&HFF,&HBE,&HF4,&HFF
21      DATA &HBF,&HF6,&HFF,&HA7,&H75,&HF3
22      DATA &HBE,&HF0,&HFF,&HBF,&HF2,&HFF,&HA7,&H75,&HC1,&HCB
23    POKE &HFFF0,&H1 : POKE &HFFF1,&H0    'MINIMUM TOGGLES ON PORT
24    POKE &HFFF4,&H10 : POKE &HFFF5,&H0     'CONTROLS WAIT PERIOD
70    HOME$=CHR$(12)
:     LF$=CHR$(10)
:     BELL$=CHR$(7)
:     QT$=CHR$(34)
:     KEY OFF
90    NHITS%=6     '# LASER SHOTS PER DATA POINT
100   DIM HIT(100), SHOT(200,1), LUMIN(100,10), REFER(100,10)
200   PRINT HOME$; BELL$
300   '
301   PRINT HOME$;"FILE HEADER DATA ---"
310     INPUT"FILE NAME ";FILENAME$
:       IF INSTR(FILENAME$,".") THEN 315
311     IF FILENAME$="" THEN FILENAME$="TESTTEST.LCD"
313     FILENAME$=LEFT$(FILENAME$,8)+".LCD"
315     PRINT
:       LINE INPUT"SUBSTANCE ";SUBSTANCE$
:       IF SUBSTANCE$="" THEN SUBSTANCE$="**"
320     PRINT
:       LINE INPUT"MISCELLANY ";MISC$
:       IF MISC$="" THEN MISC$="***"
330     PRINT
:       INPUT"WAVELENGTH (ANGSTROMS) TO START SCAN  "; LAMSTART%
:       IF LAMSTART%=0 THEN LAMSTART%=1
331     PRINT LAMSTART%
335     PRINT
:       INPUT"WAVELENGTH (ANGSTROMS) TO END SCAN    "; LAMEND%
:       IF LAMEND%=0 THEN LAMEND%=1
336     PRINT LAMEND%
```

```
340   PRINT
:     INPUT"WAVELENGTH (ANGSTROMS) STEPS FOR SCAN "; LAMSTEP%
:     IF LAMSTEP%=0 THEN LAMSTEP%=1
341   PRINT LAMSTEP%
350   PRINT
:     INPUT"CURRENT WAVELENGTH ON MONOCHROMATOR (ANGSTROMS) "; ANGORIGIN%
:     IF ANGORIGIN%=0 THEN ANGORIGIN%=1
351   PRINT ANGORIGIN%
352   ANGEND%=ANGORIGIN%
360   PRINT
:     INPUT"BOXCAR WINDOW WIDTH, MICROSECONDS  (DEFAULT=1)";WINWIDE
:     IF WINWIDE=0 THEN WINWIDE=1
361   PRINT WINWIDE
370   PRINT
:     INPUT"NUMBER OF WINDOWS AT EACH WAVELENGTH  (DEFAULT=5)";NWINDOWS%
:     IF NWINDOWS%>100 THEN PRINT BELL$;"MAXIMUM ALLOWED IS 100" : GOTO 370
371   IF NWINDOWS%<1 THEN NWINDOWS%=5
375   PRINT NWINDOWS%
380   PRINT
:     INPUT"GATE DELAY MULTIPLIER [MAX:=10; VALUE*0.1]  (DEFAULT=1)";GATEMUL
:     IF (GATEMUL*NWINDOWS%)>100 THEN PRINT BELL$
:     PRINT"MUST HAVE: 100 > WINDOWS * GATEMUL!" : GOTO 380
381   IF GATEMUL=0 THEN GATEMUL=1
382   PRINT GATEMUL
385   DVOLTS=GATEMUL*.1
390   PRINT
:     INPUT"DELAY SCALE SETTING, IN MICROSECONDS    (DEFAULT=10) ";DELAYSCALE
:        IF DELAYSCALE=0 THEN DELAYSCALE=10
395   PRINT DELAYSCALE
400   PRINT LF$;LF$;LF$;BELL$
:     PRINT"ENSURE THAT SAMPLE IS PROPERLY MOUNTED AND LASER IS READY";LF$
:     PRINT"ENTER ";QT$;"GO";QT$;" TO COMMENCE EXPERIMENT"
410   INPUT A$
:        IF NOT(A$="GO" OR A$="go") THEN 400
1000  'OPEN FILE FOR SERIAL PORT, SETUP BOXCAR INTERFACE
1010  GOSUB 10200
:     GOSUB 10300
1030  'OPEN SEQUENTIAL TEXT FILE FOR DATA
1040  OPEN "O",2,FILENAME$
1050  PRINT#2, FILENAME$
:     PRINT#2, SUBSTANCE$
:     PRINT#2, MISC$
:     PRINT#2, TIME$
:     PRINT#2, DATE$
:     PRINT#2, DELAYSCALE
:     PRINT#2, DVOLTS
1052  PRINT#2, NHITS%
:     PRINT#2, NWINDOWS%
:     PRINT#2, LAMSTART%
:     PRINT#2, LAMEND%
:     PRINT#2, LAMSTEP%
:     PRINT#2, WINWIDE
1060  CLOSE 2
```

```
1100   'CAPTURE ONE SET OF SPECTRA, N READINGS AT EACH OF M WAVELENGTHS
1110 FOR LAMDA%=LAMSTART% TO LAMEND% STEP LAMSTEP%
1120     PRINT"SLEWING TO ";LAMDA%;" ANGSTROMS"
:          ANGSTART%=ANGEND%
:          ANGEND%=LAMDA%
:          GOSUB 10100
1200     'COLLECT A DECAY CURVE AT THIS WAVELENGTH
1210     'SET DELAY TIME N BOXCAR
:          note - at default setting of 10us on DELAY SCALE,
:                    10.000v = 100us and time delay steps are in
:                    0.100v increments which becomes 1.0us steps.
1220      GOSUB 10800 : GOSUB 10800
1230      FOR NSHOT%=1 TO NWINDOWS%
1240        DY$="S8="+STR$(DVOLTS*NSHOT%)
1250        PRINT#1, DY$
1260        FOR I%=1 TO NHITS%
1270          GOSUB 10800
1272          LUMIN(NSHOT%,I%)=VAL(LUM$)
:            REFER(NSHOT%,I%)=VAL(REF$)
1280          HIT(I%)=VAL(VALUE$)
1285          IF HIT(I%)>10.2 THEN HIT(I%)=99.999
1290        NEXT I%
1300        SH1#=0
:            SH2#=0
:            SR1#=0
:            SR2#=0
1310        FOR I%=1 TO NHITS%
:              SH1#=SH1#+LUMIN(NSHOT%,I%)
:              SH2#=SH2#+LUMIN(NSHOT%,I%)*LUMIN(NSHOT%,I%)
:              SR1#=SR1#+REFER(NSHOT%,I%)
:              SR2#=SR2#+REFER(NSHOT%,I%)*REFER(NSHOT%,I%)
:            NEXT I%
1320        MEAN#=SH1#/NHITS%
:            REFMEAN#=SR1#/NHITS%
:            STDDEV#=SQR(ABS((SH2#-SH1#*SH1#/NHITS%)/(NHITS%-1)))
:            REFSD#=SQR(ABS((SR2#-SR1#*SR1#/NHITS%)/(NHITS%-1)))
1330        SHOT(NSHOT%,0)=MEAN#
:            SHOT(NSHOT%,1)=STDDEV#
1340        PRINT USING"####";LAMDA%; : PRINT"A";
:            PRINT USING"###.###";NSHOT%*DELAYSCALE*DVOLTS;
:            PRINT"us SIG=";
:            PRINT USING"##.####";SHOT(NSHOT%,0);
:            PRINT", sd=";
:            PRINT USING"##.####";SHOT(NSHOT%,1);
1342        PRINT",";
:            PRINT USING "###.#";ABS(100*SHOT(NSHOT%,1)/SHOT(NSHOT%,0));
:            PRINT "%, REF=";
:            PRINT USING"##.###";REFMEAN#;
:            PRINT " sd=";
:            PRINT USING"###.#";100*REFSD#/REFMEAN#; : PRINT"%"
1350      NEXT NSHOT%
```

```
1360      OPEN"A",2,FILENAME$
1370      FOR I%=1 TO NWINDOWS%
1371        FOR J%=1 TO NHITS%
1372          PRINT#2,USING" ##.###";LUMIN(I%,J%);
1373        NEXT J%
1374        PRINT#2," "
1375        FOR J%=1 TO NHITS%
1376          PRINT#2,USING" ##.###";REFER(I%,J%);
1377        NEXT J%
1378        PRINT#2," "
1379      NEXT I%
1380      CLOSE 2
1390    NEXT LAMDA%
1400    'SET MONOCHROMATOR BACK TO START POSITION
1500    PRINT BELL$;"RUN FOR ";FILENAME$;" COMPLETED AT ";TIME$;" ON ";DATE$
9999  GOTO 32767
:
:
:
10100 'MONOCHROMATOR DRIVER SUBROUTINE
        USE MOTHERBOARD PARALLEL PRINTER PORT
        SET MONOCHROMATOR CONTROLLER TO 20 ANGSTROMS/SEC
        THERE ARE 60 PULSES PER ANGSTROM
        DO NOT EXCEED 600 HZ PULSING!! (20 A/SEC IS MAXIMUM SPEED)
10102 '  PARALLEL PORT PIN ASSIGNMENTS:
        PIN   VALUE   FUNCTION
10104 '   2      1    TOGGLE FOR STEPPER MOTOR PULSING
          7     32    HIGH = CLOSES RELAY TO CONNECT MONOCHROMATOR
          7     32    LOW  = OPENS RELAY TO DISCONNECT MONOCHROMATOR
10110     PF=60
:         SLMAX=60000!
:         KAH%=234
:         KAL%=96
10120     SLEW =ABS(PF*(ANGEND%-ANGSTART%)) : IF SLEW <4 THEN RETURN
10125     OUT &H3BC,&H20  'TURNS MONOCHROMATOR RELAY ON
10130     PRINT"SLEWING ";SLEW/PF;" ANGSTROMS NOW - BE PATIENT"
10135     SLEW=SLEW-2 'DUE TO EXTRA TOGGLES CREATED BY ISOLATION RELAY!!!
10140     IF SLEW<=SLMAX THEN 10190
10150       SLEW=SLEW-SLMAX
10160       POKE &HFFF0,KAL%
:           POKE &HFFF1,KAH%
:           I=USR0(0)
10170       IF SLEW=0 THEN 10198
10180     GOTO 10140
10190     AH%=INT(SLEW/256)
:         AL%=INT(SLEW-256*AH%)
:         POKE &HFFF0,AL%
:         POKE &HFFF1,AH%
:         I=USR0(0)
10198     OUT &H3BC,&H0   'TURNS MONOCHROMATOR RELAY OFF
10199 RETURN
:
:
:
```

```
10200 'SERIAL COMMUNICATIONS SETUP
        SETS PORT#1 FOR 9600 BAUD, NO PARITY, 8DATA BITS, 2 STOP BITS
:
10210      OPEN"COM1:9600,N,8,2,CS,DS,CD" AS #1
:          PRINT#1,"       "
:          PRINT#1,"MR;W25"
10299  RETURN
:
:
10300 'SETUP BOXCAR INTERFACE PORTS
:
10310      PRINT#1,"I5"    'PORTS 1-5 INPUT; PORTS 6-8 OUTPUT
10320      PRINT#1,"S8=0"
10399  RETURN
:
:
10500 'LIST SHOT BY SHOT DATA ON SCREEN
10510      FOR KK%=1 TO NHITS%
:            PRINT USING" ##.###";LUMIN(NSHOT%,KK%);
:          NEXT KK%
:          PRINT
10520      FOR KK%=1 TO NHITS%
:            PRINT USING" ##.###";REFER(NSHOT%,KK%);
:          NEXT KK%
:          PRINT
10599  RETURN
:
:
10800 'FIRE LASER VIA PORT#7, TAKE LUMINESCENCE & REFERENCE PMT VALUES
10820      PRINT#1,"S6=5"
10825      PRINT#1,"S7=10"
10830      PRINT#1,"S7=0"
10840      GOSUB 30800
10870      PRINT#1,"?2"
:          INPUT#1,REF$
:          PRINT#1,"S6=0"
:          PRINT#1,"?1"
:          INPUT#1,LUM$
10899  RETURN
:
:
18100 'APPARATUS CABLE CONNECTIONS:
:
18110 'BOXCAR AVERAGER MODULE:
:
18120 'BOXCAR INPUTS:  TRIGGER - PHOTODIODE TRIGGER UNIT
:                      SIGNAL  - SIGNAL PHOTOMULTIPLIER
:
18130 'COMPUTER INTERFACE MODULE:
:
18140 'CHANNEL #1 - BOXCAR LAST SAMPLE OUTPUT
:             #2 - PEAK DETECTOR UNIT OUTPUT
:             #6 - PEAK DETECTOR UNIT RESET
:             #7 - LASER EXTERNAL TRIGGER
```

```
:                    #8 - BOXCAR EXTERNAL DELAY (ON BOXCAR REAR PANEL)
:
18150 'PEAK DETECTOR MOULE:
:
18160 'INPUT  - REFERENCE PMT
:      OUTPUT - INTERFACE CHANNEL #2
:      RESET  - INTERFACE CHANNEL #6
:
18170 'CORONA COMPUTER:
:
18180 'PARALLEL PORT - MONOCHROMATOR ISOLATION RELAY
:      SERIAL PORT   - SRS COMPUTER INTERFACE
:
18300 'NORMAL SWITCH SETTINGS:
:
18310 'MONOCHROMATOR SCANNER:
:
18320 'FRONT PANEL:
:         SCAN DIRECTION - INCREASE
:         SCAN RATE      - 20 ANGSTROMS/SEC
:         SCAN           - CONTINUOUS
:         SLEW           - OFF (BOTH SWITCHES)
:      REAR PANEL:
:         EXT. INPUT     - EXT.
:
18330 'BOXCAR MODULE:
:
18340 'TRIGGER RATE - EXT.
:              THRESHOLD - VARY
:
:      DELAY SCALE - VARY
:            MULTIPLIER - ZERO
:
:      WIDTH SCALE - VARY
:            MULTIPLIER - NORMALLY AT 1
:
18345 'SIGNAL SENSITIVITY - VARY
:              INPUT FILTER - DC
:              INPUT OFFSET - VARY
:
:      AVERAGING - LAST SAMPLE
:
18348 'REAR PANEL SWITCHES:
:         LAST SAMPLE - INVERTED
:         AVERAGE      - INVERTED
:
30800 'DELAY ROUTINE
30810      FOR FOOP=1 TO 10 : FOOQ=FOOQ : NEXT FOOP
30899 RETURN
:
32767 END
```

MONOCHROMATOR STEPPER MOTOR DRIVER ROUTINE

```
FF00  B80000      MOV      AX,0000         ; Set AX register to zero
FF03  A3F2FF      MOV      [FFF2],AX       ; Set $FFF2 to value in AX
FF06  FF06F2FF    INC      WORD PTR [FFF2] ; Add 1 to value in $FFF2
; Toggle the stepper motor line high
FF0A  BABC03      MOV      DX,03BC         ; Set DX register to $03BC
FF0D  B07F        MOV      AL,7F           ; Parallel port pin #2 high
FF0F  EE          OUT      DX,AL           ; Output AL to port DX
; Wait routine - so we don't toggle the poor stepper motor too fast
FF10  B80000      MOV      AX,0000         ; Set AX register to zero
FF13  A3F6FF      MOV      [FFF6],AX       ; Set $FFF6 to value in AX
FF16  FF06F6FF    INC      WORD PTR [FFF6] ; Add 1 to value in $FFF6
FF1A  BEF4FF      MOV      SI,FFF4         ; Set SI to value in $FFF4
FF1D  BFF6FF      MOV      DI,FFF6         ; Set DI to value in $FFF6
FF20  A7          CMPSW                    ; SI minus DI, is it zero?
FF21  75F3        JNZ      FF16            ; Jump to $FF16 if not done
; Now we toggle stepper motor line low
FF23  BABC03      MOV      DX,03BC         ; Set DX register to $03BC
FF26  B07E        MOV      AL,7E           ; Parallel port pin #2 low
FF28  EE          OUT      DX,AL           ; Output AL to port DX
; Another pause for the belabored stepper motor
FF29  B8000       MOV      AX,0000         ; Set AX register to zero
FF2C  A3F6FF      MOV      [FFF6],AX       ; Set $FFF6 to value in AX
FF2F  FF06F6FF    INC      WORD PTR [FFF6] ; Add 1 to value in $FFF6
FF33  BEF4FF      MOV      SI,FFF4         ; Set SI to value in $FFF4
FF36  BFF6FF      MOV      DI,FFF6         ; Set DI to value in $FFF6
FF39  A7          CMPSW                    ; SI minus DI, is it zero?
FF3A  75F3        JNZ      FF2F            ; Jump to $FF2F if not done
; Have we slewed the desired distance?
FF3C  BEF0FF      MOV      SI,FFF0         ; Set SI to value in $FFF0
FF3F  BFF2FF      MOV      DI,FFF2         ; Set DI to value in $FFF2
FF42  A7          CMPSW                    ; SI minus DI, is it zero?
FF43  75C1        JNZ      FF06            ; Jump to $FF06 if not done
FF45  CB          RETF                     ; Return to BASIC program
```

LUMINESCENCE DATA FILE HANDLER IN BASIC

```
1     'PROGRAM SQUEEZEM - REVISION 2.3 - 871128 - BASIC
:
2     'BY E. F. PASKI   *   (C) COPYRIGHT 1987   *   ALL RIGHTS RESERVED
:
3     'CONVERTS RAW DATA FILES FROM SPECTROMETER ACQUISITION PROGRAM:
      - COMPRESSES DATA FILES BY AVERAGING SHOT BY SHOT VALUES
      - APPLIES SYSTEM SPECTRAL RESPONSE CORRECTION
      - CREATES ENERGRAPHICS FORMAT DATA FILES FOR 3D GRAPHICS
4     '
10    PRINT"PROGRAM SQUEEZEM - REV 2.3 - 871128" : PRINT
12    PRINT"CONVERTS '.LCD' FILES TO '.SCC' FILES: SPECTRAL CORRECTION USING"
14    PRINT"CARBON TETRACHLORIDE FILTER" : PRINT:PRINT
16    'FOR METHANOL FILTER CORRECTION USE LINES 8000-8999 IN PLACE OF 7000-7999
100   OPTION BASE 1
110   'MAIN DATA ARRAY X(Q,TIME,WAVELENGTH)
:      Q=1 - SPECTRAL RESPONSE CORRECTED SPECTRUM
:      Q=2 - STANDARD DEVIATION FOR Q=1
:      Q=3 - BACKGROUND & DROOP ONLY CORRECTED SPECTRUM
:      Q=4 - DROOP CORRECTION FACTOR
118   DIM XI(20),RI(20),LUM(20),REF(20)
120   DIM X(4,31,51),C(551),ABAK(31),BBAK(31),DB$(13),DA$(13),EA$(8)
130   ZERO=1E-10
200   'INPUT DATA FILE NAMES & READ
210   GOSUB 1000
400   GOSUB 5000
610   GOSUB 6000
990   PRINT "FINISHED AT ";TIME$
999   GOTO 32767
1000  '
1001  INPUT"FIRST BACKGROUND FILE NAME";A$ : ABAKFIL$=A$
1010  IF INSTR(A$,".")=0 THEN ABAKFIL$=LEFT$(A$,8)+".LCD"
1015  OPEN"I",1,ABAKFIL$ : PRINT"FILE ";ABAKFIL$;" PRESENT" : CLOSE 1
1020  INPUT"SECOND BACKGROUND FILE NAME";A$ : BBAKFIL$=A$
1030  IF INSTR(A$,".")=0 THEN BBAKFIL$=LEFT$(A$,8)+".LCD"
1035  OPEN"I",1,BBAKFIL$ : PRINT"FILE ";BBAKFIL$;" PRESENT" : CLOSE 1
1040  INPUT"SPECTRA DATA FILENAME";A$ : DATAFILE$=A$
1050  IF INSTR(A$,".")=0 THEN DATAFILE$=LEFT$(A$,8)+".LCD"
1055  OPEN"I",1,DATAFILE$ : PRINT"FILE ";DATAFILE$;" PRESENT" : CLOSE 1
1060  GOSUB 7000 'SPECTRAL RESPONSE DATA
1090  PRINT"READING BACKGROUND NOISE FILES"
1100  OPEN"I",1,ABAKFIL$
:     OPEN"I",2,BBAKFIL$
1110  FOR I%=1 TO 13
:        INPUT #1,DA$(I%)
:        INPUT #2,DB$(I%)
:     NEXT I%
1120  NM$="A"
:     GOSUB 3000
:     IF NM$="X" THEN PRINT"FILE A = ";ABAKFIL$;", FILE B = ";BBAKFIL$
:        GOTO 2000
```

```
1130 STWL%=VAL(DA$(10))
:    ENWL%=VAL(DA$(11))
:    INWL%=VAL(DA$(12))
:    NTIMES%=VAL(DA$(9))
:    NHITS%=VAL(DA$(8))
1140 NWAVES%=1+(ENWL%-STWL%)/INWL%
1190 REFBAK=0
:    RB%=0
1200 FOR W%=1 TO NWAVES%
1210   FOR T%=1 TO NTIMES%
1220     ABK=0
:        BBK=0
1230     FOR I%=1 TO NHITS%
:          INPUT#1,X
:          ABK=ABK+X
:        NEXT I%
1240     FOR I%=1 TO NHITS%
:          INPUT#1,R
:          REFBAK=REFBAK+R
:          RB%=RB%+1
:        NEXT I%
1250     FOR I%=1 TO NHITS%
:          INPUT#2,X
:          BBK=BBK+X
:        NEXT I%
1260     FOR I%=1 TO NHITS%
:          INPUT#2,R
:          REFBAK=REFBAK+R
:          RB%=RB%+1
:        NEXT I%
1270     ABAK(T%)=ABAK(T%)+ABK/NHITS%
:        BBAK(T%)=BBAK(T%)+BBK/NHITS%
1280   NEXT T%
1290 NEXT W%
1300 FOR I%=1 TO NTIMES%
:      ABAK(I%)=ABAK(I%)/NWAVES%
:      BBAK(I%)=BBAK(I%)/NWAVES%
:    NEXT I%
1310 REFBAK=REFBAK/RB%
1320 CLOSE 1,2
2000 'READ MAIN DATA FILE, DO BACKGROUND SUBTRACTION, DISCARD OUTLIERS
2025 PRINT"READING DATA FILE  - TIME IS ";TIME$
2030 OPEN"I",1,DATAFILE$
2040 FOR I%=1 TO 13
:      INPUT#1,DA$(I%)
:    NEXT I%
2050 GOSUB 3000
:    IF NM$="X" THEN PRINT"FILE A = ";DATAFILE$;", FILE B = ";BBAKFIL$
:      PRINT"PROGRAM ABORTED"
:      GOTO 32767
2060 STWL%=VAL(DA$(10))
:    ENWL%=VAL(DA$(11))
:    INWL%=VAL(DA$(12))
:    NTIMES%=VAL(DA$(9))
```

```
:      NHITS%=VAL(DA$(8))
:      NWAVES%=1+(ENWL%-STWL%)/INWL%
:      DVOLTS=VAL(DA$(7))
:      DELAYSCALE=VAL(DA$(6))
2200 'SUBTRACT BACKGROUND
2220 FOR W%=1 TO NWAVES%
2230   FOR T%=1 TO NTIMES%
2240      X1=0
:         X2=0
:         R1=0
:         BN= ABAK(T%)-(ABAK(T%)-BBAK(T%))*((W%-1)/(NWAVES%-1))
2260      FOR I%=1 TO NHITS% : INPUT#1,LUM(I%) : NEXT I%
:         FOR I%=1 TO NHITS% : INPUT#1,REF(I%) : NEXT I%
:         J%=0 : X1=0 : X2=0
2270      FOR I%=1 TO NHITS%
:            IF REF(I%)>10.236 THEN 2300
2280         REF(I%)=REF(I%)-REFBAK
:            IF REF(I%)>RMAX THEN RMAX=REF(I%)
2285         IF REF(I%)<.4999 THEN 2300
2290         LUM(I%)=LUM(I%)-BN
:            J%=J%+1
:            XI(J%)=LUM(I%)
:            RI(J%)=REF(I%)
:            X1=X1+XI(J%)
:            X2=X2+XI(J%)*XI(J%)
:            R1=R1+RI(J%)
2300      NEXT I%
2302      IF J%=0 THEN K%=1 : X1=ZERO : R1=ZERO : SDX=X1 : GOTO 2350
2304      IF J%=1 THEN K%=1 : SDX=X1 : GOTO 2350
2310      MN=X1/J%
:         SD2=SQR((X2-X1*X1/J%)/(J%-1))
:         TV=MN-SD2
:         X1=0 : R1=0 : K%=0 : X2=0
2320      FOR I%=1 TO J%
:            IF XI(I%)<TV THEN 2340
2330         K%=K%+1
:            T=XI(I%)/RI(I%)
:            X1=X1+T
:            X2=X2+T*T
:            R1=R1+RI(I%)
2340      NEXT I%
2345      SDX=SQR((X2-X1*X1/K%)/(K%-1))
2350      REM
2352      X(2,T%,W%)=SDX
2353      X(3,T%,W%)=X1/K%
2354      X(4,T%,W%)=R1/K%
2360   NEXT T%
2370 NEXT W%
2380 CLOSE 1
2390 PRINT"FINISHED READING DATA FILES"
2600 FOR W%=1 TO NWAVES%
2605   L%=((STWL%+(W%-1)*INWL%)-2490)/10
2606   IF L%<1 THEN L%=1
2607   IF L%>551 THEN L%=551
```

```
2608    SCF=1/C(L%)
2610    FOR T%=1 TO NTIMES%
2620      X(4,T%,W%)=X(4,T%,W%)/RMAX 'NORMALIZE DROOP FACTOR
2622      X(3,T%,W%)=X(3,T%,W%)*RMAX
2624      X(2,T%,W%)=X(2,T%,W%)*RMAX*SCF 'STD. DEV. CORRECTION
2626      X(1,T%,W%)=X(3,T%,W%)*SCF 'LUMINESCENCE SPECTRAL CORRECTION
2730    NEXT T%
2740  NEXT W%
2999  RETURN
3000  'CHECK FOR MISMATCHED FILE PARAMETERS
3100  IF DA$(6)<>DB$(6) THEN NM$="X"
:       PRINT"DELAY SCALES DON'T MATCH - FILE A =";DA$(6);"  FILE B =";DB$(6)
3110  IF DA$(7)<>DB$(7) THEN NM$="X"
:       PRINT"DELAY STEPS DON'T MATCH - FILE A =";DA$(7);"  FILE B =";DB$(7)
3120  IF DA$(8)<>DB$(8) THEN NM$="X"
:       PRINT"# HITS DON'T MATCH - FILE A =";DA$(8);"  FILE B =";DB$(8)
3130  IF DA$(9)<>DB$(9) THEN NM$="X"
:       PRINT"# WINDOWS DON'T MATCH - FILE A =";DA$(9);"  FILE B =";DB$(9)
3140  IF DA$(13)<>DB$(13) THEN NM$="X"
:       PRINT"WINDOW WIDTHS DON'T MATCH - FILE A =";DA$(13);"  FILE B =";DB$(13)
3999  RETURN
5000  'SAVE BACKGROUND CORRECTED DATA
5010  BAKCORFIL$=LEFT$(DATAFILE$,INSTR(DATAFILE$,"."))+"SCC"
5020  DA$(2)="$  "+DA$(2)    'FLAG FOR CORRECTED DATA
5030  GE$="###.#### ###.#### ###.#### ###.####"
5100  PRINT : PRINT"SAVING CORRECTED DATA UNDER FILE NAME ";BAKCORFIL$
5110  OPEN"O",#1,BAKCORFIL$
5120  PRINT#1, BAKCORFIL$
   : FOR I%=2 TO 13
   :   PRINT#1, DA$(I%)
   : NEXT I%
5130  FOR M%=1 TO NWAVES%
5140    FOR N%=1 TO NTIMES%
5160      PRINT#1,USING GE$; X(1,N%,M%),X(2,N%,M%),X(3,N%,M%),X(4,N%,M%)
5170    NEXT N%
5180  NEXT M%
5190  CLOSE 1
5200  PRINT CHR$(7)
5999  RETURN
6000  '
6001  ENERFILE$=LEFT$(DATAFILE$,INSTR(DATAFILE$,"."))+"SUR"
6010  IF INSTR(ENERFILE$,".")=0 THEN ENERFILE$=LEFT$(ENERFILE$,8)+".SUR"
6012  IF INSTR(ENERFILE$,".SUR")=0 THEN ENERFILE$=LEFT$(ENERFILE$,8)+".SUR"
6030  XA$=" Time, us"
6040  YA$=" Wavelength, nm"
6050  ZA$="Relative Intensity"
6100  'SET UP ENERGRAPHICS FILE HEADER
6105  SPASE$="                                                  "
6110  EA$(1)=RIGHT$(SPASE$+DA$(2),50)
6112  TEM$=LEFT$(ENERFILE$,LEN(ENERFILE$)-4)
6114  EA$(1)=TEM$+MID$(EA$(1),LEN(TEM$))
6120  EA$(2)=DA$(5)+" at "+DA$(4)
6130  A=DELAYSCALE*DVOLTS
6132  EA$(3)=MID$(STR$(A)+SPASE$,2,5)+XA$+RIGHT$(SPASE$+STR$(A*NTIMES%),5)
```

```
6140 A=10
6142 EA$(4)=MID$(STR$(.1*STWL%)+SPASE$,2,A)+YA$+RIGHT$(SPASE$+STR$(.1*ENWL%),A)
6143 EA$(4)=MID$(STR$(.1*STWL%)+SPASE$,2,8)+YA$+RIGHT$(SPASE$+STR$(.1*ENWL%),9)
6150 EA$(5)=ZA$
6160 EA$(6)=STR$(NTIMES%)+","+STR$(NWAVES%)+",1,"+STR$(NTIMES%)+","+STR$(STWL%)
+","+STR$(ENWL%)
6162 EA$(6)=STR$(NTIMES%)+","+STR$(NWAVES%)+",1,20,3000,5000"
6170 A1$=".2," : IF NTIMES%=20 THEN A1$=".25,"
6172 A2$=".0016,.5,-200,40"
6173 IF(STWL%=3500 AND ENWL%=7000) THEN A2$=".002,.5,-350,30"
6174 IF(STWL%=2500 AND ENWL%<=5000) THEN A2$=".0029,.5,-200,25"
6175 IF(STWL%=2500 AND ENWL%=6000) THEN A2$=".002,.5,-225,50"
6176 IF(STWL%=3000 AND ENWL%=5000) THEN A2$=".0032,.5,-475,5"
6179 EA$(7)=A1$+A2$
6180 EA$(8)="60,30,3,0"
6182 EA$(7)=".25,.0032,.2,-475,5"
6200 OPEN"O",#1,ENERFILE$
6205 PRINT
:    PRINT"WRITING FILE ";ENERFILE$;" TO DISC
6210 FOR I%=1 TO 8
6220    PRINT#1,EA$(I%)
6230 NEXT I%
6240 FOR I%=1 TO NTIMES%
6250    FOR J%=1 TO NWAVES%
6260       PRINT#1, X(1,I%,J%)
6270    NEXT J%
6280 NEXT I%
6290 CLOSE 1
6999 RETURN
7000 'DATA FOR CARBON TETRACHLORIDE FILTER - SMOOTHED WITH A 3 POINT MOVING
AVERAGE
7010 FOR I%=1 TO 551 : READ C(I%) : NEXT I%
7201 DATA .00010,.01878,.02200,.01676,.01235,.03393,.03342,.03342,.00862,.00010
7202 DATA .01823,.01823,.04728,.06868,.09121,.08180,.07153,.08246,.09337,.10475
7203 DATA .10527,.12337,.10932,.10472,.08795,.10595,.11150,.12162,.13138,.14454
7204 DATA .14750,.14164,.15112,.14597,.13956,.13999,.14886,.16519,.16187,.16915
7205 DATA .16728,.17482,.17263,.17539,.17205,.18156,.19474,.20036,.20388,.20377
7206 DATA .21191,.21917,.22964,.22972,.23514,.23258,.23985,.24069,.24607,.25469
7207 DATA .26626,.27006,.27907,.27886,.28641,.28607,.28870,.29315,.29725,.30665
7208 DATA .30673,.30722,.30910,.31220,.31204,.31635,.31891,.33003,.33040,.33439
7209 DATA .33846,.34510,.34677,.34380,.34217,.34314,.34868,.35234,.35777,.36154
7210 DATA .36553,.36900,.37062,.37474,.38123,.38658,.39173,.39817,.40610,.41332
7211 DATA .42197,.42900,.43703,.44276,.45153,.45932,.46703,.47405,.47953,.48844
7212 DATA .49984,.51490,.52273,.53001,.53463,.54407,.55414,.57068,.58236,.58819
7213 DATA .59570,.60469,.61881,.63202,.64532,.65649,.65863,.66477,.67422,.69462
7214 DATA .71418,.72945,.73463,.74161,.75038,.76495,.77567,.78652,.79313,.80356
7215 DATA .81325,.83132,.84257,.85408,.85734,.86645,.87627,.88655,.89286,.89959
7216 DATA .89229,.88964,.88544,.89677,.90540,.90594,.90467,.90839,.91429,.92527
7217 DATA .92680,.92890,.92602,.92824,.93344,.93994,.94586,.95078,.95263,.95468
7218 DATA .95924,.96432,.97047,.97414,.97767,.97674,.97970,.98254,.98684,.99161
7219 DATA .99465,.99450,.99353,.99101,.99281,.98909,.98662,.98122,.97899,.97743
7220 DATA .97522,.97002,.96175,.95532,.94898,.94629,.94178,.93649,.92770,.91878
7221 DATA .91107,.90543,.89975,.89413,.88640,.88064,.87401,.86838,.86484,.86012
7222 DATA .85848,.85254,.85214,.84834,.84667,.84230,.83975,.83590,.83079,.82722
```

```
7223 DATA .82230,.81777,.81255,.80763,.80180,.79588,.79084,.78542,.78011,.77476
7224 DATA .77120,.76651,.76225,.75635,.75150,.74444,.73930,.73335,.72915,.72391
7225 DATA .71855,.71415,.70919,.70448,.69936,.69497,.69002,.68463,.67980,.67543
7226 DATA .67114,.66611,.66097,.65629,.65166,.64800,.64418,.64004,.63424,.62910
7227 DATA .62424,.62038,.61588,.61228,.60831,.60452,.60087,.59708,.59347,.58878
7228 DATA .58507,.58059,.57681,.57295,.56924,.56553,.56142,.55798,.55473,.55108
7229 DATA .54740,.54374,.54028,.53636,.53299,.52953,.52645,.52265,.52027,.51747
7230 DATA .51483,.51095,.50693,.50312,.49984,.49650,.49366,.49070,.48867,.48515
7231 DATA .48244,.47968,.47740,.47448,.47101,.46789,.46518,.46250,.46038,.45721
7232 DATA .45419,.45105,.44860,.44693,.44417,.44127,.43779,.43570,.43377,.43102
7233 DATA .42845,.42563,.42372,.42120,.41909,.41656,.41422,.41167,.40951,.40801
7234 DATA .40613,.40416,.40165,.39941,.39727,.39516,.39267,.39058,.38858,.38684
7235 DATA .38510,.38275,.38101,.37919,.37708,.37529,.37294,.37106,.36907,.36788
7236 DATA .36657,.36479,.36247,.36038,.35816,.35658,.35449,.35308,.35096,.34937
7237 DATA .34783,.34628,.34462,.34256,.34070,.33916,.33764,.33605,.33435,.33262
7238 DATA .33073,.32879,.32727,.32564,.32425,.32209,.32099,.31939,.31805,.31603
7239 DATA .31441,.31231,.31060,.30871,.30751,.30596,.30390,.30208,.30054,.29966
7240 DATA .29824,.29640,.29447,.29279,.29123,.28985,.28823,.28667,.28528,.28352
7241 DATA .28214,.28018,.27850,.27665,.27553,.27475,.27366,.27198,.27050,.26904
7242 DATA .26738,.26567,.26413,.26249,.26078,.25931,.25804,.25645,.25456,.25312
7243 DATA .25154,.25007,.24835,.24690,.24550,.24364,.24262,.24050,.23915,.23728
7244 DATA .23594,.23388,.23203,.23034,.22905,.22754,.22630,.22494,.22297,.22118
7245 DATA .21954,.21789,.21646,.21519,.21368,.21175,.20982,.20803,.20612,.20442
7246 DATA .20261,.20155,.19923,.19742,.19531,.19432,.19381,.19298,.19257,.19240
7247 DATA .19211,.19092,.18904,.18807,.18690,.18613,.18479,.18347,.18181,.18006
7248 DATA .17818,.17669,.17454,.17339,.17102,.16956,.16718,.16547,.16320,.16065
7249 DATA .15804,.15514,.15350,.15155,.14976,.14751,.14446,.14219,.13910,.13755
7250 DATA .13546,.13314,.13058,.12824,.12652,.12494,.12292,.12084,.11785,.11618
7251 DATA .11450,.11331,.11110,.10928,.10802,.10664,.10495,.10279,.10075,.09888
7252 DATA .09715,.09571,.09481,.09382,.09281,.09136,.09009,.08895,.08785,.08621
7253 DATA .08521,.08375,.08325,.08186,.08086,.07964,.07873,.07808,.07708,.07594
7254 DATA .07482,.07396,.07298,.07212,.07109,.07029,.06952,.06883,.06811,.06745
7255 DATA .06674,.06576,.06470,.06416,.06400,.06368,.06290,.06230,.06123,.06060
,.05992
7999 RETURN
8000 'DATA FOR METHANOL FILTER - SMOOTHED WITH A 3 POINT MOVING AVERAGE
8010 FOR I%=1 TO 551 : READ C(I%) : NEXT I%
8101 DATA .75168,.69409,.66074,.62706,.59737,.58709,.60040,.59013,.54360,.55848
8102 DATA .52574,.53244,.49083,.48193,.46513,.43307,.45309,.45379,.44462,.41383
8103 DATA .41005,.42855,.42507,.39957,.37681,.36086,.36434,.37313,.37368,.36028
8104 DATA .33769,.34556,.35390,.35213,.32819,.31858,.32291,.33035,.33285,.32468
8105 DATA .31673,.31745,.32528,.33141,.32661,.32637,.32837,.32814,.33062,.32770
8106 DATA .33170,.32011,.32719,.32312,.32922,.33231,.34371,.35554,.35798,.35960
8107 DATA .35716,.35937,.36073,.37281,.37868,.38230,.37445,.37457,.36741,.36728
8108 DATA .36318,.36702,.36946,.37104,.36867,.36840,.37479,.37728,.38408,.37915
8109 DATA .38609,.38482,.38081,.37153,.36162,.36055,.35561,.35703,.35530,.35921
8110 DATA .36133,.37082,.37946,.38986,.39631,.39919,.40262,.40587,.40822,.40662
8111 DATA .39941,.40052,.39791,.39942,.39642,.39517,.39488,.40118,.41814,.44637
8112 DATA .47185,.49656,.51358,.53102,.54275,.55004,.55757,.55915,.55827,.55301
8113 DATA .55187,.55446,.55318,.54484,.53028,.52445,.53754,.57059,.61292,.65225
8114 DATA .68409,.70557,.72117,.73411,.74811,.76401,.77413,.78282,.78946,.79923
8115 DATA .81001,.82513,.83697,.84580,.84481,.84607,.84868,.85449,.85776,.85883
8116 DATA .85915,.86362,.86830,.87549,.88013,.88510,.88636,.88977,.89282,.90082
8117 DATA .90235,.90457,.90220,.90538,.90802,.91510,.92173,.92820,.93109,.93375
```

```
8118 DATA .93614,.94030,.94437,.94823,.95143,.95201,.95662,.96045,.96596,.97267
8119 DATA .98029,.98813,.99146,.99465,.99565,.99277,.98909,.98672,.98825,.98850
8120 DATA .99104,.98919,.98717,.98104,.97836,.97337,.96867,.96283,.95932,.95491
8121 DATA .94964,.94414,.93929,.93348,.92922,.92634,.92577,.92867,.93129,.93361
8122 DATA .93251,.93481,.94151,.94775,.95534,.96077,.96643,.96962,.97350,.97980
8123 DATA .98297,.98477,.98318,.98523,.98849,.99378,.99600,.99590,.99636,.99674
8124 DATA .99744,.99614,.99566,.99579,.99540,.99542,.99536,.99511,.99379,.99290
8125 DATA .99231,.99031,.98755,.98462,.98288,.98222,.97948,.97842,.97460,.97331
8126 DATA .96973,.96898,.96597,.96335,.95880,.95569,.95399,.95179,.94905,.94545
8127 DATA .94182,.93951,.93587,.93328,.93055,.92776,.92551,.92230,.91951,.91407
8128 DATA .91102,.90737,.90553,.90208,.89855,.89388,.88962,.88593,.88336,.87968
8129 DATA .87593,.87160,.86794,.86471,.86067,.85529,.85090,.84776,.84455,.84012
8130 DATA .83579,.83062,.82725,.82236,.82043,.81601,.81209,.80780,.80356,.79949
8131 DATA .79370,.78950,.78514,.78242,.77782,.77416,.76864,.76557,.76164,.75860
8132 DATA .75377,.74910,.74358,.73843,.73465,.73088,.72737,.72250,.71811,.71403
8133 DATA .71135,.70724,.70256,.69806,.69443,.69119,.68627,.68187,.67703,.67184
8134 DATA .66717,.66326,.65981,.65639,.65279,.64936,.64586,.64221,.63939,.63569
8135 DATA .63131,.62680,.62316,.61943,.61591,.61119,.60811,.60413,.60122,.59656
8136 DATA .59272,.58883,.58662,.58311,.57965,.57583,.57223,.56822,.56354,.55959
8137 DATA .55521,.55065,.54648,.54225,.53860,.53481,.53053,.52661,.52175,.51735
8138 DATA .51245,.50742,.50386,.49943,.49532,.48996,.48599,.48144,.47672,.47084
8139 DATA .46720,.46290,.45933,.45432,.45032,.44540,.44073,.43608,.43261,.42782
8140 DATA .42393,.41847,.41435,.40957,.40604,.40207,.39818,.39335,.38893,.38445
8141 DATA .38112,.37703,.37268,.36762,.36323,.35979,.35636,.35281,.34878,.34438
8142 DATA .34070,.33637,.33315,.32899,.32475,.32038,.31714,.31410,.31105,.30674
8143 DATA .30256,.29839,.29489,.29142,.28803,.28415,.28124,.27771,.27467,.27093
8144 DATA .26793,.26448,.26118,.25747,.25464,.25149,.24886,.24536,.24231,.23959
8145 DATA .23694,.23422,.23068,.22754,.22445,.22136,.21864,.21578,.21347,.21088
8146 DATA .20885,.20664,.20412,.20103,.19859,.19617,.19527,.19454,.19506,.19489
8147 DATA .19480,.19364,.19246,.19086,.18992,.18870,.18720,.18510,.18308,.18125
8148 DATA .17959,.17731,.17463,.17235,.17009,.16815,.16588,.16375,.16115,.15863
8149 DATA .15578,.15307,.15041,.14815,.14622,.14406,.14138,.13854,.13585,.13385
8150 DATA .13169,.12930,.12728,.12514,.12331,.12099,.11915,.11709,.11525,.11319
8151 DATA .11144,.10974,.10825,.10661,.10502,.10363,.10258,.10162,.10048,.09881
8152 DATA .09733,.09614,.09539,.09430,.09315,.09199,.09076,.08976,.08851,.08757
8153 DATA .08630,.08531,.08430,.08342,.08259,.08183,.08097,.08010,.07905,.07811
8154 DATA .07722,.07634,.07526,.07444,.07353,.07284,.07211,.07146,.07073,.06977
8155 DATA .06908,.06832,.06757,.06671,.06603,.06559,.06482,.06415,.06338,.06291
,.06236
8999 RETURN
32767 PRINT
    : PRINT"BYE!"
    : CLOSE
    : END
```

DATA REDUCTION PROGRAM USING SIMPLEX OPTIMIZATION

```
C*******************************************************************
C*******************************************************************
C
C      PROGRAM ZECONC.FOR
C
C      DATA REDUCTION FOR MULTIDIMENSIONAL LUMINESCENCE SPECTRA - FORTRAN 77
C
C      COPYRIGHT 1988 BY E. F. PASKI - ALL RIGHTS RESERVED
C
C      REVISION 3.15 - 880303 - General version - uses four column input file
C
       DOUBLE PRECISION SAP,CP,D,DP,CTAU,SURPRM,DLY,WHW,DA,NU,P
       INTEGER N,NTIMES,NWAVES,NCOMP,PMV,PMX,WLST,WLEN,TMST,TMEN
C
       COMMON CP(5,30),CTAU(25),D(51,30),DP(51,30),DA(15),NU(51),
      X         P(30,21),SAP(51,5),SURPRM(5,5),PMX(5),
      X         NWAVES,NTIMES,N,WLST,WLEN,TMST,TMEN,DLY,WHW,NCOMP,PMV
C
C *** COMMON VARIABLES (NON DIMENSIONED):
C
C      NWAVES  = NUMBER OF WAVELENGTH CHANNELS
C      NTIMES  = NUMBER OF TIME CHANNELS
C      N       = NUMBER OF UNKNOWN SPECIES TO FIND
C      WLST    = STARTING WAVELENGTH, ANGSTROMS
C      WLEN    = END WAVELENGTH, ANGSTROMS
C      TMST    = STARTING TIME, MICROSECONDS
C      TMEN    = END TIME, MICROSECONDS
C      DLY     = DELAY TIME INTERVAL, MICROSECONDS
C      WHW     = GATE TIME WINDOW, HALF WIDTH
C      NCOMP   = NUMBER OF UNKNOWN SPECIES TO FIND
C      PMV     = NUMBER OF PARAMETERS TO VARY IN SIMPLEX OPTIMIZATION
C
C        DIMENSIONED VARIABLES:
C
C        WHERE:  T = NUMBER OF TIME CHANNELS, DEFAULT TO 30
C                W = NUMBER OF WAVELENGTH CHANNELS, DEFAULT TO 51
C                U = NUMBER OF COMPONENTS, DEFAULT TO 5
C
C        CNTRD(5*U)     = CENTROID IN SIMPLEX
C        CP(U,T)        = TIME BEHAVIOUR MATRIX
C        CPT(T,U)       = TRANSPOSE OF [CP]
C        CTAU(5*U)      = SIMPLEX FOR TIMES
C        D(T,W)         = ORIGINAL DATA MATRIX
C        DA(15)         = SPECTRUM REGION DATA MATRIX
C        DP(T,W)        = COMPUTED DATA MATRIX
C        MXI(5*U,5*U)   = MATRIX TO BE INVERTED
C        MXIPV(5*U,3)   = PIVOT FOR MATRIX INVERSION
C        NU(W)          = RECIPROCAL ANGSTROMS
C        P(5*U+5,4*U+1) = PARAMETER MATRIX FOR SIMPLEX OPTIMIZATION
C        PMX(5)         = POINTER MATRIX FOR SELECTING COMPONENTS TO VARY
```

```
C        SAP(W,U)        = WAVELENGTH BEHAVIOUR MATRIX
C        SURPRM(U,5)     = SURFACE PARAMTER MATRIX
C        TP(5*U+1)       = TEMPORARY STORAGE IN SORT ROUTINE
C
         REAL LOWAVE,HIWAVE,LOTIME,HITIME
         DOUBLE PRECISION OLDERF,ERLIM,ERF,RERF
         INTEGER ICONRD,I,J,NIT
         CHARACTER LIN(5)*80,FILNAM*12,PMVAR*12,PARMSV*12,PAS*4,README*12,
     X           PARLST*12
C
C
C**** OPEN MASTER CONTROL FILE
         ICONRD=19
         README='PCONTROL.FIL'
         OPEN(UNIT=ICONRD,FILE=README)
C
C**** INITIALIZE ALL COMMON VARIABLES
  100 CALL COMZER
C
C****    READ MASTER CONTROL FILE
         CALL CONRD(ICONRD,FILNAM,PMVAR,LOWAVE,HIWAVE,LOTIME,HITIME,
     X PARMSV)
         IF(INDEX(FILNAM,'***END***').GT.0) GO TO 32767
C
C****    OPEN FILE FOR INTERMEDIATE PARAMETER VALUES
         IF (INDEX(PMVAR,'F').EQ.0) GOTO 120
         PARLST=PARMSV(1:(INDEX(PARMSV,'.')))//'IPM'
         OPEN(UNIT=67,FILE=PARLST,STATUS='NEW')
         WRITE(67,*)'INTERMEDIATE PARAMETER VALUES FOR FILE ', FILNAM
         WRITE(67,*) PMVAR
C
  120    CONTINUE
C
C****    READ A SPECTRUM
         CALL SPEKRD(FILNAM,LIN,LOWAVE,HIWAVE,LOTIME,HITIME)
C
C****    OPTIMIZE FOR LIFETIMES
         PAS='TIME'
         OLDERF=1E10
         ERLIM=1E-5
         N=NCOMP
         NIT=0
         ERF=0
         DO 410 I=1,NCOMP
            P(1,I)=SURPRM(I,1)
  410    CONTINUE
         CALL SIMPLX(PAS,OLDERF,ERLIM,NIT,ERF,PMVAR)
C
C****    OPTIMIZE FOR SELECTED PARAMETERS
         PAS='SURF'
         OLDERF=1E10
         ERLIM=1E-5
         N=NCOMP*PMV
         CALL GAUZER
```

```
              I=0
              DO 520 J=1,NCOMP
                DO 510 K=1,PMV
                  I=I+1
                  P(1,I)=SURPRM(J,PMX(K))
      510       CONTINUE
      520     CONTINUE
C
              IF (INDEX(PMVAR,'Q').GT.0) GO TO 600
C
              CALL SIMPLX(PAS,OLDERF,ERLIM,NIT,ERF,PMVAR)
C
      600     CONTINUE
C
C****     SAVE PARAMETERS FOR REDUCED SPECTRUM
              RERF=0
              DO 620 I=1,NTIMES
                DO 610 J=1,NWAVES
                  RERF=RERF+D(J,I)
      610       CONTINUE
      620     CONTINUE
              RERF=ERF/RERF
              CALL PRMSVR(FILNAM,LIN,LOWAVE,HIWAVE,LOTIME,HITIME,ERF,RERF,
     X        PMVAR,PARMSV,NIT)
C
          IF (INDEX(PMVAR,'S').GT.0) CALL SPKSVR(PARMSV,LIN)
C
          IF (INDEX(PMVAR,'F').GT.0) CLOSE(67)
C
          GO TO 100
C
32767 CLOSE(ICONRD)
          STOP
          END
C
C*********************************************************************************
C*********************************************************************************
C
          SUBROUTINE COMZER
C
C**** INITIALIZES ALL COMMON VARIABLES
C
          DOUBLE PRECISION SAP,CP,D,DP,CTAU,SURPRM,DLY,WHW,DA,NU,P
          INTEGER N,NTIMES,NWAVES,NCOMP,PMV,PMX,WLST,WLEN,TMST,TMEN
C
          COMMON CP(5,30),CTAU(25),D(51,30),DP(51,30),DA(15),NU(51),
     X          P(30,21),SAP(51,5),SURPRM(5,5),PMX(5),
     X          NWAVES,NTIMES,N,WLST,WLEN,TMST,TMEN,DLY,WHW,NCOMP,PMV
C
          INTEGER I,J
C
          NWAVES=0
          NTIMES=0
          N=0
```

```
               WLST=0
               WLEN=0
               TMST=0
               TMEN=0
             . DLY=0
               WHW=0
               NCOMP=0
               PMV=0
               DO 100 I=1,51
                  NU(I)=0
                  DO 10 J=1,5
                     SAP(I,J)=0
       10     CONTINUE
                  DO 20 J=1,30
                     D(I,J)=0
                     DP(I,J)=0
       20     CONTINUE
      100 CONTINUE
               DO 200 I=1,5
                  PMX(I)=5
                  DO 110 J=1,5
                     SURPRM(I,J)=0
      110     CONTINUE
                  DO 120 J=1,30
                     CP(I,J)=0
      120     CONTINUE
      200 CONTINUE
               DO 210 I=1,15
                  DA(I)=0
      210 CONTINUE
               DO 220 I=1,25
                  CTAU(I)=0
      220 CONTINUE
               RETURN
               END
C
C****************************************************************************
C****************************************************************************
C
       SUBROUTINE SIMPLX(PAS,OLDERF,ERLIM,NIT,ERF,PMVAR)
C
C**** SIMPLEX OPTIMIZATION FOR MINIMUM ERROR
C           PAS    - FLAG FOR ERROR FUNCTION CALCULATION
C           OLDERF - PREVIOUS LOW ERROR FUNCTION VALUE
C           ERLIM  - VALUE FOR ACCEPTABLE RELATIVE ERROR LEVEL
C           NIT    - # ITERATIONS DONE (QUIT AFTER MAXNIT)
C           ERF    - ERROR FUNCTION VALUE
C           PMVAR  - PARAMETERS TO HOLD CONSTANT AND FLAGS
C
       DOUBLE PRECISION SAP,CP,D,DP,CTAU,SURPRM,DLY,WHW,DA,NU,P
       INTEGER N,NTIMES,NWAVES,NCOMP,PMV,PMX,WLST,WLEN,TMST,TMEN
C
       COMMON CP(5,30),CTAU(25),D(51,30),DP(51,30),DA(15),NU(51),
      X       P(30,21),SAP(51,5),SURPRM(5,5),PMX(5),
```

```
      X         NWAVES,NTIMES,N,WLST,WLEN,TMST,TMEN,DLY,WHW,NCOMP,PMV
C
        DOUBLE PRECISION CNTRD(25),TP(26),OLDP(21)
        DOUBLE PRECISION ALPHA,BETA,GAMMA,ERF,AK,OLDERF,ERLIM,SCALEF,PTST,
      X                 TTMP,ERRTST,PARMAX,PARZIP
        INTEGER PCHI,PL,PH,PNH,PR,PE,PC,I,J,IPR,IPC,NIT,MAXNIT,ENFLAG
        CHARACTER PAS*4,PMVAR*12
C
C**** LOCAL VARIABLES: CNTRD()   - CENTROID
C                      ALPHA     - REFLECTION COEFFICIENT
C                      BETA      - EXPANSION COEFFICIENT
C                      GAMMA     - CONTRACTION COEFFICIENT
C                      SCALEF    - SCALE FACTOR TO INCREASE SIMPLEX
C                      ENFLAG    - FLAG FOR DIFFERENCES IN PARAMETER VALUES
C                      ERF       - CURRENT ERROR FUNCTION VALUE
C                      ERRTST    - NORMALIZED VALUE OF ERF-OLDERF
C                      MAXNIT    - MAXIMUM # ITERATIONS ALLOWED
C                      OLDP()    - PREVIOUS LOW ERF VALUES FOR PARAMETERS
C                      PARMAX    - MAXIMUM ALLOWED VALUE FOR A PARAMETER
C                      PARZIP    - PARAMETER IS SET TO THIS IF > PARMAX
C                      PCHI      - ERROR FUNCTON COLUMN
C                      PL        - VECTOR WITH LOWEST CHISQUARE
C                      PH        - VECTOR WITH NEXT LOWEST CHISQUARE
C                      PNH       - VECTOR WITH NEXT HIGHEST CHISQUARE
C.                     PR        - VECTOR FOR REFLECTED POINT
C                      PE        - VECTOR FOR EXPANDED POINT
C                      PC        - VECTOR FOR CONTRACTED POINT
C                      PTST      - MAXIMUM RATIO ALLOWED FOR OLDP()/P()
C                      AK        - DUMMY
C
        PCHI=N+1
        PL=1
        PNH=N
        PH=N+1
        PR=N+2
        PE=N+3
        PC=N+4
        MAXNIT=1000
        ALPHA=0.9985
        GAMMA=0.4985
        BETA=1.95
        SCALEF=0.69
        ERF=1E10
        PTST=0.0001
        PARMAX=1E+8
        PARZIP=1E-8
C
C**** GENERATE PARAMETER MATRIX [P]
 1030 AK=1.1
        DO 1038 I=2,PH
          DO 1036 J=1,N
            P(I,J)=P(1,J)
            IF (P(I,J).GT.PARMAX) P(I,J)=PARZIP
            IF ((I-J).EQ.1) P(I,J)=AK*P(I,J)
```

```
 1036   CONTINUE
 1038 CONTINUE
C
C**** COMPUTE ERROR FUNCTION FOR EACH VECTOR IN [P]
      DO 1080 IPR=1,PH
        DO 1070 IPC=1,N
          CTAU(IPC)=P(IPR,IPC)
 1070   CONTINUE
        CALL ERFKAL(ERF,PAS)
        P(IPR,PCHI)=ERF
        IF (ERF .GE. OLDERF) GOTO 1078
          OLDERF=ERF
          DO 1076 I=1,PCHI
            OLDP(I)=P(IPR,I)
 1076.    CONTINUE
 1078   CONTINUE
 1080 CONTINUE
C
 1100 CONTINUE
C**** SORT [P] TO INCREASING CHISQUARE
C
      CALL SUPSRT(PCHI,PCHI,PCHI,P)
C
 1230 PL=1
      PH=N+1
      PNH=N
C
C**** CALCULATE CENTROID
      DO 1318 I=1,N
        CNTRD(I)=-P(PH,I)
        DO 1316 J=1,PH
          CNTRD(I)=CNTRD(I)+P(J,I)
 1316   CONTINUE
        CNTRD(I)=CNTRD(I)/N
 1318 CONTINUE
C
C**** CALCULATE REFLECTED POINT
 1320 CONTINUE
 1330 AK=1+ALPHA
 1340 DO 1348 I=1,N
        P(PR,I)=AK*CNTRD(I)-ALPHA*P(PH,I)
        IF (P(PR,I).GT.PARMAX) P(PR,I)=PARZIP
        CTAU(I)=P(PR,I)
 1348 CONTINUE
      CALL ERFKAL(ERF,PAS)
      P(PR,PCHI)=ERF
C
C**** TEST FOR HIGH REFLECTION SUCCESS - EXPAND IF SO
 1410 IF (P(PR,PCHI)-P(PL,PCHI)) 1420,1500,1500
 1420 PL=PH
      PH=PNH
      AK=1-BETA
      DO 1428 I=1,N
        P(PE,I)=BETA*P(PR,I)+AK*CNTRD(I)
```

```
           IF (P(PE,I).GT.PARMAX) P(PE,I)=PARZIP
           CTAU(I)=P(PE,I)
 1428 CONTINUE
      CALL ERFKAL(ERF,PAS)
      P(PE,PCHI)=ERF
 1440 IF (P(PE,PCHI).LT.P(PR,PCHI)) GO TO 1460
 1450 DO 1458 I=1,PCHI
         P(PL,I)=P(PR,I)
 1458 CONTINUE
      GOTO 1700
 1460 DO 1468 I=1,PCHI
         P(PL,I)=P(PE,I)
 1468 CONTINUE
      GOTO 1700
C
C**** TEST FOR REFLECTION FAILURE - CONTRACT IF SO
 1500 IF (P(PR,PCHI) .LT. P(PH,PCHI)) GO TO 1600
 1520 AK=1-GAMMA
      DO 1528 I=1,N
        P(PR,I)=AK*CNTRD(I)+GAMMA*P(PH,I)
        IF (P(PR,I).GT.PARMAX) P(PR,I)=PARZIP
        CTAU(I)=P(PR,I)
 1528 CONTINUE
 1530 CALL ERFKAL(ERF,PAS)
      P(PR,PCHI)=ERF
 1540 IF (P(PR,PCHI) .GT. P(PL,PCHI)) GOTO 1560
 1550 PL=PH
      PH=PNH
      DO 1558 I=1,PCHI
         P(PL,I)=P(PR,I)
 1558 CONTINUE
      GOTO 1700
 1560 IF (P(PR,PCHI) .GE. P(PH,PCHI)) GOTO 1800
C
C *** IF MODERATE SUCCESS REFLECT AGAIN
 1600 DO 1618 I=1,PCHI
         P(PH,I)=P(PR,I)
 1618 CONTINUE
      IF (P(PR,PCHI)-P(PNH,PCHI)) 1100,1100,1320
C
C *** TEST FOR CONVERGENCE
 1700 CONTINUE
      ERF=P(PL,PCHI)
      IF (INDEX(PMVAR,'F').EQ.0) GOTO 1708
      J=NCOMP*PMV
      WRITE(67,*)'AT ITERATION ',NIT,(P(PL,I), I=1,PCHI)
 1708 CONTINUE
      IF (ERF.LT.1E-20) GO TO 1999
 1710 NIT=NIT+1
      ERRTST=DABS((P(PL,PCHI)-OLDERF)/P(PL,PCHI))
      IF (P(PL,PCHI) .GE. OLDERF) GOTO 1718
         OLDERF=P(PL,PCHI)
         ENFLAG=0
         DO 1716 I=1,PCHI
```

```
                  TTMP=DABS((OLDP(I)/P(PL,I))-1.0)
                  IF(TTMP.GT.PTST) ENFLAG=1
                  OLDP(I)=P(PL,I)
 1716    CONTINUE
 1718 CONTINUE
      IF (NIT.GT.MAXNIT) GO TO 1999
 1720 IF ((ERRTST-ERLIM).GT.0.0) GOTO 1100
C
C**** TEST FOR DIFFERENCES BETWEEN OLD AND NEW PARAMETERS
      IF (ENFLAG.GT.0) GOTO 1100
      GOTO 1999
C *** SCALE UP
 1800 NIT=NIT+1
      IF(NIT.GT.MAXNIT) GO TO 1999
      DO 1838 II=1,PCHI
         DO 1836 J=1,N
            P(II,J)=P(II,J)+SCALEF*(P(PL,J)-P(II,J))
            IF (P(II,J).GT.PARMAX) P(II,J)=PARZIP
            CTAU(J)=P(II,J)
 1836    CONTINUE
 1838 CONTINUE
      GO TO 1100
C
C *** RETURN TO MAIN PROGRAM
 1999 RETURN
      END
C
C*****************************************************************************
C*****************************************************************************
C
      SUBROUTINE ERFKAL(ERF,PAS)
C
C *** MAIN SUBROUTINE FOR COMPUTING ERROR FUNCTION
C            ERF     - ERROR FUNCTION VALUE
C            PAS     - FLAG: 'SURF' = FIT SURFACE WITHIN BOUNDS
C                            'STRP' = STRIP & FIT
C
      DOUBLE PRECISION SAP,CP,D,DP,CTAU,SURPRM,DLY,WHW,DA,NU,P
      INTEGER N,NTIMES,NWAVES,NCOMP,PMV,PMX,WLST,WLEN,TMST,TMEN
C
      COMMON CP(5,30),CTAU(25),D(51,30),DP(51,30),DA(15),NU(51),
     X       P(30,21),SAP(51,5),SURPRM(5,5),PMX(5),
     X       NWAVES,NTIMES,N,WLST,WLEN,TMST,TMEN,DLY,WHW,NCOMP,PMV
C
      DOUBLE PRECISION ERF
      CHARACTER PAS*4
C
C**** NO NEGATIVES PERMITTED FOR ANY PARAMETERS
      DO 50 I=1,N
         IF (CTAU(I).LT.0) THEN
            ERF=1E10
            RETURN
         END IF
   50 CONTINUE
```

```
C
      IF (PAS.EQ.'SURF') GOTO 200
C
  100 CALL TAUEST
      CALL DPEST
      CALL CHISQU(ERF)
      RETURN
C
  200 CALL TAUNON
      CALL DPEST
      CALL CHISQU(ERF)
      RETURN
      END
C
C******************************************************************
C******************************************************************
C
      SUBROUTINE DPEST
C
C *** COMPUTES TRIAL DATA MATRIX:  [D'] = [SAP] * [C']
C
      DOUBLE PRECISION SAP,CP,D,DP,CTAU,SURPRM,DLY,WHW,DA,NU,P
      INTEGER N,NTIMES,NWAVES,NCOMP,PMV,PMX,WLST,WLEN,TMST,TMEN
C
      COMMON CP(5,30),CTAU(25),D(51,30),DP(51,30),DA(15),NU(51),
     X       P(30,21),SAP(51,5),SURPRM(5,5),PMX(5),
     X       NWAVES,NTIMES,N,WLST,WLEN,TMST,TMEN,DLY,WHW,NCOMP,PMV
C
      INTEGER I,J,K
C
      DO 2208 I=1,NWAVES
        DO 2206 J=1,NTIMES
          DP(I,J)=0
          DO 2204 K=1,NCOMP
            DP(I,J)=DP(I,J)+SAP(I,K)*CP(K,J)
 2204     CONTINUE
 2206   CONTINUE
 2208 CONTINUE
      RETURN
      END
C
C******************************************************************
C******************************************************************
C
      SUBROUTINE CHISQU(ERF)
C
C *** COMPUTE ERROR BETWEEN ARAYS [D] AND [D']
C          ERF    - ERROR FUNCTION VALUE
C
      DOUBLE PRECISION SAP,CP,D,DP,CTAU,SURPRM,DLY,WHW,DA,NU,P
      INTEGER N,NTIMES,NWAVES,NCOMP,PMV,PMX,WLST,WLEN,TMST,TMEN
C
      COMMON CP(5,30),CTAU(25),D(51,30),DP(51,30),DA(15),NU(51),
     X       P(30,21),SAP(51,5),SURPRM(5,5),PMX(5),
```

```
      X         NWAVES,NTIMES,N,WLST,WLEN,TMST,TMEN,DLY,WHW,NCOMP,PMV
C
      INTEGER I,J
      DOUBLE PRECISION CHISQ,A,PNEG,SUM,SUMNEG,ERF
C
C**** LOCAL VARIABLES: CHISQ  - SUM DIFFERENCES SQARED
C                      PNEG   - PENALTY MULTIPLIER FOR NEGATIVE VALUES
 2310 CHISQ=0
      DO 2308 I=WLST,WLEN
         DO 2306 J=TMST,TMEN
           A=D(I,J)-DP(I,J)
           CHISQ=CHISQ+A*A
 2306    CONTINUE
 2308 CONTINUE
C
C *** PENALIZE FOR NEGATIVE VALUES IN [SAP]
 2330 PNEG=100
      SUM=0
      SUMNEG=0
 2340 DO 2348 I=WLST,WLEN
         DO 2346 J=1,NCOMP
           SUM=SUM+SAP(I,J)
           IF (SAP(I,J)) 2344,2345,2345
 2344       SUMNEG=SUMNEG-SAP(I,J)
 2345      CONTINUE
 2346    CONTINUE
 2348 CONTINUE
 2350 ERF=DABS(CHISQ*(1+PNEG*SUMNEG/SUM))
 2360 RETURN
      END
C
C********************************************************************
C********************************************************************
C
      SUBROUTINE TAUEST
C
C *** COMPUTES MATRIX [SAP] FOR CASE WHERE WE WANT TO FIND LIFETIMES
C
      DOUBLE PRECISION SAP,CP,D,DP,CTAU,SURPRM,DLY,WHW,DA,NU,P
      INTEGER N,NTIMES,NWAVES,NCOMP,PMV,PMX,WLST,WLEN,TMST,TMEN
C
      COMMON CP(5,30),CTAU(25),D(51,30),DP(51,30),DA(15),NU(51),
      X       P(30,21),SAP(51,5),SURPRM(5,5),PMX(5),
      X       NWAVES,NTIMES,N,WLST,WLEN,TMST,TMEN,DLY,WHW,NCOMP,PMV
C
      INTEGER I,J,K
      DOUBLE PRECISION CPT(30,5),MXI(25,25),WFW,ZA,ZB,TTA,TTB
C
C *** COMPUTE [SAP] = [D] * [C']T * ([C'] * [C']T)INVERSE
C
C *** COMPUTE LIFETIME MATRIX [C']
      WFW=2.0*WHW
      DO 2118 I=1,NTIMES
        TTA=-DLY*I
```

```
          TTB=TTA-WFW
          DO 2116 J=1,N
            ZA=TTA/CTAU(J)
            ZB=TTB/CTAU(J)
            IF (ZA.GT.69) ZA=69
            IF (ZA.LT.-69) ZA=-69
            IF (ZB.GT.69) ZB=69
            IF (ZB.LT.-69) ZB=-69
            CP(J,I)=CTAU(J)*(DEXP(ZA)-DEXP(ZB))
 2116    CONTINUE
 2118 CONTINUE
C
C *** COMPUTE THE PSEUDOINVERSE: ([C'] * [C']T)INVERSE
      DO 2138 I=1,N
        DO 2136 J=1,N
          MXI(I,J)=0
          DO 2134 K=1,NTIMES
            MXI(I,J)=MXI(I,J)+CP(I,K)*CP(J,K)
 2134      CONTINUE
 2136    CONTINUE
 2138 CONTINUE
      CALL MXINVT(N,MXI)
C
C *** COMPUTE: [CPT] = [C']T * ([C'] * [C']T)INVERSE
      DO 2168 I=1,NTIMES
        DO 2166 J=1,N
          CPT(I,J)=0
          DO 2164 K=1,N
            CPT(I,J)=CPT(I,J)+CP(K,I)*MXI(K,J)
 2164      CONTINUE
 2166    CONTINUE
 2168 CONTINUE
C
C *** COMPUTE: [SAP] = [D] * [CPT]
      DO 218  I=1,NWAVES
        DO 2186 J=1,N
          SAP(I,J)=0
          DO 2184 K=1,NTIMES
            SAP(I,J)=SAP(I,J)+D(I,K)*CPT(K,J)
 2184      CONTINUE
 2186    CONTINUE
 2188 CONTINUE
      RETURN
      END
C
C*******************************************************************
C*******************************************************************
C
      SUBROUTINE TAUNON
C
C *** COMPUTES MATRIX [SAP] FOR CASE WHERE LIFETIMES ARE KNOWN
C
      DOUBLE PRECISION SAP,CP,D,DP,CTAU,SURPRM,DLY,WHW,DA,NU,P
      INTEGER N,NTIMES,NWAVES,NCOMP,PMV,PMX,WLST,WLEN,TMST,TMEN
```

```
C
      COMMON CP(5,30),CTAU(25),D(51,30),DP(51,30),DA(15),NU(51),
     X       P(30,21),SAP(51,5),SURPRM(5,5),PMX(5),
     X       NWAVES,NTIMES,N,WLST,WLEN,TMST,TMEN,DLY,WHW,NCOMP,PMV
C
      REAL Z,T
      INTEGER I,J,K
      DOUBLE PRECISION WFW,TTA,TTB,ZA,ZB
C
C *** PUT CTAU VALUES INTO SURFACE PARAMATER MATRIX
      I=0
      DO 8418 J=1,NCOMP
        DO 8416 K=1,PMV
          I=I+1
          SURPRM(J,PMX(K))=CTAU(I)
 8416   CONTINUE
 8418 CONTINUE
C
C *** COMPUTE LIFETIME MATRIX [C']
      WFW=2.0*WHW
      DO 4118 I=1,NTIMES
        TTA=-DLY*I
        TTB=TTA-WFW
        DO 4116 J=1,NCOMP
          ZA=TTA/SURPRM(J,1)
          ZB=TTB/SURPRM(J,1)
          IF (ZA.GT.69) ZA=69
          IF (ZA.LT.-69) ZA=-69
          IF (ZB.GT.69) ZB=69
          IF (ZB.LT.-69) ZB=-69
          CP(J,I)=SURPRM(J,1)*(DEXP(ZA)-DEXP(ZB))
 4116   CONTINUE
 4118 CONTINUE
C
C *** COMPUTE [SAP] FROM GAUSS PARAMETERS
      DO 4158 J=1,NCOMP
        DO 4156 I=1,NWAVES
          Z=(NU(I)-SURPRM(J,2))/SURPRM(J,3)
          ZA=-.5*Z*Z
          IF (ZA.GT.69) ZA=69
          IF (ZA.LT.-69) ZA=-69
          SAP(I,J)=SURPRM(J,4)*DEXP(ZA)
 4156   CONTINUE
 4158 CONTINUE
      RETURN
      END
C
C********************************************************************
C********************************************************************
C
      SUBROUTINE SUPSRT(N,C,NSC,P)
C
C**** SORTS MATRIX IN ASCENDING ORDER FOR A GIVEN COLUMN
C            N      - # ROWS
```

```
C               C        - # COLUMNS
C               NSC      - SORTING COLUMN
C               P(N,C)   - ARRAY TO SORT
C
      DOUBLE PRECISION P(30,21),TP(30)
      INTEGER N,C,NSC,D,I,J,K,JD,IP,IMD,IPD,NMD,DMINUS
C
      D=2**INT(ALOG(REAL(N))/ALOG(2.))-1
 1120 NMD=N-D
      DO 1210 I=1,NMD
        IPD=I+D
        IF (P(I,NSC).LT.P(IPD,NSC)) GO TO 1210
 1140   IP=I+D
        DO 1145 K=1,C
          TP(K)=P(IP,K)
          P(IP,K)=P(I,K)
 1145   CONTINUE
 1150   IF (I.LT.D) THEN
 1155     DO 1158 K=1,C
            P(I,K)=TP(K)
 1158     CONTINUE
          GO TO 1210
        END IF
 1160   IMD=I-D
        DMINUS=-D
        DO 1190 J=IMD,1,DMINUS
          IF (TP(NSC).GT.P(J,NSC)) GO TO 1200
 1180     JD=J+D
          DO 1185 K=1,C
            P(JD,K)=P(J,K)
 1185     CONTINUE
 1190   CONTINUE
 1200   JD=J+D
        DO 1205 K=1,C
          P(JD,K)=TP(K)
 1205   CONTINUE
 1210 CONTINUE
 1220 D=D/2
 1230 IF (D.GT.0) GO TO 1120
 1300 RETURN
      END
C
C*********************************************************************
C*********************************************************************
C
      SUBROUTINE MXINVT(N,MXI)
C
C**** INVERTS MATRIX
C            N        - # ROWS IN SQUARE MATRIX
C            MXI(N,N) - MATRIX TO BE INVERTED
C
      INTEGER N,I,J,K,L,M,PV(25,3),IR,IC,JR,JC
      DOUBLE PRECISION MXI(25,25),MAX,P,S,T
C
```

```
C        NOTES ON DIMENSIONS: DIMENSION MXI(5*NCOMP,5*NCOMP),PV(5*NCOMP,3)
C                             NCOMP IS THE MAXIMUM # OF COMPONENTS FOR PROGRAM
C                             ASSUME NCOMP IS 5.
C
C        INITIALIZE PV
         DO 20 I=1,N
           DO 10 J=1,3
             PV(I,J)=0
    10     CONTINUE
    20   CONTINUE
C
         DO 360 I=1,N
           MAX=0
           DO 170 J=1,N
             IF(PV(J,3)-1) 100,170,100
   100       DO 160 K=1,N
               IF(PV(K,3)-1) 120,160,120
   120         IF(MAX-DABS(MXI(J,K))) 130,160,160
   130         IR=J
               IC=K
               MAX=DABS(MXI(J,K))
   160       CONTINUE
   170     CONTINUE
           PV(IC,3)=PV(IC,3)+1
           PV(I,1)=IR
           PV(I,2)=IC
           IF(IR-IC) 220,270,220
   220     DO 260 L=1,N
             S=MXI(IR,L)
             MXI(IR,L)=MXI(IC,L)
             MXI(IC,L)=S
   260     CONTINUE
   270     P=MXI(IC,IC)
           MXI(IC,IC)=1
           DO 295 L=1,N
             MXI(IC,L)=MXI(IC,L)/P
   295     CONTINUE
           DO 350 M=1,N
             IF(M-IC) 320,350,320
   320       T=MXI(M,IC)
             MXI(M,IC)=0
             DO 345 L=1,N
               MXI(M,L)=MXI(M,L)-MXI(IC,L)*T
   345       CONTINUE
   350     CONTINUE
   360   CONTINUE
         DO 470 I=1,N
           L=N-I+1
           IF(PV(L,1)-PV(L,2)) 400,470,400
   400     JR=PV(L,1)
           JC=PV(L,2)
           DO 460 K=1,N
             S=MXI(K,JR)
             MXI(K,JR)=MXI(K,JC)
```

```
            MXI(K,JC)=S
  460    CONTINUE
  470 CONTINUE
      RETURN
      END
C
C****************************************************************
C****************************************************************
C
      SUBROUTINE GAUZER
C
C**** COMPUTES SPECTRUM PARAMETERS ASSUMING GAUSSIAN PEAKS
C
      DOUBLE PRECISION SAP,CP,D,DP,CTAU,SURPRM,DLY,WHW,DA,NU,P
      INTEGER N,NTIMES,NWAVES,NCOMP,PMV,PMX,WLST,WLEN,TMST,TMEN
C
      COMMON CP(5,30),CTAU(25),D(51,30),DP(51,30),DA(15),NU(51),
     X       P(30,21),SAP(51,5),SURPRM(5,5),PMX(5),
     X       NWAVES,NTIMES,N,WLST,WLEN,TMST,TMEN,DLY,WHW,NCOMP,PMV
C
      DOUBLE PRECISION SATMP(51),Q0,Q1,Q2,Q3,Q4,SKEW,KURT,EM1P,EM2P,EM3P
     X,EM4P,EM3,EM4
      INTEGER I,J,K,LMAX,MINRT,MINLFT
C
C     LOCAL VARIABLES: LMAX   - MAXIMUM VALUE IN SPECTRUM
C                      MINLFT - MINIMUM TO LEFT SIDE OF LMAX
C                      MINRT  - MINIMUM TO RIGHT SIDE OF LMAX
C                      SKEW   - SKEWNESS IN GAUSSIAN
C                      KURT   - KURTOSIS IN GAUSSIAN
C                      SATMP()- DUMMY, SPECTRUM VECTOR FOR ONE EMITTER
C
      DO 800 I=1,NCOMP
        DO 100 J=1,NWAVES
          SATMP(J)=SAP(J,I)
          IF (SATMP(J).LE.0) SATMP(J)=1E-8
  100   CONTINUE
        CALL SVSMTH(NWAVES,SATMP)
        DO 110 J=1,NWAVES
          IF (SATMP(J).LE.0) SATMP(J)=1E-8
  110   CONTINUE
C
C****   FIND MAXIMA, THEN LOCAL MINIMA ON EACH SIDE
C
        LMAX=1
        DO 200 J=1,NWAVES
          IF (SATMP(J).GT.SATMP(LMAX)) LMAX=J
  200   CONTINUE
        DO 210 J=LMAX,NWAVES-1
          MINRT=J
          IF (SATMP(J).LT.SATMP(J+1)) GO TO 220
  210   CONTINUE
  220   DO 230 J=LMAX,2,-1
          MINLFT=J
          IF (SATMP(J).LT.SATMP(J-1)) GO TO 240
```

196

```fortran
  230    CONTINUE
  240    CONTINUE
C
C****    COMPUTE SUMS
         Q0=0
         Q1=0
         Q2=0
         Q3=0
         Q4=0
         DO 300 J=MINLFT,MINRT
           Q0=Q0+SAP(J,I)
           Q1=Q1+SAP(J,I)*NU(J)
           Q2=Q2+SAP(J,I)*NU(J)*NU(J)
           Q3=Q3+SAP(J,I)*NU(J)*NU(J)*NU(J)
           Q4=Q4+SAP(J,I)*NU(J)*NU(J)*NU(J)*NU(J)
  300    CONTINUE
C
C****    SUBSTITUTE VALUES INTO SURFACE PARAMETER ARRAY
C
         SURPRM(I,1)=CTAU(I)
         SURPRM(I,2)=Q1/Q0
         SURPRM(I,3)=DSQRT(DABS((Q2/Q0)-(SURPRM(I,2)*SURPRM(I,2))))
         SURPRM(I,4)=SATMP(LMAX)
         EM1P=Q1/Q0
         EM2P=Q2/Q0
         EM3P=Q3/Q0
         EM4P=Q4/Q0
         EM3=EM3P - 3*EM1P*EM2P + 2*EM1P**3
         EM4=EM4P - 4*EM1P*EM3P + 6*EM2P*EM1P**2 - 3*EM1P**4
         SKEW=EM3/(SURPRM(I,3)**3)
         KURT=EM4/(SURPRM(I,3)**4)
         SURPRM(I,5)=SKEW
C
C****    JUST IN CASE THE MATH WENT WILD ----
         IF(SURPRM(I,2).GT.NU(1)) THEN
           SURPRM(I,2)=NU(1)
           SURPRM(I,3)=0.1*SURPRM(I,2)
           SURPRM(I,4)=SATMP(LMAX)
         END IF
         IF(SURPRM(I,2).LT.NU(NWAVES)) THEN
           SURPRM(I,2)=NU(NWAVES)
           SURPRM(I,3)=0.1*SURPRM(I,2)
           SURPRM(I,4)=SATMP(LMAX)
         END IF
C
  800 CONTINUE
      RETURN
      END
C
C******************************************************************
C******************************************************************
C
      SUBROUTINE SVSMTH(NW,RAW)
C
```

```
C**** SAVITZKY-GOLAY 5 POINT SMOOTHING - RETURNS SMOOTHED DATA VECTOR
C      NOTE: FIRST TWO AND LAST TWO ELEMENTS OF DATA VECTOR ARE SET TO ZERO!
C              NW       - # ELEMENTS IN VECTOR
C              RAW(NW)  - VECTOR TO SMOOTH
C
       INTEGER I,J,K,KA,MS,NW
       DOUBLE PRECISION RAW(51),SMTHD(51),PTS(5)
C
C**** INITIALIZE
C
       MS=NW-4
       DO 100 I=2,5
         J=I-1
         PTS(I)=RAW(J)
  100 CONTINUE
       DO 110 I=1,NW
         SMTHD(I)=0
  110 CONTINUE
C
C**** SMOOTH
C
       DO 300 I=1,MS
         J=I+4
         DO 200 K=1,4
           KA=K+1
           PTS(K)=PTS(KA)
  200    CONTINUE
         PTS(5)=RAW(J)
         SMTHD(I+2)=(-3*PTS(1)+12*PTS(2)+17*PTS(3)+12*PTS(4)-3*PTS(5))/35
  300 CONTINUE
C
C**** SUBSTITUTE SMOOTHED VECTOR TO RAW VECTOR
       DO 400 I=1,NW
         RAW(I)=SMTHD(I)
  400 CONTINUE
       RETURN
       END
C
C*************************************************************************
C*************************************************************************
C
       SUBROUTINE RESPLN(A0,A1,A2)
C
C *** COMPUTES PLANE EQUATION FOR RESIDUALS:  [R] = [DA] - [DP]
C
C *** EQUATION IS:  Z = A0 + A1*X + A2*Y
C
       DOUBLE PRECISION SAP,CP,D,DP,CTAU,SURPRM,DLY,WHW,DA,NU,P
       INTEGER N,NTIMES,NWAVES,NCOMP,PMV,PMX,WLST,WLEN,TMST,TMEN
C
       COMMON CP(5,30),CTAU(25),D(51,30),DP(51,30),DA(15),NU(51),
     X        P(30,21),SAP(51,5),SURPRM(5,5),PMX(5),
     X        NWAVES,NTIMES,N,WLST,WLEN,TMST,TMEN,DLY,WHW,NCOMP,PMV
C
```

```fortran
      INTEGER I,J,K
      DOUBLE PRECISION T,EN,SR,SX,SY,SX2,SY2,SXR,SYR,SXY,AO,A1,A2,DE
C
C *** SUM SUMS:
C
      EN=0
      SR=0
      SX=0
      SY=0
      SX2=0
      SY2=0
      SXR=0
      SYR=0
      SXY=0
      DO 210 J=TMST,TMEN
        T=DLY*J+WHW
        DO 200 I=WLST,WLEN
          R=D(I,J)-DP(I,J)
          EN=EN+1.0
          SR=SR+R
          SX=SX+NU(I)
          SY=SY+T
          SX2=SX2+NU(I)*NU(I)
          SY2=SY2+T*T
          SXR=SXR+NU(I)*R
          SYR=SYR+T*R
          SXY=SXY+NU(I)*T
  200   CONTINUE
  210 CONTINUE
C
C *** COMPUTE LEAST SQUARES PLANE COEFFECIENTS
C
      DE=EN*SX2*SY2-EN*SXY*SXY-SX*SX*SY2+SX*SXY*SY+SY*SX*SXY-SY*SX2*SY
      AO=(SR*SX2*SY2-SR*SXY*SXY-SX*SXR*SY2+SX*SXY*SYR+SY*SXR*SXY-SY*SX2*
     XSYR)/DE
      A1=(EN*SXR*SY2-EN*SXY*SYR-SR*SX*SY2+SR*SXY*SY+SY*SX*SYR-SY*SXR*SY)
     X/DE
      A2=(EN*SX2*SYR-EN*SXR*SXY-SX*SX*SYR+SX*SXR*SY+SR*SX*SXY-SR*SX2*SY)
     X/DE
C
      RETURN
      END
C
C*******************************************************************
C*******************************************************************
C
      SUBROUTINE PRMSVR(FILNAM,LIN,LOWAVE,HIWAVE,LOTIME,HITIME,ERF,RERF,
     XPMVAR,PARMSV,NIT)
C
C**** SAVES PARAMETERS FOR REDUCED SPECTRUM
C          FILNAM - FILE NAME OF ORIGINAL DATA FILE
C          LIN()  - DESCRIPTIVE FILE DATA
C          LOWAVE - LOW WAVELENGTH OF DATA REDUCTION WINDOW
C          HIWAVE - HIGH WAVELENGTH        "
```

```
C              LOTIME - LOW TIME                  "
C              HITIME - HIGH TIME                 "
C              ERF    - ERROR - SUM OF SQUARED DIFFERENCES
C              RERF   - RELATIVE ERROR
C              PMVAR  - PARAMETERS TO HOLD CONSTANT & FLAGS
C              PARMSV - SPECTRUM PARAMETER FILE NAME
C              NIT    - # ITERATIONS
C              AO     - TERM IN RESIDUALS PLANE: Z=AO + A1*TIME + A2*WAVELENGTH
C              A1     -   "
C              A2     -   "
C
      DOUBLE PRECISION SAP,CP,D,DP,CTAU,SURPRM,DLY,WHW,DA,NU,P
      INTEGER N,NTIMES,NWAVES,NCOMP,PMV,PMX,WLST,WLEN,TMST,TMEN
C
      COMMON CP(5,30),CTAU(25),D(51,30),DP(51,30),DA(15),NU(51),
     X       P(30,21),SAP(51,5),SURPRM(5,5),PMX(5),
     X       NWAVES,NTIMES,N,WLST,WLEN,TMST,TMEN,DLY,WHW,NCOMP,PMV
C
      DOUBLE PRECISION ERF,RERF,AO,A1,A2
      REAL LOWAVE,HIWAVE,LOTIME,HITIME
      INTEGER I,MOUT,NIT
      CHARACTER FILNAM*12,LIN(5)*80,PMVAR*12,PARMSV*12,BRDR*12
C
C
      MOUT=12
      OPEN(UNIT=MOUT,FILE=PARMSV, STATUS='NEW')
C
      WRITE(MOUT,10) PARMSV
   10 FORMAT('SIMPLEX OPTIMIZED PARAMETERS FOR FILE ',A12)
      DO 200 I=1,5
         WRITE(MOUT,*) LIN(I)
   20    FORMAT(1X,A80)
  200 CONTINUE
      WRITE(MOUT,30) ERF
   30 FORMAT(1X,'ERROR FUNCTION = ',E15.5)
      WRITE(MOUT,40) RERF
   40 FORMAT(1X,'RELATIVE ERROR = ',E15.5)
      WRITE(MOUT,50) NIT,PMVAR
   50 FORMAT(1X,I5,' ITERATIONS, CONSTANT PARAMETERS: ',A12)
      CALL RESPLN(AO,A1,A2)
      WRITE(MOUT,53) AO,A1,A2
   53 FORMAT(1X,'RESIDUAL PLANE: AO, A1, A2 =', 3D15.5)
      WRITE(MOUT,60) LOWAVE,HIWAVE
   60 FORMAT(1X,'SPECTRUM WINDOW:',F10.1,' TO ',F10.1,' ANGSTROMS')
      WRITE(MOUT,70) LOTIME,HITIME
   70 FORMAT(1X,'                  ',F10.5,' TO ',F10.5,' MICROSECONDS')
      WRITE(MOUT,*)'COMPONENT             ',(I,'             ',I=1,NCOMP)
   80 FORMAT(1X,'COMPONENT               ',5I15)
      WRITE(MOUT,*)'LIFETIME, US          ', (SURPRM(I,1), I=1,NCOMP)
   90 FORMAT(1X,'LIFETIME, US          ',5E15.6)
      WRITE(MOUT,*)'PEAK MAXIMA, 1/ANGSTROMS ', (SURPRM(I,2), I=1,NCOMP)
  100 FORMAT(1X,'PEAK MAXIMA, 1/ANGSTROMS ',5E15.6)
      WRITE(MOUT,*)'PEAK S.DEV., 1/ANGSTROMS ', (SURPRM(I,3), I=1,NCOMP)
  110 FORMAT(1X,'PEAK S.DEV., 1/ANGSTROMS ',5E15.6)
```

```
      WRITE(MOUT,*)'PEAK INTENSITY           ', (SURPRM(I,4), I=1,NCOMP)
  120 FORMAT(1X,'PEAK INTENSITY           ',5E15.6)
      WRITE(MOUT,*)'PEAK ASSYMETRY            ', (SURPRM(I,5), I=1,NCOMP)
  130 FORMAT(1X,'PEAK ASSYMETRY           ',5E15.6)
      BRDR='************'
      WRITE(MOUT,140) (BRDR,J=1,6)
  140 FORMAT('0',6A12)
C
      CLOSE(MOUT)
      WRITE(*,*)'FILE ',PARMSV,' SAVED'
      RETURN
      END
C
C*****************************************************************************
C*****************************************************************************
C
      SUBROUTINE SPEKRD(FILNAM,LIN,LOWAVE,HIWAVE,LOTIME,HITIME)
C
C**** READ A SPECTRUM, SET BOUNDS FOR DATA REDUCTION REGION IN SPECTRUM
C             FILNAM - FILE NAME OF ORIGINAL DATA FILE
C             LIN()  - DESCRIPTIVE FILE DATA
C             LOWAVE - LOW WAVELENGTH OF DATA REDUCTION WINDOW
C             HIWAVE - HIGH WAVELENGTH         "
C             LOTIME - LOW TIME               "
C             HITIME - HIGH TIME              "
C
      DOUBLE PRECISION SAP,CP,D,DP,CTAU,SURPRM,DLY,WHW,DA,NU,P
      INTEGER N,NTIMES,NWAVES,NCOMP,PMV,PMX,WLST,WLEN,TMST,TMEN
C
      COMMON CP(5,30),CTAU(25),D(51,30),DP(51,30),DA(15),NU(51),
     X       P(30,21),SAP(51,5),SURPRM(5,5),PMX(5),
     X       NWAVES,NTIMES,N,WLST,WLEN,TMST,TMEN,DLY,WHW,NCOMP,PMV
C
C
      REAL STWL,ENWL,INWL,ALAM,LOWAVE,HIWAVE,LOTIME,HITIME
      INTEGER MIN,I,J,NTT
      CHARACTER FILNAM*12,LIN(5)*80
C
      WRITE(*,*)'WORKING HARD ON FILE ',FILNAM
      MIN=10
      OPEN(UNIT=MIN,FILE=FILNAM)
C
      DO 100 I=1,5
         READ(MIN,10) LIN(I)
   10    FORMAT(A80)
  100 CONTINUE
C
      DO 200 I=6,13
         READ(MIN,*) DA(I)
  200 CONTINUE
C
      STWL=DA(10)
      ENWL=DA(11)
      INWL=DA(12)
```

```
      IF (STWL.GT.ENWL) THEN
         STWL=DA(11)
         ENWL=DA(10)
      END IF
      WHW=0.5*DA(13)
      DLY=DA(6)*DA(7)
      NTIMES=DA(9)
      NWAVES=(ENWL-STWL+INWL)/INWL
      ALAM=STWL-INWL
      DO 300 I=1,NWAVES
         ALAM=ALAM+INWL
         NU(I)=1/ALAM
  300 CONTINUE
C
      DO 410 I=1,NWAVES
         DO 400 J=1,NTIMES
            READ(MIN,*) D(I,J),X,X,X
   40       FORMAT(F8.4,2X,F8.4,2X,F8.2,2X,F8.2)
  400    CONTINUE
  410 CONTINUE
C
      CLOSE(UNIT=MIN)
C
C *** CHECK BOUNDS FOR LIMITING AREA OF SPECTRUM FOR DATA REDUCTION
      IF ((LOWAVE.LT.STWL).OR.(LOWAVE.GT.ENWL)) THEN
         LOWAVE=STWL
         WLST=1
      END IF
      IF ((HIWAVE.LT.STWL).OR.(HIWAVE.GT.ENWL)) THEN
         HIWAVE=ENWL
         WLEN=NWAVES
      END IF
      IF (HIWAVE.LT.LOWAVE) THEN
         LOWAVE=STWL
         HIWAVE=ENWL
         WLST=1 .
         WLEN=NWAVES
         GO TO 500
      END IF
      NTT=INT((LOWAVE-STWL)/INWL)
      WLST=1+NTT
      LOWAVE=STWL+NTT*INWL
      NTT=INT((ENWL-HIWAVE)/INWL)
      WLEN=NWAVES-NTT
      HIWAVE=ENWL-NTT*INWL
  500 CONTINUE
      STIM=DLY
      ETIM=NTIMES*DLY
      IF ((LOTIME.LT.STIM).OR.(LOTIME.GT.ETIM)) THEN
         LOTIME=STIM
         TMST=1
      END IF
      IF ((HITIME.LT.STIM).OR.(HITIME.GT.ETIM)) THEN
         HITIME=ETIM
```

202

```
            TMEN=NTIMES
         END IF
         IF (LOTIME.GT.HITIME) THEN
            LOTIME=STIM
            HITIME=ETIM
            TMST=1
            TMEN=NTIMES
            GO TO 520
         END IF
         NTT=INT((LOTIME-STIM)/DLY)
         TMST=1+NTT
         LOTIME=STIM+NTT*DLY
         NTT=INT((ETIM-HITIME)/DLY)
         TMEN=NTIMES-NTT
         HITIME=ETIM-NTT*DLY
  520 CONTINUE
      RETURN
      END
C
C*********************************************************************
C*********************************************************************
C
      SUBROUTINE CONRD(ICONRD,FILNAM,PMVAR,LOWAVE,HIWAVE,LOTIME,HITIME,
     X     XPARMSV)
C
C**** READS MASTER CONTROL FILE - TELLS WHAT FILES TO READ & WHAT TO
C                                 HOLD CONSTANT & SPECTRUM WINDOW TO
C                                 OPTIMIZE OVER.
C            ICONRD - UNIT # FOR CONTROL FILE
C            FILNAM - FILE NAME OF ORIGINAL DATA FILE
C            LOWAVE - LOW WAVELENGTH OF DATA REDUCTION WINDOW
C            HIWAVE - HIGH WAVELENGTH            "
C            LOTIME - LOW TIME                   "
C            HITIME - HIGH TIME                  "
C            PARMSV - SPECTRUM PARAMETER FILE NAME
C            PMVAR  - PARAMETERS TO HOLD CONSTANT, SET FLAGS
C                     T - LIFETIME
C                     M - PEAK MAXIMA
C                     W - PEAK WIDTH
C                     I - PEAK INTENSITY
C                     A - PEAK ASSYMETRY
C                     Q - QUIT AFTER FIRST STAGE
C                     S - FLAG TO SAVE COMPUTED SPECTRUM
C                     F - FLAG TO SAVE INTERMEDIATE PARAMETER VALUES
C
      DOUBLE PRECISION SAP,CP,D,DP,CTAU,SURPRM,DLY,WHW,DA,NU,P
      INTEGER N,NTIMES,NWAVES,NCOMP,PMV,PMX,WLST,WLEN,TMST,TMEN
C
      COMMON CP(5,30),CTAU(25),D(51,30),DP(51,30),DA(15),NU(51),
     X       P(30,21),SAP(51,5),SURPRM(5,5),PMX(5),
     X       NWAVES,NTIMES,N,WLST,WLEN,TMST,TMEN,DLY,WHW,NCOMP,PMV
C
      REAL LOWAVE,HIWAVE,LOTIME,HITIME
      INTEGER ICONRD
```

```
      CHARACTER FILNAM*12,BASEFL*12,PMVAR*12,PARMSV*12
C
   90 CONTINUE
C
C**** FILE TO READ
      READ(ICONRD,100) FILNAM
  100 FORMAT(A12)
      IF(INDEX(FILNAM,'***END***').GT.0) RETURN
      IF(INDEX(FILNAM,' ').GT.0) FILNAM=FILNAM(1:(INDEX(FILNAM,' '))-1)
C
C**** FILE TO STORE REDUCED PARAMETERS
      READ(ICONRD,110) BASEFL
  110 FORMAT(A12)
      IF(INDEX(BASEFL,'*').GT.0) BASEFL=FILNAM(1: )
      IF(INDEX(BASEFL,' ').GT.0) BASEFL=BASEFL(1:(INDEX(BASEFL,' '))-1)
      IF(INDEX(BASEFL,'.').GT.0) BASEFL=BASEFL(1:(INDEX(BASEFL,'.'))-1)
      IF(LEN(BASEFL).GT. ) THEN
        PARMSV=BASEFL(1: )//'.SLP'
        GO TO 115
      END IF
      PARMSV=BASEFL//'.SLP'
  115 CONTINUE
C
C**** SET PARAMETERS TO VARY IN SIMPLEX OPTIMIZATION
      READ(ICONRD,120) PMVAR
  120 FORMAT(A12)
      PMV=0
      IF(INDEX(PMVAR,'T').EQ.0) THEN
C****    VARY LIFETIMES
        PMV=1
        PMX(PMV)=1
      END IF
      IF(INDEX(PMVAR,'M').EQ.0) THEN
C****    VARY PEAK MAXIMA
        PMV=PMV+1
        PMX(PMV)=2
      END IF
      IF(INDEX(PMVAR,'W').EQ.0) THEN
C****    VARY PEAK WIDTH (STANDARD DEVIATION)
        PMV=PMV+1
        PMX(PMV)=3
      END IF
      IF(INDEX(PMVAR,'I').EQ.0) THEN
C****    VARY PEAK PRE-EXPONENTIAL INTENSITY FACTOR
        PMV=PMV+1
        PMX(PMV)=4
      END IF
      IF(INDEX(PMVAR,'A').EQ.0) THEN
C****    VARY PEAK ASSYMETRY
        PMV=PMV+1
        PMX(PMV)=5
      END IF
C
C**** NUMBER OF EMITTING COMPONENTS IN SPECTRUM
```

```
      READ(ICONRD,*) NCOMP
  130 FORMAT(I5)
C
C**** SURFACE PARAMETERS FOR EACH EMITTING COMPONENT
      DO 150 I=1,NCOMP
        READ(ICONRD,*) (SURPRM(I,J),J=1,5)
  140   FORMAT(5G15.6)
  150 CONTINUE
C
C**** BOUNDARIES FOR LIMITING OPTIMIZATION TO A REGION OF SPECTRUM
      READ(ICONRD,*) LOWAVE,HIWAVE,LOTIME,HITIME
  160 FORMAT(4G15.6)
C
C**** SKIP TO NEXT SPECTRUM IF A ".SLP" FILE EXISTS
      OPEN(UNIT=69,ERR=200,FILE=PARMSV,STATUS='OLD')
      WRITE(*,*) 'SKIPPING FILE ',FILNAM,' - FILE ',PARMSV,' FOUND'
      GO TO 90
C
  200 CONTINUE
C
C**** SKIP TO NEXT SPECTRUM IF THE DATA FILE DOES NOT EXIST
      OPEN(UNIT=69,ERR=220,FILE=FILNAM,STATUS='OLD')
      GO TO 300
  220 WRITE(*,*) 'FILE ',FILNAM,' DOES NOT EXIST'
      GO TO 90
C
  300 CONTINUE
      RETURN
      END
C
C***********************************************************************
C***********************************************************************
C
      SUBROUTINE SPKSVR(PARMSV,LIN)
C
C**** SAVES COMPUTED AND ORIGINAL SPECTRA
C           PARMSV - SPECTRUM PARAMETER FILE NAME
C           LIN()  - DESCRIPTIVE DATA
C
      DOUBLE PRECISION SAP,CP,D,DP,CTAU,SURPRM,DLY,WHW,DA,NU,P
      INTEGER N,NTIMES,NWAVES,NCOMP,PMV,PMX,WLST,WLEN,TMST,TMEN
C
      COMMON CP(5,30),CTAU(25),D(51,30),DP(51,30),DA(15),NU(51),
     X       P(30,21),SAP(51,5),SURPRM(5,5),PMX(5),
     X       NWAVES,NTIMES,N,WLST,WLEN,TMST,TMEN,DLY,WHW,NCOMP,PMV
C
C
      INTEGER MOUT,I,J
      REAL X,Y
      CHARACTER FILNAM*12,LIN(5)*80,PARMSV*12
C
      FILNAM=PARMSV(1:INDEX(PARMSV,'.'))//'SSP'
      Y=1.0
C
```

```
      MOUT=22
      OPEN(UNIT=MOUT, FILE=FILNAM, STATUS='NEW')
      WRITE(MOUT,*) 'COMPUTED ',FILNAM
  20  FORMAT(1X,A12)
      DO 800 I=1,4
        WRITE(MOUT,*) LIN(I)
 800  CONTINUE
  30  FORMAT (1X,A18)
      DO 810 I=6,13
        WRITE(MOUT,35) DA(I)
  35    FORMAT(1X,E15.5)
 810  CONTINUE
      DO 830 I=1,NWAVES
        DO 820 J=1,NTIMES
          X=D(I,J)-DP(I,J)
          WRITE(MOUT,40) X,DP(I,J),D(I,J),Y
  40      FORMAT(1X,F8.4,2X,F8.4,2X,F8.4,2X,F8.4)
 820    CONTINUE
 830  CONTINUE
      CLOSE(MOUT)
      RETURN
      END
```